FEM Simulation of Laser Bending for D-36 Ship Building Steel

Saswat Rajowar[1], Polash Pratim Dutta[2]

[1,2]Department of Mechanical Engineering, Tezpur University, Assam, India-784028

[1]saswatrajowar8@gmail.com

[2]polashd@tezu.ernet.in

Abstract— **Laser forming is a process used for forming of various metals. In this work deformation of a D-36 steel sheet using laser is studied using FEM simulation. The laser beam power, beam size, scan speed and number of laser passes determine the shape of the final product. Laser beam of suitable power is allowed to pass over the work-piece material due to which thermal stress is developed along the path of laser irradiation.The sheet was first analysed for the change in angle for a single pass and thereafter double pass was analysed for the sheet.**

Keywords— **Laser bending, Thermal analysis, Structural analysis, Bending angle, Heat flux.**

1. Introduction

Laser forming is a way of processing materials in an ideal manner, which would be difficult using conventional manufacturing methods. Laser forming can use combinations of curve and straight scan lines to produce three-dimensional formed components. Laser forming is of significant value to industries that previously relied on expensive stamping dies and presses for prototype evaluations, which include aerospace, automotive, microelectronics and shipbuilding. Laser forming involves heating sheet metal work piece along a certain path with a focused laser beam directed normal to the surface.Based on the direction of bending of the workpiece after the incident of the laser beam, laser bending can be divided into two types [1]:

1) Positive laser bending: If the bending of the workpiece occurs towards the incident beam, it is called as positive laser bending. Normally it is observed in most of the cases.

2) Negative laser bending: If the bending of the workpiece occurs away from the incident beam then it is called as negative laser bending.

Laser bending is an advanced manufacturing process in which the metal sheet is bent by using thermally induced plastic strains. Thermal stresses are induced due to laser beam irradiation over the workpiece surface. These stresses lead to the plastic strains. The process is controlled by various parameters such as laser power, beam diameter, scanning velocity and irradiation path etc. Instead of costly tools, dies or presses, a controlled and concentrated laser beam works as an operational tool to bend the workpiece. Spring back is eliminated in laser bending process which often changes the performance of traditional mechanical bending operation. Laser bending is now becoming popular due to its advantages such as accurate and easy control over determination of energy beam on work surface, forming of parts, minimal work piece degradation due to smaller heat affected zone, generation of complex shapes, generation of small and accurate bend angles or shapes and bending of brittle materials.

Kant et al. [2] carried out a numerical investigation on curvilinear laser bending of magnesium M1A alloy sheets. Three-dimensional sequential transient thermomechanical numerical model was developed by using finite element method. The model was validated by comparing the predicted results with those obtained in the experiments. Fetene et al. [3] carried finite element simulations of bending of small sized sheets using the ABAQUS package. The temperature and strain-rate dependent material properties of D-36 shipbuilding steel sheet were considered. Simulation results throw light on the bending behavior of small sized sheet components. Fetene et al. [4] developed an artificial neural network (ANN) model of laser-assisted bending based on the data obtained from a finite element method (FEM) model. Ji et al. [5] showed a simplified computational model and corresponding solving method under the conditions of neglecting thermo-mechanical coupling. Then, FEM analysis of the three-dimensional transient temperature field produced by laser beam scanning on the forming sheet is carried out. Liu et al. [6] presented a finite element method (FEM) based three-dimensional laser forming process design methodology for thin plates to determine the laser scanning paths and heating conditions. The strain fields were first calculated via FEM. The laser scanning paths were chosen perpendicular to the averaged principal minimum strain direction. Zhang et al. [7] built a finite element model of heat flux based on scanning path described with B-spline curve. Then, FE simulation of laser beam scanning on the forming sheet metals was carried out. And transient temperature fields, displacement fields, stress fields and strain fields were investigated. Cheng et al. [8] described an analytical model to describe the three-dimensional temperature field for a finite plate with a Gaussian heat source moving at a constant velocity. Earlier Nath et al. [9] carried thermal analysis for SOLID70 element by using ANSYS. The deformation of a sheet, subjected to an irradiation, has been studied through a single pass of the workpiece using FEM.

Fabrication and Vibration Analysis of Shaft of a Pedal Powered Washing Machine

Sanjana Talukdar[1], Narayan Das[1], Debangshu Sinha[1], Sumit Patni[1], Gaurav Kumar[1], Bhupendra Kumar Meena[1], Polash Pratim Dutta[2], Sushen Kirtania[2]

[1,2]*Department of Mechanical Engineering, Tezpur University, Assam-784028, India.*

[1]Sanjana26812@gmail.com

[2]sushen@tezu.ernet.in

[2]polashd@tezu.ernet.in

Abstract— **In a developing nation like India, where most of the population lives in villages or rural areas, washing of clothes is a noteworthy issue. Individuals in these zones cannot afford to purchase the conventional washing machines. In addition, these regions are either in complete absence or lack of electricity. The goal of our work is to develop an efficient, low cost pedal powered washing machine using scrap parts that are easily available, cheap and easy to maintain. The existing fabricated washing machine produced rigorous vibration and leakage during washing the clothes. In the present work, the causes of vibration have been identified and possible solutions were implemented to reduce vibration and leakage. A simple mathematical model of the output shaft has been proposed to predict resonance and safe operating frequency range while washing the clothes.**

Keywords— **Pedal powered washing machine, Problem identification, Vibration, Leakage, Low cost, Rural application.**

1. Introduction

A washing machine is a popular electronic home appliance, which is found in almost every household in the urban regions. The first washing machine was designed by James King in 1851 [1]. The washing machine used a drum device that is still used often in washing machines of today's generation. However it required hand power. The first drum based electric washing machine called the Thor was invented by Alva J. Fisher and manufactured by the Hurley Machine Company in 1908 [2]. The Thor was a drum type washing machine with a galvanized tub and an electric motor. Bendix Corporation introduced the first domestic automatic washing machine in 1937 [3]. In appearance and mechanical detail, this first machine was similar to the front loading automatic washers used today but the machine lacked drum suspension and it was very expensive. The drum speed change was facilitated by a 2-speed gearbox built to a heavy duty standard like a car synchromesh gearbox. The timer used miniature electric motors to sequence the washing and extraction process. A large number of US manufacturers introduced competing automatic machines (mainly of the top-loading type) in the late 1940s and early 1950s. Several manufacturers produced semi-automatic machines, requiring the user to intervene at one or two points in the wash cycle. A common semi-automatic type included two tubs: one with an agitator or impeller for washing, plus another smaller tub for water extraction or centrifugal rinsing.

During early 90's machines were available in the market that used microcontrollers for the timing process. With the passage of time more improvement was made in the field of washing machines and today's modern consumer washing machines incorporate many new features. In this 21st century, due to environmental concerns and water scarcity problems, the focus has shifted in developing technology associated with washing machines which can overcome these issues. The Xerox washing machine is one such new kinds of machine that uses primary nylon polymer beads and very little water [4]. Works are going on to develop washing machines of low cost and which do not require electricity. Ranjan et al. [5] developed a pedal powered washing machine using a transmission system connecting the bicycle frame to the front loaded washing machine. Ajay et al. [6] designed a pedal powered washer where inner drum is constructed by modifying a plastic utility tub. Other pedal powered washing machine developments have been reported which are low cost and energy saving devices [7-9]. Recognizing the need of low cost washing machine for rural India, the aim of the present work is to develop a low cost pedal powered washing machine (PPWM) with readily available scrap parts which can be used for washing sufficient quantities of clothes.

The washing machine generally involves rotating masses which rotate to agitate the clothes inside a drum creating turbulence to clean them. However, rotating machineries might involve problems like misalignment, unbalanced masses leading to vibration and noise which are unavoidable. A great challenge for the fabrication of the washing machine is to carefully eliminate these ill effects.

2. Detailed Set Up

Figure 1 shows the front view of the fabricated pedal powered washing machine. It consists of a shaft (length 1 m, inner diameter = 0.04 m, outer diameter = 0.45 m) which is connected to the sprocket of the cycle. The shaft rotates when the cycle is pedalled. The inner drum with

Academic Science

DIIF

Conference Info

Reference No.:NITTTR323

2nd International Conference on Engineering Technology, Science and Management Innovation (ICETSMI-2017)

Venue-
National Institute of Technical Teachers Training & Research (NITTTR),
MHRD,Govt of India, Chandigarh, India
on 15th January 2017

Certificate of Presentation

This is to certify that

B.Chowdhury
Department of Mechanical Engineering, Tezpur University, Tezpur, Assam, India

Presented a paper titled as

"Cause-Effect Diagram Versus System Dynamic Model – A case study of Manufacturing Defects analysis"

Organized by Conference Info in Association with Academic Science at
National Institute of Technical Teachers Training & Research(NITTTR),
MHRD, Govt of India, Chandigarh, India
on 15th January 2017

Dr K. Agarwal
Editor, Academic Science

Convener

2021/5/28 22:10
SHOT ON POCO F1
POCO

National Conference on

SUSTAINABLE MECHANICAL ENGINEERING: TODAY AND BEYOND

SMETB 2017

March 25-26, 2017

Department of Mechanical Engineering, Tezpur University, Assam, India

This is to certify that Prof./Dr./Mr./Ms. Barnali Chowdhury *of* Tezpur University *participated and presented a paper titled* Analysis of manufacturing defects using FMEA - a step towards defect prevention. *in the* ***National Conference on SUSTAINABLE MECHANICAL ENGINEERING: TODAY AND BEYOND****, 2017 held at Tezpur University , Assam , India.*

SMETB 2017

(Dr. Partha P. Dutta)	(Prof. Tapan K. Gogoi)	(Dr. Seikh M. Kamal)
Chairman	Organizing Secretary	Joint Organizing Secretary

POCO
SHOT ON POCO F1
2021/5/28 22:11

INTERNATIONAL CONFERENCE

on

Sustainable Approaches in Food Engineering and Technology

(SAFETy-2021)

24th-25th June, 2021

Certificate

BARNALI CHOWDHURY

This is to certify that Dr./Mr./Ms. ..... has participated as Oral Presenter *..... at SAFETy-2021, organized by the Department of Food Engineering & Technology, Tezpur University, Assam, India, and Department of Food Science & Technology, University of Georgia, Georgia (US) in Association with AFST(I) Tezpur Chapter during 24th-25th June, 2021.*

Title: Design and analysis of a water pumping device - A solution for hilly terrains

Author(s): Chowdhury, B., Maitra, S., Das, M. & Krishna, K.

Dr. Amit Baran Das	Dr. Abhinav Mishra	Prof. Nandan Sit	Prof. Manpreet Singh
Organizing Secretary	Organizing Secretary	Chairperson	Chairperson
TEZPUR UNIVERSITY	UNIVERSITY OF GEORGIA	TEZPUR UNIVERSITY	UNIVERSITY OF GEORGIA

Analysis of Performance Parameters of a Shell and Tube Heat Exchanger using Design of Experiments

Bikshya Saikia[1] and Barnali Chowdhury[2]

[1]*Department of Mechanical Engineering, Tezpur University, Tezpur, India.*
[2]*Department of Mechanical Engineering, Tezpur University, Tezpur, India.*

[1]bsaikia221@gmail.com
[2]barnali@tezu.ernet.in

Abstract

A heat exchanger is important equipment used for the regulation of heat in a wide range of domestic and industrial processes and as a means of waste heat recovery. Therefore it is necessary to find out the optimum combination of parameters that influence the performance of heat exchangers. Experimental analysis is the most basic form of analysis of the performance parameters of a system. However such an analysis has certain limitations and may not always give the desired results. Hence in this work an attempt has been made to carry out a statistical analysis of a shell and tube heat exchanger in order to determine the significant parameters that affect its performance. The performance parameters of the heat exchanger namely log mean temperature difference and effectiveness are analysed with the help of a statistical tool called the Design of Experiments (DOE). Mathematical models are then developed and optimum parameters are obtained.

Keywords –Heat exchangers, DOE, statistical analysis, optimization.

Time Series Analysis of Manufacturing Defects – A Case of Refrigerator Liner Manufacturing

Barnali Chowdhury [1] and Sudip Kumar Deb[2]

[1]*Department of Mechanical Engineering , Tezpur University, Tezpur, India.*
[2]*Department of Mechatronics Engineering, Assam Engineering College,Gauhati University Guwahati, India,*

[1]barnali@tezu.ernet.in
[2]sudipkumardeb@gmail.com

Abstract

Defects play a significant role in enhancing the performance of a product and improving the productivity of an organization. Further, defects cannot be isolated or completely removed from a process or a product but can only be reduced. Defect data analysis are being done using commonly used tools namely cause–effect diagram, Pareto analysis, Failure Modes and Effects Analysis etc. since the time when enhancing productivity and reducing cost of poor quality were given due importance. However, these are inadequate to ascertain any persistence behavior or significant correlation among the defect data and cannot provide any forecast based on the existing situation. This inadequacy of commonly used tools in carrying out such effective and exploratory data analysis may be overcome by using time series approach. Hence in this paper, a humble attempt has been made to analyze manufacturing defect data using time series approach and discover significant correlations among them, which would further enable to understand, forecast trend and diagnose manufacturing process problems at a grave depth.

Keywords -Time series, rejection data, forecast, liner manufacturing.

TEQIP III

NATIONAL CONFERENCE FOR STUDENTS ON ADVANCES IN MECHANICAL ENGINEERING

DEPARTMENT OF MECHANICAL ENGINEERING
ASSAM ENGINEERING COLLEGE

CERTIFICATE OF PARTICIPATION

This is to certify that

Barnali Chowdhury of **Tezpur University**

has participated and successfully prsented a paper in TEQIP-III sponsored **"National Conference for Students on Advances in Mechanical Engineering"** organized by Department of Mechanical Engineering, Assam Engineering College on 6th of March 2020.

DR. SUDIP KUMAR DEB	DR. PRADIP BAISHYA	DR. RANJIT KUMAR DUTTA
	TEQIP III Cordinator	Prof. & HOD

CERTIFICATE

61st National Convention
of
Indian Institution of Industrial Engineering
&
5th International Conference
on

Industrial Engineering (ICIE 2019)

This is to certify that Dr./Prof./Mr./Ms.

B. Chowdhury

has attended 61st National Convention of Indian Institution of Industrial Engineering
& 5th International Conference on **Industrial Engineering (ICIE 2019)**
Hosted by Indian Institution of Industrial Engineering (IIIE) Surat Chapter,
S. V. National Institute of Technology, Surat, India during December 12-14, 2019
and presented a paper entitled

Application of Design of Experiments in the analysis of Thermoforming Process Parameters that affect Rejection Rate of Thermoformed Refrigerator Liners

Dr. Ravi Kant
Convener

Dr. Tushar N. Desai
Convener

Shri D. V. Bhagat
Chairman, IIIE National Council

v

Certificate of Appreciation

International Congress on

Advances in Materials Science and Engineering (CAMSE-2020)

www.camse.in

December 28-30, 2020

This is to certify that

Dr. Barnali Chowdhury, Tezpur University, Tezpur, Assam, India has participated and presented a research paper titled **Optimizing thermoforming of refrigerator liners to reduce liner rejection rate- a case study using fractional factorial design of experiments** in the International Conference - **CAMSE-2020** held in Virtual format in association with **Shobhit University Gangoh** and Technically supported by **STEM-Research Society** and **Dr. B. R. Ambedkar National Institute of Technology, Jalandhar, Punjab.**

Dr. Tarun K. Sharma
Organizing Chair

In association with

Dr. Om Prakash Verma
Organizing Co-Chair

Proceedings in LNME Series

Springer

Technically Supported by:

SONA COLLEGE OF TECHNOLOGY
Learning is a Celebration!

SONA COLLEGE OF TECHNOLOGY

An Autonomous Institution | Approved by AICTE | ISO 9001 : 2015 Certified | NAAC Accredited - A Grade
All Eligible Programmes NBA Accredited | Affiliated to Anna University, Chennai

Junction Main Road, Salem - 636 005. Tamil Nadu. India.
Phone: +91 427 4099 999 | www.sonatech.ac.in

63 Years of Excellence in EDUCATION AND INDUSTRY

Certificate of Presentation

Awarded to

DR.BARNALI CHOWDHURY, Tezpur University, Assam

for presenting a research paper titled

TIME SERIES ANALYSIS OF MANUFACTURING DEFECTS – A CASE OF REFRIGERATOR LINER MANUFACTURING

at the International Virtual Conference on APPLIED SCIENCE, TECHNOLOGY MANAGEMENT AND LANGUAGE STUDIES (ASTMLS - 2020) on 11th & 12th December, 2020.

[Associate Sponsors]

IEEE · IETE · The Institution of Engineers (India) · ISTE · ICI

Coordinator
Dr. D. Senthilkumar
Professor & Head / Mechanical, Dean - Students Affair
Sona College of Technology

Convenor
Dr.S.Chandrasekar
Dean - Research and Development
Sona College of Technology

Patron
Dr. S.R.R. Senthilkumar
Principal
Sona College of Technology

FINITE ELEMENT ANALYSIS OF LASER BENDING PROCESS FOR D36 SHIPBUILDING STEEL

M. K. Nath[1], P. P. Dutta[2], A. Chowdhury[3], A. Das[4]
[1, 3]M.Tech Student, Tezpur University, Tezpur, India
[2]Assistant Professor, Tezpur University, Tezpur, India, e-mail: polashd@tezu.ernet.in
[4]Assistant Professor, Tezpur University, Tezpur, India

ABSTRACT: Laser bending process is one of the advanced bending processes which can be achieved by elasto-plastic deformation through the local introduction of thermal stresses. It is a thermo-mechanical process in which a laser heat source of suitable power is used for bending the material rather than any external force. In this work, sequential structural analysis is carried out for SOLID45 element by using ANSYS. The deformation of a sheet, subjected to an irradiation, has been studied through a sequentially coupled thermo-mechanical elasto-plastic simulation by using the finite element method (FEM). D36 shipbuilding steel sheet has been taken as the work-piece material for the analysis. A parametric study has been performed to investigate the effect of three most influential operating parameters in laser bending process, viz. laser power, scanning speed and sheet thickness.

Keywords: Laser bending process, bending angle, FEM

1. INTRODUCTION

Laser bending is a non-contact process of forming the sheet by localized heating with the help of a laser beam which induces thermal stress gradients throughout the thickness of the sheet, causing localized plastic deformation of the sheet without use of any external force. Laser bending process is superior to conventional bending process as it does not require any external tool. The process is free from spring-back effect and suitable for materials that are difficult to form by mechanical approaches. Laser bending mechanisms mainly include temperature gradient mechanism (TGM), buckling mechanism (BM) and upsetting mechanism (UM). Potential applications of laser manufacturing include cutting of complex shapes, drilling on curved surfaces, surface treatment, welding of dissimilar metals etc. With increasing knowledge, the process offers significant potential value to industry such as aerospace, shipbuilding, microelectronics etc.

In case of laser bending process, bending angle plays an important role which is affected by different operating parameters. Among different operating parameters; intensity of laser power, scanning speed of laser beam and sheet thickness of the work-piece are considered to be the most influential. Bending angle can be calculated with the help of these parameters. Various researchers developed different models for the prediction of

LIANGKHUN KETIBU KHUANG

A Learner's Book of the Liangmai Language

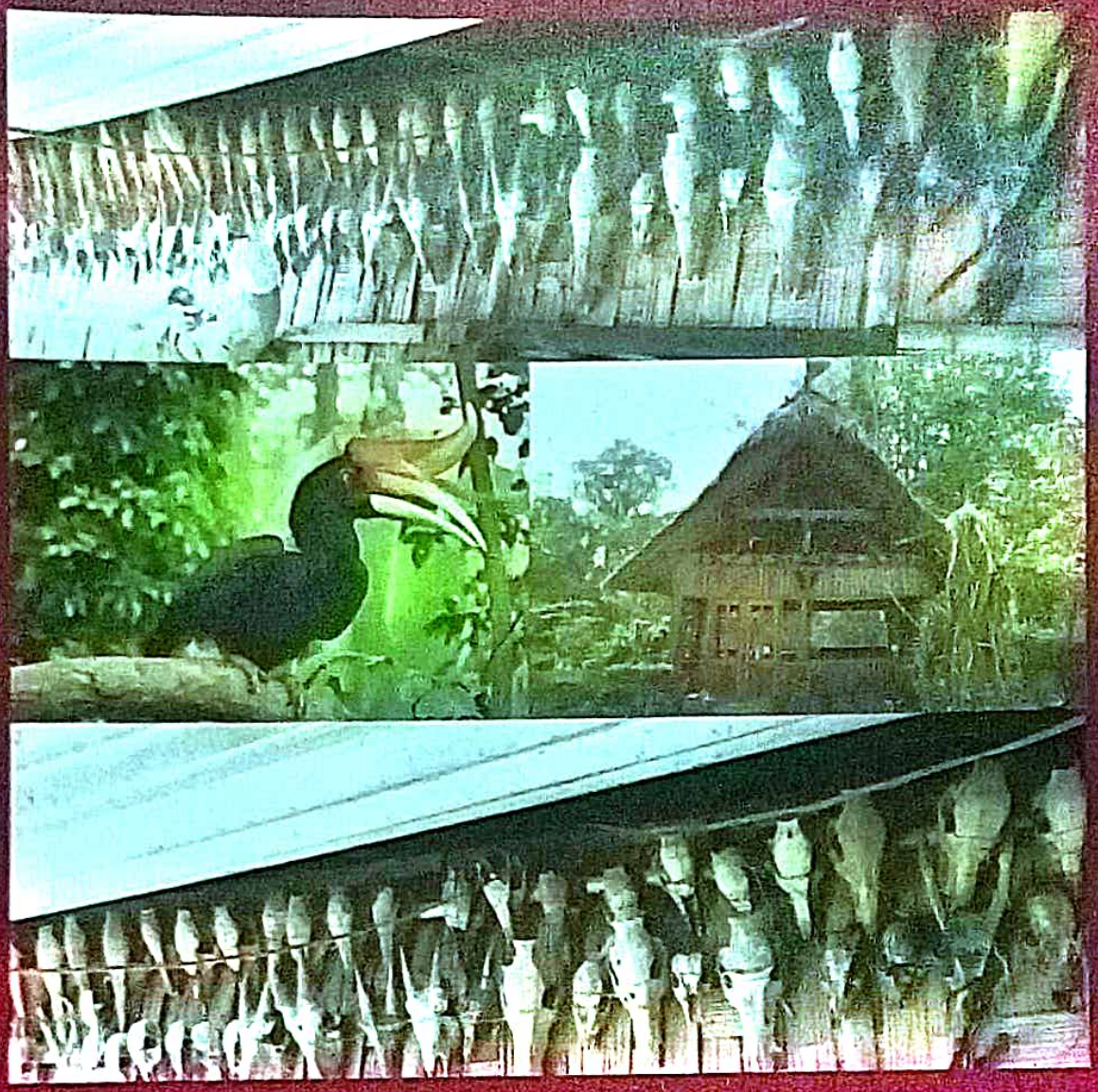

Author

Charengna Widinibou

Editors

Bipasha Patgiri

Amalesh Gope

Centre for Endangered Languages

Tezpur University

LIANGKHUN KETIBU KHUANG: *A Learner's Book of the Liangmai Language* Produced by the Centre for Endangered Languages, Tezpur University

© Tezpur University

First Published: September 2017

Published by:
Registrar
Tezpur University
Tezpur, Assam

Price Rs. 150/-

ISBN: 978-81-935387-9-1

Printed in India at
Bhabani Offset & Imaging Systems Pvt. Ltd.
7 Lachit Lane, Rajgarah Road, Guwahati-781007

CONTENTS

Introduction 1

1 Literature and Theory 5

1.1 Introduction 5

1.2 Theory 11

1.3 Classification of Data Structures 17

1.4 Trees 25

2 Types of Trees 34

2.0 Introduction 34

2.1 Binary 42

2.2 Traversing 46

2.3 Applications 58

2.4 Trees 71

2.5 Algorithms 82

2.6 Implementation 97

3 Searching 104

3.0 Introduction 104

3.1 Trees 108

3.1.1 Binary Trees 108

3.1.2 Red Trees 115

3.1.3 Search Trees 126

3.2 Types of Searching 136

3.2.1 Sequential Searching 136

3.2.2 Binary Searching 145

3.2.3 Interpolation Searching 157

3.2.4 Hashing 177

3.3 Efficiency of Searching 190

3.3.1 Complexity 196

3.3.2 Comparisons 208

3.3.3 Searching 221

3.4 Trees (Trees) 240

4 Basic Conversation --- 31
5 Basic Vocabulary --- 38
6 Folklore --- 50
Short Stories --- 60
Folk song, Lullabies --- 65
Proverbs --- 66
7 The Liangmai Community --- 69
7.1 Migration --- 70
7.2 Alternative names --- 72
7.3 Official status of Liangmai --- 73
7.4 Myth of Liangmai --- 73
7.5 Endangerment level --- 74
7.6 Social and cultural life --- 74
7.7 Traditional attire --- 74
7.8 Food habit --- 75
7.9 Livelihood --- 75
7.10 Religion --- 75
7.11 Youth dormitory --- 76
7.12 Khangchiu --- 77
7.13 Liuchiu --- 77
7.14 Taboo --- 78
7.15 Festival --- 79
7.16 Chaga ngee --- 80
7.17 Miukeng kibo --- 82
7.18 Kariudungbo --- 82
7.19 Karinggen gibo --- 83
7.20 Tadiabo (Period of mourning) --- 83
7.21 Duangtipbo --- 84

Pictorial wordlist
Liangmai Language Consultants
References

INTRODUCTION

A Learner's Book of the Liangmai Language is aimed primarily at absolute beginners who want to learn how to speak Liangmai and at native speakers who have some knowledge of the language without much formal training. The book is designed as an accessible vocabulary and reference grammar of Liangmai. *A Learner's Book of the Liangmai Language* is a thorough collection of the greetings, sounds, word classes, sentences, folktales, folk songs, stories, proverbs and lullabies. Additionally, it includes a range of comprehensive basic conversations which may help the learners to practice their lessons and researchers to understand the structure of the language. It also contains a pictorial glossary of indigenous terms of the Liangmai community.

A Learner's Book is also a modest attempt to illustrate Liangmai oral literature to the younger generation of the community, interested readers and researchers. With this endeavour, revitalization of the rich traditions of Liangmai language, literature and culture has been aspired for. Apart from learning how to speak the language, the younger generation of the Liangmai community will be acquainted with their own linguistic and cultural heritage through *A Learner's Book of the Liangmai Language.* The book describes the Liangmai variety spoken in Nagaland (especially Ntu village and Tening sub-division of Peren district) which is enormously different from the variety spoken in Manipur. Liangmai (ISO 639-3: njn), belongs to the Tibeto-Burman branch of the larger Sino-Tibetan language family and is spoken in Manipur and Nagaland in the North Eastern region of India. It is an endangered language with a rich but undocumented oral tradition. The language does not have its own script and hence, has been using the Roman script for all its purposes. We hope that our efforts will be well-received by the Liangmai community and the society at large. We would gladly appreciate comments from all sections of the community to enhance the content in future editions of *A Learner's of Book of the Liangmai Language.*

ONAEME LEIH DANGDO LAIREIBOUNG

A Learner's Book of the Onaeme Language

Authors

Niharika Dutta

Bobita Sarangthem

Editor

Gautam K. Borah

Centre for endangered languages

Tezpur university

Onaeme Leih Dangdo Laireiboung: A *Learner's Book of the Onaeme Language.* Produced by the Centre for Endangered Languages, Tezpur University.

©Tezpur University

First Published: September, 2017

Published by:
Registrar
Tezpur University
Tezpur, Assam

Price: ₹150/-

ISBN: 978-81-935387-7-7

Printed in India at
Bhabani Offset & Imaging Systems Pvt. Ltd.
7 Lachit Lane, Rajgarh Road, Guwahati-781007

Contents

INTRODUCTION 1

1 THE SOUND SYSTEM 4

1.1 The Consonants 4

1.2 The Vowels 8

2 THE WORD CLASSES 11

2.1 Nouns 11

2.1.1 Count Nouns 11

2.1.2 Mass Nouns 11

2.1.3 Proper Nouns 12

2.1.4 Abstract Nouns 12

2.1.5 Compound Nouns 13

2.1.6 Borrowed Nouns 13

2.1.7 Gender 14

2.2 Pronouns 15

2.2.1 Personal Pronouns 15

2.2.2 Possessive Pronouns 16

2.2.3 Interrogative Pronouns 16

2.2.4 Demonstrative Pronouns 17

2.3 Verbs 17

2.3.1 Stative Verbs 17

2.3.2 Dynamic Verbs 17
2.4 Postpositions 18
2.5 Adjectives 18
2.5.1 Qualitative Adjectives 19
2.5.2 Quantitive Adjectives 19
2.6 Adverbs 20
2.6.1 Adverbs of Place 20
2.6.2 Adverbs of Time 20
2.6.3 Adverbs of Frequency 21
2.7 Connectives 22
3 SENTENCES 23
3.1 Declarative Sentences 23
3.2 Interrogative Sentences 24
3.3 Negative Sentences 25
3.4 Imperative Sentences 26
4 BASIC CONVERSATION 27
5 FOLKLORE 34
5.1 The Story of the Origin of Onaeme 34
5.2 The Story of Pou Rini 38
5.3 Tiilu Nga (Paddy Transplantation) 42
5.4 The Sun, Moon, and the Rooster 44
5.5 Proverbs 48
6 THE OINAM PEOPLE 49
6.1 Introduction 49
6.2 Migration 49
6.3 Marriage and Death 50
6.4 Pottery 50
6.5 Social and Economic Life 51
PICTURES 52
WORD LIST 59
PHOTOS OF LANGUAGE CONSULTANTS 77
FIELDWORK PICTURES 81

INTRODUCTION

The reader is a collection of folktales, folksongs, proverbs, words, and some basic sentences of Onaeme. Onaeme is a Tibeto-Burman language, spoken by a small community of around 4000 speakers. Although the language is considered unclassified, the data and their ethnic identity show that it is rather closely related to the Poumai Naga group of the Tibeto-Burman family. This book is an attempt to preserve the richness of this endangered language mainly through documentation and archiving of the language as spoken at the present time. The book is bilingual in nature where we have used English as the medium of writing the description. The International Phonetic Alphabet (IPA) is used in Chapter 1 to show a correspondence between the Roman script used for writing the language and its sound system.

Demographic Overview

Oinam, one of the Poumai Naga villages, is situated 88.4 km away from the district headquarters of Senapati. The distance between Imphal and Oinam is 168.4 kms. As per the 2011 Census, Oinam has a total population of 4,328. It is worth mentioing here that Poumai Nagas as a tribe live in about 100 villages and their present poplulation is 1,27,000 (according to the 2011 Census). Because of the pressure of an increasing population on land, many villagers had migrated and established new villages. Some of these are: Ngamju, Tingsong, Sorbung, and Taphou Oinam.

Biate Ṭong Riseina Bu

A Learner's Book of the Biate Language

Authors
Daimalu Brahma
Raju Ram Boro
Editor
Monali Longmailai

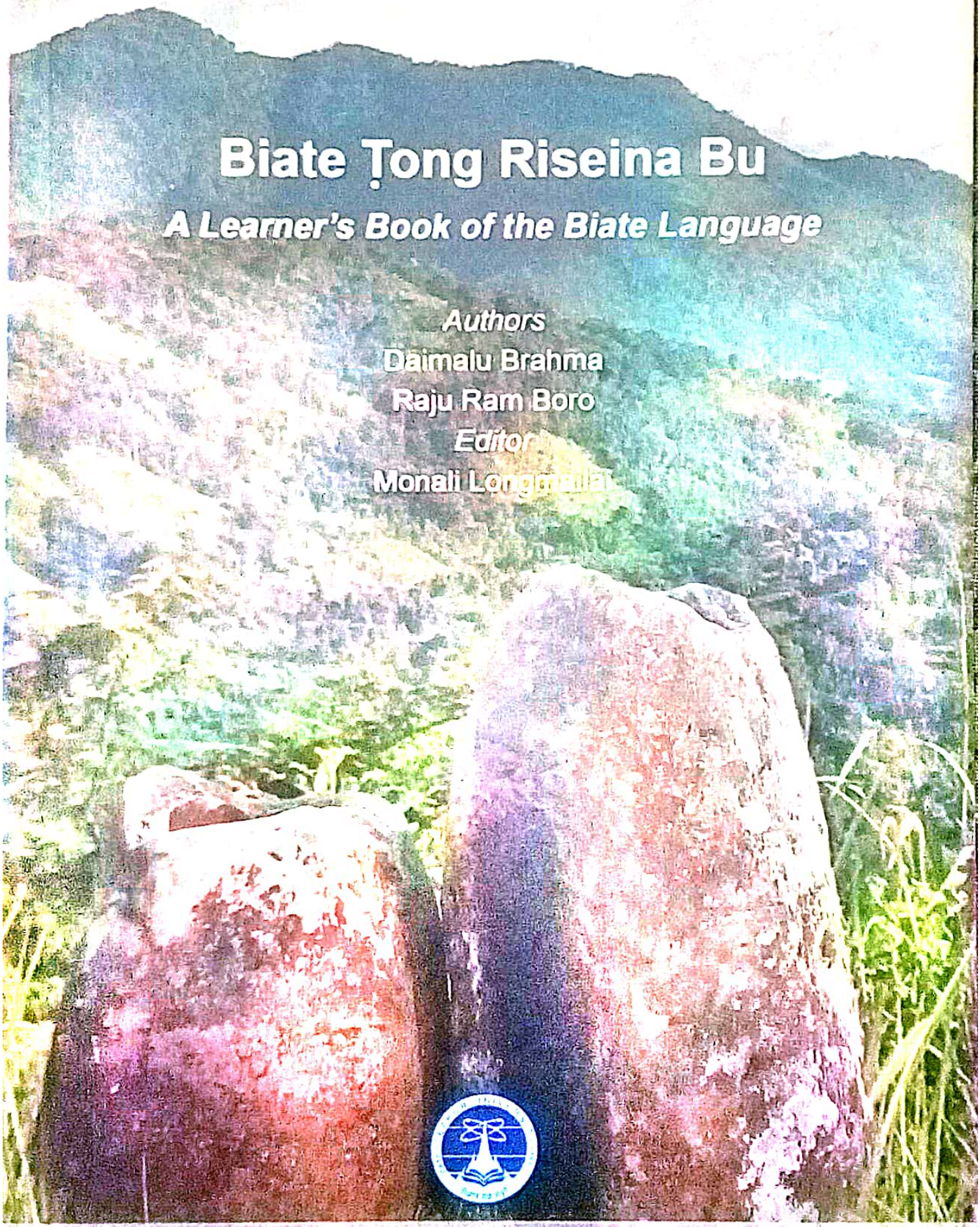

Centre for Endangered Languages
Tezpur University

Biate Ṭong Riseina Bu: *A Learner's Book of the Biate Language.* Produced by the Centre for Endangered Languages, Tezpur University.

© Tezpur University

First Published: September 2017

Photograph Courtesy: *Authors & Editor*

Published by:
Registrar
Tezpur University
Tezpur, Assam

Price. ₹150/-

ISBN: 978-81-935387-4-6

Printed in India at
Bhabani Offset & Imaging Systems Pvt. Ltd.
7 Lachit Lane, Rajgarh Road, Guwahati-781007

CONTENTS

Abbreviations..... x
List of Figures..... x
Introduction..... 1
1. Consonants and Vowels in Biate..... 7
1.1 Consonants..... 7
1.2 Vowels..... 11
1.3. Diphthongs..... 12

2. Parts of Speech..... 13
2.1 Nouns..... 13
2.1.1 Proper Nouns..... 13
2.1.2 Common Nouns..... 13
2.1.3 Count Nouns..... 13
2.1.4 Mass Nouns..... 13
2.1.5 Borrowed Nouns..... 14
2.1.6 Singular and Non-singular Nouns..... 14
2.2 Pronouns..... 14
2.2.1 Personal Pronouns..... 14
2.2.1.1 Free Forms..... 15
2.2.1.2 Proclitic Forms..... 15
2.2.1.3 Enclitic Forms..... 15
2.2.2 Interrogative Pronouns..... 15
2.2.3 Demonstrative Pronouns..... 16
2.3 Adjectives..... 16
2.3.1 Types of Adjectives..... 16
2.4 Verbs..... 18
2.5 Adverbs..... 20
2.5.1 Manner Adverbs..... 20
2.5.2 Temporal Adverbs..... 21
2.6 Postpositions..... 22

3. Sentences and Basic Conversations..... 23
3.1 Declarative Sentences..... 23
3.2 Affirmative Sentences..... 23

3.3 Negative Sentences..... 24
3.4 Interrogative Sentences..... 24
3.5 Imperative Sentences..... 25
3.6 Basic Conversations..... 25

4. Pictorial Wordlist..... 29
4.1 Traditional Items..... 29
4.2 Vegetables and Herbs..... 32

5. Word Vocabulary..... 36
5.1 Universe..... 36
5.2 Names of Trees, Plants and Grass..... 38
5.3 Names of Fruits, Vegetables and their related words..... 40
5.4 Names of Animals..... 43
5.5 Names of Birds..... 45
5.6 Names of Fish..... 46
5.7 Names of Insects..... 47
5.8 Body Parts..... 48
5.9 Kinship Terms..... 52
5.10 Profession and Occupation..... 60
5.11 Ailment and Body Conditions..... 61
5.12 Religious and Ritual Terms..... 63
5.13 Traditional Dress and Ornaments..... 64
5.14 Food Items and Curry..... 66
5.15 Utensils and House Articles..... 69
5.16 Cardinal Numerals..... 71
5.17 Ordinal Numerals..... 73

6. Proverbs, Narratives and Folk Songs..... 75
6.1 Proverbs..... 75
6.2 Narratives..... 76
6.2.1 Umai Ka Fangma Zong (Two Sisters Searching for Cucumber)..... 76
6.2.2 Biate Riphutna (The Origin of Biate)..... 79
6.2.3 Mairingthanga Phung (The Story of Mairingthanga)..... 80

6.2.4 Imeng Neh Sakei Thurchi (The Story of a Cat and a Tiger)..... 81
6.3 Folk Songs..... 82
6.3.1 Pipu La (Lit: Grandfather's song 'An Ode to Ancestors')..... 82
6.3.2 Ram Thlang La (An Ode to Nature)..... 83
6.3.3 Bu Koi La (Harvest Song)..... 83
6.3.4 Rung RungVatenu (Lullaby)..... 84

7. Ethnographic Information of Biate..... 85
7.1 The Community..... 85
7.2 Origin and History..... 85
7.3 Demography..... 86
7.4 Status of Biate..... 87
7.5 Culture and Tradition..... 87
7.6 Nulding Kut Festival..... 87
7.7 Life and Economy..... 88
References..... 89
Metadata of Informants..... 90

INTRODUCTION

According to G. A. Grierson (1904), the Biate (BĒTĒ) language belongs to the Kuki-Chin group of the Sino-Tibetan language family. UNESCO report shows that the Biate is a *Definitely Endangered Language* in North-Eastern India. There is very little or no information of previous research on the Biate language, though there have been literary contributions on history, origin, culture, religion and language by community members. Special mention can be made of Ramdina Lalsim, Ezra Lalsim, Remsiama Ngamlai, Rev. L. Thiate, among a handful of others. Recent linguists have shown an interest in the comparative study of Kuki-Chin languages, including Biate, and scholars are emerging from the Biate community in documenting the language. The Centre for Endangered Languages, Tezpur University, also has initiated the documentation of Biate, which will lead to compilation of sketch grammar and an outline dictionary. The Centre, therefore, decided to conduct a pilot fieldwork in the Dima Hasao (formerly North Cachar Hills) district of Assam.

The Biate speakers live mainly in the **Haflong** area in the Dima Hasao (N C Hills) district. Dima Hasao is one of the twin hill districts of Assam. Haflong is the only hill station of Assam, also known by the local people as 'Switzerland of the East' and 'Second Shillong'. The district has the highest mountain peak of Assam, Mt Thumjang (1866 metres high) located near Mahur and the second highest Mt Hempeupet (1748 metres high) near the Leikul village. The fieldwork was conducted in **Fiangpui** (locality of Biate Speakers) in Haflong and adjacent villages of Biate speakers. Fiangpui and Haflong are surrounded by the Barail mountain range, a portion of the greater Himalayan mountain belt. The Biate people at Fiangpui comprise nearly 300 households, at present, according to the former Gaonburah of the village. However, other speakers of Biate believe that they will be 2000 approximately in Fiangpui and the surrounding Haflong town, due to new migration and settlement of the Biates from other villages within the Dima Hasao district to the Fiangpui village for its easy access to the Haflong town, the headquarters of the said district. Biate people are said to be peace loving and they have been living

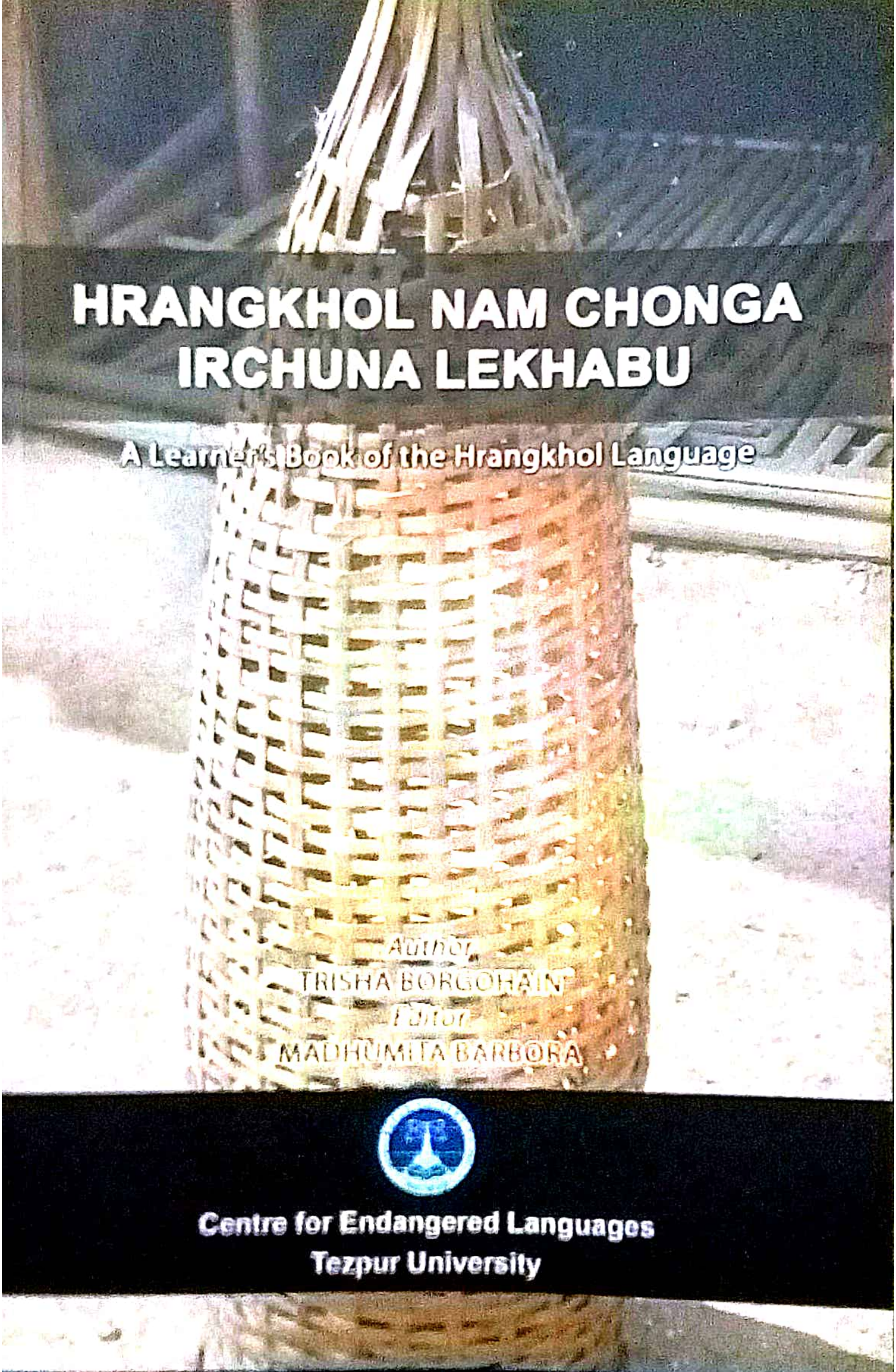

HRANGKHOL NAM CHONGA IRCHUNA LEKHABU

A Learner's Book of the Hrangkhol Language

Author

TRISHA BORGOHAIN

Tutor

MADHUMITA BARBORA

Centre for Endangered Languages

Tezpur University

Hrangkhol Nam Chonga Irchuna Lekhabu: *A Learner's Book of the Hrangkhol Language*. Produced by the Centre for Endangered Languages, Tezpur University.

© Tezpur University

First Published: September 2017

Published by:
Registrar
Tezpur University
Tezpur, Assam

Price. ₹ 150/-

ISBN: 978-81-935387-6-0

Printed in India at
Bhabani Offset & Imaging Systems Pvt. Ltd.
7 Lachit Lane, Rajgarh Road, Guwahati-781007

Table of Contents

Introduction -- 1
1. Hrangkhol Sounds -- 5
2. Hrangkhol Word Classes
   - 2.1 Noun -- 10
   - 2.2 Pronoun -- 14
   - 2.3 Adjective -- 16
   - 2.4 Verb -- 18
   - 2.5 Adverb -- 19
   - 2.6 Postposition -- 20
   - 2.7 Conjunction -- 20
3. Sentence patterns in Hrangkhol -- 21
4. Basic Conversation -- 24
5. Folklore
   - 5.1 Folk Tales
     - 1. Ralngam -- 30
     - 2. Pangam and Suiting -- 46
   - 5.2 Rhymes
     - 1. Rite Rite Ei Vok -- 60
     - 2. Um Um Umin Zola -- 60
     - 3. Tutu Lu Um Mekoite -- 61
   - 5.3 Folk Song
     - 1. Dongheai Kan Ram Tang -- 61
     - 2. A Nu Kha Bukul Chuan A Fe -- 62
   - 5.4 Proverbs -- 64
6. Ethnolinguistic Information of the Hrangkhol Community
   - 6.1 Migration and History -- 65
   - 6.2 Religion -- 66
   - 6.3 Family Structure -- 66
   - 6.4 Right of Inheritance -- 66
   - 6.5 Birth Rituals -- 67
   - 6.6 Marriage -- 67
   - 6.7 Divorce -- 68
   - 6.8 Death Rituals -- 68
   - 6.9 Dress Patterns -- 69
   - 6.10 Village Administration -- 69
   - 6.11 Traditional Festivals -- 70
7. Pictorial Wordlist -- 72
8. Basic Word list -- 77

Photos of Language Consultants -- 89
Field Work Photos -- 91
References -- 94

INTRODUCTION

The publication of the book *Hrangkhol Nam Chonga Irchuna Lekha* is an endeavour undertaken by the Centre for Endangered Languages, Tezpur University. This book is the result of two rigorous field works carried out in Haflong of the Dima Hasao district in Assam, India. This book includes the sound system of Hrangkhol, basic sentences, parts of speech, folk tales, folk songs, lullabies, proverbs, ethnolinguistic information about the community and a word list covering the basic domains.

Hrangkhol is a Tibeto-Burman language, spoken in parts of Assam and Tripura. The language shares a close affinity with the Kukish languages. The degree of mutual intelligibility between the Kuki languages, namely, Hmar, Biate, Purum, Khelma, Mizo, etc., and Hrangkhol has been observed to be rather high. The language has been marked as '*Vulnerable*' according to the UNESCO Endangerment Index. The total population of the Hrangkhol community has been estimated at 18,700 according to Ethnologue sources (2000). As the language does not have a script of its own, the Roman script has been adopted in the recent times to document the language.

The work for bringing out this book started after our first visit to Haflong during the month of February, 2017. The first help that we received then was from Mr. Ron Kemprai who introduced us to our much valuable informants. Since then, we have been in constant contact with our informants, Mr. Bulthoikhup (Dumkar) Hrangkhol, Mr. Roilalbul (Phoitong) Hrangkhol, and Mr. Lalphirthoi (Dumkar) Hrangkhol for the analysis of the data collected during the two field trips to Haflong, Dima Hasao, Assam. The second field trip was conducted during the month of August, 2017.

KHELMA CHONG ANCHUNA LEKHABU

A Learner's Book of the Khelma Language

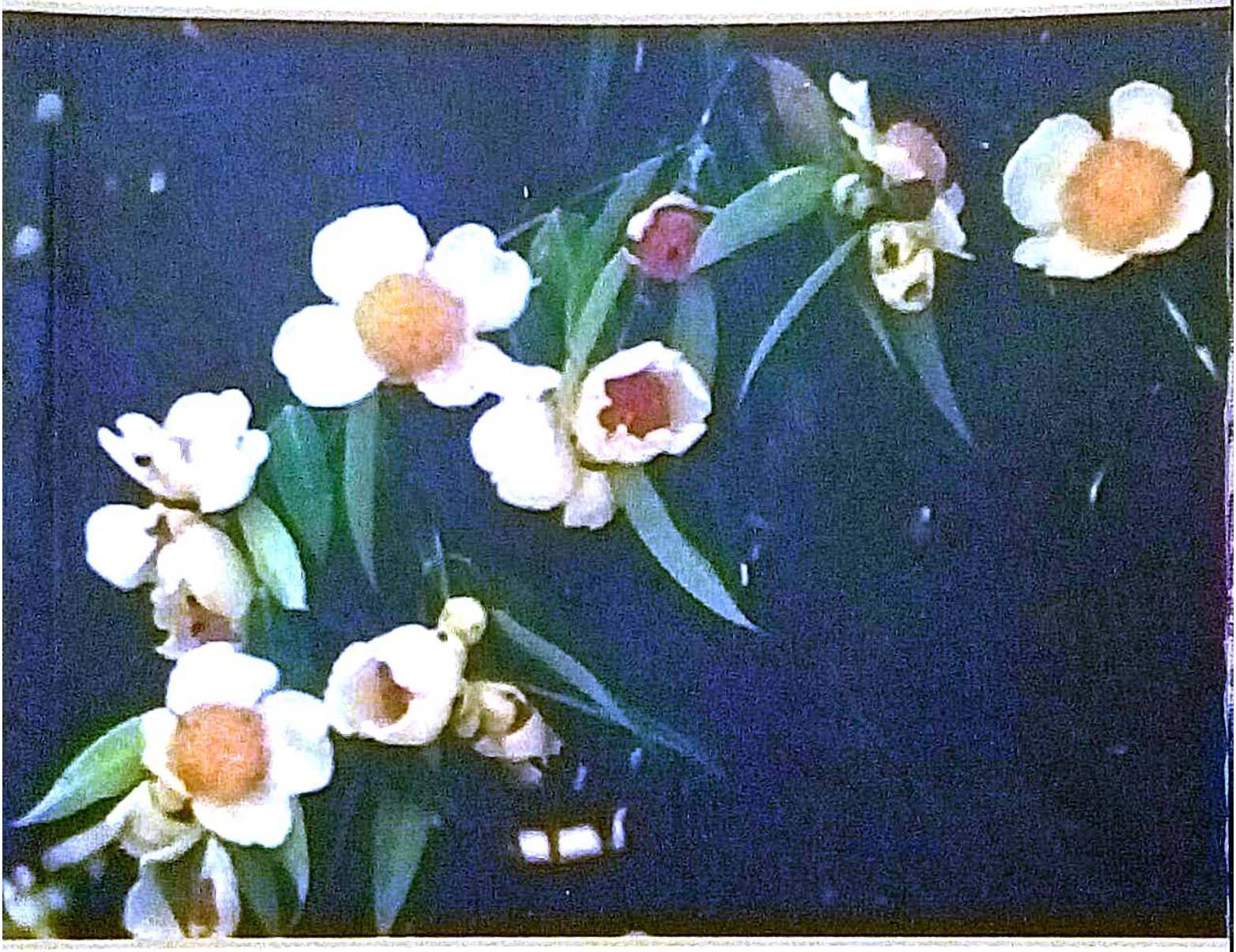

Authors

Pushpa Renu Bhattacharyya

Barshapriya Dutta

Editor

Arup Kumar Nath

Centre for Endangered Languages

Tezpur University

KHELMA CHONG ANCHUNA LEKHABU: *A Learner's Book of the Khelma Language* prepared by the Centre for Endangered Languages, Tezpur University Assam.

The cover page shows the *Kerseidon* (mesua-ferrea) used by the Khelmas in *Paarsem kut*.

© Tezpur University

First Published: September 2017

Published by:
Registrar
Tezpur University
Tezpur, Assam

Price. ₹150/-

ISBN: 978-81-935387-5-3

Printed in India at
Bhabani Offset & Imaging Systems Pvt. Ltd.
7 Lachit Lane, Rajgarh Road, Guwahati-781007

Contents

Page

Introduction 1

1 Latin sounds 3
1.1 Introduction 3
1.1.1 Vowel sounds 4
1.1.1.1 Vowel sounds in Latin words with visual illustrations 5
1.1.2 Consonants 6
1.1.2.1 Consonant sounds in Latin words with visual illustrations 7

2 Latin word classes 9
2.1 Nouns 9
2.1.1 Common nouns 9
2.1.2 Proper nouns 9
2.1.3 Pronouns 9
2.1.3.1 Personal pronouns 9
2.1.3.2 Demonstrative pronouns 10–11
2.1.3.3 Relative pronouns 11
2.1.3.4 Interrogative pronouns 11
2.1.3.5 Indefinite pronouns 11–12
2.2 Adjectives 12
2.3 Verbs 12

2.4 Adverbs 13-14
2.5 Postpositions 14

3. Khelma basic sentences 15-18
3.1 Declarative sentences 15
3.2 Affirmative sentences 15
3.3 Negative sentences 16-17
3.4 Interrogative sentences 17
3.5 Imperative sentences 18

4. Basic Conversations 19-25

5. Folklore 26-47
5.1 Lullaby 26-27
5.2 Folkongs 27-29
5.3 Proverbs 29-31
5.4 Folktales 31-40
5.5 The three main rituals of Khelmas 40-47
5.5.1 Birth ritual 40-42
5.5.2 Marriage ritual 42-45
5.5.3 Death ritual 45-47

6. Ethnographic Description of the Khelmas 48-60
6.1 Introduction 48
6.2 History 48-49
6.3 Clan 49
6.4 Geographical distribution of the area and Demographic description of the Khelmas 49-51
6.5 Education 52
6.6 Economy 52
6.7 Handloom and handicraft 52-54
6.8 Housing 54
6.9 Religion 54-56
6.10 Festivals 56
6.11 Games and sports 56-57
6.12 Customs and traditions 57

6.13 Village administration 57-58
6.14 Food habits 58
6.15 Language, script and literature 58-60
6.15.1 Number 60
6.15.2 Gender 60
6.16 Endngerment level 60

7. Basic wordlist 61-74

Pictorial wordlist 75-86
Language consultants 87-88

INTRODUCTION

The Khelma, also known as Sakachep is a lesser-known community inhabiting in some parts of Assam, Nagaland, Mizoram and Tripura. The language of the Khelmas is known by the same ethnic name Khelma (Sakachep), which is an unclassified language. Khelma is an undocumented language and in an endangered stage. Khelma speakers talk in their language at home domains only.

So far, no anthropological or linguistic research of the Khelmas has been documented. As a result, the name *Khelma* is not very familiar to most of the people. It must be mentioned that except Dima Hasao, the Khelmas are known as Sakachep in other districts of Assam and neighbouring states like Mizoram, Tripura and Nagaland.

The book is an outcome of the collected information gathered from the native speakers during four fieldtrips to ten Khelma villages that comes under the Umrangso circle under the New Sangbar block, Dima Hasao district of Assam. The fieldtrips were conducted by the Research Associate and Field Assitant of CFEL, Tezpur University.

Demographic information

The Dima Hasao district is one of the hilliest and undulated districts of Assam. The Dima Hasao district has common boundaries with three North-Eastern States and three other districts of Assam. On its eastern side are the states of Nagaland and Manipur. On its south the Cachar districts of Assam. On the western side is the state of Meghalaya. On its north are Nagaon and Karbi Anglong districts of Assam.

The field work was carried out in different phases. The initial exploratory visit to the Khelma villages and the bulk of the data collection, took place during four separate time periods: the first being

Purum Chong Kinchung Zedetrubu

A Learner's Book of the Purum Language

Author
Elangbam Manimohon Meitei
Editor
Dhanapati Shougrakpam

Centre For Endangered Languages
Tezpur University

Purum Chong Kinchuna Zedetrubu: *A Learner's Book of the Purum Language.* Produced by the Centre for Endangered Languages, Tezpur University.

© Tezpur University

First Published: September 2017

Published by:
Registrar
Tezpur University
Tezpur, Assam

Price. ₹ 150/-

ISBN: 978-81-935387-8-4

Printed in India at
Bhabani Offset & Imaging Systems Pvt. Ltd.
7 Lachit Lane, Rajgarh Road, Guwahati-781007

Contents

1. Introduction..... 1

2. Purum Sound System..... 4

3. Parts of Speech..... 12

4. Basic conversation in Purum 22

5. Sentences in Purum..... 29

6. Folk Tales 34

7. Folk songs 38

8. Proverbs 46

9. Ethnolinguistic Account of the Purum community 47

Word list of Purum..... 52

Pictorial word list 81

Informants' Photos..... 92

References 94

1 INTRODUCTION

The book is a comprehensive introduction to the Purum language. It is intended to serve as a Reader or must have for any beginner in Purum. This fruitful integration of scholarly overview and practical application provides a reader that is more than a simple grammar or an introduction to the language. It is written in a style designed for beginners and the book avoids technical language and strives for a reader-friendly inductive approach.

The Purum Reader is a product of the research work carried out at the Centre for Endangered languages (CFEL), Tezpur University. It describes the sound system with pictorial illustrations, parts of speech, basic conversation, sentences, folk tales, folk songs and proverbs of the community; brief overview of the ethnolinguistic account of the community; word list of basic vocabulary; and pictorial wordlist of indigenous items of the community.

The present field work is carried out at Purum Likli village, under Saikul sub-division of Kangpokpi District. There are only two Purum villages found in Manipur- Purum Likli and Purum Khullen. The population of Purums according to the Manipur Census 2011 is 2728. The Purum Likli village is located about 38 kms away from Imphal. It is located on a narrow plain between the Iril river and a small hillock that lies in Saikul sub-division. The Iril river which lies on the eastern side of the village flows from the north to southward direction marking the eastern boundary of the village. The Imphal Saikul road marks the western boundary. The northern boundary is marked by Purum Kokpak, a Nepali village while the southern boundary is marked by Litanpokpi, a Meetei village. The serene beauty of the village is a captivating sight for onlookers.

DYF Selected Papers

Studies on Dimasa

History, Language and Culture

Volume 2

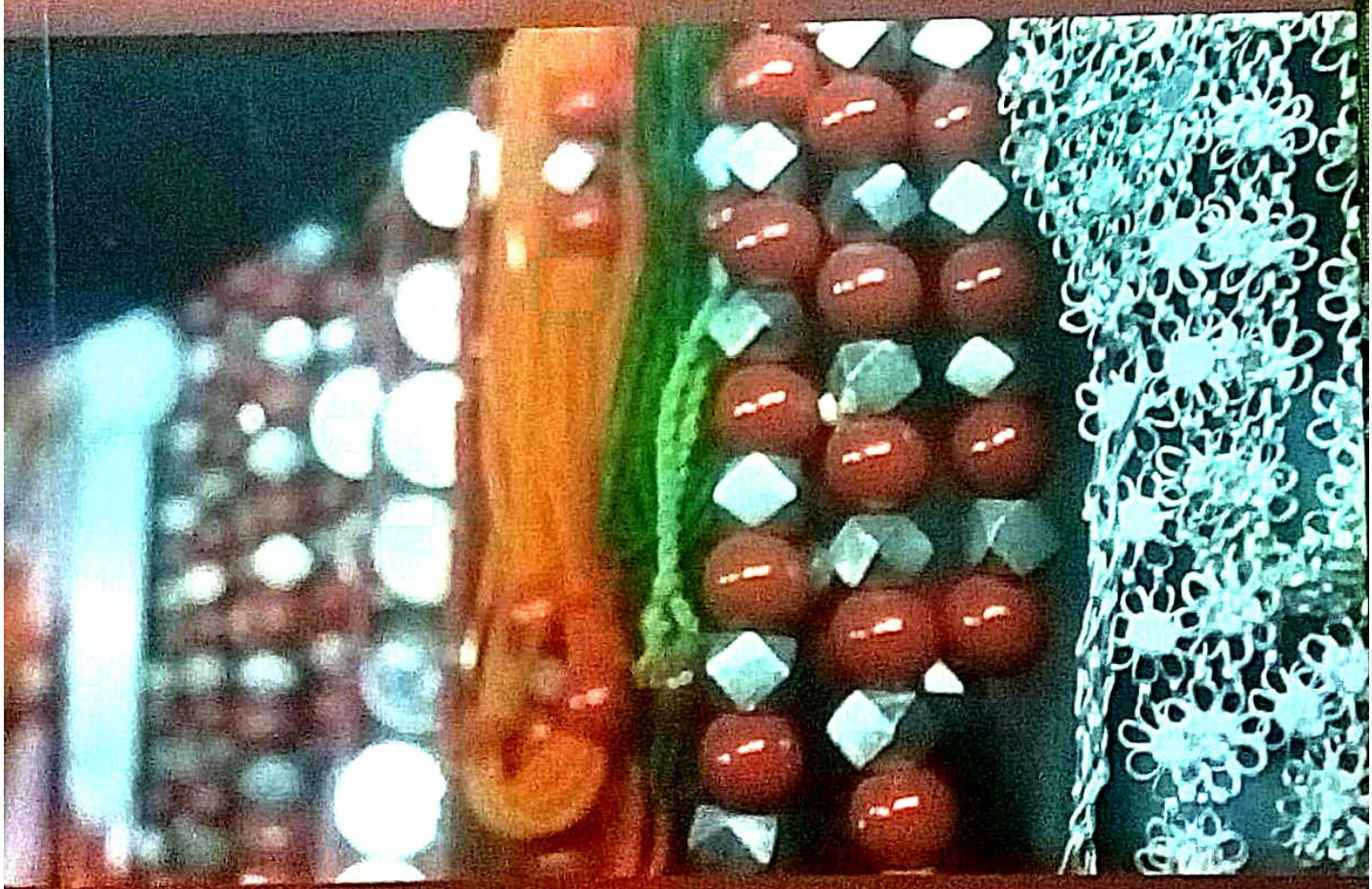

Edited by
Monali Longmailai

Copyright © author

All rights reserved. No part of this publication may be reproduced, stored in a retrieval system, or transmitted, in any form or by any means, electronic, mechanical, photocopying, recording or otherwise, without the prior permission of the copyright owner and the publishers.

The view expressed in this book are those of the authors not necessarily that of the publisher. The publisher is not responsible for the views of the authors and the authenticity of the data, in any way whatsoever.

First Published 2019

DVS PUBLISHERS
H. B. Road, Panbazar, Guwahati - 781 001
Phone : 2638295, 2730057
Fax : 0361-2511789
e-mail : dvspub@gmail.com, dvspublisher@gmail.com
website : www.dvspublishers.com

Cover Design : Chandan Das
Cover Photos : Dimasa traditional ornaments & Stone House at Maibang
Photograph Courtesy : Monali Longmailai

Type setting : Pankaj Saikia

ISBN: 978-93-85839-32-0

Printed at : Bhabani Offset Private Limited.

CONTENTS

i. Foreword : *Partha Sarathi Misra* v

ii. Acknowledgements viii

iii. Introduction ix

iv. Detail of Contributors xiii

History: Evidences from Archaeology, Sedimentology and Religion

1. Exquisite Monolithic Monuments of Dimasas 1
Alok Tripathi and Shring Dao Langthasa

2. The Migration of the Dimāsās in North East India 11
Raktim Ranjan Saikia and Nurul Amin

3. Hinduization of the Genealogy of Dimasa Kachari Rulers: an Appraisal 20
Chiranjeev Nunisa

Language and Linguistics: Sounds, Words and Syntax to Ethnolinguistics

4. Dimasa Generative Phonology and Phonological Rules 31
Partha Sarathi Misra

5. Nonverbal Predicate Clause in Dimasa and Bodo 45
Jelina Moshahary and Madhumita Barbora

6. Spread and Contact Situation of Dimasa 66
Monali Longmailai

7. Cultural Metaphor in Dimasa and Meitei- an Ethnolinguistic Aspect 86
Monali Longmailai and Bobita Sarangthem

Cultural Metaphor in Dimasa and Meitei-an Ethnolinguistic Aspect

Monali Longmailai and Bobita Sarangthem

1. Introduction

Dimasa and Meitei are neighbouring Tibeto-Burman speech communities from north-east India. Both the communities have had cultural and political ties from the mediaeval period, including the matrimonial alliances between the two royalties during 17th-18th centuries (Hasnu 2017: 47). Sarangthem and Longmailai (2017) also observed the shared cultural elements, especially taboo words, present in Dimasa and Meitei. This paper makes another attempt to study the ethnolinguistic aspects present in these two languages, with the help of folkloristics. Ethnolinguistics studies the relation between language and culture and how different cultures conceptualize the world with language in use, while folkloristics deals with studies entirely on folklore. The reading of culture and folklore bring out at least a transmission of culture, a common cultural history of mankind and a possible contact in the past. Nevertheless, there are cultural specifics and hard forms of culture and folklore. George and Trimbur (2007: 3), mention that, "Culture means all the familiar pursuits and pleasures that shape people's identities and that enable and constrain what they do and what they might become". Folklore, on the other hand, expresses the

DYF Selected Papers

Studies on DIMASA

History, Language and Culture

Volume 1

Edited by
Monali Longmailai

Copyright © editor

All rights reserved. No part of this publication may be reproduced, stored in a retrieval system, or transmitted, in any form or by any means, electronic, mechanical, photocopying, recording or otherwise, without the prior permission of the copyright owner and the publishers.

The view expressed in this book are those of the authors not necessarily that of the publisher. The publisher is not responsible for the views of the authors and the authenticity of the data, in any way whatsoever.

First Published 2017

DVS PUBLISHERS

H. B. Road, Panbazar, Guwahati - 781 001, Assam, India
Phone : 2638295, 2730057

WZ-33, Lane No.2, Shiv Nagar, New Delhi - 110058, India

e-mail : dvspub@gmail.com, dvspublisher@gmail.com
website : www.dvspublishers.com

Cover Design & Photo editing : Chandan Das
Cover photos : Dimasa handloom & musical instruments 'khram' (drum) and 'muri' (pipe)
Photograph courtesy : Monali Longmailai
Type setting : Pankaj Saikia

ISBN: 978-93-85839-08-5

Printed at : Bhabani Offset Private Limited.

Contents

i. Foreword v

ii. Acknowledgements vii

iii. Introduction viii

iii. Detail of Contributors ix

History: Genesis and Myths to Colonial Records

1. A Review on N.K. Barman's "The Queens of Cachar or Herambo and The History of the Kachchhari"
Ruthi Lallawmkim Thanglet 1

2. The Kamarupa State as They Remember: Interpreting Dimasa Social Memory
Uttam Bathari 16

3. Colonial Archives and the Representations of Pre-colonial Dimasa Pasts
Santosh Hasnu 41

Language and Literature: Origin, Folkloristics and Linguistics

4. Engendering the Origin of the Dimasas: Cosmos, Body and Gender in the narratives of the Dimasas
Vandana Thousen 56

5. Language, Identity and Origin of Dimasa
Monali Longmailai 66

6. A Feminist Reading of the Dimasa Folktale of the Story of *Queen Dishru*

Supriya Bodo 86

7. Consonant Clusters in Dimasa

Kh. Dhiren Singha 95

8. A Study on the Verbal Deixis in Bodo and Dimasa

Daimalu Brahma 120

People and Culture: Beliefs, Practices and Cultural Aspects

9. Beliefs and Dreams: A Comparative Narrative between the Seng Khasi and the Dimasa Tribes

Deepshikha Carpenter 131

10. Semkhor Daikho: Outlining the Sacred Groves of Semkhor

Humi Thaosen 145

11. Taboos Prevailing in Conservative Manipuri and Dimasa Societies

Bobita Sarangthem and Monali Longmailai 158

12. Physico-chemical and Biochemical Properties of Judima (Rice Beer)

Ron Kemprai 170

Index 180

Language, Identity and Origin of Dimasa[1]

Monali Longmailai[2]

1. Introduction

Dimasa is racially Indo-Mongoloid (Barpujari 1997:6) and linguistically belongs to the Tibeto-Burman language family, sub-classified under the Bodo-Garo group of languages (Lewis, Simons and Fennig 2016). It is spoken mainly in Assam and Dimapur district in Nagaland in northeast India. Hasao spoken in Dima Hasao in Assam is the standard dialect. Dimasa consists of 110,976 peoples approximately (2001 Census) and the Dimasa language is included in the eighth schedule of the Constitution of India. It is a tonal language, highly agglutinating (several morphemes

[1] I would like to acknowledge Kh Dhiren Singha for his fruitful comments and suggestions for writing this paper. I would also like to express my thanks to Famiebar Gorlosa, Silpi Thaosen and her father, for discussions on Dilaobra Sanggibra, Delina Srongphang in documenting the Rice pounding song, Jaan Kemprai for his data on Dembra dialect, Santosh Hasnu and Uttam Bathari for discussions on Dimasa history, François Jacquesson, late J.K. Thaosen and Spelling and Glossary Committee (Dimasa Sahitya Sabha) for their encouragements towards pursuing research work on Dimasa.

[2] The data provided in the paper are based on the intuition of the author, who is a native speaker of Dimasa.

Taboos Prevailing in Conservative Manipuri and Dimasa Societies

Bobita Sarangthem and Monali Longmailai[1]

1. Introduction

The North East India has often been described as a precious store-house of data for linguistic research. In this small land, four major language families are present with a sizeable number of different speakers. It has been observed that due to close contiguity and social and political cohesion among various language communities over centuries, there have been a lot of linguistic convergence among the various languages. Manipuri and Dimasa have developed certain features which show similarities in their social life.

Manipur is one of the eight sisters in north east India. The State has a population of 2721756 (2011 census report). There are thirty-three recognised scheduled tribes. Interestingly, Manipuri or Meiteilon is the only

---

[1] The authors of the paper are native speakers of Manipuri (Meiteilon) and Dimasa languages. Primary data have been collected on taboo words based on intuition and linguistic knowledge of these speakers.

Springer Link

Introduction to Mechanical Engineering pp 137-178 | Cite as

Basics and Applications of Thermal Engineering

Authors | Authors and affiliations

T. K. Gogoi, U. S. Dixit

Chapter
First Online: 29 April 2018

2k
Downloads

Part of the Materials Forming, Machining and Tribology book series (MFMT)

CERTIFICATE

61st National Convention
of
Indian Institution of Industrial Engineering
&
5th International Conference
on

Industrial Engineering (ICIE 2019)

This is to certify that Dr./Prof./Mr./Ms.

B. Chowdhury

has attended 61st National Convention of Indian Institution of Industrial Engineering
& 5th International Conference on **Industrial Engineering (ICIE 2019)**
Hosted by Indian Institution of Industrial Engineering (IIIE) Surat Chapter,
S. V. National Institute of Technology, Surat, India during December 12-14, 2019
and presented a paper entitled

Application of Design of Experiments in the analysis of Thermoforming Process Parameters that affect Rejection Rate of Thermoformed Refrigerator Liners

Dr. Ravi Kant
Convener

Dr. Tushar N. Desai
Convener

Shri D. V. Bhagat
Chairman, IIIE National Council

v

A comparative investigation of annular fins of different profiles using multi-objective genetic algorithm

Abhijit Deka
Department of Mechanical Engineering
Tezpur University
Napaam, Tezpur - 784 028, India.
Email: adeka13@tezu.ernet.in

Dilip Datta
Department of Mechanical Engineering
Tezpur University
Napaam, Tezpur - 784 028, India.
Email: ddatta@tezu.ernet.in / datta_dilip@rediffmail.com

***Abstract*—The present work carries out a comparative study among various annular fin profiles, namely uniform thickness, variable thickness and step change in thickness. The design of a fin, under one-dimensional heat transfer with constant base temperature and variable thermal conductivity, is formulated as a multi-objective optimization problem for maximizing heat transfer rate and minimizing fin volume as the primary objectives. For further assessment of the fin performances, its efficiency is considered as another objective to be maximized. Evaluating the heat transfer rate by the hybrid spline difference method, a multi-objective genetic algorithm, namely NSGA-II, is employed to arrive at a Pareto front containing a set of trade-off solutions in terms of various combination of the three objective functions. Finally, the Pareto fronts obtained for the considered three fin profiles are compared in order to facilitate a designer to choose a compromise solution for practical use.**

I. Introduction

Performance of a heat exchanger having cylindrical primary surface can be enhanced by using annular fins. An annular fin increases the heat transfer rate as a result of enhanced convective and radiative heat transfer areas. However, the material and fabrication costs associated with a fin increases the overall production cost, thus requiring optimum design of fins to identify the effective configurations that would dissipate maximum amount of heat but use minimum amount of fin material. The simplest design is the conventional uniform thickness fin. Such a fin suffers from the disadvantage that the material near its tip is not fully engaged in heat dissipation, which raises the issues of optimum fin profile of variable thickness (shape optimization) and fin with step change in thickness (size optimization) [1]. Though the practical application of fin profiles of variable thickness is limited due to the complex fabrication processes involved with them; a fin with step change in thickness, which is a modification of the uniform thickness annular fin, not only involves a simple fabrication process, but also dissipates heat making effective utilization of the fin material to certain extend.

978-1-5090-5674-3/17/$31.00 ©2017 IEEE

The rate of heat transfer from a fin and the fin volume are conflicting in nature, causing an optimized solution with respect to one of them unacceptable in terms of the other. A reasonable approach, thus, would be to tackle the fin design as a multi-objective optimization problem for arriving at a set of trade-off solutions. However, to the best knowledge of the authors, no work comparing performances of different optimized annular fin profiles under multi-objective optimization has been reported in the specialized literature. Hence, the present work is taken up to fill up such a gap in literature.

The present work puts forward a complete methodology for multi-objective optimization of various profiles of an annular fin. The fin is optimized with respect to some fin performance related objective functions, in particular the heat transfer rate and fin efficiency are maximized and the fin volume is minimized by tuning the selected design variables. Evaluating the objective values sequentially with the application of the hybrid spline difference method (HSDM) [2], they are optimized simultaneously by employing the nondominated sorting genetic algorithm II (NSGA-II) [3]. The main purpose of this study is to present a comparative analysis of the trade-off optimal scenarios of various fin profiles in terms of some conflicting objective functions, so as to facilitate a designer to arrive at a suitable fin profile and a corresponding compromise solution depending upon the availability and practicability of information and resources.

II. Literature review

Kraus et al. [4] presented a comprehensive study on heat transfer through fins. The optimum dimensions of constant thickness radial fins were evaluated by Brown [5] using Bessel functions. Ullmann and Kalman [6] extended the work of Brown [5] by determining the efficiency along with the optimized dimensions for fins of rectangular, triangular, parabolic and hyperbolic profiles under constant heat transfer coefficient, where the parabolic profile was found outperforming others.

An analytical approach for maximizing the heat transfer rate in fins of constant volume rectangular profile with thermally non-symmetric convective boundary conditions was proposed by Arslanturk [7] considering constant thermal conductivity of the fin material. Another analytical method based on differential transformation was put forward by Yu and Chen [8] for thermal analysis and constant volume optimization of a rectangular profile fin considering variable thermal conductivity and convective heat transfer coefficient. Using the incremental differential quadrature method, Malekzadeh and Rahideh [9] analyzed two-dimensional nonlinear transient heat transfer characteristics of variable section annular fins. Optimization of annular fins with specified geometries can be found in many other works, e.g., in [1], [10]–[15].

Kundu [16] analyzed the performance of a stepped annular fin under fully and partially wet surface conditions, where it was observed that the heat transfer rate per unit volume in a stepped annular fin is more than that in a concentric annular disc fin. The same findings were reported in [17], [18] also.

III. Problem Statement and Formulation

The problem in the present study is an annular fin of various profiles (namely uniform thickness, variable thickness, and step change in thickness) attached to a heat exchanger of cylindrical primary surface. The thickness of the fin is considered to be much smaller than its radius enabling to study it with one-dimensional heat transfer in the radial direction. The heat dissipation from the fin surface takes place through natural convection to the ambient and radiation to the surrounding. Steady-state heat transfer with a constant convective heat transfer coefficient and negligible internal heat generation are other assumptions made in this study. Fig. 1 shows the schematic diagram of annular fins of various profiles, where r is the radial distance with r_b and r_o respectively as its radial values at the inner and outer surfaces of each fin, while r_1 is its radial value at the point of step change in the case of the fin with step change in thickness. Similarly, t represents the cross-sectional half-thickness with t_b as its value at the base of the uniform and variable thickness fins. For variable thickness fin, t_o is the cross-sectional half-thickness at the tip of the fin while t_1 and t_2 respectively as its values at the base and tip of the fin with step change in thickness.

A. Formulation of the heat transfer model

As thermal conductivity k varies linearly with temperature T_i in most of the fin materials, they can be related as in Eq. (1) [2].

$$k = k_a \left\{1 + \beta \left(T_i - T_\infty\right)\right\} \tag{1}$$

In Eq. (1), T_∞ is ambient temperature, k_a is the value of k at T_∞, and β is a parameter that controls the variation in k. Further, $T_i = T$ in uniform and variable thickness fins, while i in T_i indicates the steps in the fin with step change in thickness ($i = 1$ in the first step and $i = 2$ in the second step).

Considering a constant temperature T_b at the base of the fin and heat dissipation to the surrounding from the tip of the fin by both convection and radiation, one-dimensional steady-state energy balance governing equations for the studied fin profiles can be obtained based on Eq. (1) as follows:

1) Uniform and variable thickness fins: The main governing equation and boundary conditions for the uniform and variable thickness fins are derived from the basic energy balance equation, and these are expressed by Eqs. (2) and (3), respectively.

$$\begin{aligned} &\frac{d}{dr}\left[r\left\{1+\beta\left(T-T_\infty\right)\right\}\frac{dT}{dr}\right] \\ &+\left[r\left\{1+\beta\left(T-T_\infty\right)\right\}\frac{dT}{dr}\right]\frac{t'}{t} \\ &-\frac{hr}{k_a t}\left\{T-T_\infty+\frac{\sigma\epsilon\left(T^4-T_\infty^4\right)}{h}\right\}\left(1+t'^2\right)^{\frac{1}{2}}=0 \end{aligned} \tag{2}$$

$$T = T_b \ ; \ \text{at } r = r_b \tag{3a}$$

$$\begin{aligned} -k_a\left\{1+\beta\left(T-T_\infty\right)\right\}\frac{dT}{dr} =& h\left(T-T_\infty\right) \\ &+\sigma\epsilon\left(T^4-T_\infty^4\right) \ ; \ \text{at } r = r_o \end{aligned} \tag{3b}$$

In Eqs. (2) and (3), ϵ is the emissivity of the fin material, h is the convective heat transfer coefficient on fin surface, σ is the Boltzmann constant ($\sigma = 5.67 \times 10^{-8}$ W/m^{2}K^4), and $t' = 0$ for uniform thickness fin.

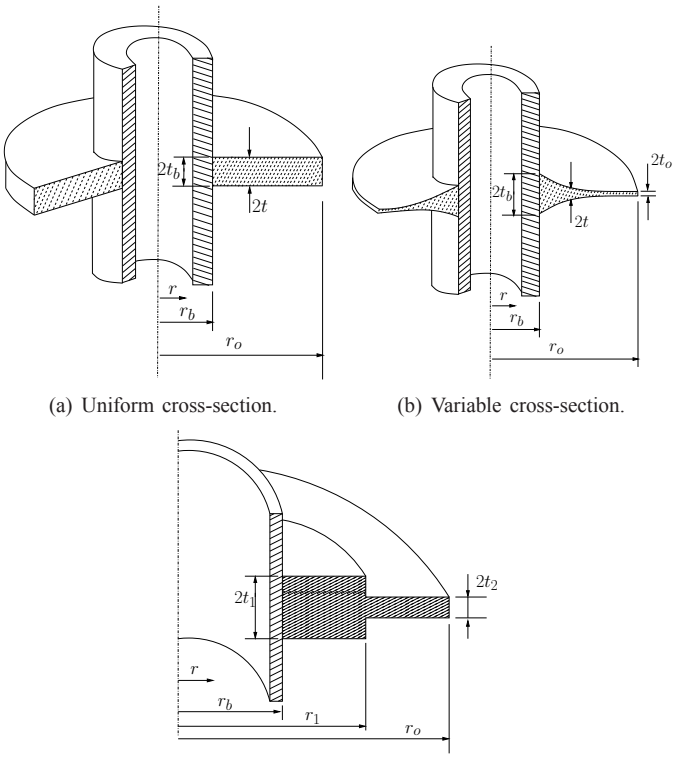

(a) Uniform cross-section. (b) Variable cross-section.

(c) Two-stepped rectangular cross-section.

Fig. 1. Schematic diagram of annular fins of different profiles.

For normalizing Eqs. (2) and (3), the temperature distribution and fin dimensions as shown in Figs. 1(a) and 1(b) are normalized by defining some dimensionless parameters, which are given by Eq. (4).

$$\left.\begin{array}{lll} X=\frac{r}{r_b} & X_o=\frac{r_o}{r_b} & \zeta=\frac{t_b}{r_b} \\ \delta_d=\beta T_\infty & \gamma_c=\frac{t}{t_b} & Bi=\frac{hr_b}{k_a} \\ \omega=\frac{T}{T_\infty} & \omega_b=\frac{T_b}{T_\infty} & \delta_c=\frac{\beta T_\infty}{(1-\beta T_\infty)} \\ \gamma=\frac{hr_b^2}{t_b k_a(1-\beta T_\infty)} & n_c=\frac{r_b^2\sigma T_\infty^3\epsilon}{t_b k_a(1-\beta T_\infty)} & m_c=\frac{r_b\sigma T_\infty^3\epsilon}{k_a} \end{array}\right\} \quad (4)$$

In Eq. (4), X and ω are dimensionless radial coordinate and temperature, respectively.

Using the parameters defined in Eq. (4), Eqs. (2) and (3) are normalized as given by Eqs. (5) and (6), respectively.

$$\begin{aligned} \gamma_c\left\{(1+\delta_c\omega)\frac{d^2\omega}{dX^2}+(1+\delta_c\omega)\frac{1}{X}\frac{d\omega}{dX}+\delta_c\left(\frac{d\omega}{dX}\right)^2\right\} & \\ +\gamma_c{}'(1+\delta_c\omega)\frac{d\omega}{dX} & \\ -\left\{\gamma(\omega-1)+n_c\left(\omega^4-1\right)\right\}\left(1+\gamma_c{}'^2\zeta^2\right)^{\frac{1}{2}}=0 & \end{aligned} \quad (5)$$

$$\omega=\omega_b \ ; \ \text{at } X=1 \quad (6a)$$

$$\begin{aligned} (1-\delta_d+\delta_d\omega)\frac{d\omega}{dX} & \\ +Bi(\omega-1)+m_c\left(\omega^4-1\right)=0 \ ; \ \text{at } X=X_o & \end{aligned} \quad (6b)$$

In Eq. (5), $\gamma_c{}'=0$ for uniform thickness fin.

2) Fin with step change in thickness: In a similar way as in the case of uniform and variable thickness fins, the main governing equation and boundary conditions for the step fin are derived as expressed by Eq. (7).

$$\left.\begin{array}{ll} & \frac{d}{dr}\left[r\left\{1+\beta\left(T_i-T_\infty\right)\right\}\frac{dT_i}{dr}\right] \\ & -\frac{hr}{k_a t_i}\left\{T_i-T_\infty+\frac{\sigma\epsilon\left(T_i^4-T_\infty^4\right)}{h}\right\}=0 \\ \text{where,} & r_b\le r\le r_1 \ , \quad \text{for} \quad i=1 \\ & r_1\le r\le r_o \ , \quad \text{for} \quad i=2 \end{array}\right\} \quad (7)$$

Since the continuity of temperature and energy balance must exist at the interface of the two sections of the step fin, Eq. (7) will be subjected to the boundary conditions given by Eq. (8).

$$T_1=T_b \ ; \ \text{at } r=r_b \quad (8a)$$

$$\begin{aligned} -k_a\left\{1+\beta\left(T_2-T_\infty\right)\right\}\frac{dT_2}{dr} & =h\left(T_2-T_\infty\right) \\ & +\sigma\epsilon\left(T_2^4-T_\infty^4\right) \ ; \ \text{at } r=r_o \end{aligned} \quad (8b)$$

$$T_1=T_2 \ ; \ \text{at } r=r_1 \quad (8c)$$

$$\begin{aligned} -t_1k_a\left\{1+\beta\left(T_1-T_\infty\right)\right\}\frac{dT_1}{dr} & =-t_2k_a\left\{1+\beta\left(T_2-T_\infty\right)\right\}\frac{dT_2}{dr} \\ & +h_s\left(t_1-t_2\right)\times \\ & \left\{T_1-T_\infty+\frac{\sigma\epsilon\left(T_1^4-T_\infty^4\right)}{h_s}\right\}; \\ & \text{at } r=r_1 \end{aligned} \quad (8d)$$

In Eqs. (7) and (8), h is the convective heat transfer coefficient on fin surface and h_s is that on the step surface.

For normalizing Eqs. (7) and (8), the temperature distribution and fin dimensions shown in Fig. 1(c) are normalized, as given in Eq. (9), by defining some dimensionless parameters.

$$\left.\begin{array}{lll} \theta=\frac{T_1-T_\infty}{T_b-T_\infty} & \phi=\frac{T_2-T_\infty}{T_b-T_\infty} & \delta=\frac{T_\infty}{T_b-T_\infty} \\ R_f=\frac{\sigma\epsilon(T_b-T_\infty)^3}{h} & R_{f_s}=\frac{\sigma\epsilon(T_b-T_\infty)^3}{h_s} & \alpha=\left(T_b-T_\infty\right)\beta \\ R=\frac{r}{r_o} & R_1=\frac{r_b}{r_o} & R_o=\frac{r_1}{r_o} \\ y_s=\frac{t_2}{t_1} & \xi=\frac{t_1}{r_b} & \\ \text{Bi}=\frac{hr_b}{k_a} & \text{Bi}_s=\frac{h_sr_b}{k_a} & \end{array}\right\} \quad (9)$$

In Eq. (9), θ and ϕ are respectively the dimensionless temperatures in the first and second steps of the fin; R is the dimensionless radial coordinate with R_1 and R_o as its radial values at the inner surface and step change in thickness; y_s is the thickness ratio; and Bi and Bi_s are the Biot numbers at the side and step surface.

Using the parameters defined in Eq. (9), Eqs. (7) and (8) are normalized as given by Eqs. (10) and (11), respectively.

$$\left.\begin{array}{ll} & (1+\alpha\kappa)\frac{d^2\kappa}{dR^2}+\left\{\alpha\frac{d\kappa}{dR}+\frac{1}{R}(1+\alpha\kappa)\right\}\frac{d\kappa}{dR} \\ & -Z^2\kappa\left\{1+R_f\left(4\delta^3+6\delta^2\kappa+4\delta\kappa^2+\kappa^3\right)\right\}=0 \\ \text{where,} & \kappa=\theta \ , \ Z=\frac{Z_0}{R_1} \ ; \quad \text{if} \quad R_1\le R\le R_o \\ & \kappa=\phi \ , \ Z=\frac{Z_1}{\sqrt{y_s}} \ ; \quad \text{if} \quad R_o\le R\le 1 \\ & Z_0=\left(\frac{Bi}{\xi}\right)^{\frac{1}{2}} \\ & Z_1=\frac{Z_0}{R_1} \end{array}\right\} \quad (10)$$

$$\theta=1 \ ; \ \text{at } R=R_1 \quad (11a)$$

$$\begin{aligned} -(1+\alpha\phi)\frac{d\phi}{dR} & =\frac{Bi}{R_1}\phi\left\{1+R_f\left(4\delta^3+6\delta^2\phi+4\delta\phi^2+\phi^3\right)\right\}; \\ & \text{at } R=1 \end{aligned} \quad (11b)$$

$$\theta=\phi \ ; \ \text{at } R=R_o \quad (11c)$$

$$\begin{aligned} R_1(1+\alpha\theta)\frac{d\theta}{dR} & =y_sR_1(1+\alpha\phi)\frac{d\phi}{dR} \\ & -Bi_s(1-y_s)\theta \\ & \times\left\{1+R_{f_s}\left(4\delta^3+6\delta^2\theta+4\delta\theta^2+\theta^3\right)\right\}; \\ & \text{at } R=R_o \end{aligned} \quad (11d)$$

IV. Optimization Modeling of Annular Fin

It is stated in Section I that the performance of the studied annular fin of various profiles will be evaluated in different combinations of three performance functions, which are heat transfer rate, fin volume and fin efficiency. Accordingly, the multi-objective optimization problem is formulated here in a general form for maximizing the heat transfer rate ($f_1(\boldsymbol{x})$) and fin efficiency ($f_3(\boldsymbol{x})$) and minimizing the fin volume ($f_2(\boldsymbol{x})$).

A. Formulation of the uniform and variable thickness fins

The profile of the variable thickness fin as shown in Fig. 1(b) is represented by a B-spline curve, which is defined by some

control points. Hence, m number of such control points, $P_i(x_i, y_i)$ ($i = 1$ to m), are taken as the design variables, whose x values will represent the radial distances starting from the base of the fin and associated y values will define the half-thickness of the fin falling on the B-spline curve. On the other hand, the profile of the uniform thickness fin, as shown in Fig. 1(a), is defined by a single point $P_1 = (x, y)$, whose x and y values will give respectively the outer radius and half-thickness of the fin. Accordingly, the optimization problem for both the profiles can be formulated jointly as given by Eq. (12).

$$\left.\begin{array}{rrcl} \text{Determine} & \boldsymbol{x} & \equiv & \{P_i | P_i \ ; \ i = 1 \text{ to } m\} \\ \text{to maximize} & \boldsymbol{z}(\boldsymbol{x}) & \equiv & \{f_1(\boldsymbol{x}), f_3(\boldsymbol{x})\} \\ \text{minimize} & \boldsymbol{f}(\boldsymbol{x}) & \equiv & \{f_2(\boldsymbol{x})\} \\ \text{subject to} & g_1(\boldsymbol{x}) & \equiv & x_1 < x_2 \leq \cdots \leq x_m \\ & g_2(\boldsymbol{x}) & \equiv & y_1 \geq y_2 \geq \cdots \geq y_m \end{array}\right\} \quad (12)$$

In the case of the variable thickness fin, $P_i = (x_i, y_i)$ in Eq. (12) is the ith control point of the B-spline curve representing the fin profile and m is the total number of control points. According to the notations used in Fig. 1(b), $x_1 = r_b$, $y_1 = t_b$, $x_m = r_o$ and $y_m = t_o$. Constraints $g_1(\boldsymbol{x})$ and $g_2(\boldsymbol{x})$ in Eq. (12) ensure that the control points are distributed along the radially outward direction of the fin with non-increasing values in the direction of the fin thickness, so as to avoid any unpleasant fin profile. Further, $y_m > 0$ can be set in order to represent a practical scenario by avoiding a sharp outer edge of the fin.

In Eq. (12), $m = 1$ for uniform thickness fin, indicating a single design point as stated above. Further, constraints $g_1(\boldsymbol{x})$ and $g_2(\boldsymbol{x})$ are not applicable in this case.

B. Formulation of the fin with step change in thickness

The geometry of the step fin, as shown in Fig. 1(c), is defined in terms of four parameters, which are radius of the fin at the point of step change in thickness (r_1), outer radius of the fin (r_o), cross-sectional half thickness of the thick (first) step of the fin (t_1), and cross-sectional half thickness of the thin (second) step of the fin (t_2). Taking these four parameters as the variables, the design of the step fin can be formulated as a multi-objective optimization problem as given by Eq. (13).

$$\left.\begin{array}{rrcl} \text{Determine} & \boldsymbol{x} & \equiv & (r_1, r_o, t_1, t_2)^{\mathrm{T}} \\ \text{to maximize} & \boldsymbol{z}(\boldsymbol{x}) & \equiv & \{f_1(\boldsymbol{x}), f_3(\boldsymbol{x})\} \\ \text{minimize} & \boldsymbol{f}(\boldsymbol{x}) & \equiv & \{f_2(\boldsymbol{x})\} \\ \text{subject to} & g_1(\boldsymbol{x}) & \equiv & r_1 > r_b \\ & g_2(\boldsymbol{x}) & \equiv & r_o > r_1 \\ & g_3(\boldsymbol{x}) & \equiv & t_1 > t_2 \\ & & & r_1, r_o, t_1, t_2 \geq 0 \ . \end{array}\right\} \quad (13)$$

In Eq. (13), the existence of two steps in the fin is ensured by constraints $g_1(\boldsymbol{x})$ and $g_2(\boldsymbol{x})$, while two different cross-sectional thicknesses of the two steps are ensured by constraint $g_3(\boldsymbol{x})$. The last line in Eq. (13) makes the design variables non-negative.

C. Formulation of objective functions

The three objective functions, $f_1(\boldsymbol{x})$–$f_3(\boldsymbol{x})$ expressed in Eqs. (12) and (13), are the heat transfer rate, fin volume, and fin efficiency, respectively. The maximization of $f_1(\boldsymbol{x})$ and $f_3(\boldsymbol{x})$ enhances the overall thermal performance of the fin, while the minimization of $f_2(\boldsymbol{x})$ reduces the fin material cost. In terms of the notations and formulations of the thermal modeling of the fin as presented in Section III, these can be given by Eq. (14).

$$f_1(\boldsymbol{x}) = -kA_b \left.\frac{dT_i}{dr}\right|_{r=r_b} \quad (14a)$$

$$f_2(\boldsymbol{x}) = V \quad (14b)$$

$$f_3(\boldsymbol{x}) = \frac{f_1(\boldsymbol{x})}{hA_s\left(T_b - T_\infty\right) + \sigma\epsilon A_s\left(T_b^4 - T_\infty^4\right)} \quad (14c)$$

where, $A_b = \begin{cases} 4\pi r_b t_b \ ; \ \text{for uniform/variable thickness fins} \\ 4\pi r_b t_1 \ ; \ \text{for step fin.} \end{cases}$

In Eq. (14a), A_b is the base area of the fin. The fin volume V, appearing in Eq. (14b), is expressed by Eq. (15).

$$V = \begin{cases} \frac{4}{3}\pi \sum_{n=2,\ 4,\ \ldots}^{N} r_{n-1}\left(r_n - r_{n-1}\right) \\ \times \left(t_{n-2} + 4\ t_{n-1} + t_n\right) \ ; \ \text{for variable thickness} \\ 2\pi t_b \left({r_o}^2 - {r_b}^2\right) \ ; \ \text{for uniform thickness} \\ 2\pi \left\{t_1\left({r_1}^2 - {r_b}^2\right) + t_2\left({r_o}^2 - {r_1}^2\right)\right\} \ ; \ \text{for step fin.} \end{cases} \quad (15)$$

Further, the heat transfer surface area A_s, appearing in Eq. (14c), is expressed by Eq. (16).

$$A_s = \begin{cases} 4\pi r_o t_o + 2\pi \sum_{n=1}^{N}\left(r_n + r_{n-1}\right) \times \\ \left\{\left(r_n - r_{n-1}\right)^2 + \left(t_{n-1} - t_n\right)^2\right\}^{\frac{1}{2}} \ ; \ \text{for variable thickness} \\ 2\pi\left({r_o}^2 - {r_b}^2\right) + 4\pi r_o t_b \ ; \ \text{for uniform thickness} \\ 2\pi\left({r_o}^2 - {r_b}^2\right) + 4\pi\left\{r_1\left(t_1 - t_2\right) + r_o t_2\right\} ; \ \text{for step fin.} \end{cases} \quad (16)$$

In Eqs. (15) and (16), n and (N+1) are respectively the grid index of space and total number of grid points.

V. Solution procedure

A widely applied multi-objective genetic algorithm, namely the non-dominated sorting genetic algorithm II (NSGA-II) proposed by Deb et al. [3], is employed here for solving the fin design problem formulated by Eqs. (12) and (13) as multi-objective optimization models (since NSGA-II is a well-established algorithm, its detail is skipped here).

In the cycles of NSGA-II, the heat transfer rate, $f_1(\boldsymbol{x})$, is evaluated through Eqs. (5) and (6) for uniform and variable thickness fins, while that through Eqs. (10) and (11) for step fin. The non-dimensional temperature distributions (ω, θ and ϕ) along the length of the fins are first evaluated by solving the sets of equations using a highly accurate numerical method, namely the hybrid spline difference method (HSDM) presented by Wang et al. [2], [19]–[21].

Then a temperature distribution, ν, and its derivatives, ν' and ν'', are discretized by applying the concept of HSDM

as expressed by Eq. (17) [2], where Δr, $N^{(i)}+1$, n and p represent the grid size, total number of grid points, grid index of space, and spline parameter, respectively.

$$\nu_n = \frac{p_{n-1}^{(i)} + 10p_n^{(i)} + p_{n+1}^{(i)}}{12} \tag{17a}$$

$$\nu'_n = \frac{p_{n+1}^{(i)} - p_{n-1}^{(i)}}{2\Delta r} - \Delta\nu'_n \tag{17b}$$

$$\nu''_n = \frac{p_{n-1}^{(i)} - 2p_n^{(i)} + p_{n+1}^{(i)}}{\Delta r^2} \tag{17c}$$

$$\text{where,}\quad \Delta\nu'_n = \begin{cases} \frac{\left(-3\nu''_n + 4\nu''_{n+1} - \nu''_{n+2}\right)\Delta r}{24}\ ; & n = 0 \\ \frac{\left(\nu''_{n+1} - \nu''_{n-1}\right)\Delta r}{24}\ ; & n = 1 \text{ to } N^{(i)} - 1 \\ \frac{\left(3\nu''_n - 4\nu''_{n-1} + \nu''_{n-2}\right)\Delta r}{24}\ ; & n = N^{(i)} \end{cases} \tag{17d}$$

In Eq. (17), $i \in \{1, 2\}$ for step fin, while $p^{(i)} = p$ and $N^{(i)} = N$ for variable and uniform thickness fins. Further, $\nu = \omega$ for uniform and variable thickness fins as formulated in Eq. (12), while $\nu = \kappa$ for step fin as formulated in Eq. (13).

Using Eq. (17), the two sets of equations, i.e., Eqs. (5) and (6), and Eqs. (10) and (11), are solved for $p_n^{(i)}$ using the variant of the Thomas algorithm proposed by Martin and Boyd [22]. After evaluating the $p_n^{(i)}$ values, the dimensionless temperature distributions ω, θ and ϕ along with their derivatives up to the second order at all the grid points are evaluated from Eq. (17). Finally, the temperature gradient at the base of the fin, i.e., $\frac{dT_i}{dr}\big|_{r=r_b}$, is obtained from the non-dimensional temperature gradient at that point, which is then used in Eq. (14a) to evaluate $f_1(\boldsymbol{x})$.

VI. Numerical Experimentation and Discussion

In the present study, the annular fins of various profiles, namely uniform thickness, variable thickness and step change in thickness, are analyzed in a convective and radiative environment with a constant temperature at the base of the fin and variable thermal conductivity for the fin material. The proposed procedure is coded in C programming language, and all the test cases are executed in the Ubuntu 12.04.5 LTS Linux environment in a 32-bit HP Desktop.

The considered operating conditions and thermal properties of the fin material along with fin geometry with reference to Fig. 1 are listed in Table I, while the user defined algorithmic parameter settings for NSGA-II are fixed based on some trial runs as given in Table II. Since cubic curves with open uniform knot vector and of order 4 are sufficient in most of the engineering analysis, the same is considered for the B-Spline curve representing the profile of the variable thickness fin. Further, since the number of control points of a B-spline curve must be more than the chosen polynomial degree by at least two units in order to have a local control on the curve [23], five control points are considered here to define the B-spline curve.

With the above sets of input values and randomly generated NSGA-II population, the fin design problem formulated in Eqs. (12) and (13) is studied with various combinations of the three objective functions, f_1–f_3, given by Eq. (14).

TABLE I
Operating conditions, material properties, and fin geometry.

Parameter	Value/ Range of value
Ambient temperature, T_∞	300 K
Temperature of the fin at the base, T_b	600 K
Convective heat transfer coefficient on fin surface, h	50 W/m^{2}K
Convective heat transfer coefficient on step surface, h_s	50 W/m^{2}K
Thermal conductivity of the fin material at T_∞, k_a	186 W/mK
Parameter for variable thermal conductivity, β	-0.00018 K^{-1}
Emissivity of the fin material, ϵ	0.8
Base radius, r_b	2.0 cm
Outer radius, r_o	2.5–6.0 cm
Fin half-thickness, t (for uniform/variable thickness fin)	0.01–0.2 cm
Radius of step change in thickness, r_1 (for step fin)	2.5–6.0 cm
Half thickness of the first step, t_1 (for step fin)	0.01–0.2 cm
Half thickness of the second step, t_2 (for step fin)	0.01–0.2 cm

TABLE II
User-defined parameter setting in the context of NSGA-II.

Parameter	Value/ Range of value
Population size	100
Number of generations	400
Crossover probability	90%
Distribution index for the crossover operator of NSGA-II	10
Mutation probability	0–1%
Distribution index for the mutation operator of NSGA-II	100

The Pareto fronts for the three fin profiles obtained by maximizing the heat transfer rate (f_1) and minimizing fin volume (f_3) are shown in Fig. 2, where the conflicting nature

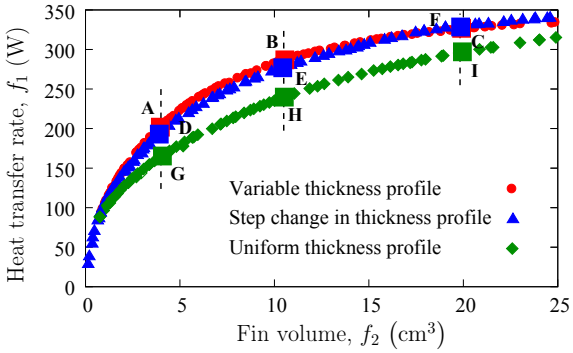

Fig. 2. Pareto fronts in terms of f_1 and f_2.

of the heat transfer rate and fin volume is clearly visible, i.e., one objective cannot be improved without degrading the other at least by some amount. It is also seen in Fig. 2 that the variable thickness fin has the best performance among the three profiles, followed by that of the step fin. In fact, near the end of the Pareto fronts where both the heat transfer rate and fin volume reach their maximum values, the performance of the step fin is slightly better than that of the variable thickness fin. Nine selective efficient fin geometries (three solutions from each fin profile), corresponding to solutions A–I of Fig. 2, are shown in Fig. 3, where the patterns of significant geometric

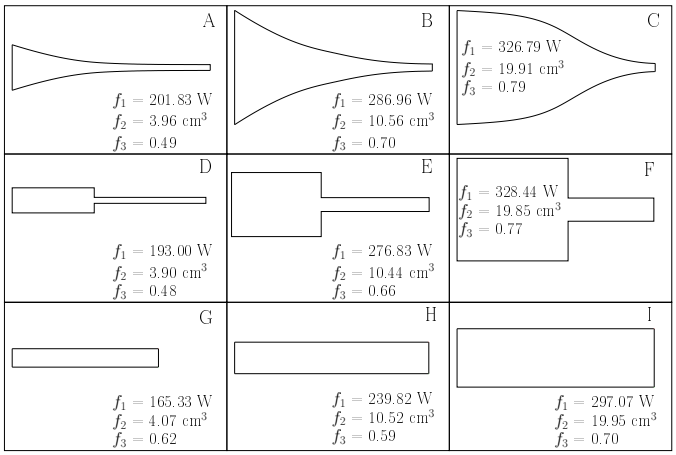

Fig. 3. Nine efficient fin geometries corresponding to solutions A–I of Fig. 2 (a larger scale in thickness direction is used to make the variation in thickness prominent).

variations are clearly noticeable. For these configurations, the values of the third objective (f_3) are also computed and shown in Fig. 3.

For further assessment, the problem is studied in the second step for simultaneously maximizing the heat transfer rate (f_1) and fin efficiency (f_3). The obtained Pareto fronts are shown in Fig. 4, which reveal the conflicting nature between the heat

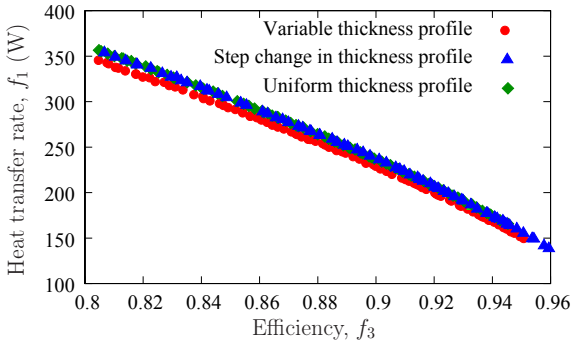

Fig. 4. Pareto fronts in terms of f_1 and f_3.

transfer rate and fin efficiency also. It is also seen in Fig. 4 that the variable thickness fin has the lowest efficiency among the three fin profiles. The Pareto fronts of the other two fins overlap with each other, indicating almost the same efficiency in both the cases. This is due to the fact that both the optimized step fin and uniform thickness fin takes almost similar shapes.

VII. Conclusion

A comparative analysis of multi-objective optimization of various profiles of annular fins under one-dimensional heat transfer in convective and radiative environments is presented. Fin performance related three parameters are taken as objective function of the problem, which are maximization of the heat transfer rate and fin efficiency and minimization of fin volume. Evaluating by the hybrid spline difference method (HSDM), the objective functions are optimized using the nondominated sorting genetic algorithm (NSGA-II). In the numerical experimentation, it is observed that the variable thickness fin has a lower efficiency but a higher heat dissipation rate per unit volume, followed by those of the step fin.

References

[1] B. Kundu, K.-S. Lee, and A. Campo, "An ease of analysis for optimum design of an annular step fin," *Int. J. Heat Mass Trans.*, vol. 85, pp. 221–227, 2015.

[2] C.-C. Wang, W.-J. Liao, and C.-Y. Yang, "Hybrid spline difference method for heat transfer and thermal stresses in annular fins," *Numer. Heat Trans., B*, vol. 64, no. 1, pp. 71–88, 2013.

[3] K. Deb, A. Pratap, S. Agarwal, and T. Meyarivan, "A fast and elitist multi-objective genetic algorithm: NSGA-II," *IEEE Trans. Evol. Comput.*, vol. 6, no. 2, pp. 182–197, 2002.

[4] A. D. Kraus, A. Aziz, and J. Welty, *Extended Surface Heat Transfer*. New York: John Wiley & Sons, 2001.

[5] A. Brown, "Optimum dimensions of uniform annular fins," *Int. J. Heat Mass Trans.*, vol. 8, no. 4, pp. 655–662, 1965.

[6] A. Ullmann and H. Kalman, "Efficiency and optimized dimensions of annular fins of different cross-section shapes," *Int. J. Heat Mass Trans.*, vol. 32, no. 6, pp. 1105–1110, 1989.

[7] C. Arslanturk, "Performance analysis and optimization of a thermally non-symmetric annular fin," *Int. Commun. Heat Mass Trans.*, vol. 31, no. 8, pp. 1143–1153, 2004.

[8] L.-T. Yu and C.-K. Chen, "Optimization of circular fins with variable thermal parameters," *J. Franklin Inst.*, vol. 336, no. 1, pp. 77–95, 1999.

[9] P. Malekzadeh and H. Rahideh, "IDQ two-dimensional nonlinear transient heat transfer analysis of variable section annular fins," *Energy Convers. Manage.*, vol. 48, no. 1, pp. 269–276, 2007.

[10] H. S. Kang and D. C. Look, "Thermally asymmetric annular rectangular fin optimaztion," *J. Thermophys. Heat Trans.*, vol. 18, no. 3, pp. 406–409, 2004.

[11] K. Laor and H. Kalman, "Performance and optimum dimensions of different cooling fins with a temperature-dependent heat transfer coefficient," *Int. J. Heat Mass Trans.*, vol. 39, no. 9, pp. 1993–2003, 1996.

[12] H. S. Kang and D. C. Look, Jr., "Optimization of a trapezoidal profile annular fin," *Heat Trans. Eng.*, vol. 30, no. 5, pp. 359–367, 2009.

[13] N. Nagarani, K. Mayilsamy, and A. Murugesan, "Fin effectiveness optimization of elliptical annular fins by genetic algorithm," *Procedia Eng.*, vol. 38, pp. 2939–2948, 2012.

[14] H. Nemati and S. Samivand, "Performance optimization of annular elliptical fin based on thermo-geometric parameters," *Alex. Eng. J.*, vol. 54, no. 4, pp. 1037–1042, 2015.

[15] S. Pashah, A. Moinuddin, and S. M. Zubair, "Thermal performance and optimization of hyperbolic annular fins under dehumidifying operating conditions-analytical and numerical solutions," *Int. J. Refrig.*, vol. 65, pp. 42–54, 2016.

[16] B. Kundu, "Analysis of thermal performance and optimization of concentric circular fins under dehumidifying conditions," *Int. J. Heat Mass Trans.*, vol. 52, no. 11–12, pp. 2646–2659, 2009.

[17] B. Kundu and K.-S. Lee, "Analytical tools for calculating the maximum heat transfer of annular stepped fins with internal heat generation and radiation effects," *Energy*, vol. 76, pp. 733–748, 2014.

[18] B. Kundu and P. Das, "Performance analysis and optimization of annular fin with a step change in thickness," *J. Heat Trans.*, vol. 123, no. 3, pp. 601–604, 2001.

[19] C.-C. Wang, H. Chen-Hung, and D.-J. Yang, "Hybrid spline difference method for steady-state heat conduction," *Numer. Heat Trans., B*, vol. 60, no. 6, pp. 472–485, 2011.

[20] C.-C. Wang, L.-P. Chao, and W.-J. Liao, "Hybrid spline difference method (HSDM) for transient heat conduction," *Numer. Heat Trans., B*, vol. 61, no. 2, pp. 129–146, 2012.

[21] C.-C. Wang, W.-J. Liao, and Y.-S. Hsu, "Hybrid spline difference method for the Burgers' equation," *Appl. Math. Comput.*, vol. 219, no. 3, pp. 1031–1039, 2012.

[22] A. Martin and I. D. Boyd, "Variant of the Thomas algorithm for opposite-bordered tridiagonal systems of equations," *Int. J. Numer. Method. Biomed. Eng.*, vol. 26, no. 6, pp. 752–759, 2010.

[23] L. Piegel and W. Tiller, *The NURBS Book*. Berlin: Springer-Verlag, 1997.

Bi-level Problem as a Plain Multi-Objective Optimization Problem: A Preliminary Study

Pooja Dutta
Department of Mechanical Engineering
Tezpur University
Napaam, Tezpur - 784 028, India.
Email: poojadutta132@gmail.com

Dilip Datta
Department of Mechanical Engineering
Tezpur University
Napaam, Tezpur - 784 028, India.
Email: ddatta@tezu.ernet.in / datta_dilip@rediffmail.com

***Abstract*—The bi-level problem is an embedded decentralized optimization process at two levels arisen in hierarchy-based organizations. The activities of the lower-level are governed by the upper-level, while the performance of the latter is dependent upon that of the former. Though consists of two decentralized levels, their embedding nature makes the solution procedure of the bi-level problem complicated. In the present work, a multi-objective differential evolution algorithm is employed to solve this problem as a plain multi-objective optimization problem by combining its two levels. The proposed procedure is found very potential in identifying promising trade-off optimal solutions for a number of benchmark problems.**

I. Introduction

The bi-level problem was introduced in the field of game theory by Stackelberg in the year 1934, in which two players of a game compete with each other in such a way that the leader optimizes its objectives by anticipating the optimal reactions of the follower against the initiative movements of the leader. That is, the bi-level problem is a sequential hierarchical optimization process, which involves two decision makers that have different objective functions, variables and constraints. In other words, the bi-level problem consists of two optimization problems, one embedded (nested) within another as a hierarchical structure. The outer optimization problem is commonly referred to as the upper or top level (or leader) problem, and the inner one as the lower or bottom level (or follower) problem. The variables associated with the upper-level problem are known as the upper-level variables and those associated with the lower-level problem are known as the lower-level variables. The constraints are also referred in similar ways according to their association with the upper-level and lower level problems.

The bi-level problem has applications in various real-world domains, including agriculture [1], environmental economics [2], decision-making [3], portfolio management [4], government policy making [5], transportation [6], [7], and engineering [8], [9], [10], [11], [12], among others.

The bi-level problem is usually studied under certain categories, such as linear bi-level problem [13], nonlinear bi-level problem and multi-objective bi-level problem. The bi-level problem is linear if all the objective functions and constraints of both the levels are linear, while the problem is nonlinear if any of them is nonlinear. On the other hand, the problem is called multi-objective if more than one objective function are to be optimized at any level.

II. The bi-level problem formulation

Since the bi-level problem consists of two optimization problems one embedded (nested) within another as a hierarchical structure, it in a general form can be formulated mathematically as expressed by Eq. (1).

$$\left.\begin{array}{ll} \underset{\boldsymbol{x}\in\boldsymbol{X},\boldsymbol{y}\in\boldsymbol{Y}}{\text{Minimize}} & F_r^{(\mathrm{u})}(\boldsymbol{x},\boldsymbol{y})\ ;\ r=1 \text{ to } Q^{(\mathrm{u})} \\ \text{subject to} & G_i^{(\mathrm{u})}(\boldsymbol{x},\boldsymbol{y})\leqslant 0\ ;\ i=1 \text{ to } M^{(\mathrm{u})} \\ & \boldsymbol{y}\in \arg\min_{\boldsymbol{z}\in\boldsymbol{Y}} \left\{F_s^{(\mathrm{l})}(\boldsymbol{x},\boldsymbol{z}) : G_j^{(\mathrm{l})}(\boldsymbol{x},\boldsymbol{z})\leqslant 0\right\}\ ; \\ & \qquad\qquad s=1 \text{ to } Q^{(\mathrm{l})}\ ;\ j=1 \text{ to } M^{(\mathrm{l})} \\ & \boldsymbol{X}\subseteq \boldsymbol{R}^{n_x} \\ & \boldsymbol{Y}\subseteq \boldsymbol{R}^{n_y} \end{array}\right\} \quad (1)$$

In Eq. (1), F and G represent respectively the sets of objective functions to be minimized (optimized) and inequality constraints to be satisfied, while Q and M are the sizes of these two sets with the superscripts (u) and (l) denoting respectively the upper-level and lower-level problems. On the other hand, $\boldsymbol{x}$ and $\boldsymbol{y}$ represent respectively the upper-level and lower-level decision vectors.

In principle, the bi-level problem formulated in Eq. (1) is to be solved sequentially in an interactive mode as follows: the lower-level problem is first optimized for its variable vector $\boldsymbol{y}$ against an initial guess to the upper-level variable vector $\boldsymbol{x}$, which in turn is improved by optimizing the upper-level problem with the obtained $\boldsymbol{y}$. Then the optimization of the lower-level problem is repeated for its new variable vector $\boldsymbol{y}$ against the updated $\boldsymbol{x}$, followed by optimization of the upper-level problem again for further improvement of $\boldsymbol{x}$. In this way, the process is continued until it converges. Although sounds simple and interesting, the implementation of the process is not so easy, particularly when a level involves multiple objectives

978-1-5090-5674-3/17/$31.00 ©2017 IEEE

leading not to a single $\boldsymbol{x}$ or $\boldsymbol{y}$ but to a set. If the problem is tackled in its original form, classical optimization techniques often require some simplifications, like linearity, convexity, or single-objective transformation. Hence, it becomes essential to develop some alternative approaches.

Aiyoshi and Shimuzu [14] tackled the single-objective bi-level problem (i.e., in Eq. (1), $Q^{(\mathrm{u})} = Q^{(\mathrm{l})} = 1$) with a well-known penalty function method by transforming the bi-level problem into a one-level single-objective optimization problem, in which it was claimed that a sequence of solutions to the transformed problem would converge to the solution of the original bi-level problem. In the domain of evolutionary algorithms, some researchers converted the bi-level problem into a single level problem using the Karush-Kuhn-Tucker (KKT) conditions [15], [16]. Sinha et al. [17] have recently introduced a hybridized bi-level evolutionary algorithm based on quadratic approximations of optimal lower level variables with respect to the upper level variables.

In the multi-objective bi-level problem as in Eq. (1), the rational response of the follower against a decision of the leader is deterministic if the lower-level problem is single-objective, i.e., $Q^{(\mathrm{l})} = 1$ in Eq. (1). In the case of a multi-objective lower-level problem, however, there is no single solution to the follower to respond, but a set of trade-off solutions (i.e., no solution is better than any other solution in terms of all the objective values), which makes it difficult to device a procedure for providing effective solutions at the upper-level [18]. For such cases, Shi and Xia [19], [20] proposed an interactive algorithm that transforms the original bi-level problem into a separate multi-objective problem at each level with a satisfactory concept to model the preferences of the upper-level decision maker. Zhang et al. [21] presented a branch-and-bound algorithm for solving linear bi-level problems with the provision for handling multiple objectives at any level through some fuzzy parameters. Deb and Sinha [22] suggested a co-evolutionary algorithm with two interacting populations for pursuing both the upper-level and lower-level problems simultaneously through iterations, instead of a serial optimization of the lower-level problem against every solution of the upper-level problem.

III. The proposed plain multi-objective problem formulation

Aiyoshi and Shimuzu [14] transformed the single-objective bi-level problem into a one-level single-objective optimization problem with a claim that the solution of the transformed problem would be same with the solution of the original bi-level problem. In a similar line, the bi-level problem in the present work is transformed into a one-level problem. However, unlike forming a single weighted objective function by combining those of the upper and lower levels as in Aiyoshi and Shimuzu [14], the objective functions of the two levels are considered here to be optimized simultaneously as a multi-objective problem. Accordingly, the original bi-level problem given by Eq. (1) is transformed into a plain multi-objective optimization problem as expressed by Eq. (2).

$$\left.\begin{array}{ll} \text{Minimize} & f_q(\boldsymbol{x},\boldsymbol{y},\boldsymbol{z}) \ ; \ \boldsymbol{x} \in \boldsymbol{X}; \boldsymbol{y},\boldsymbol{z} \in \boldsymbol{Y} \\ \text{subject to} & g_k(\boldsymbol{x},\boldsymbol{y},\boldsymbol{z}) \leqslant 0 \\ \text{where} & q = 1 \text{ to } Q^{(\mathrm{u})} + Q^{(\mathrm{l})} \\ & k = 1 \text{ to } M^{(\mathrm{u})} + M^{(\mathrm{l})} \\ & \boldsymbol{X} \subseteq \boldsymbol{R}^{n_x} \\ & \boldsymbol{Y} \subseteq \boldsymbol{R}^{n_y} \end{array}\right\} \quad (2)$$

In Eq. (2), f_q ($q = 1$ to $Q^{(\mathrm{u})} + Q^{(\mathrm{l})}$) is a set comprising $F_r^{(\mathrm{u})}$ ($r = 1$ to $Q^{(\mathrm{u})}$) and $F_s^{(\mathrm{l})}$ ($s = 1$ to $Q^{(\mathrm{l})}$) as given in Eq. (1). Similarly, g_k ($k = 1$ to $M^{(\mathrm{u})} + M^{(\mathrm{l})}$) is another set comprising $G_i^{(\mathrm{u})}$ ($i = 1$ to $M^{(\mathrm{u})}$) and $Q_j^{(\mathrm{l})}$ ($j = 1$ to $M^{(\mathrm{l})}$) as given in Eq. (1).

IV. Numerical experimentation and discussion

For evaluating the proposed multi-objective transportation of the bi-level problem, three test problems of different nature are considered, details of which are given in Table I. Test problem 1 is a simple case of one leader and one follower, each involving a single objective function to be minimized. Further, the leader is subject to one constraint and the follower is subject to two constraints. Test problem 2 also has one leader and one follower, but each having two objective functions to be maximized simultaneously, where the leader is subject to one constraint and the follower only needs a non-negative variable. In comparison to Test problems 1 and 2, Test problem 3 is complicated. It involves one leader and three followers with each having one objective function to be minimized, in which information exchange takes place among the followers also. Moreover, the variables of the leader and followers 2 and 3 are to be positive without any fixed lower boundary. Additionally, follower 3 is subject to an equality constraint, which is difficult to handle by any numerical optimization technique.

A multi-objective version of the differential evolution (DE) algorithm, presented by Datta and Figueira [25], is chosen for solving the multi-objective optimization problem formulated in Eq. (2). In case of each of the above three test problems, a DE population (i.e., a set of solutions) of size 60 is evolved for 500 iterations with DE perturbance factor of 0.7 and crossover probability of 90%. Analyzing the constraints of the test problems, their variable limits are fixed as follows: $0 \leqslant x_1, x_2 \leqslant 50$ and $-10 \leqslant y_1, y_2 \leqslant 20$ for Test Problem 1, $0 \leqslant x_1, x_2 \leqslant 4$ for Test problem 2, and $0.001 \leqslant x_1 \leqslant 10$, $0.001 \leqslant x_2 \leqslant 5$, $1 \leqslant y_{11} \leqslant 9$, $2 \leqslant y_{12} \leqslant 3$, $0.001 \leqslant y_{21} \leqslant 9$, $0.001 \leqslant y_{22} \leqslant 3$, $0.001 \leqslant y_{31} \leqslant 2.5$ and $0.001 \leqslant y_{32} \leqslant 1.7$ for Test problem 3. Further, the equality constraint of Test problem 3 is converted into an inequality constraint as $\left|\frac{2y_{31}+3y_{32}}{5} - 1\right| \leqslant 0.001$.

The final 2-objective Pareto front obtained for Test problem 1 is shown in Fig. 1 along with its best known solution as given in Table I, where it is seen that the best known solution is nothing but the extreme point of the Pareto front corresponding to the overall maximum of $F^{(\mathrm{u})}$ and minimum of $F^{(\mathrm{l})}$ as expressed in Table I. However, an extreme solution

TABLE I
DETAIL OF THE STUDIED TEST PROBLEMS.

SN	Test problem		Best known solution	Reference
1	Minimize $(\boldsymbol{x})$	$F^{(\mathrm{u})}(\boldsymbol{x},\boldsymbol{y}) \equiv 2x_1 + 2x_2 - 3y_1 - 3y_2 - 60$	$(x_1^*, x_2^*) = (25, 30)$ $(y_1^*, y_2^*) = (5, 10)$ $F^{(\mathrm{u})*} = 5$ $F^{(\mathrm{l})*} = 0$	Aiyoshi and Shimuzu [14]
	Subject to	$\boldsymbol{y} \in \arg\min_{(\boldsymbol{y})} \left\{ \begin{array}{l} F^{(\mathrm{l})}(\boldsymbol{x},\boldsymbol{y}) \equiv (y_1 - x_1 + 20)^2 + (y_2 - x_2 + 20)^2 \\ x_1 - 2y_1 \geqslant 10 \\ x_2 - 2y_2 \geqslant 10 \\ -10 \leqslant y_1, y_2 \leqslant 20 \end{array} \right\}$		
		$x_1 + x_2 + y_1 - 2y_2 \leqslant 40$		
		$0 \leqslant x_1, x_2 \leqslant 50$		
2	Maximize (x_1)	$\left\{ \begin{array}{l} F_1^{(\mathrm{u})}(x_1, x_2) \equiv x_1^2 + x_2^2 \\ F_2^{(\mathrm{u})}(x_1, x_2) \equiv (x_1 - 1)^2 + x_2^2 \end{array} \right\}$	$x_1^* = 0$ $x_2^* = 4$ $\left(F_1^{(\mathrm{u})*}, F_2^{(\mathrm{u})*}\right) = (16, 17)$ $\left(F_1^{(\mathrm{l})*}, F_2^{(\mathrm{l})*}\right) = (-7, 64)$	Baky and Abo-Sinna [23]
	Subject to	$x_2 \in \arg\max_{(x_2)} \left\{ \begin{array}{l} F_1^{(\mathrm{l})}(x_1, x_2) \equiv (x_1 - 3)^2 - 4x_2 \\ F_2^{(\mathrm{l})}(x_1, x_2) \equiv 2x_1 + (x_2 + 4)^2 \end{array} \right\}$		
		$x_1 + x_2 \leqslant 4$		
		$x_1, x_2 \geqslant 0$		
3	Minimize $(\boldsymbol{x})$	$F^{(\mathrm{u})}(\boldsymbol{x}, \boldsymbol{y_1}, \boldsymbol{y_2}, \boldsymbol{y_3}) \equiv \frac{3(y_{11}+y_{12})^2 + 5(y_{21}+y_{22})^2 + 10(y_{31}+y_{32})^2}{2x_1^2 + x_2^2 + 3x_1x_2}$	$(x_1^*, x_2^*) = (5.768, 2.116)$ $(y_{11}^*, y_{12}^*) = (2.885, 2.0)$ $(y_{21}^*, y_{22}^*) = (1.699, 1.414)$ $(y_{31}^*, y_{32}^*) = (1.183, 0.878)$ $F^{(\mathrm{u})*} = 1.510$ $F_1^{(\mathrm{l})*} = 12.323$ $F_2^{(\mathrm{l})*} = 6.225$ $F_3^{(\mathrm{l})*} = 0.835$	Liu [24]
	Subject to	$x_1 + 2x_2 \leqslant 10$		
		$x_1, x_2 > 0$		
		$\boldsymbol{y_1} \in \arg\min_{(\boldsymbol{y_1})} \left\{ \begin{array}{l} F_1^{(\mathrm{l})}(\boldsymbol{y_1}) \equiv y_{11}^2 + y_{12}^2 \\ y_{11} + y_{21} + y_{31} \geqslant x_1 \\ y_{12} + y_{22} + y_{32} \geqslant x_2 \\ y_{11} \geqslant 1 \\ y_{12} \geqslant 2 \end{array} \right\}$		
		$\boldsymbol{y_2} \in \arg\min_{(\boldsymbol{y_2})} \left\{ \begin{array}{l} F_2^{(\mathrm{l})}(\boldsymbol{y_2}) \equiv y_{21} + y_{22} + \frac{y_{11}}{y_{21}} + \frac{y_{12}}{y_{22}} \\ y_{21}, y_{22} > 0 \end{array} \right\}$		
		$\boldsymbol{y_3} \in \arg\min_{(\boldsymbol{y_3})} \left\{ \begin{array}{l} F_3^{(\mathrm{l})}(\boldsymbol{y_3}) \equiv \frac{(y_{31}-y_{21})^2}{y_{31}} + \frac{(y_{32}-y_{22})^2}{y_{32}} \\ 2y_{31} + 3y_{32} = 5 \\ y_{31}, y_{32} > 0 \end{array} \right\}$		

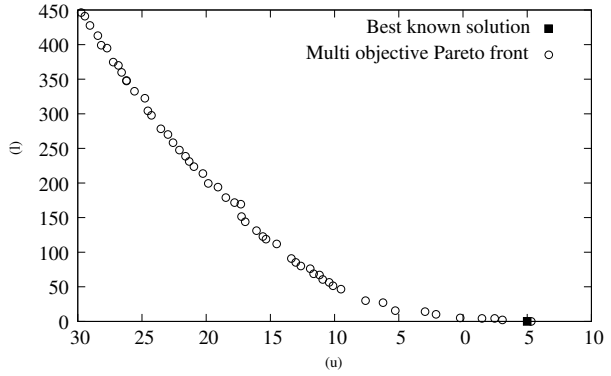

Fig. 1. Pareto front for Test problem 1 given in Table I.

always may not be preferred in real life, but a compromise one due to many reasons, such as the management (the leader) of a manufacturing company may prefer to cut the profit to some extent by improving its product quality (the follower) in order to survive in the competitive market. In that case, it seems that the multi-objective transformation of the bi-level problem as proposed in the present work would be a good choice, whose Pareto front will provide multiple trade-off solutions to select an appropriate compromise solution for implementation.

Since there is no mechanism to visualize the 4-objective Pareto front of Test problem 2, only numerical values of some of its points are shown in Table II. It is seen here that the

TABLE II
NUMERICAL VALUES OF THE PARETO FRONT FOR TEST PROBLEM 2 GIVEN IN TABLE I.

Solution	x_1	x_2	$F_1^{(\mathrm{u})}$	$F_2^{(\mathrm{u})}$	$F_1^{(\mathrm{l})}$	$F_2^{(\mathrm{l})}$
1	0.000	4.000	16.000	17.000	-7.000	64.000
2	0.000	3.970	15.761	16.761	-6.880	63.522
3	0.000	3.873	15.001	16.001	-6.493	61.987
4	0.004	3.790	14.363	15.356	-6.181	60.689
5	0.000	3.735	13.953	14.953	-5.941	59.835
⋮	⋮	⋮	⋮	⋮	⋮	⋮
52	0.002	0.482	0.232	1.227	7.060	20.089
53	0.000	0.399	0.159	1.159	7.406	19.347
54	0.000	0.222	0.049	1.049	8.112	17.825
55	0.000	0.127	0.016	1.016	8.492	17.033
56	0.000	0.000	0.000	1.000	9.000	16.000

best known solution of Test problem 2 is also nothing but an extreme point (i.e., solution number 1) of its Pareto front corresponding to the overall maximum of $F_1^{(u)}$, $F_2^{(u)}$ and $F_2^{(l)}$ and minimum of $F_1^{(l)}$ as expressed in Table I. Hence, the same conclusion as in Test problem 2 can be drawn that the multi-objective transformation of the bi-level problem has merits in terms of providing a set of trade-off solutions as multiple alternatives to choose a suitable compromise solution for implementation. Further, since both the leader and follower of Test problem 2 have two objective functions to be optimized simultaneously, there should be a 2-objective Pareto front for each of them. Since the proposed multi-objective transformation will not give such separate Pareto fronts but a combined one, the objective values of the leader and follower are extracted from the combined Pareto front whose truncated numerical values are shown in Table II. Then $F_1^{(u)}$ versus $F_2^{(u)}$ and $F_1^{(l)}$ versus $F_2^{(l)}$ are plotted as shown in Fig. 2, where it

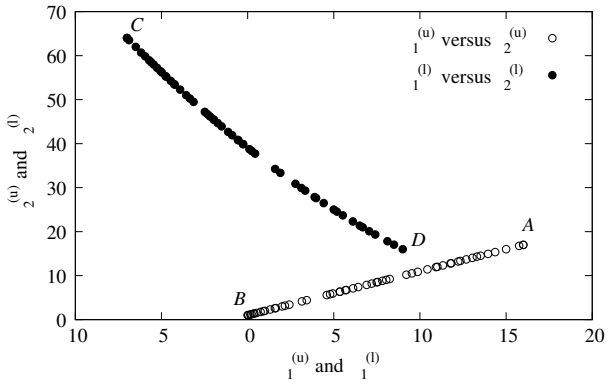

Fig. 2. Plots of the leader and follower objective values for Test problem 2 given in Table I.

is observed that $F_1^{(u)}$ and $F_2^{(u)}$ are correlated, i.e., both are improved or degraded simultaneously. On the other hand, $F_1^{(l)}$ and $F_2^{(l)}$ conflict with each other, i.e., one cannot be improved without degrading the other one by some amount and *vice versa*. In order to confirm these observations, each of the two sets of objective functions is also optimized separately as a two-objective problem (plots are not shown here), in which it is found that the optimized $F_1^{(u)}$ and $F_2^{(u)}$ converge at point *A* shown in Fig. 2, while $F_1^{(l)}$ and $F_2^{(l)}$ form a Pareto front that overlaps with *CD* of Fig. 2. Therefore, it is clear in Fig. 2 that the optimized $F_1^{(u)}$ and $F_2^{(u)}$ converge at different values along *AB* corresponding to the trade-off values of $F_1^{(l)}$ and $F_2^{(l)}$ along their Pareto front *CD*. That is, points A and C of Fig. 2 together form a solution of Test problem 2, points B and D form another solution, and so on in the cases of the intermediate points of *AB* and *CD*.

As in the case of Test problem 2, due to the non-availability of any technique to visualize the 4-objective Pareto front of Test problem 3, only numerical values of some of its points are shown in Table III, where it is observed that the best known solution of the problem is dominated by at least one solution of its Pareto front, specifically solution number 42 as shown in the table.

V. Conclusion

Owing the complicacy of solving the bi-level problem, particularly when it involves multiple objective functions at any level, the problem is transformed here as a plain multi-objective optimization problem by combining its both the levels into a single one. The solution of the transformed problem will be a Pareto front containing a set of trade-off solutions in terms of all the objective functions of the original bi-level problem, even in the case of a single-objective bi-level problem. Employing a multi-objective differential evolution (DE) algorithm to the transformed problem, Pareto fronts containing sets of promising trade-off solutions could be obtained for three test problems of different nature in terms of numbers of followers and objective functions.

References

[1] Z. Tao and X. Qian, "A bilevel programming model for an agriculture production-distribution system with fuzzy random parameters," in *Eighth International Conference on Management Science and Engineering Management*, ser. Advances in Intelligent Systems and Computing, vol. 280. Springer, 2014, pp. 59–72.

[2] A. Sinha, P. Malo, A. Frantsev, and K. Deb., "Multi-objective stackelberg game between a regulating authority and a mining company: A case study in environmental economics," in *IEEE Congress on Evolutionary Computation (CEC-2013)*. IEEE Press, 2013.

[3] G. Zhang, J. Han, and J. Lu, "Fuzzy bi-level decision-making techniques: A survey," *International Journal of Computational Intelligence Systems*, vol. 9, pp. 25–34, 2016.

[4] S. Ma, "A nonlinear bilevel programming approach for product portfolio management," *Springerplus*, vol. 5, no. 1, p. 727, 2016.

[5] J. F. Bard, J. Plummer, and J. C. Sourie, "A bilevel programming approach to determining tax credits for biofuel production," *European Journal of Operational Research*, vol. 120, no. 1, pp. 30–46, 2000.

[6] R. E. Msigwa, Y. Lu, Y. Ge, and L. Zhang, "A smoothing approach for solving transportation problem with road toll pricing and capacity expansions," *Journal of Inequalities and Applications*, p. 237, 2015.

[7] Sonia, A. Khandelwal, and M. C. Puri, "Bilevel time minimizing transportation problem," *Discrete Optimization*, vol. 5, no. 4, pp. 714–723, 2008.

[8] P. Caillard, F. Gillon, S.-A. Randi, and N. Janiaud, "Mono and bi-level optimization architectures for powertrain design," *International Journal for Computation and Mathematics in Electrical and Electronic Engineering*, vol. 35, no. 3, pp. 847–859, 2016.

[9] P. Garcia-Herreros, L. Zhang, P. Misra, E. Arslan, S. Mehta, and I. E. Grossmann, "Mixed-integer bilevel optimization for capacity planning with rational markets," *Computers & Chemical Engineering*, vol. 86, pp. 33–47, 2016.

[10] E. Ghotbi, "Bi- and multi level game theoretic approaches in mechanical design," Ph.D. dissertation, The University of Wisconsin–Milwaukee, USA, 2013.

[11] A. Najafi, H. Falaghi, J. Contreras, and M. Ramezani, "A Stochastic Bilevel Model for the Energy Hub Manager Problem," *IEEE Transactions on Smart Grid*, vol. PP, no. 99, 2016.

[12] J. Xu, S. Zhao, Z. Li, and Z. Zeng, "Bilevel construction site layout optimization based on hazardous-material transportation," *Journal of Infrastructure Systems*, vol. 22, no. 3, p. 04016014, 2016.

[13] O. B. Ayed, "Bi-level linear programming," *Computers & Operations Research*, vol. 20, no. 5, pp. 485–501, 1993.

[14] E. Aiyoshi and K. Shimuzu, "A solution method for the static constrained Stackelberg problem via penalty method," *IEEE Transactions on Automatic Control*, vol. 29, no. 12, pp. 1111–1114, 1984.

[15] H. Li and Y. Wang, "An evolutionary algorithm with local search for convex quadratic bilevel programming problems," *Applied Mathematics and Information Sciences*, vol. 5, no. 2, p. 139146, 2011.

TABLE III
NUMERICAL VALUES OF THE PARETO FRONT FOR TEST PROBLEM 3 GIVEN IN TABLE I.

Solution	x_1	x_2	y_{11}	y_{12}	y_{21}	y_{22}	y_{31}	y_{32}	$F^{(\mathrm{u})}$	$F_1^{(\mathrm{l})}$	$F_2^{(\mathrm{l})}$	$F_3^{(\mathrm{l})}$
1	6.015	1.990	1.631	2.000	1.963	0.001	2.433	0.044	1.071	6.659	2002.795	0.133
2	6.015	1.991	1.631	2.000	1.963	0.049	2.433	0.044	1.079	6.659	43.928	0.091
3	5.696	2.146	1.000	2.000	2.442	0.001	2.263	0.158	1.087	5.000	2002.853	0.170
⋮	⋮	⋮	⋮	⋮	⋮	⋮	⋮	⋮	⋮	⋮	⋮	⋮
42	4.557	2.345	1.944	2.000	1.190	1.022	1.477	0.682	1.489	7.781	5.803	0.225
43	4.539	2.537	1.891	2.000	1.537	1.025	1.446	0.702	1.513	7.574	5.743	0.155
⋮	⋮	⋮	⋮	⋮	⋮	⋮	⋮	⋮	⋮	⋮	⋮	⋮
50	4.475	2.566	1.690	2.000	2.071	1.052	1.553	0.631	1.693	6.856	5.840	0.454
52	4.250	2.123	1.064	2.000	1.572	1.590	2.287	0.142	2.026	5.132	5.096	14.952
53	3.990	2.296	1.144	2.000	2.313	1.479	2.023	0.318	2.420	5.310	5.639	4.288

[16] G. Wang, Z. Wan, X. Wang, and Y. Lv, "Genetic algorithm based on simplex method for solving linear-quadratic bilevel programming problem," *Computers & Mathematics with Applications*, vol. 56, no. 10, pp. 2550–2555, 2008.

[17] A. Sinha, P. Malo, and K. Deb, "Evolutionary algorithm for bilevel optimization using approximations of the lower level optimal solution mapping," *European Journal of Operational Research*, 2016, doi: http://dx.doi.org/10.1016/j.ejor.2016.08.027.

[18] I. Nishizaki and M. Sakawa, "Stakelberg solutions to multiobjective two-level linear programming problems," *Journal of Optimization Theory and Applications*, vol. 103, pp. 161–182, 1999.

[19] X. Shi and H. Xia, "Interactive bilevel multi-objective decision making," *The Journal of the Operational Research Society*, vol. 48, no. 9, pp. 943–949, 1997.

[20] ——, "Model and interactive algorithm of bi-level multi-objective decision-making with multiple interconnected decision makers," *Journal of Multi-Criteria Decision Analysis*, vol. 10, pp. 27–34, 2001.

[21] G. Zhang, J. Lu, and T. Dillon, "Decentralized multi-objective bilevel decision making with fuzzy demands," *Knowledge-Based Systems*, vol. 20, pp. 495–507, 2007.

[22] K. Deb and A. Sinha, "Solving bilevel muti-objective optimization problems using evolutionary algorithms," ser. Lecture Notes in Computer Science (LNCS), M. Ehrgott *et al.*, Eds., vol. 5467. Springer, 2009, pp. 110–124.

[23] I. A. Baky and M. A. Abo-Sinna, "TOPSIS for bi-level MODM problems," *Applied Mathematical Modelling*, vol. 37, pp. 1004–1015, 2015.

[24] B. Liu, "Stackelberg-Nash equilibrium for multilevel programming with multiple followers using genetic algorithms," *Computers & Mathematics with Applications*, vol. 36, no. 7, pp. 79–89, 1998.

[25] D. Datta and J. R. Figueira, "Graph partitioning by multi-objective real-valued metaheuristics: A comparative study," *Applied Soft Computing*, vol. 11, no. 5, pp. 3976–3987, 2011.

Multi-objective optimization of the multi-floor facility layout problem

Zahnupriya Kalita
Department of Mechanical Engineering
Tezpur University
Tezpur - 784 028, Assam, India
Email: zk@tezu.ernet.in

Dilip Datta
Department of Mechanical Engineering
Tezpur University
Tezpur - 784 028, Assam, India
Email: ddatta@tezu.ernet.in / datta_dilip@rediffmail.com

***Abstract*—The multi-floor facility layout problem (MFLP) involves the optimal arrangement of given facilities in multiple floors. Considering that the facilities are to be arranged in multiple floors starting from the left origin of each floor, the MFLP is formulated here as a multi-objective optimization problem for simultaneously minimizing the number of floors and the overall material handling cost. The overall material handling cost involves the individual material handling cost among the facilities arranged in the same floor as well as in different floors. The horizontal and vertical material handling costs between two given facilities are considered to be different as the vertical flow of materials requires the install of elevators also. Solving the present formulation of the MFLP by customizing a permutation-based genetic algorithm, results of a number of test instances of varying sizes are provided as benchmark.**

I. Introduction

The facility layout problem (FLP) usually seeks an optimal arrangement of facilities by minimizing the material handling cost among them. The FLP has applications in the manufacturing and service industries. It deals with the arrangement of various machines in a manufacturing line, as well as the arrangement of various departments in service sectors such as office, hospital, etc. The single row facility layout problem (SRFLP) has been studied extensively, where the facilities are arranged along a single row. However, expensive and limited land supply specially in urban areas, as well as the requirement for reducing material handling cost, makes it essential to arrange given facilities even in multiple floors, which is known as the multi-floor facility layout problem (MFLP).

Initially some heuristic techniques were applied to solve the MFLP [1], [2]. Due to the limitation of the heuristic techniques in getting stuck at local optimum, various meta-heuristics are being investigated. Meller et al. [3] proposed a simulated annealing based approach, named as SABLE, to attain the global optimum solutions. Some two-stage approaches, such as STABLE [4] and FAF/TS [5], were also investigated, which combine heuristic techniques with exact methods. In the first stage of a two-stage approach, exact methods such as the mixed integer linear programming (MIP) are used to arrange the facilities in different floors based on their vertical flow cost. Then some heuristic techniques such as Tabu search are applied in the second stage for optimizing the layout of each floor. However, the approach faced the limitation of facility exchange among different floors. An alternative approach, known as the FLEX, was proposed by Meller and Bozer [6], which outperformed STABLE [4] both in overcoming this limitation and in computational aspect. Another two-stage approach was proposed by Bernardi and Anjos [7], where an MIP model was used in the first stage and another mathematical-programming framework in the second stage.

Based on practical scenarios, such as number, location and utilization of elevators, the MFLP was handled by Matsuzaki et al. [8] using simulated annealing and genetic algorithm. Lee et al. [9] investigated a genetic algorithm to arrange the compartments in a ship as an MFLP model. In another study, Goetschalckx and Irohara [10] provided an MFLP formulation for manufacturing industries to serve by elevators only at two or three adjacent floors, and another formulation for office buildings to serve at any floor.

In all of the above works, the MFLP was studied for minimizing the overall material handling cost among the facilities under the consideration of fixed number of floors, each of equal length. No work could be found in specialized literature studying the MFLP with flexibility to length and number of floors.

Motivated by the above research gap in literature and practical requirement, the MFLP is formulated here as a multi-objective optimization problem for simultaneously minimizing the overall material handling cost among the facilities and the number of floors in which the given facilities can be arranged. Further, a permutation-based genetic algorithm is customized to handle the MFLP model. In the numerical experimentation, a number of test instances of sizes in the range of [9,30] are solved and the comparison with their SRFLP results is presented.

The paper is organized as follows: the problem is described in Section II, followed by its formulation in Section III and the solution procedure in Section IV. Presenting the computational

978-1-5090-5674-3/17/$31.00 ©2017 IEEE

results in Section V, the article is concluded in Section VI summarizing the present work and highlighting the future scope on the theme.

II. Problem description

In the MFLP model studied in the present work, a given set of facilities are to be placed in multiple floors so as to simultaneously minimize the overall material handling cost among the facilities and the number of floors in which the facilities are to be placed. Various assumptions made in the MFLP model are as follows:

1) The placement of the facilities is started from the left corner of every floor.
2) Inter-floor interaction occurs through the nearest one out of the two elevators located at the two corners of a floor.
3) There is no physical gap between two consecutive facilities placed in a floor.
4) All the floors are of the same height.
5) The total height of the floors cannot be greater than the maximum floor length. This restriction is imposed just to create an upper bound to the total height of the floors.

III. Problem formulation

For formulating the MFLP model at hand, the following notations are defined:

Indices

i, j	: Indices of facilities
k, l	: Indices of floors
π	: Index of a permutation of given facilities

Fixed parameters

m	: Number of facilities to be arranged
l_i	: Length of the ith facility
L	: Average length of m number of facilities
c_{ij}	: Horizontal material handling cost between the ith and jth facilities (i.e., when the facilities are placed in the same floor)
c'_{ij}	: Vertical material handling cost between the ith and jth facilities (i.e., when the facilities are placed in different floors)
h	: Height of a floor

Variables

N	: Total number of floors
L_k	: Length of the kth floor
d_{ij}	: Horizontal distance between the ith and jth facilities (i.e., when the facilities are placed in the same floor)
n_i	: Floor in which the ith facility is placed

Objective function

f_1	: Overall material handling cost among all the given m facilities
f_2	: Number of required floors.

In terms of the above notations, the proposed MFLP is formulated as given by Eqs. (1)–(3).

$$\text{Minimize} \quad f_1^\pi = \sum_{i=1}^{m-1} \sum_{j=i+1}^{m} \left[c_{ij} d_{ij}^\pi + c'_{ij} h |n_i^\pi - n_j^\pi| \right] \quad (1)$$

$$\text{Minimize} \quad f_2^\pi = N^\pi \quad (2)$$

$$\text{Subject to} \quad N^\pi h \leq \max \{ L_k | L_k \ ; \ k = 1, 2, \ldots, N^\pi \} \quad (3)$$

Equations (1) and (2) represent the two objective functions to be minimized, which are respectively the overall material handling cost among all the facilities and the number of floors for their placement. Equation (3) is a constraint that creates an upper limit to the total height of all the floors. The computations of the horizontal distance d_{ij}^π and vertical distance $h|n_i^\pi - n_j^\pi|$ between the ith and jth facilities of the permutation π, used in Eq. (1), are explained in Section III-B.

A. Forming MFLP solution

Any permutation π of given m facilities will not directly represent a solution of the MFLP. Therefore, a valid MFLP solution is to be formed before evaluating it using Eqs. (1)–(3), which is explained here.

An MFLP solution from a permutation π of given m facilities is formed by distributing the facilities into N floors. This is done as follows:

The average length L of each of the N floors is first calculated using Eq. (4).

$$L = \frac{\sum_{i=1}^{m} l_i}{N} \quad (4)$$

Then, a floor is formed by placing the facilities of π in it one by one until the total length of the floor becomes L. However, since the length of a facility is a discrete one, the following two cases may arise as illustrated in Fig. 1:

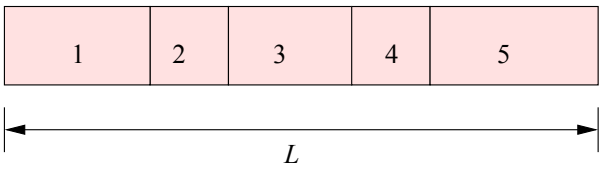

(a) Floor length equals its average value.

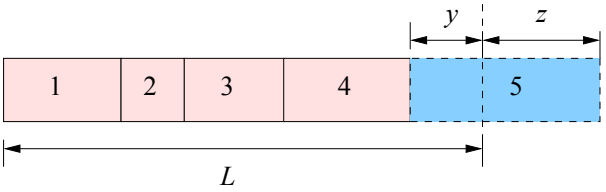

(b) Floor length deviates from its average value.

Fig. 1. Forming an MFLP solution from a permutation of given facilities.

1) As shown in Fig. 1(a), the length of the kth floor will become exactly L if facilities 1–5 are placed in it. Hence, the kth floor is formed with facilities 1–5 and the remaining facilities are taken to the other floor(s).

2) As shown in Fig. 1(b), the length of the kth floor will be shorter by y from L if facilities 1–4 are placed in it, while it will exceed by z if facilities 1–5 are placed in it. Hence, in order to avoid excessive deviation from the average floor length L, the kth floor will be formed with facilities 1–4 if $y < z$ and with facilities 1–5 if $z < y$, while it can be formed randomly either with facilities 1–4 or facilities 1–5 if $y = z$.

B. Distance between two facilities

Once an MFLP solution is formed as explained in Section III-A, the total number of floors N^{π} (used in Eqs. (2) and (3)), in which the facilities of permutation π are placed, is obtained automatically.

The computation of the distance between two given facilities, required in Eq. (1), is explained below with the help of Fig. 2:

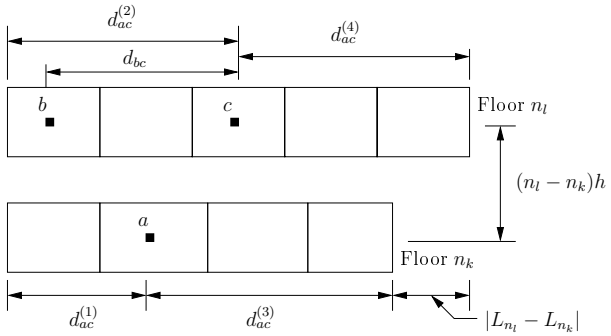

Fig. 2. Distance between two facilities in a permutation.

1) If the two facilities are placed in the same floor, the horizontal distance between them would simply be their centroidal distance in the horizontal direction. This is illustrated in Fig. 2 by d_{bc} as the horizontal distance between facilities b and c. Further, since the facilities are placed in the same floor, they will have no vertical distance, i.e., their vertical distance is zero.
2) If the two facilities are placed in two different floors, they can be interacted through any of the two elevators located at their two corners. However, the shortest distance is considered for reducing the material handling cost between them. This is illustrated in Fig. 2 as the interaction between facilities a and c placed in floor n_k and n_l, respectively. Their horizontal distance through the left elevator is $(d_{ac}^{(1)} + d_{ac}^{(2)})$ and through the right elevator is $(d_{ac}^{(3)} + d_{ac}^{(4)} + |L_{n_l} - L_{n_k}|)$. Hence, the minimum of $(d_{ac}^{(1)} + d_{ac}^{(2)})$ and $(d_{ac}^{(3)} + d_{ac}^{(4)} + |L_{n_l} - L_{n_k}|)$ will be used in Eq. (1) as the horizontal distance between facilities a and c. Further, being in different floors, their vertical distance will be $h(n_l - n_k)$.

IV. Solution procedure

The proposed MFLP model is investigated by customizing the permutation based genetic algorithm (pGA) presented in [11], [12] for studying facility layout problem. The steps followed in the customized GA are outlined below:

1) The GA population is formed with a set of D solutions, where a solution is an array representing a permutation of given m number of facilities. Each solution of the GA population is initialized with a random population using the technique presented in [12].
2) MFLP solutions are formed as explained in Section III-A.
3) The objective values of the MFLP solutions are calculated using Eqs. (1) and (2).
4) Applying the crowded tournament selection operator, a temporary GA population of size D is formed by multiple copies of the solutions of the original GA population based on their non-dominating ranks and crowding distances.
5) Applying the crossover operator, used in [12], a new GA population of size D is generated by exploiting the temporary GA population formed in Step (4) above. In this operator, a new solution is formed from two random solutions taken from the temporary GA population. The positions of the new solutions are filled up by taking facilities from the same positions of any of the two parent solutions. If a position cannot be filled up by taking facilities from the parents, it is kept in reserved. Finally, all the reserved positions are filled up by taking the remaining facilities in a random order.
6) In the mutation, the neighborhood of each new solution generated by the crossover is explored by interchanging the facilities of two random positions.
7) Repeating Steps (2) and (3) for the solutions obtained in Step (6) above, MFLP solutions are formed and evaluated.
8) The GA population for the next iteration is formed by the best 50% solutions from the combination of the original and new GA populations based on the non-dominated ranks and crowding distances of their solutions.
9) Steps (2)–(8) are repeated until a predefined number of GA iterations are performed.

V. Computational experiments and discussion

The procedure proposed in the present work is coded in C programming language and executed in the Fedora 15 Linux environment in a HP Desktop. The computational experiment is performed with instances of different sizes varying in the range of [9,30].

A. Experimental setup

For handling the above instances to evaluate the proposed MFLP model, the range of floors, in which the facilities of an instance can be arranged, is fixed as [1,5] for instances of sizes up to 11 and as [1,15] for the remaining instances. The height of a floor is taken as 3 in all the instances. Further, since the vertical material handling costs for none of these instances are

available in literature, it is taken as 1.5 times of the horizontal material handling cost of each pair of facilities.

Since the pGA is a stochastic optimization tool, the solutions may vary with its parameter settings. Hence, multiple runs are performed for comparison with different sets of initial solutions. Other parameter values, fixed based on some trial runs, are given in Table I.

TABLE I
GA PARAMETER VALUES USED IN THE NUMERICAL COMPUTATION.

GA parameter	Value
Population size	60
Crossover probability	50%
Mutation probability	10%
Number of iterations	500 (for permutation sizes ≤ 11) 10000 (for permutation sizes > 11)
Number of runs	30

B. Results

With the experimental setup stated in Section V-A, a total of 14 instances of different sizes are considered for evaluating the proposed MFLP model. Two instances each of size 9 with different lengths of the facilities, which were originally introduced by Simmons [13] for evaluating a SRFLP model, are studied first. In each of the 30 runs of the GA for both the instances, the final Pareto front was found containing multiple trade-off solutions placing the facilities in a maximum of 4 floors. The detail results against the minimum and maximum number of floors, including the facilities and length of each floor, obtained in a random run for the instances are given in Table II. It may be noticed in Table II that both the overall material handling cost (f_1) and floor length could be reduced in the MFLP model by arranging the facilities in multiple floors over the SRFLP model arranging them in a single floor (row).

TABLE II
RESULTS OF THE MFLP INSTANCES OF 9 FACILITIES.

Instance	Size	Flow cost (f_1)	No. of floors (f_2)	Floor number	Facilities placed in the floor	Floor length
S9 [13]	9	2469.5	1	1	2 3 6 9 1 5 7 4 8	56
		2227.5	4	1	7 2	14
				2	6 3	13
				3	5 1 9	14
				4	4 8	15
S9h [13]	9	4695.5	1	1	9 5 2 1 7 3 6 4 8	59
		3697.5	4	1	3 5	13
				2	8 2	15
				3	6 7 1	16
				4	4 9	15

Studying two more small-size instances of sizes 10 and 11, which were also originally introduced by Simmons [13] for evaluating his SRFLP model, similar results as in Table II are obtained. These results are given in Table III.

After the two sets of small-size instances, a set of 5 instances each of size 25 with different facility lengths and flow costs, which were originally introduced by Nugent et al. [14] for evaluating a SRFLP model, are studied. The results containing the objective values of these instances, obtained in one of the 30 runs of the GA, are presented in Table IV. Though the final Pareto fronts of the instances contained multiple trade-off solutions in terms of the two objective functions (except instance N25_01, whose Pareto front converged to a single solution), only the solutions arranging the facilities in the maximum number of floors are presented in Table IV. For illustration, the plots of the Pareto fronts, obtained in different GA runs for instance N25_04, are also shown in Fig. 3.

TABLE III
RESULTS OF THE MFLP INSTANCES OF 10 AND 11 FACILITIES.

Instance	Size	Flow cost (f_1)	No. of floors (f_2)	Floor number	Facilities placed in the floor	Floor length
S10 [13]	10	2781.5	1	1	9 3 1 7 5 10 4 2 6 8	60
		2467	4	1	10 7	15
				2	5 2 4 6	15
				3	8 1	15
				4	3 9	15
S11 [13]	11	6933.5	1	1	11 9 7 2 1 10 6 4 3 5 8	67
		5882	4	1	9 11	16
				2	7 1 2	17
				3	3 4 6	17
				4	10 8 5	17

TABLE IV
OBJECTIVE VALUES OF THE MFLP INSTANCES OF 25 FACILITIES.

Instance	Size	f_1	f_2	Floor length
N25_01 [14]	25	4618	1	25
N25_02 [14]	25	18140.5	9	28
N25_03 [14]	25	13976	8	20
N25_04 [14]	25	21145.5	12	29
N25_05 [14]	25	10956.5	6	16

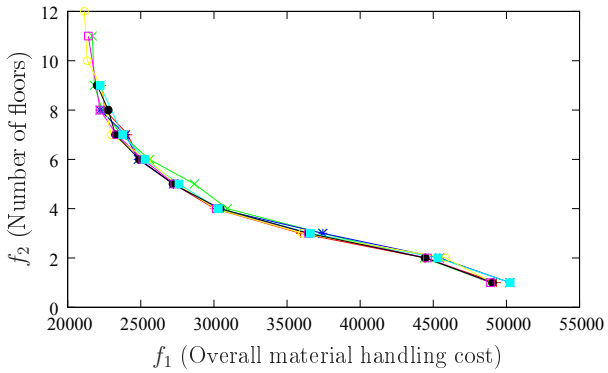

Fig. 3. Pareto fronts obtained in different GA runs for instance N25_04 of Table IV.

Finally, another set of 5 instances each of size 30 with different facility lengths and flow costs are studied, which were also originally introduced by Nugent et al. [14] for evaluating

their SRFLP model, are studied. The results containing the objective values of these instances, obtained in one of the 30 runs of the GA, are presented in Table V in a similar way as in Table IV. Here, the Pareto front of instance N30_01

TABLE V
OBJECTIVE VALUES OF THE MFLP INSTANCES OF 30 FACILITIES.

Instance	Size	f_1	f_2	Floor length
N30_01 [14]	30	8278	1	30
N30_02 [14]	30	15143.5	6	14
N30_03 [14]	30	23478.5	8	24
N30_04 [14]	30	26417	9	29
N30_05 [14]	30	39766	14	40

converged to a single solution, and those of all other 4 instances converged at a set of trade-off solutions. However, only the solutions arranging the facilities in the maximum number of floors are presented in Table V. Further, the plots of the Pareto fronts, obtained in different GA runs for instance N30_05, are also shown in Fig. 4.

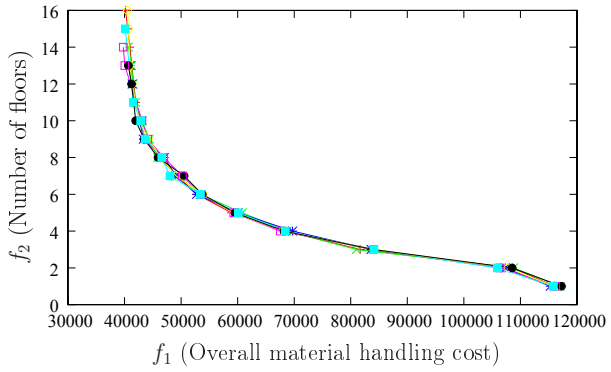

Fig. 4. Pareto fronts obtained in different GA runs for instance N30_05 of Table V.

VI. CONCLUSION

A new model of the multi-floor facility layout problem (MFLP) is proposed here. It is formulated as a multi-objective optimization problem for arranging given facilities in multiple floors by simultaneously minimizing the overall material handling cost among the facilities and the maximum number of floors required for their placement. It is considered that facilities are placed in a floor, starting from its left end, without allowing any physical gap between two facilities. Two facilities placed in two different floors are allowed to interact only through one of the elevators placed at two corners of the floors. Further, an upper bound to the total height of the floors is also created by imposing a constraint.

Customizing a permutation-based multi-objective genetic algorithm, available in literature, a set of MFLP instances of different sizes in the range of [9,30] are studied and their detail results are presented. It is observed that both material handling cost and floor size can be reduced by arranging given facilities in multiple floors, instead of a single floor (row) as studied under the single-row facility layout problem (SRFLP).

All the instances studied in the present work are one dimensional, i.e., the facilities have only lengths. The proposed MFLP model may be extended to study more realistic cases considering both length and width of the facilities.

REFERENCES

[1] R. V. Johnson, "Spacecraft for multi-floor layout planning," *Management Science*, vol. 28, no. 4, pp. 407–417, 1982.
[2] Y. A. Bozer, R. D. Meller, and S. J. Erlebacher, "An improvement-type layout algorithm for single and multiple-floor facilities," *Management Science*, vol. 40, no. 7, pp. 918–932, 1994.
[3] R. D. Meller and Y. A. Bozer, "A new simulated annealing algorithm for the facility layout problem," *International Journal of Production Research*, vol. 34, no. 6, pp. 1675–1692, 1996.
[4] R. D. Meller and K.-Y. Gau, "The facility layout problem: recent and emerging trends and perspectives," *Journal of manufacturing systems*, vol. 15, no. 5, pp. 351–366, 1996.
[5] S. Abdinnour-Helm and S. W. Hadley, "Tabu search based heuristics for multi-floor facility layout," *International Journal of Production Research*, vol. 38, no. 2, pp. 365–383, 2000.
[6] R. D. Meller and Y. A. Bozer, "Alternative approaches to solve the multi-floor facility layout problem," *Journal of Manufacturing Systems*, vol. 16, no. 3, pp. 192–203, 1997.
[7] S. Bernardi and M. F. Anjos, "A two-stage mathematical-programming method for the multi-floor facility layout problem," *Journal of the Operational Research Society*, vol. 64, no. 3, pp. 352–364, 2013.
[8] K. Matsuzaki, T. Irohara, and K. Yoshimoto, "Heuristic algorithm to solve the multi-floor layout problem with the consideration of elevator utilization," *Computers & Industrial Engineering*, vol. 36, no. 2, pp. 487–502, 1999.
[9] K.-Y. Lee, M.-I. Roh, and H.-S. Jeong, "An improved genetic algorithm for multi-floor facility layout problems having inner structure walls and passages," *Computers & Operations Research*, vol. 32, no. 4, pp. 879–899, 2005.
[10] M. Goetschalckx and T. Irohara, "Efficient formulations for the multi-floor facility layout problem with elevators," *Optimization Online*, pp. 1–23, 2007.
[11] D. Datta, A. R. Amaral, and J. R. Figueira, "Single row facility layout problem using a permutation-based genetic algorithm," *European Journal of Operational Research*, vol. 213, no. 2, pp. 388–394, 2011.
[12] Z. Kalita and D. Datta, "Solving the bi-objective corridor allocation problem using a permutation-based genetic algorithm," *Computers & Operations Research*, vol. 52, pp. 123–134, 2014.
[13] D. M. Simmons, "One-dimensional space allocation: An ordering algorithm," *Operations Research*, vol. 17, no. 5, pp. 812–826, 1969.
[14] C. E. Nugent, T. E. Vollmann, and J. Ruml, "An experimental comparison of techniques for the assignment of facilities to locations," *Operations research*, vol. 16, no. 1, pp. 150–173, 1968.

Operational cost minimization in heat exchanger network under milk fouling

Dimbalita Deka
Department of Mechanical Engineering
Tezpur University
Napaam, Tezpur, Assam–784028
Email: dimbalitadeka@gmail.com

Dilip Datta
Department of Mechanical Engineering
Tezpur University
Napaam, Tezpur, Assam–784028
Email: ddatta@tezu.ernet.in / datta_dilip@rediffmail.com

***Abstract*—Milk pasteurization processes in dairy industries, carried out in heat exchanger network (HEN), undergo severe fouling because of the complex biological composition of milk. The formation of fouling gradually reduces the heat transfer capacity requiring to maintain the performance of a HEN by its periodic cleaning for fouling, which not only involves very high cleaning cost but also leads to production loss due to shutdown of the production process during cleaning. Hence, the HEN needs to be scheduled in a way to minimize the cleaning cost satisfying different process conditions as well as avoiding loss in the net production. In this work, the problem is formulated as a single-objective optimization problem for minimizing operational cost and then it is solved using a genetic algorithm. Further, along with the economic criteria, the effects of energy consumption and heating medium flow rate in the process are also discussed.**

I. Introduction

Milk is pasteurized by heating to destroy the micro-organisms dissolved in milk, so that it can be consumed safely [1]. However, the process suffers from the rapid formation of fouling on the heating surface. The major causes of milk fouling are protein denaturation and calcium precipitation, which form precipitated layers on the surfaces of heat exchangers [2], [10]. Milk fouling leads to numerous undesirable phenomena, such as decrease in heat transfer coefficient, increase in pressure drop, loss in product, etc. [2]. Various fouling models, involving such phenomena, are proposed in [4], [11]–[13].

Fouling can be reduced either by improving the design of heat exchangers [3], [4] or through process control by adjusting physical parameters like air content, temperature, pressure, flow rate, preheating, etc. [5]–[7]. Still a heat exchanger is to be cleaned periodically to maintain a low fouling rate. Dairy industries require the cleaning of a heat exchanger for 5–6 hours on daily basis [21].

Industrial heat exchangers are generally cleaned by cleaning-in-place (CIP), cleaning-out-of place (COP) and manual cleaning techniques [8], out of which CIP is found to be the most effective one for dairy industries as it can be applied in the plant itself without disassembling a heat exchanger network (HEN) [9]. However, the CIP technique requires the production process to be stopped in the heat exchanger under cleaning. Moreover, it consumes more water, chemicals and energy, thus involving high cost (cost of cleaning, cost of steam, cost of manpower, cost of electricity, etc.) [14], [15]. Hence, CIP systems require some modifications to make them more efficient [16]. Manufacturing companies, such as ECOLAB [17], OPTEK [18], SIEMENS [19] and SPX [20], have developed some improved CIP systems.

Accordingly, an effective cleaning schedule of the heat exchangers of a HEN becomes essential to minimize the cleaning cost by avoiding any production loss. Many works have been reported on optimal operation of the milk pasteurization process [1], [22], [23], while some other on optimal scheduling of a HEN [21], [24]–[28]. It is found in all of these works that cleaning is scheduled either for a single heat exchanger or a small-size HEN. Also, the optimization models are solved by various classical methods, which are usually inadequate to handle large-size instances of the problem. Further, the classical optimization methods need to transform this mixed integer non-linear programming (MINLP) problem into an equivalent mixed integer linear programming (MILP) model.

Motivated by above mentioned research gap, the milk pasteurization in a serial HEN is formulated here as a mixed integer non-linear single-objective optimization problem for minimizing total cleaning cost subject to some processing conditions. In the numerical experimentation, the effectiveness and limitations of this formulation are demonstrated by solving a case-study using a genetic algorithm (GA).

II. Problem formulation

The optimization of a milk pasteurization process carried out in a serial HEN over a given time period is considered here. The problem is broadly defined as follows:

- Determine
  1) Operational status (heating or cleaning) of each heat exchanger at every time instant.
  2) Final outlet temperature of the steam (heating medium) from the HEN at every time instant.
  3) Final outlet temperature of the milk (processing fluid) from the HEN at every time instant.

978-1-5090-5674-3/17/$31.00 ©2017 IEEE

- To minimize
  1) Total cleaning cost.
- Subject to
  1) Constraint on amount of mass deposition on the surface of a heat exchanger.
  2) Constraint on maximum operating time of a heat exchanger.
  3) Constraint on residence time of milk in the HEN.
  4) Constraint on cleaning of a heat exchanger at two consecutive time instants.
  5) Constraint on temperature difference between steam and milk.
  6) Constraint on temperature of milk at the outlet of the HEN.

The following are the notations to be used in the optimization formulation of the problem:

- *Indices*
  i : ith heat exchanger.
  t : tth time instant.
- *Parameters*
  N : Total number of heat exchangers in the HEN.
  T : Duration of the production cycle.
  A_i : Surface area of the heat exchanger.
  Γ_i : Permitted period of continuous operation.
  ζ_{ij} : Heat transfer coefficient after the jth time instant ($\zeta_{ij} \leqslant \Gamma_i$) of operation.
  Θ_t^{hinit} : Initial temperature of steam.
  Θ_t^{finit} : Initial temperature of milk.
  Θ_t^{fmin} : Required minimum temperature of milk at the outlet of the HEN.
  $\delta\Theta_t$: Minimum temperature difference between steam and milk.
  c^{h} : Specific heat capacity of steam.
  c^{f} : Specific heat capacity of milk.
  F^{f} : Flow rate of milk.
  δ_i^{crit} : Critical amount of mass deposition (fouling).
  γ_i : Slope of the profile of mass deposition.
  r_i : Residence time of milk during operation.
  $r^{\min}$: Minimum overall residence time in the HEN.
  C_t^{h} : Cost coefficient of steam.
  C_{it}^{fix} : Fixed cost coefficient associated with CIP.
  C_{it}^{var} : Variable cost coefficient associated with CIP.
- *Main variables*
  u_{it} : Operational status.
  Θ_t^{hfinal} : Steam temperature at the outlet of the HEN.
  Θ_t^{ffinal} : Milk temperature at the outlet of the HEN.
- *Auxiliary variables*
  h_{it} : Heat transfer coefficient under fouling.
  τ_{it} : Number of continuous operational time instants ($\tau_{it} \leqslant \Gamma_i$).
  Θ_{it}^{hin} : Inlet temperature of steam.
  Θ_{it}^{fin} : Inlet temperature of milk.
  $\Theta_{it}^{\text{fout}}$: Outlet temperature of milk.
  ϕ_t : Total number of operational heat exchangers.

The operational status of the heat exchangers over the time instants (u_{it}) can be expressed by Eq. (1).

$$u_{it} = \begin{cases} 0\ ; & \text{if } i\text{th heat exchanger is cleaned at } t\text{th instant} \\ 1\ ; & \text{otherwise.} \\ & i = 1, 2, \ldots, N \text{ and } t = 1, 2, \ldots, T\ . \end{cases} \tag{1}$$

The total number of operational heat exchangers (ϕ_t) can be computed using Eq. (2).

$$\phi_t = \sum_{i=1}^{N} u_{it}\ ; \quad t = 1, 2, \ldots, T\ . \tag{2}$$

The number of continuous operational time instants of the ith heat exchanger at the tth time instant (τ_{it}) can be obtained using Eq. (3).

$$\tau_{it} = \begin{cases} 0\ ; & \text{if } \ u_{it} = 0\ ,\ \forall t = 1, 2, \ldots, T \\ c\ ; & \text{if } \ t = T\ ;\ u_{i,t-j+1} = 1\ ; \\ & \quad\ u_{i,t-c} = 0\ ;\ j = 1 \text{ to } c \\ 1 + \tau_{iT}\ ; & \text{if } \ u_{it} = 1 \text{ and } t = 1 \\ 1 + \tau_{i,t-1}\ ; & \text{if } \ u_{it} = 1 \text{ and } 1 < t < T \end{cases} \tag{3}$$

The decreased heat transfer co-efficients (h_{it}) due to increased mass deposition on the heat exchanger surface over time, can be calculated using Eq. (4) as a function of τ_{it}.

$$h_{it} = \begin{cases} \zeta_{i,\tau_{it}}\ ; & \text{if } \tau_{it} > 0 \\ 0\ ; & \text{otherwise.} \end{cases} \tag{4}$$

In Eq. (4), $\zeta_{i,\tau_{it}}$ can be obtained experimentally or computational analysis of the complete milk pasteurization process.

The steam temperature at the entry (Θ_{it}^{hin}) of a heat exchanger can be obtained by uniformly distributing ($\Theta_t^{\text{hinit}} - \Theta_t^{\text{hfinal}}$) over all the operational heat exchangers of a time instant as given by Eq. (5).

$$\Theta_{it}^{\text{hin}} = \begin{cases} \Theta_t^{\text{hinit}}\ ; & \text{if } i \leqslant s_t \\ \Theta_{i-1,t}^{\text{hin}}\ ; & \text{if } i > s_t \text{ and } u_{i-1,t} = 0 \\ \Theta_{i-1,t}^{\text{hin}} - \Delta_t\ ; & \text{if } i > s_t \text{ and } u_{i-1,t} = 1 \end{cases} \tag{5a}$$

$$\text{where,} \quad s_t = \min\{p \mid u_{pt} = 1\ ;\ p = 1, 2, \ldots, N\} \tag{5b}$$

$$\text{and,} \quad \Delta_t = \frac{\Theta_t^{\text{hinit}} - \Theta_t^{\text{hfinal}}}{\phi_t - 1} \tag{5c}$$

In Eq. (5), s_t is the first operational heat exchanger at time instant t. It is considered in Eq. (5a) that steam temperature in a heat exchanger at a time instant will be lost by an amount of Δ_t if the heat exchanger is in operation at that time instant.

Milk temperatures at the entry and exit of a heat exchanger and at the outlet of the HEN at different time instants may be obtained as given by Eq. (6).

$$\Theta_{it}^{\text{fin}} = \begin{cases} \Theta_t^{\text{finit}}\ ; & \text{if } i = 1 \\ \Theta_{i-1,t}^{\text{fout}}\ ; & \text{otherwise.} \end{cases} \tag{6a}$$

$$\Theta_{it}^{\text{fout}} = \begin{cases} \Theta_{it}^{\text{fin}}\ ; & \text{if } u_{it} = 0 \\ \frac{A_i h_{it}\left(2\Theta_{it}^{\text{hin}} - \Theta_{it}^{\text{fin}}\right) + 2F^{\text{f}}c^{\text{f}}\Theta_{it}^{\text{fin}}}{A_i h_{it} + 2F^{\text{f}}c^{\text{f}}}\ ; & \text{otherwise.} \end{cases} \tag{6b}$$

$$\Theta_t^{\text{ffinal}} = \Theta_{Nt}^{\text{fout}} \tag{6c}$$

Finally, the optimization of the milk pasteurization process can be formulated mathematically as given by Eqs. (7) and (8).

$$\text{Minimize} \quad f \equiv \sum_{t=1}^{T} C_t^{\mathrm{h}} \Theta_t^{\mathrm{hinit}} + \sum_{i=1}^{N} \sum_{t=1}^{T} \left\{ C_{it}^{\mathrm{fix}} \left(1 - u_{it}\right) + C_{it}^{\mathrm{var}} d_{it} \right\} \quad (7a)$$

$$\text{with} \quad d_{it} = \begin{cases} \tau_{iT} \ ; & \text{if } t = 1 \\ \tau_{i,t-1} \ ; & \text{if } t > 1 \end{cases} \quad (7b)$$

$$\text{Subject to} \quad g_1 \equiv \ \gamma_i \Gamma_i \leqslant \delta_i^{\mathrm{crit}} \quad (8a)$$

$$g_2 \equiv \ \tau_{it} \leqslant \Gamma_i \quad (8b)$$

$$g_3 \equiv \ \sum_{i=1}^{N} r_i u_{it} \geqslant r^{\min} \quad (8c)$$

$$g_4 \equiv \ \left(1 - u_{i\alpha}\right)\left(1 - u_{it}\right) \neq 0 \ ; \quad \alpha = T \text{ if } t = 1, \text{ else } \alpha = t - 1 \quad (8d)$$

$$g_5 \equiv \ \Theta_{it}^{\mathrm{hin}} - \Theta_{it}^{\mathrm{fin}} \geqslant \delta\Theta_t \quad (8e)$$

$$g_6 \equiv \ \left(\Theta_{it}^{\mathrm{hin}} - u_{it}\delta\Theta_t\right) - \Theta_{it}^{\mathrm{fout}} \geqslant \delta\Theta_t \quad (8f)$$

$$g_7 \equiv \ \Theta_t^{\mathrm{ffinal}} \geqslant \Theta_t^{\mathrm{fmin}} \quad (8g)$$

In Eq. (7a), the objective function f represents the total clean-in-place (CIP) cost, which includes the cost of steam, fixed cleaning cost and variable cleaning cost. Also, d_{it} in Eq. (7b) indicates the number of continuous operational time instants prior to the cleaning time instant. The constraints given by g_1–g_7 in Eqs. (8a)–(8g) represent, respectively, the amount of mass deposition, continuous operational time, residence time of milk in the HEN, cleaning of a heat exchanger at two consecutive time instants, temperature difference between steam and milk at the entry of the heat exchanger, temperature difference between steam and milk at the exit of the heat exchanger, and temperature of milk at the outlet of the HEN. Since these constraints are hard to handle, some repairing mechanisms may be used for their forced satisfaction.

III. Genetic algorithm for solving the problem

In the present optimization problem, a HEN of N heat exchangers is to be scheduled over T time instants. Accordingly, the problem involves $N \times T$ number of $\{0,1\}$ binary variables (u_{it}; $i = 1, \ldots, N$ and $t = 1, \ldots, T$) and T number of real variables ($\Theta_t^{\mathrm{hfinal}}$; $t = 1, \ldots, T$).

A binary-real-coded version of genetic algorithm (GA), employed by Datta [29] to a problem of similar nature, namely the unit commitment problem in the area of power systems, is adopted here for solving the present problem. In this GA, solution comparison is made with the binary tournament selection operator. The single-point crossover operator and swapping mutation operator are used for working with the binary variables (u_{it}) of the problem, while the simulated binary crossover (SBX) operator and polynomial mutation operator are used for handling the real variables $\Theta_t^{\mathrm{hfinal}}$ (Deb et al. [30] may be referred for detail of these operators).

IV. Numerical experimentation and discussion

The application of the optimization model given by Eqs. (7) and (8) is demonstrated by solving it for a case-study using the GA mentioned in Section III.

A. Case study

A HEN consisting of 15 plate type heat exchangers with counter-current flow, taken from Georgiadis and Papageorgiou [21], is investigated here. All the data related to the HEN and the heat treatment process are kept the same with those given in [21]. The data set includes fixed parameter values related to heat exchanger and heat treatment process (N, A_i, T, $\Theta_t^{\mathrm{hinit}}$, $\Theta_t^{\mathrm{finit}}$, c^{h}, c^{f}, F^{f}, $\delta\Theta_t$, Θ_t^{fmin}, r_i, $r_{\min}$, δ_i^{crit}), heat transfer co-efficients under milk fouling (ζ_{it}), rate of mass deposition on the surfaces of heat exchangers (γ_i) and cleaning cost co-efficients associated with CIP (C_t^{h}, C_{it}^{fix}, C_{it}^{var}).

B. Experimental setup

The problem is solved 30 times with different initial solutions and other user-defined algorithmic parameter values to analyze the statistical performances of the investigated GA. The user-defined algorithmic parameter values are provided in Table I.

TABLE I
User-defined parameter values used in the investigated GA.

Parameter	Value
Population size	100
Maximum number of generations performed	20000
Crossover probability	90%
Distribution index for SBX operator	20
Mutation probability	1%
Distribution index for polynomial mutation operator	35
Number of runs	30

C. Results and discussion

The schedule of the HEN obtained in one out of the 30 independent runs of the GA is given in Table II, where '1' indicates that the corresponding heat exchanger is in operation,

TABLE II
Scheduling of the HEN of 15 heat exchangers over 24 time instants.

Time inst.	Schedule	No. of operating HEs	Time inst.	Schedule	No. of Operating HEs
1	111011111011110	12	13	101011111111110	12
2	111111111100011	12	14	111101111010011	11
3	111110110111101	12	15	111111010111101	12
4	011111101111110	12	16	111110111101111	13
5	111111011010111	12	17	101111101110111	12
6	101111111111011	13	18	011101111011110	11
7	111001111101111	12	19	110111011111001	11
8	110111111111100	12	20	111011111011110	12
9	111110110110111	12	21	101110101101111	11
10	011111011011111	12	22	111111110110011	12
11	110111101111001	11	23	011101011111111	12
12	111111111101111	14	24	100111111111101	12

while '0' means it is under cleaning. It can be observed that the schedule satisfies the residence time constraint (residence time of $r_i = 6$ seconds in a heat exchanger and overall minimum residence time of $r_{\min} = 60$ seconds in the HEN at a time instant), which demands at least 10 operating heat exchangers at each time instant.

The total number of cleaning instants and the corresponding cleaning cost obtained at different runs of the GA are visualized in Fig. 1 (the cleaning cost has been expressed in rmu,

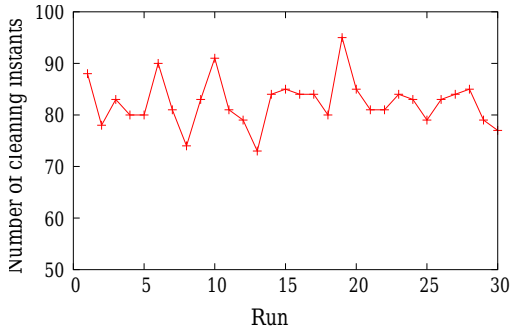

(a) Cleaning instants.

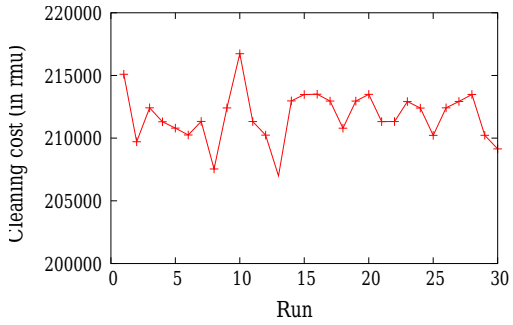

(b) Cleaning cost.

Fig. 1. Number of cleaning instants and cleaning cost obtained at different runs of the GA.

which means relative monetary unit). The statistical analysis of the overall cleaning cost (best, worst, average and standard deviation) over 30 independent runs of the GA is presented in Table III.

TABLE III
STATISTICAL ANALYSIS OF THE CLEANING COST OVER 30 INDEPENDENT RUNS OF THE GA.

Cleaning cost f	Value
Best	206990 rmu
Worst	216737 rmu
Average	211757 rmu
Standard deviation	0.96%

Along with satisfying the economic criteria (minimizing the cleaning cost), thermal balance is also required during the milk heat treatment process to avoid high energy consumption and high steam flow rate. Hence, outlet temperatures of milk and steam are two major issues of concern. It is to be ensured that milk is not overheated consuming excess energy during the process. The steam outlet temperature should also be within some lower bound so as to utilize its heat content completely by maintaining an aspired temperature difference between milk and steam. Hence, for the schedule given in Table II, the temperatures of milk and steam at the outlet of the HEN at different time instants are investigated, the plots of which are shown in Fig. 2. It is observed in Fig. 2(a) that milk leaves

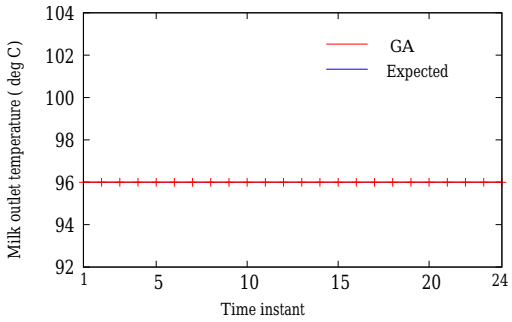

(a) Milk (processing fluid).

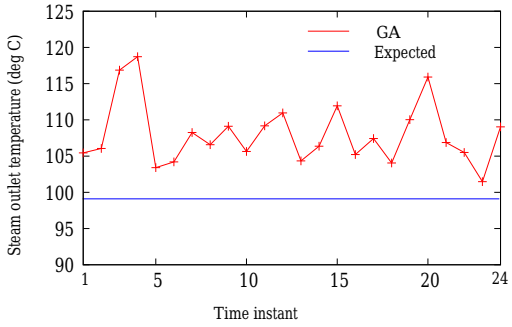

(b) Steam (heating medium).

Fig. 2. Milk and steam temperatures at the outlet of the HEN at different time instants.

the last heat exchanger of the HEN exactly at the expected temperature ($\Theta_t^{\text{fmin}} = 96\,^{\circ}\text{C}$) at all the 24 time instants. On the other hand, it is seen in Fig. 2(b) that steam leaves the HEN at higher temperatures than its minimum possible value ($\Theta_t^{\text{fmin}} + \delta\Theta_t = 99\,^{\circ}\text{C}$) almost at all the 24 time instants, which depicts that the heat of steam is not utilized fully, thus requiring a higher steam flow rate.

In view of above, multi-objective optimization of the milk pasteurization process may be performed for arriving at a set of trade-off solutions by simultaneously minimizing operational cost as well as energy consumption.

V. CONCLUSION

Motivated by the requirement of minimizing cleaning cost of heat exchangers in dairy industries under milk fouling, a mixed-integer optimization problem is formulated in the present work. This cost minimization necessitates scheduling of a heat exchanger network (HEN) and controlling of processing fluid (milk) and heating medium (steam) outlet temperatures at any time instant. Accordingly, a binary-real-coded genetic algorithm (GA) is investigated here for scheduling of a serial HEN over a given time period. The GA could minimize the cleaning cost and maintain the milk outlet

temperatures at the required level. However, the steam outlet temperatures are found to be significantly above the minimum possible level, thus demanding a higher steam flow rate. Hence, further investigation may be carried out for balancing both the economic and thermal performance criteria.

REFERENCES

[1] M. H. Manik, C. S. Bildea, J. Grievink, and C. Marshman, "Modelling and Optimisation of Milk Pasteurisation Processes," (European Symposium on Computer-Aided Process Engineering), 2004.

[2] T. J. M. Jeurnink, *Milk fouling in heat exchangers*. PhD thesis, Wageningen University,The Netherlands, 1996.

[3] A. B. Kananeh and J. Peschel, *Fouling in plate heat exchangers: some practical experience. Heat Exchangers- Basic Design Applications*. http://cdn.intechopen.com/pdfs/30779.pdf: GEA PHE Systems, Germany, 2012.

[4] M. P. Murugesan and R. Balasubramanian, "To study the fouling of corrugated plate type heat exchanger in the dairy industry," *Research Journal of Engineering Sciences*, vol. 2, pp. 5–10, 2013.

[5] B. Bansal and X. D. Chen, "A critical review of milk fouling in heat exchangers," *Comprehensive reviews in food science and food safety*, vol. 5, pp. 27–33, 2009.

[6] S. D. Changani, M. T. Belmar-Beiny, and P. J. Fryer, "Engineering and chemical factors associated with fouling and cleaning in milk processing," *Experimental Thermal and Fluid Science*, vol. 14, pp. 392–406, 1997.

[7] P. D. Jong, "Impact and control of fouling in milk processing," *Trends in Food Science and Technology*, vol. 8, pp. 401–405, 1997.

[8] OZONE, "Study of the cleaning-in-place techniques: public report," (http://ec.europa.eu/environment/life/project/Projects/index.cfm-fuseaction=home.showFile\&rep=file\&fil=OZONECIP_cleaningtechniques.pdf, accessed in January 2014), 2014.

[9] A. Thomas and C. T. Sathian, "Cleaning-in-place (CIP) system in Dairy plant- review," *Journal of Environmental Science, Toxicology and Food technology*, vol. 8, pp. 41–44, 2014.

[10] M. T. B. Beiny and P. J. Fryer, "Preliminary stages of fouling from Whey Protein Solutions," *Journal of Dairy Research*, vol. 60, pp. 467–483, 1993.

[11] P. D. Jong, M. C. te Giffel, H. Straatsma, and M. M. M. Vissers, "Reduction of fouling and contamination by predictive kinetic models," *International Dairy Journal*, vol. 12, pp. 285–292, 2002.

[12] S. June and V. M. Puri, "A 2D dynamic model for fouling performance of plate heat exchangers," *Journal of Food Engineering*, vol. 75, pp. 364–374, 2006.

[13] W. Choi, S. Jun, L. T. Nguyen, N. Rungraeng, H. Yi, S. Balasubramanian, V. M. Puri, and J. Lee, "3-D milk fouling modeling of plate heat exchangers with different surface finishes using computational fluid dynamics codes," *Journal of Food Processing Engineering*, vol. 36, pp. 439–449, 2012.

[14] COST, "Cost of CIP usage," (www.tts-ciptech.com, accessed in January, 2015), 2015.

[15] P. Sandfort, "CIP (Clean-in-place) 3-A Standards defined : Food process consulting," (http://foodprocessconsulting.com/cip-clean-in-place-is-defined-by-the-3-a-standards-eleventh- edition-of-the-model-document-as-the-removal-of-soil-from-product-contact-surfaces-in-their-process-position, accessed in January 2014), 2014.

[16] B. Jude and E. Lemaire, "How to optimize cleaning-in-pace (CIP) processes in food and beverage operations," (www.scheinder-electric.com/documents/support/white-papers/energy-efficiency/how-to-optimize-clean-in-place-CIP-processes.pdf, accessed in July 2014), 2013.

[17] ECOLAB, "CIP in food and Beverage production: Ecolab united Kingdom," (www.uk.ecolab.eu/all-applications/cleaning-in-place, accessed in July, 2014), 2014.

[18] OPTEK, "Clean-in-place (CIP) applications," (www.optek.com/ApplicationNote/General/English/3/Clean-in-place_CIP_applications.asp, accessed in January, 2014), 2014.

[19] SIEMENS, "Flexible cleaning-in-place (CIP) system for perfectly clean dairy operations: Food and beverage," (www.industry.siemens.com/verticals/global/en/food-beverage/dairy-technology/cip-system/pages/default.aspx, accessed in January, 2014), 2014.

[20] SPX, "CIP and sanitation of process plant: white paper," (www.spx.com/en/assets/pdf/CIP_systems, accessed in October, 2014), 2014.

[21] M. C. Georgisdis and L. G. Papageorgiou, "Optimal energy and cleaning management in heat exchanger networks under fouling," *Applied Thermal Engineering*, vol. 78, no. 1, pp. 168–179, 2000.

[22] E. M. Ishiyama, W. R. Paterson, and D. I. Wilson, "Optimum cleaning cycles for heat transfer equipment undergoing fouling and ageing," *Chemical Engineering Science*, vol. 66, pp. 604–612, 2011.

[23] M. Markowski and K. Urbaniec, "Optimal cleaning schedule for heat exchangers in a heat exchanger network," *Applied Thermal Engineering*, vol. 25, pp. 1019–1032, 2005.

[24] E. Bonsignour, "CIP is a food safety must, but can it be optimized to increase your bottom line result? : Food and Beverage," (http://blog.schneider-electric.com/authors/ebonsignour, accessed in November, 2013), 2013.

[25] M. C. Georgisdis and L. G. Papageorgiou, "Optimal scheduling of heat-integrated multipurpose plants under fouling conditions," *Applied Thermal Engineering*, vol. 21, pp. 1675–1697, 2001.

[26] T. Pogiatzis, E. M. Ishiyama, W. R. Paterson, V. S. Vassiliadis, and D. I. Wilson, "Identifying optimal cleaning cycles for heat exchangers subject to fouling and ageing," *Applied Energy*, vol. 89, pp. 60–66, 2012.

[27] S. Sanaye and B. Niroomand, "Simulation of heat exchanger network (HEN) and the optimum cleaning schedule," *Energy Conversion and Management*, vol. 48, pp. 1450–1461, 2007.

[28] F. Smaili, V. S. Vassiliadis, and D. I. Wilson, "Long term scheduling of cleaning of heat exchanger networks," *Institution of Chemical Engineers*, vol. 80, no. 1, pp. 561–578, 2002.

[29] D. Datta, "Unit commitment problem with ramp rate constraint using a binary-real-coded genetic algorithm," *Applied Soft Computing*, vol. 13, no. 9, pp. 3873–3883, 2013.

[30] K. Deb, S. Agarwal, A. Pratap, and T. Meyarivan, "A fast and elitist multi-objective genetic algorithm: NSGA-II," *IEEE Transactions on Evolutionary Computation*, vol. 6, no. 2, pp. 182–197, 2002.

Performance Analysis of a Coal-Fired Open Cycle MHD Plant at Constant Subsonic Inlet Nozzle Mach Number with Variation in Nozzle–Area Ratio

Prabin Haloi and Tapan Kumar Gogoi

Abstract In the present work, a coal-fired magnetohydrodynamics (MHD) power plant is analyzed to predict its performance using constant nozzle inlet Mach number. Two supersonic nozzles, namely, *A* and *B* are taken with the variation in throat to exit area ratio. The nozzle exit parameters, adiabatic flame temperature for coal combustion, and the performance parameters of the segmented Faraday-type MHD generator are calculated using each nozzle separately. It has been found that an increase/decrease in nozzle–area ratio resulted in an increase/decrease in gas velocity at MHD generator inlet but with a reduction in temperature. The nozzle efficiency is found to be almost independent of either the area ratio or Mach number at nozzle exit. The maximum voltage and power are found to increase with increase in area ratio. The nozzle exit velocity and efficiencies are found to vary with area ratio.

1 Introduction

Energy demand worldwide has seen a dramatic increase in power demand in the last few decades. The conventional methods of power generation that widely depends upon fossil fuels have been reduced to some extent due to the advancement of technology and use of nonconventional methods of energy production. Solar, wind, tidal, nuclear energy sources, etc. have been explored and harnessed to meet the demand. At the same time all these sources and their harnessing methods could not reduce dependency on fossil fuels because of their various existing limitations compared to fossil fuel energy resources. Gas and steam turbines have been made more efficient with higher inlet temperature due to the advancement in metallurgy and high-temperature blade and other materials. The use of conventional and most nonconventional technologies of power generation is limited by the maximum material temperature limit, wear and tear, aging, etc. The role of magnetohydrodynamics as a means of power

P. Haloi (✉) · T. K. Gogoi
Department of Mechanical Engineering, Tezpur University, Tezpur, Assam 784028, India
e-mail: haloi_p@tezu.ernet.in

T. K. Gogoi
e-mail: tapan_g@tezu.ernet.in

© Springer Nature Singapore Pte Ltd. 2020

B. B. Biswal et al. (eds.), *Advances in Mechanical Engineering*, Lecture Notes in Mechanical Engineering, https://doi.org/10.1007/978-981-15-0124-1_64

Exergy Modelling of a Coal-Fired MHD Power Plant

Prabin Haloi and Tapan Kumar Gogoi

Abstract Energy quality can be best measured through the application of the proven method of exergy analysis. Exergy analysis of thermal systems provides a better way to determine the deficient sub-components and also estimate the amount of losses that occurred in such components. The present work models a coal-fired open-cycle Magneto-hydrodynamics (MHD) power generation system in terms of exergy analysis. The exergy analysis is carried out side-to-side energy analysis in order to determine the components with major energy losses and exergy destruction in the modelled plant. It is observed that the nozzle has the maximum energy losses as well as exergy destruction followed by the generator. Energy losses for the compressor, combustor, air preheater, seed recovery unit, sulphur removal unit and the stack showed a higher value of energy losses in comparison to that of exergy destruction values in these components. From the exergy point, it has been found that the components that require most improvement ar×e the nozzle and the generator.

Keywords Magneto-hydrodynamics · Energy loss · Exergy · Exergy destruction

Nomenclature

$\xi^{0,ch}$	Chemical exergy of dry coal (kJ/kg)
NCV	Net calorific value (kJ/kg)
$\emptyset_{\text{dry}}$	Ratio of chemical exergy to NCV (dimensionless)
HHV	Higher heating value (MJ/kg)
T(K)	Temperature (K)
$\dot{m}$	Mass flow rate (kg/s)
p	Pressure (bar)

P. Haloi (✉) · T. K. Gogoi
Department of Mechanical Engineering, Tezpur University, Tezpur, Assam 784028, India
e-mail: haloi_p@tezu.ernet.in

T. K. Gogoi
e-mail: tapan_g@tezu.ernet.in

© Springer Nature Singapore Pte Ltd. 2020

H. K. Voruganti et al. (eds.), *Advances in Applied Mechanical Engineering*,
Lecture Notes in Mechanical Engineering,
https://doi.org/10.1007/978-981-15-1201-8_10

ResearchGate

See discussions, stats, and author profiles for this publication at: https://www.researchgate.net/publication/338981253

A Multi-objective Optimization Method Based on Nelder–Mead Simplex Search Method

Chapter · January 2020

DOI: 10.1007/978-981-15-1201-8_72

CITATIONS
0

READS
72

2 authors:

Vivek Kumar Mehta
Tezpur University
17 PUBLICATIONS **41** CITATIONS
SEE PROFILE

Bhaskar Dasgupta
Indian Institute of Technology Kanpur
64 PUBLICATIONS **2,351** CITATIONS
SEE PROFILE

Some of the authors of this publication are also working on these related projects:

Course Project View project

All content following this page was uploaded by Vivek Kumar Mehta on 26 August 2020.

The user has requested enhancement of the downloaded file.

A Multi-objective Optimization Method Based on Nelder–Mead Simplex Search Method

Vivek Kumar Mehta and Bhaskar Dasgupta

Abstract In this paper, a method based on Nelder and Mead's simplex search method is developed for solving multi-objective optimization problems. Unlike other multi-objective optimization algorithms based on classical methods, this method does not require any *a priori* knowledge about the problem. Moreover, it does not need any pre-defined weights or additional constraints as it works without scalarizing the multi-objective problem. The algorithm works with a population of points and is capable of generating a multitude of Pareto optimal solutions. Equipped with the constraint handling strategy adopted in this work, the method is found to be competitive with respect to the existing algorithms.

Keywords Simplex search method · Multi-objective optimization · Pareto optimal solutions

1 Introduction

Nelder and Mead's simplex search method [14] is a well-known direct search classical algorithm for single-objective optimization. The method was introduced for solving the usual single-objective unconstrained optimization problems. In a problem having n design variables, it works with a simplex, which with its $n + 1$ vertices forms a convex hull. Starting with an initial simplex in the design space, the method evaluates the objective function value at each vertex of the simplex and on the basis of these function values determines the worst $\mathbf{x}_w$, second worst $\mathbf{x}_s$, and the best $\mathbf{x}_b$ among them. Next, the algorithm attempts to improve the current simplex by replacing the worst vertex with a potentially better point in the design space. It does so by exploring

V. K. Mehta (✉)
Tezpur University, Tezpur, Assam, India
e-mail: vkmehta@tezu.ernet.in

B. Dasgupta
IIT Kanpur, Kanpur, India
e-mail: dasgupta@iitk.ac.in

© Springer Nature Singapore Pte Ltd. 2020

H. K. Voruganti et al. (eds.), *Advances in Applied Mechanical Engineering*,
Lecture Notes in Mechanical Engineering,
https://doi.org/10.1007/978-981-15-1201-8_72

vkmehta@tezu.ernet.in

the region around the points (other than the worst point) with the help of a reflection followed by a considered option of an expansion, contraction, or shrink.

In recent years, there have been attempts to exploit the potential of this algorithm for multi-objective optimization problems [7, 8, 11, 12]. Using simplex search method for local search along with the usual operations of reproduction, crossover, and mutation involved in genetic algorithm, Koduru et al. [7] proposed a hybrid algorithm, fuzzy simplex genetic algorithm (FSGA), which uses the concept of fuzzy dominance. Martnez and Coello [11] have proposed a method for hybridizing the NSGA-II algorithm with the simplex search method. They have also employed the simplex search method for local exploration and found their method performing better than NSGA-II. However, their method can only handle bound constraints. Kuriger and Grant [8] proposed a lexicographic Nelder–Mead-based simulation optimization (LNM-SO) method. They have used preemptive goal programming strategy for handling multiple objectives. In addition to setting the target value for each goal, the strategy demands the decision maker to rank the goals in order of decreasing importance.

Martinez et al. [12] proposed a nonlinear simplex search-based approach for solving unconstrained multi-objective optimization problems. They have adopted the penalty boundary intersection (PBI) approach [20], which uses weight vectors and a penalty value to convert the multi-objective problem to several single-objective problems. Then, they solve each of these subproblems using simplex search method to obtain several solutions on the Pareto front.

In this paper, a multi-objective optimization method based purely on Nelder–Mead's simplex search method has been developed. The suggested method works without converting the multi-objective optimization problem into single-objective optimization problem and, yet, is capable of generating a multitude of Pareto optimal solutions. The proposed method uses only the basic operations of simplex search method and is capable of handling constraints efficiently. In Sect. 2, the proposed method has been described in detail. Section 3 describes the constraint handling strategy used with the proposed method. Sections 4 and 5 present the results obtained by the proposed method for unconstrained and constrained problems, respectively, followed by the conclusion in Sect. 6.

2 Proposed Algorithm

Evolutionary algorithms work with a population, because of which they are capable of generating several solutions for a multi-objective optimization problem in a single run. Like evolutionary algorithms, the simplex search method, in a way, also works with a population of points. One obvious question than one could ask is the following.

> Could it be used to generate several solutions for a multi-objective optimization problem and that too in a single run?

vkmehta@tezu.ernet.in

This is precisely the question that has been addressed in this work, and the proposed method is an answer to this question. Though the proposed method is based on the simplex search method, it is different from the basic simplex method in two significant aspects.

1. The basic simplex method works with $n + 1$ points and a single simplex, whereas the proposed method works with more than $n + 1$ points and multiple simplices.
2. In the basic simplex method, two points in the design space are compared on the basis of objective function values, whereas in the case of the proposed method, two points are compared on the basis of dominance.

Moreover, in the proposed algorithm the number of vertices used to form a simplex, nps, is also taken as a parameter. In the usual simplex method, the number of vertices to form a simplex, nps, is taken as $(n + 1)$. To explore an n-dimensional space, it is imperative for a simplex to have $(n + 1)$ vertices so that no region of the domain is outside the reach of such simplices. However, working with more than one simplex, in a multi-objective scenario, gives an opportunity to explore the effect of changing nps on the performance of the algorithm. Since the algorithm works with more than one simplices, a region of the domain left unexplored by one of the simplex could be covered by others.

Algorithm As discussed earlier, for solving an n-dimensional multi-objective optimization problem, the proposed algorithm which is based on simplex search method works with more than $n + 1$ points and multiple simplices. Further, the number of vertices used to form a simplex, nps, is also considered as a parameter. Hence, it is must to decide the population size, the number of simplices, and the number of vertices for the simplex at the beginning of the algorithm. Let the population size be denoted as P_s, and the number of simplices is denoted as N. Now, the task in hand is to generate the new improved solutions using this initial population of solutions. For generating the new solutions, at each iteration, $iter$, usual operations of simplex search method, i.e., reflections, contraction, and expansion, are performed for each of the N simplices. The stopping criterion for the simplex loop is $Smax_{iter}$. New solutions are generated till the maximum iteration, Max_{iter}, is reached. Below are the steps involved in the proposed algorithm.

- Decide population size P_s, number of simplices N, number of vertices to form a simplex nps, maximum iteration of the outer loop Max_{iter}, and maximum iteration for the simplex loop or the inner loop $Smax_{iter}$.
- Generate P_s points to form the initial population and assign front value to each point of the population.
- Outer loop: For $iter = 1$ to $iter = Max_{iter}$, generate random combination of points for N simplices.
  - Inner loop: For each simplex, follow the usual procedure of basic simplex method of reflection, expansion/contraction to generate new solutions and compare different solutions on the basis of domination.

vkmehta@tezu.ernet.in

It is interesting to note that if $Smax_{iter} = 1$, then by the end of every outer iteration, the algorithm must have generated and explored at most $2N$ additional points (generated by reflection and expansion/contraction). It is quite possible that in one of the inner iterations, the algorithm accepts a point from the tenth front,[1] whereas in another it rejects a point which corresponds to the fifth front. Discarding or accepting points in every inner loop severely hampers the efficiency of the algorithm because in doing so it is quite likely that the algorithm discards a point having a better front value.

To overcome this difficulty, an additional population of points generated by reflection and expansion/contraction is maintained at the end of every outer loop iteration. This additional population is then combined with original P_s points. Out of these points, P_s points are chosen from the fronts having the highest front value. In the vocabulary of evolutionary algorithms, this can be seen as preserving *elites*.

While selecting P_s points from a combined population of points, a condition may arise when to complete the set of P_s points, and the algorithm needs to choose only a subset of points from the points available on a front. In that case, those points from the front can be chosen, which form a better spread of that front. This can be done by introducing another measure, *crowding distance* [3], that will help the algorithm identify such points from a front.

3 Constraint Handling with Simplex Search Method

A method for handling constraints with simplex search method for single-objective constrained optimization problems has been proposed by the authors [13]. It treats constraint violation and objective function separately and provides appropriate measures to handle all the cases of a simplex lying in any of the three regions, namely (i) feasible region: where all the points of the simplex are feasible, (ii) boundary region: where some of the $n + 1$ points are feasible and other infeasible, and (iii) infeasible region: where all the points of the simplex are infeasible. In case all the points are either feasible or infeasible, the algorithm tries to minimize the objective function value or constraint violation, respectively. If the simplex lies in the boundary region, the infeasible points are assigned a consolidated function value which is equal to the sum of objective function value of the worst feasible point and the constraint violation of that infeasible point. In this way, the point having the largest value of constraint violation would become the worst point among $n + 1$ points and the algorithm would try to move away from that point.

The same strategy of assigning function value is used here for handling constraints in multi-objective scenario. The function value assignment for each point of the population P_s is as follows:

[1] To compare two points on the basis of dominance, a front value is assigned to each point depending on the front on which the point lies. All the points on a particular front have the same front value which is equal to the number of points which are dominated by that front.

vkmehta@tezu.ernet.in

– For each point of the population, evaluate the constraint violations and identify the infeasible points.
– Evaluate the objective function values at all the feasible points, identify the worst feasible function value for all the objectives f_i, $i = 1, 2, \ldots, m$, and store them in a vector $\mathbf{f}^w = [f_1^{worst} \quad f_2^{worst} \ldots f_m^{worst}]^T$.
– To each of the infeasible points, assign a consolidated value

$$\mathbf{F} = \mathbf{f}^w + \text{cv}[1\ 1 \ldots 1]^T_{R^{m\times 1}},$$

where for a general multi-objective problem having inequality and equality constraints defined as $g_i(\mathbf{x}) \leq 0$ for $i = 1, \ldots, p$, $h_j(\mathbf{x}) = 0$ for $j = 1, \ldots, q$; the constraint violation (cv[2]) is defined as:

$$\text{cv} = \sum_{j=1}^{p} max\left\{0, g_j(\mathbf{x})\right\} + \sum_{j=1}^{q} max\left\{0, (|h_k(\mathbf{x})| - \delta)\right\} + R\sum_{j=1}^{q}|h_k(\mathbf{x})|^2.$$

Thus, all the points of the population will be assigned function values. The point having the highest constraint violation will be dominated by all the other points, and the proposed algorithm would try to move away from that point.

4 Unconstrained Problems

The proposed method has been tested on several unconstrained multi-objective test problems shown in Table 1. The results are compared with the NSS-MO [12] and NSGA-II [3] algorithms. The comparison with NSS-MO is on the basis of performance metrics spacing S [17] and hypervolume [22], whereas with NSGA-II, it is based on Υ and Δ [3]. The metrics Υ and hypervolume measure the convergence of the solution points obtained to the global Pareto front, whereas the metrics Δ and S give a measure of the diversity of the obtained solution set.

Martinez et al. [12] have compared their algorithm NSS-MO with that of Zhang and Li [20] for the problems LIS, FON, and DTLZ5 and concluded their algorithm to be superior than MOEA/D. For bi-objective problems LIS and FON, Martinez et al. have taken $P_s = 100$ and maximum function evaluations to be 4000 and for three-objective problem, DTLZ5, they have taken $P_s = 300$ and maximum function evaluations to be 12,000. For comparison, 30 independent runs of the proposed algorithm have been considered, with same P_s and maximum function evaluations, along with $N = 100$, $nps = n + 1$ and $Smax_{iter} = 1$.

Figure 1 shows the typical convergence of the population points of the proposed algorithm for problems LIS, FON, and DTLZ5. Table 2 shows the comparison of the results obtained from the proposed algorithm with that of the NSS-MO (as reported in [12]). For each problem, boldface values correspond to the algorithm which performs

[2]For discussion on R and δ in the expression, see Mehta and Dasgupta [13].

vkmehta@tezu.ernet.in

Table 1 Unconstrained multi-objective optimization test problems

Problem	n	Variable bounds	Objective function	Nature of Pareto front
SCH Schaffer [16]	1	$[-10^3, 10^3]$	$f_1(x) = x^2$ $f_2(x) = (x-5)^2$	Convex Connected
LIS Lis and Eiben [10]	2	$[-5, 10]$	$f_1(\mathbf{x}) = \sqrt[8]{x_1^2 + x_2^2}$ $f_2(\mathbf{x}) = \sqrt[4]{(x_1-0.5)^2 + (x_2-0.5)^2}$	Non-convex Connected
FON Fonseca et al. [6]	3	[-4, 4]	$f_1(\mathbf{x}) = 1 - \exp(-3\sum_{i=1}^{3}(x_i - \frac{1}{\sqrt{3}})^2)$ $f_2(\mathbf{x}) = 1 - \exp(-3\sum_{i=1}^{3}(x_i + \frac{1}{\sqrt{3}})^2)$	Non-convex Connected
POL Poloni et al. [15]	2	$[-\pi, \pi]$	$f_1(\mathbf{x}) = 1 + (A_1 - B_1)^2 + (A_2 - B_2)^2$ $f_2(\mathbf{x}) = (x_1+3)^2 + (x_2+1)^2$ $A_1 = 0.5\sin 1 - 2\cos 1 + \sin 2 - 1.5\cos 2$ $A_2 = 1.5\sin 1 - \cos 1 + 2\sin 2 - 0.5\cos 2$ $B_1 = 0.5\sin x_1 - 2\cos x_1 + \sin x_2 - 1.5\cos x_2$ $B_2 = 1.5\sin x_1 - \cos x_1 + 2\sin x_2 - 0.5\cos x_2$	Disconnected, Non-convex
KUR Kursawe [9]	3	$[-5, 5]$	$f_1(\mathbf{x}) = \sum_{i=1}^{n-1}(-10\exp(-0.2\sqrt{x_i^2 + x_{i+1}^2}))$ $f_2(\mathbf{x}) = \sum_{i=1}^{n}, (\lvert x_i\rvert^{0.8} + 5\sin x_i^3)$	Non-convex Disconnected
VNT Viennet et al. [19]	2	$[-3, 3]$	$f_1(\mathbf{x}) = 0.5(x_1^2 + x_2^2) + \sin(x_1^2 + x_2^2)$ $f_2(\mathbf{x}) = \frac{(3x_1 - 2x_2 + 4)^2}{8} + \frac{(x_1 - x_2 + 1)^2}{27} + 15$ $f_3(\mathbf{x}) = (x_1^2 + x_2^2 + 1)^{-1} - 1.1\exp[-(x_1^2 + x_2^2)]$	Non-convex Disconnected
DTLZ5 Deb et al. [5]	12	[0, 1]	$f_1(\mathbf{x}) = \cos(\theta_1)\cos(\theta_2)(1 + g(\mathbf{x}_M))$ $f_2(\mathbf{x}) = \cos(\theta_1)\sin(\theta_2)(1 + g(\mathbf{x}_M))$ $f_3(\mathbf{x}) = \sin(\theta_1)(1 + g(\mathbf{x}_M))$ $g(\mathbf{x}_M) = \sum_{x_i \in \mathbf{x}_M}(x_i - 0.5)^2$ $\theta_1 = \frac{\pi}{2}x_1$ $\theta_2 = \frac{\pi}{4(1+g(\mathbf{x}_M))}(1 + 2g(\mathbf{x}_M x_2))$ $\mathbf{x}_M = [x_3, x_4, x_5, x_6, x_7, x_8, x_9, x_{10}, x_{11}, x_{12}]$	Non-convex Connected Degenerate

better. Clearly, as the convergence of the proposed algorithm is better in two out of three cases, whereas the spacing metric values are better for the NSS-MO algorithm in two cases, one cannot say which algorithm performs better on these problems. However, it is important to note that the proposed algorithm has performed similar to the NSS-MO without using any weight vector and penalty value and without converting the multi-objective problem to single-objective problem.

For comparison, the NSGA-II[3] algorithm has been run for 250 generations (or Max_{iter}) with a population size of $N = 100$, crossover probability 0.9, and a mutation probability of $1/n$ (where n is the number of design variables). The distribution indices for mutation and crossover operators were taken as $\eta_m = 20$ and $\eta_c = 20$, respectively. To keep the function evaluations of the proposed algorithm same as that of NSGA-II, the runs for the proposed algorithm were taken with maximum number

[3]The authors gratefully acknowledge the availability of the source codes for NSGA-II algorithm on the Web site http://www.iitk.ac.in/kangal/codes.shtml, from where these were downloaded on September 8, 2011.

vkmehta@tezu.ernet.in

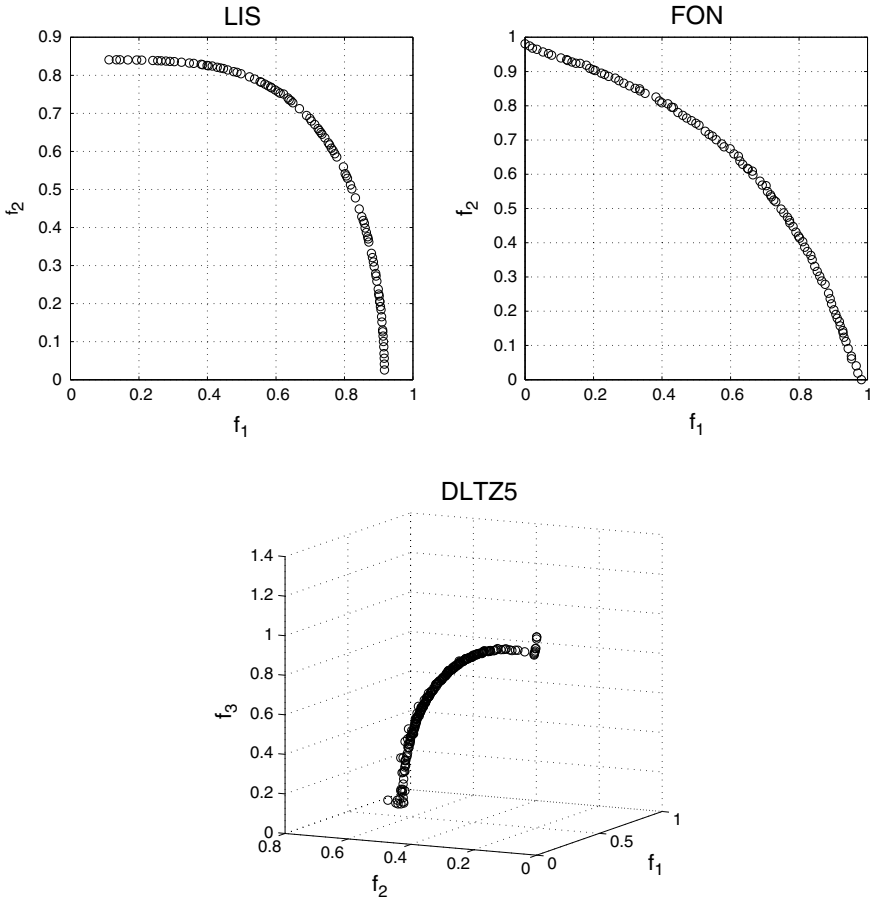

Fig. 1 Typical results of the proposed algorithm for problems LIS, FON, and DTLZ5

Table 2 Comparison of the proposed algorithm with NSS-MO. The hypervolume calculation is based on reference vector $r = [1\ \ 1]^T$ for LIS, $r = [1.1\ \ 1.1]^T$ for FON and $r = [1.1\ \ 1.1\ \ 1.1]^T$ for DLTZ5

Problem	NSS-MO	Proposed algorithm	NSS-MO	Proposed algorithm
	Hypervolume		Spacing	
	Mean (variance)	Mean (variance)	Mean (variance)	Mean (variance)
LIS	**0.309713** (0.007686)	0.281162 (0.000029)	0.005861 (0.000812)	**0.005823** (0)
FON	0.542006 (0.001476)	**0.543569** (0)	**0.004454** (0.000218)	0.005823 (0.000001)
DLTZ5	0.429676 (0.000917)	**0.432870** (0.000006)	**0.007064** (0.001211)	0.019799 (0.000289)

vkmehta@tezu.ernet.in

Table 3 Comparison of different algorithms of the basis of mean and variance of metrics Υ and Δ

Problem	Algorithm	$\bar{\Upsilon}$	σ_Υ	$\bar{\Delta}$	σ_Δ	$\bar{N}_f$
SCH	NSGA-II	0.003173	0	0.430332	0.001196	25,000
	Proposed algorithm $(n+1)$	**0.003162**	0	**0.393513**	0.000722	25,000
FON	NSGA-II	0.002589	0	0.373326	0.000566	25,000
	Proposed algorithm (2)	**0.002173**	0	**0.293504**	0.000539	25,000
	Proposed algorithm $(n+1)$	0.002240	0	0.323102	0.000674	25,000
POL	NSGA-II	**0.014194**	0.000001	0.415517	0.001060	25,000
	Proposed algorithm (2)	0.015238	0.000001	0.339555	0.000244	25,000
	Proposed algorithm $(n+1)$	0.016869	0.000001	**0.322245**	0.000290	25,000

of function evaluations as 25,000. Ten independent runs for each of the algorithms have been considered for those problems for which the true Pareto front is known. For the proposed algorithm, the run was carried out with two values of nps. The average performance of the algorithms, on the basis of Υ and Δ, is shown in Table 3. As is evident from the values shown in the table, except the value of $\bar{\Upsilon}$ for the problem POL, all the results of the proposed algorithm are better than NSGA-II.

For the problems, KUR and VNT (for which the true Pareto front is not known), the results are compared using set converge metrics [21] C_{AB} and C_{BA}, where A corresponds to the solution set obtained by the proposed algorithm and B corresponds to the solution set obtained by the NSGA-II algorithm.

Table 4 shows the mean and standard deviation for these metrics. As discussed earlier, the metric C_{AB} gives the fraction of solutions in set B, which are dominated by solutions of set A and C_{BA} gives the fraction of solutions in set A, which are dominated by solutions of set B. As evident from the table, for the problem KUR, on an average more number of solutions of set A, i.e., solutions obtained by the proposed algorithm are dominated by the solutions of set B. Hence, the algorithm NSGA-II performs better on the problem KUR. For the problem VNT, on an average more number of solutions of set B, i.e., solutions obtained by the NSGA-II algorithm are dominated by the solutions of set A. So, the proposed algorithm performs better in case of the problem VNT.

vkmehta@tezu.ernet.in

Table 4 Comparison of different algorithms on the basis of set converge metric

Problem	Algorithm	$\bar{C}_{AB}$	$\sigma_{C_{AB}}$	$\bar{C}_{BA}$	$\sigma_{C_{BA}}$	$\bar{N}_f$
KUR	A: Proposed algorithm ($nps = n + 1$) B: NSGA-II	**0.0854**	0.0251	0.4227	0.0375	25,000
	A: Proposed algorithm ($nps = 2$) B: NSGA-II	**0.1177**	0.0366	0.2219	0.0438	25,000
VNT	A: Proposed algorithm ($nps = n + 1$) B: NSGA-II	0.1023	0.0303	**0.0774**	0.0290	25,000
	A: Proposed algorithm ($nps = 2$) B: NSGA-II	0.1132	0.0344	**0.0667**	0.0248	25,000

5 Constrained Problems

The proposed multi-objective optimization algorithm equipped with the constraint handling procedure discussed in Sect. 3 is tried on some problems (Table 5) available in the literature. These problems include two problems of mechanical component design: two-bar truss design problem and welded-beam design problem. The results have been compared with NSGA-II. The results of NSGA-II were obtained with 250 generations (or Max_{iter}), a population size of $N = 100$, crossover probability 0.9 and a mutation probability of $1/n$ (where n is the number of design variables). The distribution indices for mutation and crossover operators were taken as $\eta_m = 100$ and $\eta_c = 20$, respectively. To keep the function evaluations of the proposed algorithm same as that of NSGA-II, the results of the proposed algorithm have been obtained with the maximum number of function evaluations as 25,000.

Figure 2 shows the typical convergence of the proposed algorithm on these constrained test problems, along with that of NSGA-II. Except the welded-beam design problem, where both the algorithms have fallen short of locating the minimum of objective function f_1, the performance of both the algorithms is good, as all the points of the population have converged close to the actual Pareto front and a decent spread has been maintained by both the algorithms. To compare the average performance of the algorithms quantitatively, ten runs of both the algorithms were taken and mean and variance of the performance metrics Υ and Δ are shown in Table 6. As shown in the table, except the SRN and truss design problem, the convergence metric Υ

vkmehta@tezu.ernet.in

Table 5 Constrained multi-objective optimization test problems

Problem	n	Variable bounds	Definition
DEB Deb et al. [3]	2	$x_1 \in [0.1, 1.0]$ $x_2 \in [0, 5]$	**Minimize** $f_1(\mathbf{x}) = x_1$ **Minimize** $f_2(\mathbf{x}) = \frac{1+x_2}{x_1}$ **Subject to** $g_1(\mathbf{x}) = 6 - x_2 - 9x_1 \leq 0$ $g_2(\mathbf{x}) = 1 + x_2 - 9x_1 \leq 0$
SRN Chankong and Haimes [1]	2	$x_1 \in [-20, 20]$ $x_3 \in [-20, 20]$	**Minimize** $f_1(\mathbf{x}) = (x_1 - 2)^2 + (x_2 - 1)^2 + 2$ **Minimize** $f_2(\mathbf{x}) = 9x_1 - (x_2 - 1)^2$ **Subject to** $g_1(\mathbf{x}) = x_1^2 + x_2^2 - 225 \leq 0$ $g_2(\mathbf{x}) = x_1 - 3x_2 + 10 \leq 0$
TNK Tanaka et al. [18]	2	$x_1 \in [-\pi, \pi]$ $x_2 \in [-\pi, \pi]$	**Minimize** $f_1(\mathbf{x}) = x_1$ **Minimize** $f_2(\mathbf{x}) = x_2$ **Subject to** $g_1(\mathbf{x}) = -x_1^2 - x_2^2 + 1 + 0.1\cos(16\arctan\frac{x}{y}) \leq 0$ $g_2(\mathbf{x}) = (x_1 - 0.5)^2 + (x_2 - 0.5)^2 - 0.5 \leq 0$
Welded beam Deb and Srinivasan [4]	4	$h \in [0.125, 5]$ $t \in [0.1, 10]$ $l \in [0.1, 10]$ $b \in [0.125, 5]$	**Minimize** $f_1 = (1.10471h^2l + 0.04811tb(14 + l))$ **Minimize** $f_2 = (2.1952/(t^3b))$ **Subject to** $g_1 = \tau - 13600$ $g_2 = \sigma - 30600$ $g_3 = h - b$ $g_4 = 6000 - P_c$ where $\tau_p = 6000/(\sqrt{2}hl)$ $\tau_{dp} = 6000(14 + 0.5l)\frac{\sqrt{0.25(l^2+(h+t)^2))}}{(1.414lh((l^2/12)+0.25(h+t)^2)}$ $P_c = 64746.022(1 - 0.0282346t)tb^3$ $\sigma = 504000/(t^2b)$ $\tau = \sqrt{\tau_p^2 + \tau_{dp}^2 + \frac{l\tau_p\tau_{dp}}{\sqrt{0.25(l^2+(h+t)^2)}}}$
Two-bar Truss design Deb [2, pp. 450–451]	3	$x_1 \in [0, 0.01]$ $x_2 \in [0, 0.01]$ $y \in [1.0, 3.0]$	**Minimize** $f_1 = x_1\sqrt{16 + y^2} + x_2\sqrt{1 + y^2}$ **Minimize** f_2=max$(\sigma_{AC}, \sigma_{BC})$ **Subject to** g_1 =max$(\sigma_{AC}, \sigma_{BC}) \leq 10^5$ where $\sigma_{AC} = \frac{20\sqrt{16+y^2}}{yx_1}$ $\sigma_{AC} = \frac{80\sqrt{1+y^2}}{yx_2}$

has a better value for the proposed algorithm. Also, the metric Δ, which signifies the spread of the points of the population over the Pareto front, has better value in all the cases.

With the above discussions, it is clear that the proposed method which is based on a classical direct search algorithm is capable of generating a multitude of solutions for multi-objective optimization problems. The method is capable of handling constraints neatly and efficiently and can solve engineering problems. Apart from the problems discussed here, the proposed method has been tested on few other problems and the performance is found to be comparable with the existing algorithms.

vkmehta@tezu.ernet.in

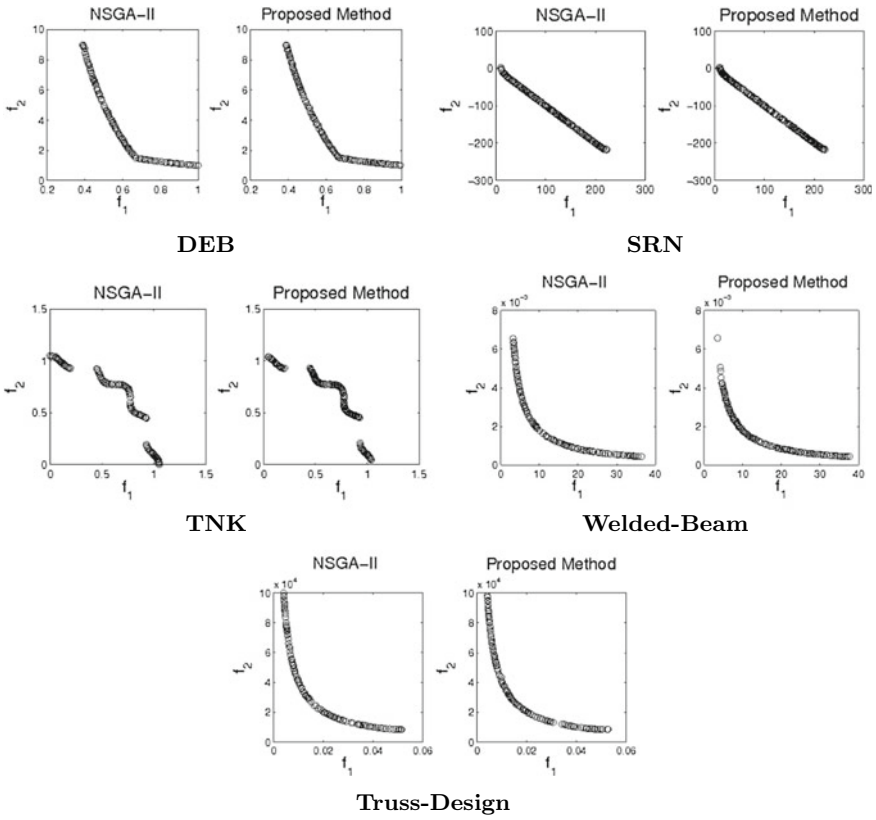

Fig. 2 Typical results of NSGA-II and the proposed algorithms for constrained problems

However, to exploit the true potential of the proposed algorithm and to further develop the idea of using the simplex search method as the multi-objective optimization tool, detailed studies on the area are needed.

6 Conclusion

In this paper, a multi-objective optimization method based on Nelder and Mead's simplex search method has been developed. The method is easy to implement and unlike NSS-MO [12], which is another multi-objective algorithm based on Nelder and Mead's simplex search method, is capable of handling constraints. The proposed method does not need any *a priori* and additional information about the problem, and it works without converting the multi-objective optimization problem to single-objective problem using weights or additional constraints.

vkmehta@tezu.ernet.in

Table 6 Comparison of different algorithms of the basis of mean and variance of metrics Υ and Δ

Problem	Algorithm	$\bar{\Upsilon}$	σ_Υ	$\bar{\Delta}$	σ_Δ	$\bar{N}_f$
DEB	NSGA-II	0.004666	0	0.691395	0.002342	25,000
	Proposed algorithm (2)	**0.004419**	0	0.604383	0.000834	25,000
	Proposed algorithm $(n+1)$	0.005127	0	**0.568830**	0.000738	25,000
SRN	NSGA-II	**0.287146**	0.000615	0.380772	0.001154	25,000
	Proposed algorithm (2)	0.341309	0.000752	**0.365620**	0.000429	25,000
	Proposed algorithm $(n+1)$	0.341737	0.000501	0.376241	0.000849	25,000
TNK	NSGA-II	0.005242	0	0.719209	0.000585	25,000
	Proposed algorithm (2)	**0.003374**	0	**0.626290**	0.001373	25,000
	Proposed algorithm $(n+1)$	0.003420	0	0.630787	0.000284	25,000
Welded beam	NSGA-II	0.049928	0.000925	0.760862	0.004857	25,000
	Proposed algorithm (2)	0.100432	0.032677	0.730994	0.009236	25,000
	Proposed algorithm $(n+1)$	**0.044968**	0.000030	**0.552562**	0.003877	25,000
Truss design	NSGA-II	**265.8680**	713.1869	0.740586	0.001752	25,000
	Proposed algorithm (2)	273.7213	976.5151	0.640583	0.001531	25,000
	Proposed algorithm $(n+1)$	279.8505	782.431	**0.624337**	0.001124	25,000

It has been shown that the proposed algorithm is capable of generating multiple solutions closer to the true Pareto front of a problem with decent spread and that too in a single run, and its performance is comparable to well-established algorithm NSGA-II. It has been found that several parameters influence the performance of

vkmehta@tezu.ernet.in

the algorithm. A detailed study of these effects on the performance of the proposed method could be taken up further for understanding and enhancing the capabilities of the proposed method.

References

1. Chankong V, Haimes Y (1983) Multiobjective decision making: theory and methodology, vol 8. North-Holland, New York
2. Deb K (2001) Multi-objective optimization using evolutionary algorithms, vol 16. Wiley, Hoboken
3. Deb K, Pratap A, Agarwal S, Meyarivan T (2002) A fast and elitist multiobjective genetic algorithm: NSGA-II. IEEE Trans Evol Comput 6(2):182–197
4. Deb K, Srinivasan A (2006) Innovization: innovating design principles through optimization. In: Proceedings of the 8th annual conference on genetic and evolutionary computation. ACM, pp 1629–1636
5. Deb K, Thiele L, Laumanns M, Zitzler E (2002) Scalable multi-objective optimization test problems. In: WCCI. IEEE, pp 825–830
6. Fonseca C, Fleming P (1995) An overview of evolutionary algorithms in multiobjective optimization. Evol Comput 3(1):1–16
7. Koduru P, Dong Z, Das S, Welch S, Roe J, Charbit E (2008) A multiobjective evolutionary-simplex hybrid approach for the optimization of differential equation models of gene networks. IEEE Trans Evol Comput 12(5):572–590. https://doi.org/10.1109/TEVC.2008.917202
8. Kuriger G, Grant F (2011) A lexicographic Nelder Mead simulation optimization method to solve multi-criteria problems. Comput Ind Eng 60:555–565
9. Kursawe F (1991) A variant of evolution strategies for vector optimization. In: Parallel problem solving from nature, pp 193–197
10. Lis J, Eiben Á (1996) A multi-sexual genetic algorithm for multiobjective optimization. In: 1997 IEEE international conference on evolutionary computation. IEEE, pp 59–64
11. Martínez, S., Coello, C.: A proposal to hybridize multi-objective evolutionary algorithms with non-gradient mathematical programming techniques. In: Parallel problem solving from nature—PPSN X, pp 837–846
12. Martinez S, Montanando A, Coello Coello C (2011) A nonlinear simplex search approach for multi-objective optimization. In: 2011 IEEE congress on evolutionary computation (CEC), pp 2367 –2374. https://doi.org/10.1109/CEC.2011.5949910
13. Mehta VK, Dasgupta B (2012) A constrained optimization algorithm based on the simplex search method. Eng Optim 44(5):537–550
14. Nelder JA, Mead R (1965) A simplex method for function minimization. Comput J 7(4):308–313
15. Poloni C, Giurgevich A, Onesti L, Pediroda V (2000) Hybridization of a multi-objective genetic algorithm, a neural network and a classical optimizer for a complex design problem in fluid dynamics. Comput Meth Appl Mech Eng 186(2–4):403–420
16. Schaffer JD (1984) Some experiments in machine learning using vector evaluated genetic algorithms (artificial intelligence, optimization, adaptation, pattern recognition). Ph.D. thesis, Nashville, TN, USA. AAI8522492
17. Schott J (1995) Fault tolerant design using single and multicriteria genetic algorithm optimization. Technical report. DTIC Document
18. Tanaka M, Watanabe H, Furukawa Y, Tanino T (1995) GA-based decision support system for multicriteria optimization. In: IEEE international conference on systems, man and cybernetics. Intelligent systems for the 21st century, vol 2. IEEE, pp 1556–1561
19. Viennet R, Fonteix C, Marc I (1996) Multicriteria optimization using a genetic algorithm for determining a pareto set. Int J Syst Sci 27(2):255–260

vkmehta@tezu.ernet.in

View publication stats

20. Zhang Q, Li H (2007) MOEA/D: a multiobjective evolutionary algorithm based on decomposition. IEEE Trans Evol Comput 11(6):712–731. https://doi.org/10.1109/TEVC.2007.892759
21. Zitzler E (1999) Evolutionary algorithms for multiobjective optimization: methods and applications. Shaker Verlag, Aachen-Maastricht, Berichte aus der Informatik
22. Zitzler E, Thiele L (1998) Multiobjective optimization using evolutionary algorithms—a comparative case study. In: Parallel problem solving from nature—PPSN V. Springer, pp 292–301

vkmehta@tezu.ernet.in

Sociology of Northeast India

Empirical Reality and Disciplinary Practice

Edited by

Jyoti Prasad Saikia

Partha Pratim Borah

Copyright © editors

All rights reserved. No part of this publication may be reproduced, stored in a retrieval system, or transmitted, in any form or by any means, electronic, mechanical, photocopying, recording or otherwise, without the prior permission of the copyright owner and the publishers.

The view expressed in this book are those of the authors not necessarily that of the publisher. The publisher is not responsible for the views of the authors and the authenticity of the data, in any way whatsoever.

First Published 2018

DVS PUBLISHERS

H. B. Road, Panbazar, Guwahati - 781 001, Assam, India
Phone : 2638295, 2730057

WZ-33, Lane No.2, Shiv Nagar, New Delhi - 110058, India
e-mail : dvspub@gmail.com, dvspublisher@gmail.com
website : www.dvspublishers.com

Type setting : Pankaj Saikia

ISBN: 978-93-85839-24-5

Printed at : Bhabani Offset Private Limited

Content

Acknowledgement

Introduction

Sociology of Northeast India: Empirical Reality and Disciplinary Practice 1
Partha Pratim Borah
Jyoti Prasad Saikia

Part I

A Critical Understanding of Sociology of Northeast India: Geo-Political History and Migration 17
Kedilezo Kikhi

Northeast India: Historical Evolution and Diverse Conceptualizations of a Region 34
Partha Pratim Borah & Rabin Deka

Challenges to Manage Pluralism in Assam: A Sociological Observation 56
Jyoti Prasad Saikia

Part II

Peace building Activities of Civil Society in Northeast India 66
M Amarjit Singh

Violence, State Response and Civil-Society Intervention for Peace: An Evaluation in the Context of Northeast India 82
Hriday Ranjan Kalita

Changing Face of Death in Northeast India 102
Hoineilhing Sitlhou

Part III

Interrogating Development in Northeast India: Instances from Assam and Nagaland 121
Jagritee Ghosh & Amiya Kumar Das

A Critical Understanding of Sociology of Northeast India

Geo-Political History and Migration

Kedilezo Kikhi

Introduction

Understanding Northeast (NE) posits a danger of too much generalisation or visualizing knowing northeast while we may not? NE has to be understood as varied diversities in terms of its different ethnic groups, linguistic families, and political units ranging from authoritarian hereditary monarchy to democracy bordering anarchy, social organisation and cultural dimensions, family organisation and kinship, religious diversities and various art forms. While all this varied diversities are embedded in its history. This chapter attempts to look at migration (or immigration) in NE India by placing it in the background of its geo-political entity and historical context. Geographically, NE is at the extreme north-eastern part of India, and has international boundaries with Bhutan, Tibet, China, Myanmar and Bangladesh. The region is geographically isolated from the rest of India because its only land link with the rest of the country is through a narrow strip of land in the state of West Bengal. At the same time, the northeast is a geographically 'recognisable entity' (Gopalakrishnam, 1991). However, there are significant variations within the region where each of these states

Investigating Weldability in Microalloyed Al Alloys

Sanjib Banerjee, Rakesh Bhadra, Sanjib Gogoi and Ravi shankar Dutta

Abstract Aluminum (Al) alloys, especially the 2xxx series due to high strength to weight ratio have found extensive use in aerospace, marine, and automobile industries. The present research trend is microalloying (wt.% < 0.1) these alloys with trace elements viz. Cd, Sn, Ag, In, etc. For these applications, welding becomes an inevitable technique, which is a tougher challenge for Al alloys, and Friction Stir Welding (FSW) is recently explored. In present work, 2219Al alloy and the same alloy microalloyed with 0.06 wt.% Cd were processed by casting route. They were then welded by FSW and mechanical properties and microstructure of the welded joints were studied. The hardness value increased while the impact toughness decreased due to trace addition of Cd. The microstructural study revealed three zones viz. weld nugget zone (WNZ), thermo mechanically affected zone (TMAZ) and heat affected zone (HAZ), identified by the formation of fine, columnar, and spherical grains, respectively.

Keywords Aluminum alloys · Microalloying · Friction stir welding · Weldability

1 Introduction

Nowadays, the automobile, aeronautic, and marine industries are undoubtedly most focused fields of research. Actually, mechanical strength, corrosion resistance, residual stress, weight reduction, joining techniques, etc., are the prime painstaking issues. The continuous strive for obtaining higher strength to weight ratio, shifted the focus from ferrous to lightweight nonferrous alloys of Al, Mg, etc. Al alloys due to lightweight but high strength brought a new era of excellence in the field of aerospace. Among the various Al alloys, especially the 2xxx series is the most common as it encompasses various engineering fields due to its commendatory mechanical properties. Again from this 2xxx series, 2219Al alloy owing to the exemplary blend of its unique properties, is used in the construction of liquid cryogenic rocket fuel tanks, space boosters, etc. The present research trend is microalloying (< 0.1 wt.%) these

S. Banerjee (✉) · R. Bhadra · S. Gogoi · R. Dutta
Department of Mechanical Engineering, Tezpur University, Tezpur, India
e-mail: sanjibb@tezu.ernet.in

© Springer Nature Singapore Pte Ltd. 2020

B. B. Biswal et al. (eds.), *Advances in Mechanical Engineering*, Lecture Notes in Mechanical Engineering, https://doi.org/10.1007/978-981-15-0124-1_25

Academic Science

DIIF

Conference Info

Reference No.:NITTTR323

2nd International Conference on Engineering Technology, Science and Management Innovation (ICETSMI-2017)

Venue-
National Institute of Technical Teachers Training & Research (NITTTR),
MHRD,Govt of India, Chandigarh, India
on 15th January 2017

Certificate of Presentation

This is to certify that

B.Chowdhury
Department of Mechanical Engineering, Tezpur University, Tezpur, Assam, India

Presented a paper titled as

"Cause-Effect Diagram Versus System Dynamic Model – A case study of Manufacturing Defects analysis"

Organized by Conference Info in Association with Academic Science at
National Institute of Technical Teachers Training & Research(NITTTR),
MHRD, Govt of India, Chandigarh, India
on 15th January 2017

Dr K. Agarwal
Editor, Academic Science

Convener

2021/5/28 22:10
SHOT ON POCO F1
POCO

National Conference on

SUSTAINABLE MECHANICAL ENGINEERING: TODAY AND BEYOND

SMETB 2017

March 25-26, 2017

Department of Mechanical Engineering, Tezpur University, Assam, India

This is to certify that Prof./Dr./Mr./Ms. Barnali Chowdhury *of* Tezpur University *participated and presented a paper titled* Analysis of manufacturing defects using FMEA - a step towards defect prevention. *in the* ***National Conference on SUSTAINABLE MECHANICAL ENGINEERING: TODAY AND BEYOND****, 2017 held at Tezpur University , Assam , India.*

SMETB 2017

(Dr. Partha P. Dutta)	(Prof. Tapan K. Gogoi)	(Dr. Seikh M. Kamal)
Chairman	Organizing Secretary	Joint Organizing Secretary

POCO
SHOT ON POCO F1
2021/5/28 22:11

INTERNATIONAL CONFERENCE

on

Sustainable Approaches in Food Engineering and Technology

(SAFETy-2021)

24th-25th June, 2021

Certificate

BARNALI CHOWDHURY

This is to certify that Dr./Mr./Ms. ..... has participated as Oral Presenter *..... at SAFETy-2021, organized by the Department of Food Engineering & Technology, Tezpur University, Assam, India, and Department of Food Science & Technology, University of Georgia, Georgia (US) in Association with AFST(I) Tezpur Chapter during 24th-25th June, 2021.*

Title: Design and analysis of a water pumping device - A solution for hilly terrains

Author(s): Chowdhury, B., Maitra, S., Das, M. & Krishna, K.

Dr. Amit Baran Das	Dr. Abhinav Mishra	Prof. Nandan Sit	Prof. Manpreet Singh
Organizing Secretary	Organizing Secretary	Chairperson	Chairperson
TEZPUR UNIVERSITY	UNIVERSITY OF GEORGIA	TEZPUR UNIVERSITY	UNIVERSITY OF GEORGIA

Evolutionary Algorithms for Scheduling of Crude Oil Preheating Process Under Linear Fouling

Dimbalita Deka(✉) and Dilip Datta

Department of Mechanical Engineering, Tezpur University, Tezpur 784 028, India
dimbalitadeka@gmail.com, ddatta@tezu.ernet.in, datta_dilip@rediffmail.com

Abstract. The crude oil preheating process in refineries is required to be scheduled in a way to minimize the processing cost involved with it, subject to the satisfaction of various process related constraints. The process forms a mixed-integer optimization problem as the scheduling of the processing units involves binary variables, while the discharges from the running units are real valued. The two parts of such problems are usually handled by two different algorithms, where the optimum scheduling obtained by one algorithm is fed to another algorithm for optimizing its discharge process. In the present work, formulating the crude oil preheating process under the effect of linear fouling as a mixed-integer nonlinear programming (MINLP) model, three binary-real coded evolutionary algorithms (EAs) are investigated in order to demonstrate that a single EA can successfully tackle its both binary and real parts. Further, the statistical analysis of the performances of the EAs are also presented through their application to a benchmark instance of the problem.

Keywords: Evolutionary algorithms · Optimization
Crude oil preheating process

1 Introduction

Evolutionary algorithms (EAs) are known to have the ability to find approximate solutions in reasonable time for such problems also, where classical optimization methods either become too expensive or even ineffective. EAs are usually independent of problem domains unlike classical optimization methods, which are restricted to specific classes of problems only. Hence, EAs have found applications in a wide range of real-life problems, including linear and nonlinear, convex and non-convex, continuous and discrete, and many more.

However, EAs still could not be generalized in case of many classes of discrete or mixed-discrete problems, but require the incorporation of some problem information for their effective performance. Unit scheduling of continuous flow process systems in industries is such a problem, which consists of two optimization sub-problems. The first part is the integer-valued scheduling of the

© Springer International Publishing AG, part of Springer Nature 2018
P. Korošec et al. (Eds.): BIOMA 2018, LNCS 10835, pp. 113–125, 2018.
https://doi.org/10.1007/978-3-319-91641-5_10

processing units, while the second part is concerned with the optimization of the discharge process based on the scheduling of the first part. Accordingly, the optimization of an industrial continuous flow process system essentially becomes a mixed-integer non-linear programming (MINLP) problem involving both integer variables to represent operational status of the units and real variables to represent the flows from the running units. Due to the complexities involved with such MINLP problems, two parts of a problem are often tackled separately through two different algorithms, where the first algorithm is employed to schedule the processing units over a time horizon and then the second algorithm optimizes the flow processes in the schedule of the first algorithm [1,2]. However, such an isolating system may suffer from the drawback of missing better solutions as the possibility of more promising solutions cannot be denied if both the parts of the problem were tackled interactively [3,4].

In view of above, three EAs are investigated here for handling an MINLP based two-step continuous flow process system by a single EA. The studied problem is the optimum scheduling of the crude oil preheating process arising in refineries, which is carried out through a crude preheat train (CPT) over a time horizon. The aim of preheating is to increase the crude oil temperature to a certain degree before its entry into a furnace, so that the energy (fuel) requirement in the furnace gets reduced. The CPT consists of a network of heat exchangers, commonly known as the heat exchanger network (HEN), to run a productive heat treatment process. The heat exchangers of HEN require periodic shutting down for the purpose of cleaning or other maintenance. This demands the effective scheduling of the HEN in order to get the optimum performance from the active units.

2 Literature Review

In the case of EAs, mixed-integer problems involving distinct real and integer valued parts are often solved by hybridizing two optimization techniques, allowing one technique to handle the integer part and another to handle the real part. As an example, Trivedi et al. [5] solved the mixed-integer unit commitment problem, where binary variables are evolved using a genetic algorithm (GA) and the continuous variables using a differential evolution (DE). Similar hybridization procedures are found in many other works, such as hybridization of GA and particle swarm optimization (PSO) [6,7], artificial bee colony (ABC) and GA [8], and DE and PSO [9].

Some works are also found where both integer and real parts of mixed-integer problems are handled by a single algorithm [3,4]. However, no such work on scheduling the crude oil preheating process in refineries could be found in specialized literature.

3 Problem Description and Formulation

The studied problem of crude oil preheating process in a CPT is adopted from Smaïli et al. [10], which is shown schematically in Fig. 1. In this problem, the

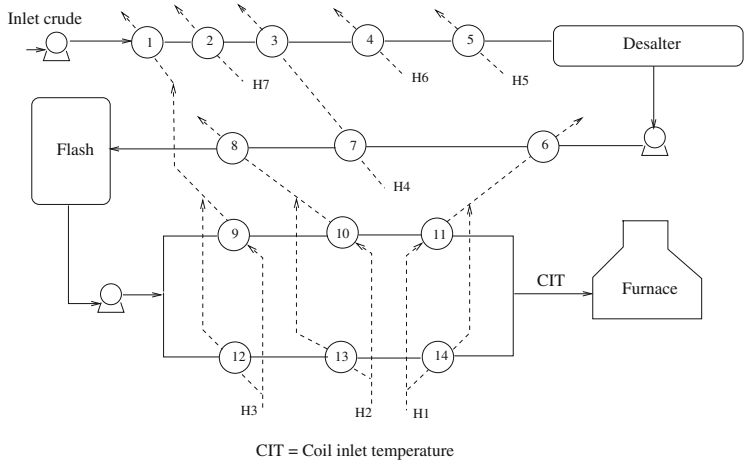

Fig. 1. Crude oil preheating process in a CPT [10].

raw crude oil passes through 14 heat exchangers (marked in Fig. 1 by 1 to 14), where it is preheated by 7 heating streams (marked in Fig. 1 by H1 to H7) prior to entering into the furnace. Heat exchangers 1–8 are connected in series; while the remaining 6 heat exchangers are arranged in two parallel lines, one containing heat exchangers 9–11 and the other connecting heat exchangers 12–14. The desalter and flash used in the processing line remove, respectively, any salt and vapour dissolved in the crude oil. The preheated crude oil is then burnt in the furnace at a higher temperature, after which it is distilled into different products.

During the preheating process of the crude oil, some impurities mixed with the crude oil get precipitated/deposited on the inner surfaces of the heat exchangers, which is called fouling. Such deposition forms a thick layer over time, which gradually reduces the performance of heat exchangers. In other words, the crude oil cannot be heated up to the possible level, which consequently increases the energy requirement in the furnace, thus increasing the energy cost. Further, the periodic cleaning of the heat exchangers for mitigating fouling is associated with cleaning cost. Hence, the process needs optimization for minimizing the total operational cost (i.e., the total of energy cost and cleaning cost) subject to some processing constraints.

Since the process is operated continuously over several years without any interruption, it can be considered that a cycle of a shorter time period is repeated in the entire time horizon. For the purpose of analysis, the cycle can further be divided equally into a certain number of time instants. At a time instant, a unit (heat exchanger) will remain either in full operation or partially/fully shutdown. In a shutting down instant, a unit may go through cleaning process also. Accordingly, the general optimization problem of a cycle of the process can be defined as follows:

– Determine
  1. Operational status of each unit at every time instant.
  2. Outlet temperature of the crude from the CPT at every time instant.
– To minimize total cost (cleaning cost plus energy cost).
– Subject to
  1. Limit on operational units in each series segment at every instant.
  2. Limit on operational units in each parallel segment at every instant.
  3. Limit on operational units in each heating line at every instant.
  4. Limit on crude oil temperature from the outlet of the CPT.
  5. Limit on cleaning instants of each unit in the entire time horizon.
  6. Limit on cleaning a unit at consecutive time instants.

The above optimization problem is formulated in Eqs. (1) and (2).

$$\text{Minimize} \qquad f = C^{\text{cl}} \sum_{i=1}^{N} \sum_{t=1}^{T} \beta_{it} + C^{\text{ener}} F_N^{\text{f}} c_N^{\text{f}} \sum_{t=1}^{T} \left(\Theta^{\text{fmax}} - \Theta_{Nt}^{\text{f,out}} \right) \tag{1}$$

$$\text{Subject to} \qquad g_1 \equiv \sum_{j=1}^{\text{nsu}_i} u_{\text{su}_{ij},t} \geqslant \text{su}_i^{\text{on}}; \qquad t = 1, 2, \cdots, T;\ i = 1, 2, \cdots, \text{ns} \tag{2a}$$

$$g_2 \equiv \sum_{k=1}^{\text{npsu}_{ij}} u_{\text{psu}_{ijk},t} \geqslant \text{psu}_{ij}^{\text{on}}; \qquad \begin{matrix} t = 1, 2, \cdots, T;\ j = 1, 2, \cdots, \text{nps}_i \\ i = 1, 2, \cdots, \text{npl} \end{matrix} \tag{2b}$$

$$g_3 \equiv \sum_{j=1}^{\text{nhlu}_i} u_{\text{hlu}_{ij},t} \geqslant \text{hlu}_i^{\text{on}}; \qquad t = 1, 2, \cdots, T;\ i = 1, 2, \cdots, \text{nhl} \tag{2c}$$

$$g_4 \equiv \Theta_{Nt}^{\text{f,out}} \leqslant \Theta^{\text{fmax}}; \qquad t = 1, 2, \cdots, T \tag{2d}$$

$$g_5 \equiv \sum_{t=1}^{T} v_{it} \geqslant 1; \qquad i = 1, 2, \cdots, N \tag{2e}$$

$$g_6 \equiv (1 - u_{ip})(1 - u_{it}) \neq 0; \qquad p = \begin{cases} T; & \text{if } t = 1 \\ t - 1; & \text{otherwise.} \end{cases} \quad t = 1, 2, \cdots, T;\ i = 1, 2, \cdots, N \tag{2f}$$

The objective function, f, in Eq. (1) represents the total operational cost, where the two summing terms on the right side represent the cleaning cost and energy cost, respectively. The constraints, g_1–g_3, in Eqs. (2a)–(2c) represent,

respectively, the minimum number of operational units in series segments, parallel segments, and heating medium flow lines; while the constraints, g_4–g_6, in Eqs. (2d)–(2f) ensure the specified temperature of the crude oil at the outlet of the CPT, cleaning of each unit at least once in the entire time horizon, and avoiding the cleaning of a unit at two consecutive time instants, respectively.

In Eqs. (1) and (2), N and T are respectively the total number of units (heat exchangers) and time instants in a production cycle, C^{cl} is the cleaning cost coefficient per cleaning instant for the ith unit at the tth time instant (in practice, C^{cl} may remain same in all units and time instants), C^{ener} is the energy cost coefficient per unit of energy requirement, F_N^{f} is the flow rate in the last unit (Nth unit), c_N^{f} is the specific heat transfer capacity of the crude oil in the last unit, $\Theta_{Nt}^{\mathrm{f,out}}$ is the crude outlet temperature from the last unit at the tth time instant, Θ^{fmax} is the temperature up to which the crude is to be heated in the furnace, ns is the number of series segments, nsu_i is the number of units in the ith series segment with su_{ij} as its jth unit and $\mathrm{su}_i^{\mathrm{on}}$ as the required minimum number of operational units, npl is the number of parallel segments, nps_i is the number of branches in the ith parallel segment with npsu_{ij} as the number of units in its jth branch and psu_{ijk} as the kth unit while $\mathrm{psu}_{ij}^{\mathrm{on}}$ as the required minimum number of operational units in that branch, nhl is the number of heating lines with nhlu_i as the number of units in the ith heating line and hlu_{ij} as the jth unit and $\mathrm{hlu}_i^{\mathrm{on}}$ as the required minimum number of operational units in that heating line.

The cleaning time (β_{it}), operational status (u_{it}) and cleaning status (v_{it}) of the units, as used in Eqs. (1) and (2), are expressed by Eq. (3), where $v_{it} = 1$ means that the ith unit will be cleaned at the tth time instant.

$$u_{it} = \begin{cases} 1; & \text{if the } i\text{th unit is fully in operation} \\ 0; & \text{if the } i\text{th unit is shutdown partially} \\ & t = 1, 2, \cdots, T;\ i = 1, 2, \cdots, N. \end{cases} \tag{3a}$$

$$v_{it} = \begin{cases} 0; & \text{if } u_{it} = 1 \\ \{0, 1\}; & \text{otherwise} \\ & t = 1, 2, \cdots, T;\ i = 1, 2, \cdots, N. \end{cases} \tag{3b}$$

$$\beta_{it} = \begin{cases} 0; & \text{if } v_{it} = 0 \\ \in [0, \alpha_{it}]; & \text{otherwise} \\ & t = 1, 2, \cdots, T;\ i = 1, 2, \cdots, N. \end{cases} \tag{3c}$$

For obtaining the crude oil outlet temperatures from the last unit at different time instants, $\Theta_{Nt}^{\mathrm{f,out}}$ used in Eqs. (1) and (2d), the same for different units are computed using Eq. (4a), where $t = 1, 2, \cdots, T$ and $i = 1, 2, \cdots, N$.

$$\Theta_{it}^{\mathrm{f,out}} = \begin{cases} \Theta_{it}^{\mathrm{f,in}}; & \text{if } u_{it} = 0 \\ \phi_{it}^{h}\Theta_{i}^{\mathrm{hinit}}(1-\alpha_{it}) + \{\alpha_{it} + (1-\alpha_{it})\phi_{it}^{c}\}\,\Theta_{it}^{\mathrm{f,in}}; & \text{otherwise.} \end{cases} \tag{4a}$$

where,
$$\Theta_{it}^{\mathrm{f,in}} = \begin{cases} \Theta^{\mathrm{f,inlet}}; & \text{if } i = 1 \\ \Theta_{i-1,t}^{\mathrm{f,out}}; & i \in \{2-14; i \neq 6, 12\} \\ \Theta_{5,t}^{\mathrm{f,out}} - \Theta^{\mathrm{desalter}}; & \text{if } i = 6 \\ \Theta_{8,t}^{\mathrm{f,out}}; & \text{if } i = 12 \end{cases} \tag{4b}$$

$$\phi_{it}^{h} = \frac{(1-x)C_{\min}}{(1-xR_i)c_i^{\mathrm{f}}} \tag{4c}$$

$$\phi_{it}^{c} = \frac{(1-xR_i)c_i^{\mathrm{f}} - (1-x)C_{\min}}{(1-xR_i)c^{\mathrm{f}}} \tag{4d}$$

$$C_{\min} = \min\{F_i^{\mathrm{f}}c_i^{\mathrm{f}}, F_i^{\mathrm{h}}c_i^{\mathrm{h}}\} \tag{4e}$$

$$x = \exp\left\{-\frac{h_{it}A_i}{C_{\min}}(1-R_i)\right\} \tag{4f}$$

$$\mathrm{R}_i = \frac{C_{\min}}{C_{\max}} \tag{4g}$$

$$\alpha_{it} = \begin{cases} 0; & \text{if } u_{it} = 1 \\ \in (0,1); & \text{otherwise} \\ & t = 1, 2, \cdots, T;\ i = 1, 2, \cdots, N. \end{cases} \tag{4h}$$

In Eq. (4), $\Theta_{it}^{\mathrm{f,out}}$ is the crude outlet temperature from ith unit at tth time instant, $\Theta_{it}^{\mathrm{f,in}}$ is the crude oil inlet temperature of ith unit at tth time instant, $\Theta_{i}^{\mathrm{hinit}}$ is the initial temperature of heating medium of ith unit, α_{it} is the partial shutdown time during operation, $\Theta^{\mathrm{f,inlet}}$ is the crude oil temperature at the inlet of the CPT, $\Theta^{\mathrm{desalter}}$ is the temperature drop in desalter, $C_{\min}$ is the minimum heat capacity rate, $C_{\max}$ is the maximum heat capacity rate, F_i^{f} is the flow rate of crude oil of ith unit, c_i^{f} is the specific heat capacity of crude oil of ith unit, F_i^{h} is the flow rate of heating medium of ith unit, c_i^{h} is the specific heat capacity of heating medium of ith unit, h_{it} is the heat transfer co-efficient of ith unit at tth time instant and A_i is the area of ith unit.

The heat transfer co-coefficients for cleaning/shutdown sub-period (h_{it}^{cl}) and processing sub-period (h_{it}^{pr}) can be obtained from the linear fouling rates ($\dot{R}_t^{\mathrm{f}}$), which are expressed by Eq. (5).

$$\dot{R}_{it}^{\mathrm{f,pr}} = \dot{R}_{it}^{\mathrm{f,cl}} = \dot{R}_t^{\mathrm{f}} \tag{5a}$$

$$h_{it}^{\mathrm{cl}} = \frac{h_{i,t-1}^{\mathrm{pr}}}{1 + \{h_{i,t-1}^{\mathrm{pr}}\dot{R}_{i,t-1}^{\mathrm{f,pr}}(1-\alpha_{it})\Delta t\}} \tag{5b}$$

$$h_{it}^{\mathrm{pr}} = \frac{h_{it}^{\mathrm{cl}}}{1 + (h_{it}^{\mathrm{cl}}\dot{R}_{i,t-1}^{\mathrm{f,cl}}\beta_{it}\Delta t)} + (v_{it}h_{it}^{\mathrm{clean}}) \tag{5c}$$

In Eq. (5), $\dot{R}_{it}^{\mathrm{f,pr}}$ is the fouling resistance under processing sub-period, $\dot{R}_{it}^{\mathrm{f,cl}}$ is the fouling resistance under cleaning sub-period and Δt is the duration of each time interval.

4 Evolutionary Algorithms (EAs) for Solving the Problem

The optimization problem studied in the present work seeks the scheduling of the crude oil preheating process in a CPT of N heat exchangers over T time instants, so as to minimize the total cost arising from the requirement of external energy for additional heating of the crude oil and periodic cleaning of the heat exchangers. The scheduling of the heat exchangers needs $2NT$ number of $\{0, 1\}$ binary variables (u_{it} and v_{it}; $i = 1, \ldots, N$ and $t = 1, \ldots, T$), while the crude preheating process requires NT number of real variables (α_{it}; $i = 1, \ldots, N$ and $t = 1, \ldots, T$). For solving the problem, three mixed-binary EAs are investigated here, which are genetic algorithm (GA), differential evolution (DE) and particle swarm optimization (PSO). In all the three EAs, an individual (solution representation) for the problem at hand consists of two one-dimensional arrays, the first one of size $2NT$ takes the $\{0, 1\}$ binary variables and the second one of size NT takes the real variables.

The investigated binary-real coded GA (brGA) is the one applied by Datta [3] to a problem of similar nature, namely the unit commitment problem arising in the area of power systems, which involves the scheduling of given power generating units and optimization of discharge from the operational units in a way to meet the hourly power demand at a minimum production cost subject to a series of system related fixed and dynamic constraints. In the brGA, the standard binary tournament selection operator, single-point crossover operator and swapping mutation operators are used for handling the $\{0, 1\}$ valued binary variables; while the binary tournament selection operator, simulated binary crossover (SBX) operator [11] and polynomial mutation operator [11] are used for handling the real variables of a problem.

Datta and Figueira [12] proposed a real-integer-discrete coded differential evolution (ridDE) algorithm for working with any type of variables (real, binary, integer, or discrete) without any conversion, which was also applied successfully to the unit commitment problem by Datta and Dutta [2]. The ridDE replaces the real valued mutation operator of the 'DE/rand/1/bin' variant of DE [13] by a binary valued mutation operator, which generates only $\{0, 1\}$ valued binary mutant elements with a mutation probability based on some basic properties of DE and such binary numbers. The ridDE is investigated here as another EA for solving the problem at hand.

Similar to the ridDE [12], Datta and Figueira [14] proposed a real-integer-discrete coded particle swarm optimization (ridPSO) algorithm for working with any type of variables (real, binary, integer, or discrete) without any conversion, whose application was demonstrated on various engineering design problems. The ridPSO defines particle vectors by $\{0, 1\}$ valued binary elements with a

mutation probability, based on some basic properties of PSO and such binary numbers. The ridPSO is investigated here as the third EA for solving the crude oil preheating problem.

Since all the three EAs are stochastic in nature, there is no guarantee that the new individuals formed in a generation (iteration) will be better than those of the current individuals from where they were generated. Hence, in order to prevent the search from moving opposite to the optimum in worst cases, the elite individuals at every generation are preserved using the mechanism proposed by Deb et al. [15]. In this case, instead of forming the population for the next generation directly with the newly generated individuals, they are first combined with the existing individuals of the current population. Then the best 50% of them, based on their objective values, are taken as the population for the next generation.

5 Numerical Experimentation

The EAs stated in Sect. 4 are coded in the `C` programming language by incorporating the optimization problem formulated in Eqs. (1) and (2). Then the performances of the EAs are evaluated with the help of a case study.

5.1 Case Study

The investigated case study of crude oil preheating is taken from Smaïli et al. [10]. As shown in Fig. 1, the CPT in the case study consists of 14 number of shell and tube heat exchangers ($N = 14$) of the type of counter-current flow. The heat exchanger network (HEN) starts with two series segments (ns = 2); the first one contains units (heat exchangers) 1–5, followed by a desalter, and then the second series segment containing units 6–8. Fixing a flash after the second series segment, the remaining six units are then arranged in a parallel segment (npl = 1) having two branches; the first one contains units 9–11 and the second one contains units 12–14. At the end of the HEN, a furnace is placed for further heating of the crude oil, if required.

There are seven heating lines (nhl = 7) in the HEN, which are marked in Fig. 1 as H1–H7. The units (heat exchangers) covered by the heating lines are as follows—H1: (1, 9, 12), H2: (8, 10, 13), H3: (6, 11, 14), H4: (3, 7), H5: (2), H6: (4) and H7: (5).

The case study is subjected to some operational constraints in the form of minimum number of units to be made always fully operational. Each of the two series segments and the two branches of the parallel segment requires minimum of two of its units to be made fully operational. Some heating lines also have similar requirement, which are as follows—H1: 2, H2: 2, H3: 2 and H4: 1.

For solving the problem, a repeating production cycle of 3 years is considered, which is divided into 36 time instants ($T = 36$), i.e., each time instant is of a duration of one month. Except the cost coefficients, the problem related other input parameters are taken from Smaïli et al. [10] and given in Table 1 in terms of

Table 1. Design and fouling data for the case study (source: Smaïli et al. [10])

Unit	Θ_i^{hinit} (°C)	F_i^{h} (kg/s)	F_i^{f} (kg/s)	c_i^{h} (kJ/kgK)	c_i^{f} (kJ/kgK)	h_{it}^{clean} (W/m^{2}K)	A_i (m^2)	$\dot{R}_t^{\text{f}} \times 10^{-7}$ (m^{2}K/J)
HE-1	194	19.1	95	2.8	1.92	0.5	56.6	0.6
HE-2	296	3.3	95	2.9	1.92	0.5	8.9	0.9
HE-3	197	55.8	95	2.6	1.92	0.5	208.3	0.6
HE-4	170	49.7	95	2.6	1.92	0.5	112.9	0.8
HE-5	237	49.7	95	2.6	1.92	0.5	121.6	0.8
HE-6	285	34.8	95	2.8	2.3	0.5	110.1	1.5
HE-7	205	55.8	95	2.6	2.3	0.5	67.2	1.1
HE-8	254	45.5	95	2.9	2.3	0.5	67.1	1.5
HE-9	249	9.5	46	2.8	2.4	0.5	91.0	1.6
HE-10	286	22.8	46	2.9	2.4	0.5	61.3	1.8
HE-11	334	17.4	46	2.8	2.4	0.5	55.6	1.9
HE-12	249	9.5	46	2.8	2.4	0.5	91.0	1.6
HE-13	286	22.8	46	2.9	2.4	0.5	61.3	1.8
HE-14	334	17.4	46	2.8	2.4	0.5	55.6	1.9

the notations used in the problem formulation in Eqs. (1)–(5). The cleaning cost coefficient (C^{cl}) and energy cost coefficient (C^{ener}) are taken from Tian et al. [16], which are 20000 $ per cleaning instant and 15.5 $ per MWh, respectively. Further, the initial temperature of the crude oil at any time instant is considered to be 26 °C ($\Theta_t^{\text{finit}} = 26\,^{\circ}\text{C}$), requiring it to be preheated up to 250 °C ($\Theta^{\text{fmax}} = 250\,^{\circ}\text{C}$) with a drop of 10 °C in the desalter ($\Theta^{\text{desalter}} = 10\,^{\circ}\text{C}$).

5.2 Experimental Setup

The considered EA related parameter values are given in Table 2, where a non-applicable value is marked by (–). Since the performance of a stochastic optimizer is likely to be influenced by the user-defined algorithmic parameter setting, instead of fixed values, some parameter values in Table 2 are made self-adaptive within given ranges with an attempt to reduce their influences on the performance of an EA. In this process, every time a random value for such a parameter is generated within its given range. Further, in order to analyze the statistical performance, 30 number of independent runs of each EA are performed with different sets of initial individuals (solutions).

5.3 Results and Discussion

With the above problem and algorithm related input information, each of the EAs are executed for 30 independent runs. For the purpose of illustration, the best schedule obtained by the brGA is given in Table 3, where '1' in the schedule means that the particular unit (heat exchanger) is in fully operation at the

Table 2. User-defined parameter values for the investigated EAs.

Parameter	brGA	ridDE	ridPSO
Population size	100	100	100
Maximum number of generations performed	7000	7000	7000
Crossover probability	90%	(0, 90%]	–
Distribution index for SBX operator	20	–	–
Mutation probability	(0, 1%]	–	–
Distribution index for polynomial mutation operator	35	–	–
Mutation probability (for binary variables only)	–	(0, 15%]	(0, 15%]
Scaling factor (for real variables only)	–	(0, 70%]	–
Inertia constant (for real variables only)	–	–	(0, 0.75]
Cognitive factor (for real variables only)	–	–	(0, 1.5]
Social factor (for real variables only)	–	–	(0, 2]
Number of runs	30	30	30

Table 3. The best schedule of the case study obtained by the brGA.

Time instant	Schedule	Number of operating units	Time instant	Schedule	Number of operating units
1	01111101111111	12	19	11111110111111	13
2	11111111111110	13	20	11111111111011	13
3	11111111111101	13	21	11110111011111	12
4	11101111011111	12	22	11111110110111	12
5	01111111110111	12	23	11111101111111	13
6	11111111111111	14	24	11111111111111	14
7	11011111101111	12	25	11111011011111	12
8	11111111101111	13	26	11111111111111	14
9	11110111011111	12	27	11111111011111	13
10	11111111101111	13	28	11111111111111	14
11	11111110011111	12	29	11111111111110	13
12	11111011101111	12	30	11110111111111	13
13	11011111101111	12	31	11111111101011	12
14	11101111111011	12	32	11101111111111	13
15	11111110111111	13	33	11111111110111	13
16	11111111101111	13	34	11111111111111	14
17	11111111111101	13	35	11111111111111	14
18	11110111101111	12	36	10111111101111	12

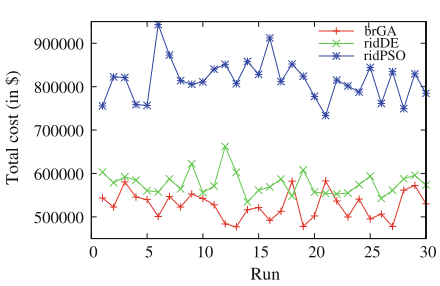

(a) Total cost.

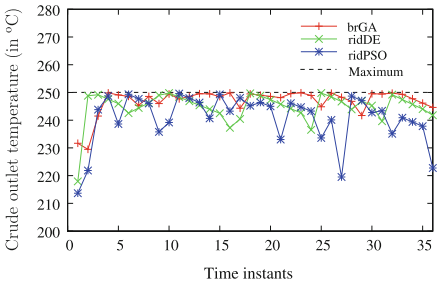

(b) Crude oil outlet temperature.

Fig. 2. Total cost over 30 runs and crude outlet temperatures over different time instants of a random run.

corresponding time instant, while '0' means it was partially shutdown during which period the unit may go through cleaning also. The schedule shows that no two units are cleaned at two consecutive time instants and each unit is cleaned at least once in the entire production cycle.

Table 4. Statistical analysis of the overall cost over 30 independent runs of the EAs.

EA	Overall cost (in $)			
	Best	Worst	Mean	Standard deviation
brGA	477150	582772	526507	31555
ridDE	534629	662064	576553	26633
ridPSO	733464	912245	815510	46860

Table 5. The t-test values for the solutions of the EAs at a significance level of 5%.

EA	brGA-vs-ridDE	brGA-vs-ridPSO	ridDE-vs-ridPSO
t-value	−6.64	−28.02	−24.28

The overall costs, i.e., the values of the objective function expressed by Eq. (1), obtained from 30 runs of each of the EAs are visualized in Fig. 2(a), where it is observed that the lowest cost could be obtained by the brGA among the three EAs. Further, the obtained crude oil outlet temperatures from the heat exchanger network at different time instants of a random run are shown in Fig. 2(b), where the outlet temperatures obtained from the brGA are found to be almost close to the required maximum furnace temperature, while those obtained from the ridPSO are found to be the worst ones.

For further detail of the performances of the EAs, a statistical analysis of the overall costs (best, worst, mean, and standard deviation) over 30 independent

runs of the EAs is performed and the obtained results are presented in Table 4. It is seen in Table 4 that the brGA has better objective values (best, worst as well as mean), followed by those of the ridDE. However, the ridDE has better standard deviation than those of the brGA and ridPSO. Therefore, finally the EAs are statistically compared by conducting pair-wise t-test between the mean objective value and standard deviation at a significance level of 5%. The obtained t values are given in Table 5, by marking a value with a '-ve' sign if the second EA in a pair is not better than the first one. Accordingly, it can be concluded that the brGA outperforms the ridDE and ridPSO, and the ridDE outperforms the ridPSO.

6 Conclusion

A typical crude oil preheating process arising in refineries is formulated as a constrained mixed-integer nonlinear programming (MINLP) problem for minimizing total of the cost of additional energy requirement and the cost for cleaning the heat exchangers of the process. It involves two separate optimization subproblems, the integer valued scheduling of the heat exchangers and the real valued heating levels in the operational heat exchangers. Such problems are usually handled by two separate algorithms, one for the integer part and another for the real part. The potentiality of thee mixed-binary evolutionary algorithms (EAs), namely genetic algorithm (GA), differential evolution (DE) and particle swarm optimization (PSO), are investigated here for handling both the parts of the problem by a single EA. From statistical analysis of the results for a benchmark problem, the GA is found outperforming both the DE and PSO, followed by the DE outperforming the PSO.

References

1. Chandrasekaran, K., Simon, S.: Multi-objective unit commitment problem using Cuckoo search Lagrangian method. Int. J. Eng. Sci. Technol. **4**, 89–105 (2012)
2. Datta, D., Dutta, S.: A binary-real-coded differential evolution for unit commitment problem. Electr. Power Energy Syst. **42**, 517–524 (2012)
3. Datta, D.: Unit commitment problem with ramp rate constraint using a binary-real-coded genetic algorithm. Appl. Soft Comput. **13**, 3873–3883 (2013)
4. Deka, D., Datta, D.: Multi-objective optimization of the scheduling of a heat exchanger network under milk fouling. Knowl.-Based Syst. **121**, 71–82 (2017)
5. Trivedi, A., Srinivasan, D., Biswas, S., Reindl, T.: A genetic algorithm differential evolution based hybrid framework: case study on unit commitment scheduling problem. Inf. Sci. **354**, 275–300 (2016)
6. Juang, C.F.: A hybrid of genetic algorithm and particle swarm optimization for recurrent network design. IEEE Trans. Syst. Man Cybern.-Part B: Cybern. **34**(2), 997–1006 (2004)
7. Kuo, R.J., Syu, Y.J., Chen, Z.Y., Tien, F.C.: Integration of particle swarm optimization and genetic algorithm for dynamic clustering. Inf. Sci. **195**, 124–140 (2012)

8. Ozturk, C., Hancer, E., Karaboga, D.: A novel binary artificial bee colony algorithm based on genetic operators. Inf. Sci. **297**, 154–170 (2015)
9. Epitropakis, M.G., Plagianakos, V.P., Vrahatis, M.N.: Evolving cognitive and social experience in particle swarm optimization through differential evolution: a hybrid approach. Inf. Sci. **216**, 50–92 (2012)
10. Smaïli, F., Vassiliadis, V.S., Wilson, D.I.: Mitigation of fouling in refinery heat exchanger networks by optimal management of cleaning. Energy Fuels **15**, 1038–1056 (2001)
11. Deb, K.: Multi-Objective Optimization Using Evolutionary Algorithms. Wiley, Chichester (2001)
12. Datta, D., Figueira, J.R.: A real-integer-discrete-coded differential evolution. Appl. Soft Comput. **13**(9), 3884–3893 (2013)
13. Storn, R., Price, K.: Differential evolution - a simple and efficient heuristic for global optimization over continuous spaces. J. Glob. Optim. **11**, 341–354 (1997)
14. Datta, D., Figueira, J.R.: A real-integer-discrete-coded particle swarm optimization for design problems. Appl. Soft Comput. **11**(4), 3625–3633 (2011)
15. Deb, K., Agarwal, S., Pratap, A., Meyarivan, T.: A fast and elitist multi-objective genetic algorithm: NSGA-II. IEEE Trans. Evol. Comput. **6**(2), 182–197 (2002)
16. Tian, J., Wang, Y., Feng, X.: Simultaneous optimization of flow velocity and cleaning schedule for mitigating fouling in refinery heat exchanger networks. Energy **109**, 1118–1129 (2016)

e-Proceedings of
International Conference on Advancements in Mechanical Engineering
(ICAME 2020)

Aliah University, Kolkata
16-18 January 2020

Finite Element based Studies on Elastic Properties of Carbon Nanotube-Reinforced Metal Matrix Composites

S. Kirtania[1] and D. Chakraborty[2]

[1]Assistant Professor, Department of Mechanical Engineering, Tezpur University, Assam, India
[2]Professor, Department of Mechanical Engineering, Indian Institute of Technology Guwahati, Assam, India
E-mail: [1]sushen@tezu.ernet.in, [2]chakra@iitg.ernet.in.

ARTICLE INFO

Keywords:
Carbon nanotube,
Metal matrix composites,
Finite element analysis,
Nonlinear,
Elastic properties

ABSTRACT

Present work deal with the evaluation of elastic properties of carbon nanotube (CNT)-reinforced metal matrix composites (MMCs) using finite element (FE) method. The Young's modulus of CNT-reinforced MMCs has also calculated theoretically using rule of mixture (ROM) formula. Results obtained from both the approaches are then compared to validate the present FE model. The effects of matrix materials and volume fraction on elastic properties have been investigated. The linear and nonlinear behavior of CNT has also been considered to calculate elastic modulus of CNT-reinforced MMCs. The Young's modulus in longitudinal direction of CNT-reinforced MMCs increased with the increase in the volume fraction of CNT. The computational values of longitudinal Young's modulus calculated by considering nonlinear behavior of CNT are always less than the computational values obtained by considering linear behavior of CNT as well as theoretical values calculated based on ROM. In general, the transverse Young's modulus calculated using FE method is more than the theoretical values, but it is found to be equal at 15% volume fraction of CNT for CNT/steel composites. Therefore, transverse Young's modulus of CNT-reinforced MMCs depends on the relative stiffness of the matrix materials.

1. Introduction

Carbon nanotube possesses excellent mechanical, thermal, electrical properties and exceptional chemical stability. Those properties of CNTs made them an ideal candidate for the reinforcement in the matrix [1]. Therefore, CNT-reinforced composite is an important research area for the last thirty years. As compared to conventional materials, composites possess high strength and stiffness. Therefore, for structural applications, CNT could be used as reinforcement in metal. Most of the literatures are available on polymer matrix composites using CNT as reinforcement. However, there are few literatures available on CNT-reinforce MMCs. Therefore, there is a need for detailed study of CNT-reinforced MMCs. Some of the important literatures on modelling and characterization of CNT-reinforced composites are presented here.

A book on CNT-reinforced MMCs edited by Agarwal et al. [2], where they presented the processing techniques, characterization, interfacial phenomena, computational studies, potential applications and future direction of CNT-reinforce MMCs. Goh et al. [3] fabricated CNT/ magnesium (Mg) composite at different volume fractions of CNT and reported the maximum improvement of yield strength, ultimate tensile strength, and ductility at 1.3 weight percentage of CNT. Thotsaphon et al. [4] fabricated multi-walled CNT (MWCNT)/titanium (Ti) composite and

e-Proceedings of
International Conference on Advancements in Mechanical Engineering
(ICAME 2020)
Aliah University, Kolkata
16-18 January 2020

Fabrication and Finite Element Analysis of L-pin Mechanism for Gearless Power Transmission

S. Gautam[1], S.A. Choudhary[2], G. Das[3] and S. Kirtania[4]

[1,2,3,4]*Department of Mechanical Engineering, Tezpur University, Assam-784028, India*
E-mail: [1]gautamsiddharth13.7@gmail.com, [2]sahilalamchoudhary@gmail.com, [3]giridharndas@gmail.com, [4]sushen@tezu.ernet.in

ARTICLE INFO

Keywords:
L-pin mechanism,
Gearless transmission,
Finite element analysis,
Stress,
Torque capacity.

ABSTRACT

The L-pin mechanism is an alternative to a gear transmission mechanism. The mechanism could replace the use of bevel gears in the transmission of power between shafts at the right angle to each other. The mechanism can be made with any number of L-pins greater than or equal to 3. It can be used for a wide variety of applications and runs smoothly even at high speed. In the present work; design, modeling, fabrication, testing, and analysis of the L-pin mechanism has been performed. It has been observed experimentally that the mechanism is capable of transmitting motion at right angles with negligible noise. Finite element (FE) analysis has also been carried out to find out the stresses and displacement of the L-pin. The torque capacity of the present mechanism has also been calculated using the result of FE analysis.

1. Introduction

Conventional geared transmission mechanism suffers from disadvantages like the high cost of production, loss of power due to friction and backlash. The L-pin mechanism is a right angle constant velocity joint that could replace the use of bevel gears in the transmission of power between shafts at right angles to each other. This L-pin mechanism can transmit power between two shafts connected other than the right angle also. The mechanism can be easily fabricated in a few simple operations with basic manufacturing equipment and common available materials. If one part of the mechanism is damaged, it can be easily replaced compared to the conventional gear transmission mechanism.

The L-pin mechanism was first used in tower clocks in 1685, notably the Big Ben clock in London [1]. The minimum number of L-pins required for the gearless power transmission mechanism to transmit power continuously is three, and increasing the number of L-pins makes it run more smoothly [2]. The advantages of transmission mechanism over gear mechanism are low backlash, ease of manufacturing, smooth operation, minimum power loss, portable, eliminates radial vibration etc. [1,2]. The applications of the mechanism are in gang drilling, lubrication pump, air blower, door shutter, compactors, printing press and many others [1,2]. Solanki *et al.* [3] performed FE analysis of L-pins mechanisms with 4, 6, and 8 L-pins and reported that the mechanism with 6 L-pins showed the least values of equivalent stress and deformation. Baradiya *et al.* [4] performed a motion analysis of the mechanism with 3 L-pins and concluded that the maximum permissible speed of the mechanism is 120 rpm due to excessive bending stress beyond 120 rpm. Yadav *et al.* [5] fabricated 3 L-pins mechanism and reported that sudden applied loads during operation should be avoided. They [5] also reported that low starting torque is required by the mechanism. Kumar and Das [6] reported that power can be transmitted between coaxial shafts of different diameter using *Z*-pin.

INVESTIGATION OF STRESS DISTRIBUTION AND STRAIN ENERGY RELEASE RATE IN CARBON NANOTUBE/ALUMINUM COMPOSITES HAVING A BROKEN CARBON NANOTUBE

Sushen Kirtania[1]* and Debabrata Chakraborty[2]

E-mail: sushen.kirtania@gmail.com

[1]Assistant Professor, Department of Mechanical Engineering, Tezpur University, Assam, India
[2]Professor, Department of Mechanical Engineering, Indian Institute of Technology Guwahati, Assam, India

Abstract: Carbon nanotubes (CNTs) are used as reinforcing materials for advanced nanocomposites due to their extraordinary mechanical, thermal and electrical properties. Even though there are few works on the fabrication and characterization of CNT/Aluminum (Al) composites, but there is no work on the fracture behavior of CNT/Al composites with a broken CNT. Therefore, the present analysis is aimed at studying the stress redistribution and determination of strain energy release rates (SERRs) of CNT/Al composites in presence of a broken CNT. Figure 1 shows the pictorial view of the finite element (FE) model of a square representative volume element (RVE) with nine-CNTs of CNT/Al composites, where the central CNT is considered to be broken. SOLID45 element embodied in ANSYS has been used for FE modeling. The nonlinear behavior of single-walled CNT has been considered.

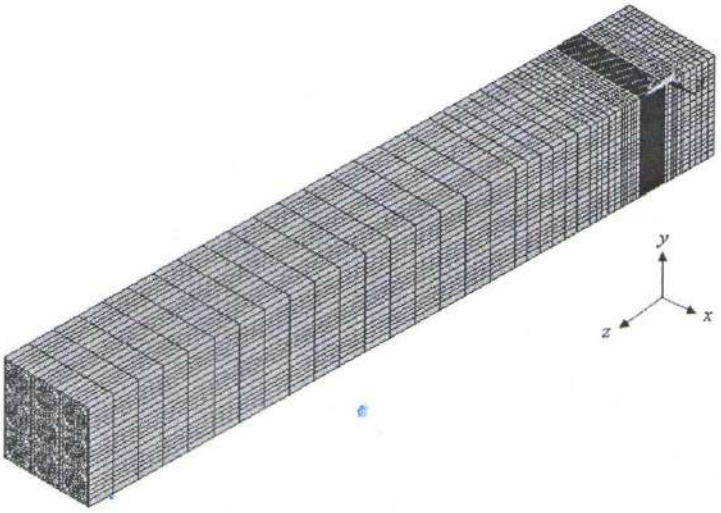

(1)

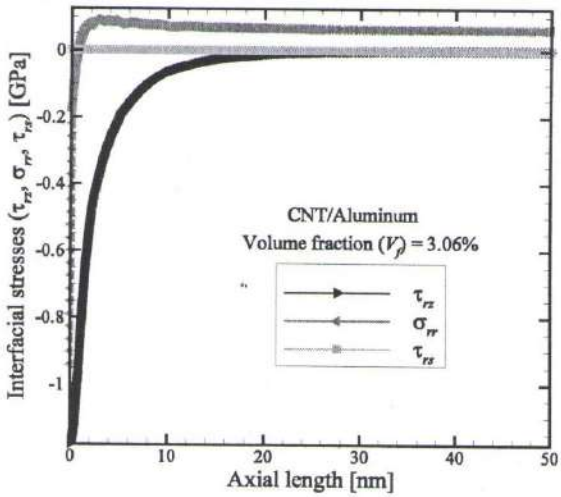

(2)

Figure 1. Finite element model of nine-CNTs square RVE. Figure 2. Distribution of interfacial stresses at the interface of broken CNT and matrix in front of crack tip.

Figure 2 shows the distribution of interfacial stresses at the interface of broken CNT and the matrix along the fiber length in CNT/Al composite for a constant volume fraction (V_f) of 3.06%. It can be seen in Fig. 2 that the values of interfacial normal (IFN) stress (σ_{rr}) and interfacial shear (IFS) stress (τ_{rs}) are negligible compared to the value of IFS stress (τ_{rz}). It could be concluded that τ_{rz} is responsible for debonding, σ_{rr} and τ_{rs} have negligible effect on debonding of CNT from the matrix materials. Virtual crack closure integral has been used for determination of the components of SERRs for mode-I, mode-II and mode-III (G_I, G_{II} and G_{III}). As expected G_I and G_{III} are negligible and G_{II} is only significant for such an axial loading. The effects of V_f have also been studied. Some of the important conclusions drawn from the present work are – (i) ineffective length of the broken CNT does not show significant changes with the change in V_f, (ii) IFS stress (τ_{rz}) is only responsible for debonding, (iii) breaking of one CNT may lead to the successive failure of the adjacent CNTs and finally the failure of nanocomposites, and (iv) SERR increases with the increase in V_f.

4th International Conference on Advanced Nanomaterials and Nanotechnology

December 08-11, 2015

Organized by

Centre for Nanotechnology
INDIAN INSTITUTE OF TECHNOLOGY GUWAHATI

ICANN 2015

This is to certify that Mr./Ms. Sushen Kirtania has made ORAL/POSTER presentation in 4th International Conference on Advanced Nanomaterials and Nanotechnology from 08-11 December, 2015 held at Centre for Nanotechnology, Indian Institute of Technology Guwahati, Guwahati - 781039, Assam, India.

Prof. Parameswar K. Iyer
(Convener)

Finite Element Analysis of Flywheels used for Punching Operation

Kalita M J [1], Das P [2, *], Mahfuz T [3], and Kiratania S [4]
[1,2,3,4] Department of Mechanical Engineering,
Tezpur University, Tezpur, Assam, India.

*pramatheshlmg21@gmail.com

Abstract. In this work, flywheel used for punching press operation has been analysed. A punch press is a stamping press operation. A punching hole uses a die and punching set which is pushed into the workpiece with extreme pressure. A flywheel is a machine component used in machines which serves as a reservoir of energy. In the present analysis, two types of flywheels viz hole type and arm type have been considered. Two types of materials viz cast iron grades of FG 220 and FG 300 have also been used. The flywheels have been modelled using Catia software, then those models have been imported in ANSYS software for finite element (FE) analysis. Stress and total deformation have been determined using FE method. To validate the computational results, the theoretical analysis has also been done. It has been observed that the differences between theoretical and computation results are comparable.

Keywords. Flywheel, Finite element analysis, Normal stress, Deformation.

1. Introduction

A punch press is driven by electric motor. In punching and shearing machines, maximum power is required only during a small part of the cycle, when the actual punching or shearing takes place. During remaining part of the cycle, negligible power is required to overcome the friction. If these machines are directly driven by an electric motor, a higher capacity motor corresponding to maximum power requirement during actual punching operation will be required. A motor of such kind will run almost idle during the remaining part of the cycle. It is obviously wasteful to provide such a large motor when its full capacity is needed but for a small fraction of the time. Providing a flywheel to these machines allow a much smaller motor to be used. During the actual punching operations, energy will be derived from the flywheel, slowing it down. During the relatively long period between two punching operations, the motor will be accelerating the flywheel back to its original speed.

The flywheel thus stores the kinetic energy during the idle portion of the work cycle by increasing its speed and delivers this kinetic energy during the peak-load period of punching. Therefore, when a flywheel is used between the motor and these machines, a smaller capacity motor will be sufficient.

Raut *et al.* carried out FE analysis of different types of flywheels. They have reported that the maximum stress is more in 4-arms flywheel than the 6 and 8 arm flywheels. Akram and Bankar reported that the mass of the flywheel changes with the change in design parameter. But, the change in mass had negligible effect on the energy storing capacity of the flywheel. Prathap and Srinivasulu carried out design of a flywheel based on the availability of the space limitation of 1m. Rajmane and Balasaheb reported that the peripheral velocity of the flywheel is governed by allowable strength of the

Finite Element Analysis of Flywheels used for Punching Operation

Kalita M J [1], Das P [2, *], Mahfuz T [3], and Kiratania S [4]
[1,2,3,4] Department of Mechanical Engineering,
Tezpur University, Tezpur, Assam, India.

*pramathoshlmg21@gmail.com

Abstract. In this work, flywheel used for punching press operation has been analysed. A punch press is a stamping press operation. A punching hole uses a die and punching set which is pushed into the workpiece with extreme pressure. A flywheel is a machine component used in machines which serves as a reservoir of energy. In the present analysis, two types of flywheels viz hole type and arm type have been considered. Two types of materials viz cast iron grades of FG 220 and FG 300 have also been used. The flywheels have been modelled using Catia software, then those models have been imported in ANSYS software for finite element (FE) analysis. Stress and total deformation have been determined using FE method. To validate the computational results, the theoretical analysis has also been done. It has been observed that the differences between theoretical and computation results are comparable.

Keywords. Flywheel, Finite element analysis, Normal stress, Deformation.

1. Introduction

A punch press is driven by electric motor. In punching and shearing machines, maximum power is required only during a small part of the cycle, when the actual punching or shearing takes place. During remaining part of the cycle, negligible power is required to overcome the friction. If these machines are directly driven by an electric motor, a higher capacity motor corresponding to maximum power requirement during actual punching operation will be required. A motor of such kind will run almost idle during the remaining part of the cycle. It is obviously wasteful to provide such a large motor when its full capacity is needed but for a small fraction of the time. Providing a flywheel to these machines allow a much smaller motor to be used. During the actual punching operations, energy will be derived from the flywheel, slowing it down. During the relatively long period between two punching operations, the motor will be accelerating the flywheel back to its original speed.

The flywheel thus stores the kinetic energy during the idle portion of the work cycle by increasing its speed and delivers this kinetic energy during the peak-load period of punching. Therefore, when a flywheel is used between the motor and these machines, a smaller capacity motor will be sufficient.

Raut *et al.* carried out FE analysis of different types of flywheels. They have reported that the maximum stress is more in 4-arms flywheel than the 6 and 8 arm flywheels. Akram and Bankar reported that the mass of the flywheel changes with the change in design parameter. But, the change in mass had neglegible effect on the energy storing capacity of the flywheel. Prathap and Srinivasulu carried out design of a flywheel based on the availability of the space limitation of 1m. Rajmane and Balasaheb reported that the peripheral velocity of the flywheel is governed by allowable strength of the

comparison to the Freundlich isotherm models, pseudo first order model. The maximum adsorption capacity of fish scale is 9.3 mg/g, 1.782 mg/g, 1.898 mg/g for fluoride, Cr(VI), Pb(VI) respectively. It gives maximum adsorption capacity of fluoride at the pH of 6.5 and at the agitation speed of 150 rpm for 3 hours of contact period i.e. 9.3 mg/g. This result shows that by using this bio-waste (fish scale) we canremove fluoride from drinking water.

Keyword: Fish scale, Langmuir isotherm model, Pseudo second order, Batch study

Comparative Study Between Composite and Conventional Steel Shafts Using Finite Element Method

Arshita Chaliha, Arjun Sarkar, Sucheta Brahma and Sushen Kirtania*

Department of Mechanical Engineering, Tezpur University, Napaam, Tezpur-784028, Assam, India.
**Corresponding Author: Email: sushen@tezu.ernet.in, Phone No: + 91-3712-275857*

A shaft is the component of a mechanical device that mainly transmits rotational motion and power. Also, a shaft, usually carries power transmitting components, such as gears, pulley etc., which exert forces on it in the transverse direction. These transverse forces cause bending in the shaft. In general, weight of vehicle could be reduced by using the composite shafts compared to conventional shaft without having any compromise in quality and reliability. The main advantages of composite materials are high stiffness to mass ratio and strength to weight ratio compared to conventional materials. Due to which, day by day conventional materials are replaced by composite materials in different engineering applications. Most of the earlier literatures reported that the existing steel shaft could be replaced by composite shafts. Therefore, the present finite element (FE) analysis has been performed considering both the conventional as well as composite shafts. A full three-dimensional FE

Representative Volume Element Based Finite Element Modeling of Carbon Nanotube (CNT)-Reinforced Composites with a Broken CNT

Sushen Kirtania[1] and Debabrata Chakraborty[2]

[1]*Department of Mechanical Engineering, Tezpur University, Assam, India.*

[1]sushen@tezu.ernet.in.

[2]*Department of Mechanical Engineering, Indian Institute of Technology Guwahati, Assam, India.*

[2]*chakra@iitg.ernet.in.*

***Abstract*— Three different types of representative volume elements (RVEs) have been considered for finite element (FE) modelling and analysis of carbon nanotube (CNT)-reinforced composites with broken CNT. In all the RVEs a CNT is considered to be broken with a small debonding ahead of the break and three dimensional FE analyses have been carried out to estimate the stress redistribution in the vicinity of the break in the form of axial normal stress in the broken CNT and interfacial normal and shear stresses at the interface between the broken CNT and the matrix. Strain energy release rate components have also been computed to assess the severity of debonding near the broken CNT. Results obtained from the three different RVEs have been compared to understand the advantages and limitations of such modelling and proper recommendations have been put forward for using appropriate RVE model in FE analysis of CNT-reinforced composites.**

***Keywords*— CNT/epoxy composites, Representative volume element, Finite element analysis, Broken CNT, Virtual crack closure integral, Stress distribution, Strain energy release rate.**

1. INTRODUCTION

Due to the exceptional properties of CNTs, CNTs are believed to be potential reinforcing materials for the next generation advanced nanocomposites. Therefore, CNT-based composites have been one of the important research areas since last twenty years. Due to their sizes, fabrication process and conducting tests for such CNT-based composites are extremely difficult and are not economical. Therefore, theoretical analysis and simulation are extensively used for understanding, analysing and designing of such nanocomposites. Generally, the volume fraction of CNT in CNT-reinforced composite is less compared to that in conventional glass or carbon fiber composites. Thus defect in CNT will have more impact on the strength and stiffness of such composites. However due to statistical distribution of strength of CNTs, it is possible that one or more CNT breaks during loading. In general, whenever there is a fiber break, it is accompanied by a small fiber matrix debonding at the vicinity of the break. Depending upon the applied load this debonding may grow. Therefore study on stress distribution and calculation of strain energy release rate (SERR) of CNT-reinforced composites with a broken CNT are important tasks those need to be addressed. In recent years, a large number of works have been reported on modelling, synthesis, characterization, load transfer mechanism and stress distribution in the broad area of CNT-reinforced composites and CNT/epoxy composite in particular. Some of these important works are discussed here.

Recently, Kausar et al. [1] presented a comprehensive review on the applications of CNT/epoxy composites in different areas. Chen and Liu [2] evaluated effective mechanical properties of CNT-based composites using three dimensional (3D) FE analyses and considering a 3D nanoscale RVE. Barber et al. [3] experimentally found the separation strength between CNT and the polymer matrix to be remarkably high, indicating the effectiveness of CNTs as reinforcement. Cheng et al. [4] reported that the Young's modulus and tensile strength of the CNT/epoxy composites could be increased by 716% and 160%, respectively compared to those of pure epoxy. Thostenson and Chou [5] fabricated and evaluated the mechanical properties of aligned CNT/polystyrene composites. The authors reported that the improvement of elastic modulus with aligned nanotube composites observed to be five times greater than that of the randomly oriented composites. Ci and Bai [6] investigated feasibility of reinforcement of CNT on different matrix materials and reported that reinforcement of CNT on soft and ductile matrix led to better performance. Haque and Ramasetty [7] developed an analytical model to study the axial stress and interfacial shear stress in single-walled carbon nanotube (SWCNT) reinforced polymer matrix composites. Fereidoon et al. [8] built a 3D FE model of a RVE near the crack tip and reported on the fracture behavior of CNT/epoxy composites. Lau and Hui [9] reported that the use of multi-walled carbon nanotubes (MWCNTs) as intrinsic reinforcements for composite structures might not allow the maximum strength to be achieved due to their non-uniform axial deformation and hence recommended the use of SWCNTs. Zuberi and Esat [10] compared the effect of two approaches viz. non-bonded interaction and perfect bonding in modelling the interface between SWCT and epoxy for determination of mechanical properties of SWCNT/epoxy composites.

Comparison betweenSquare and Hexagonal Representative Volume Elements for Evaluating Elastic Properties of CNT-reinforced Composites

Bichitra Narayon Gohain[1], Sushen Kirtania[2]

[1,2]*Department of Mechanical Engineering, Tezpur University, Assam 784028, India*

[1]*bichitrangohain55@gmail.com*

[2]*sushen@tezu.ernet.in*

Abstract— **In the present study, finite element (FE) analyses have been performed to evaluate elastic properties of CNT-reinforced composites. Two types of representative volume elements (RVEs) viz. hexagonal and square have been considered. Different types of matrix materials from low strength to high strength have been considered to observe the effect of matrix materials. Results obtained from FE simulation are compared with theoretical results calculated based on rule of mixture. It has been observed that the axial Young's modulus of CNT-reinforced composites obtained from the present FE simulations are exactly matched with the theoretical results. It has also been observed that transverse Young's modulus and Poisson's ratio obtained using square RVE are in good agreement with theoretical values than those obtained using hexagonal RVE. Effect of volume fraction on elastic properties has also been observed. It has also been observed that the axial and transverse Young's modulus of CNT-reinforced composites increase with the increase in volume fraction.But the effective Poisson's ratio decreases with the increase in volume fraction of CNT.**

Keywords— **CNT-reinforced composites, Representative volume element, Axial Young's modulus, Poisson's ratio, Finite element method, Rule of mixture**

1. INTRODUCTION

Iijima [1] in 1991 discovered CNT, which has exceptionally high strength, stiffness and resilience. Since then it is an important new research area in the field of nanotechnology. Due to these properties CNT opened a vast area of research in the field of nano-composites where CNT could be used as an excellent fiber in matrix to enhance mechanical, thermal, electrical and optical properties leading to the discovery of a new class of nano-composites. So, the evaluation of mechanical, thermal and electrical properties of CNT-reinforced compositesis important taskstodevelop new class nanocomposites. A large scale of experimental and simulation work have been published in order to determine the elastics properties, but due to their small size it is a very challenging task to conduct experimental work and also very expensive. On the other hand, it is too complicated to established analytical relation and to solve it in nanoscale level. But for characterization of CNT-reinforced composites, computer simulation furnishes an easy way for designing and analyzing of such composites. Finite element method is one of the numerical tools which is more powerful in its application in real world problems and can be used to calculate elastic properties of CNT-reinforced composites.

Many researchers reported that Young's modulus [2-4] of CNT is around 1TPa and Poisson's ratio is 0.28 [5-6]. Load carrying capacity of nanocomposites enhanced significantly due to addition of small percentage of CNT in matrix has been reported in some earlier publications [7-10]. Qian et al. [7] reported that with 1 wt% addition of CNT in epoxy, stiffness of the composites could be enhanced by 36% - 42% compared to the stiffness of pure epoxy. Liu and Chen [8] evaluated effective material properties of CNT-based composites by considering square RVEs. They showed that with the addition of 3.6% volume fraction of CNT in matrix the stiffness of the composites in axial direction can be enhanced by 33%. By adding 3.06% volume fraction of the CNT in epoxy, the effective axial Young's modulus as well as axial coefficient of thermalexpansion (CTE) of composites could be increased and decreased by 776.61% and 91%compared to theYoung's modulus and CTE of the pure epoxy [9]. Esawi et al. [10] reported that tensile strength and stiffness of CNT/Aluminum (Al) composite could be increased up to 50% and 23%, respectively, compared to pure aluminum. Literature review reveal that there are lots of works available in determination of elastic properties of CNT-reinforced composites. But there islessnumber of work available in determination of elastic properties using different types of RVEs.Therefore, the aim of the present work is to determine the elastic properties of square and hexagonal RVEs and recommended for using square RVE.

Fabrication and Vibration Analysis of Shaft of a Pedal Powered Washing Machine

Sanjana Talukdar[1], Narayan Das[1], Debangshu Sinha[1], Sumit Patni[1], Gaurav Kumar[1], Bhupendra Kumar Meena[1], Polash Pratim Dutta[2], Sushen Kirtania[2]

[1,2]*Department of Mechanical Engineering, Tezpur University, Assam-784028, India.*

[1]Sanjana26812@gmail.com

[2]sushen@tezu.ernet.in

[2]polashd@tezu.ernet.in

***Abstract*— In a developing nation like India, where most of the population lives in villages or rural areas, washing of clothes is a noteworthy issue. Individuals in these zones cannot afford to purchase the conventional washing machines. In addition, these regions are either in complete absence or lack of electricity. The goal of our work is to develop an efficient, low cost pedal powered washing machine using scrap parts that are easily available, cheap and easy to maintain. The existing fabricated washing machine produced rigorous vibration and leakage during washing the clothes. In the present work, the causes of vibration have been identified and possible solutions were implemented to reduce vibration and leakage. A simple mathematical model of the output shaft has been proposed to predict resonance and safe operating frequency range while washing the clothes.**

***Keywords*— Pedal powered washing machine, Problem identification, Vibration, Leakage, Low cost, Rural application.**

1. INTRODUCTION

A washing machine is a popular electronic home appliance, which is found in almost every household in the urban regions. The first washing machine was designed by James King in 1851 [1]. The washing machine used a drum device that is still used often in washing machines of today's generation. However it required hand power. The first drum based electric washing machine called the Thor was invented by Alva J. Fisher and manufactured by the Hurley Machine Company in 1908 [2]. The Thor was a drum type washing machine with a galvanized tub and an electric motor. Bendix Corporation introduced the first domestic automatic washing machine in 1937 [3]. In appearance and mechanical detail, this first machine was similar to the front loading automatic washers used today but the machine lacked drum suspension and it was very expensive. The drum speed change was facilitated by a 2-speed gearbox built to a heavy duty standard like a car synchromesh gearbox. The timer used miniature electric motors to sequence the washing and extraction process. A large number of US manufacturers introduced competing automatic machines (mainly of the top-loading type) in the late 1940s and early 1950s. Several manufacturers produced semi-automatic machines, requiring the user to intervene at one or two points in the wash cycle. A common semi-automatic type included two tubs: one with an agitator or impeller for washing, plus another smaller tub for water extraction or centrifugal rinsing.

During early 90's machines were available in the market that used microcontrollers for the timing process. With the passage of time more improvement was made in the field of washing machines and today's modern consumer washing machines incorporate many new features. In this 21st century, due to environmental concerns and water scarcity problems, the focus has shifted in developing technology associated with washing machines which can overcome these issues. The Xerox washing machine is one such new kinds of machine that uses primary nylon polymer beads and very little water [4]. Works are going on to develop washing machines of low cost and which do not require electricity. Ranjan et al. [5] developed a pedal powered washing machine using a transmission system connecting the bicycle frame to the front loaded washing machine. Ajay et al. [6] designed a pedal powered washer where inner drum is constructed by modifying a plastic utility tub. Other pedal powered washing machine developments have been reported which are low cost and energy saving devices [7-9]. Recognizing the need of low cost washing machine for rural India, the aim of the present work is to develop a low cost pedal powered washing machine (PPWM) with readily available scrap parts which can be used for washing sufficient quantities of clothes.

The washing machine generally involves rotating masses which rotate to agitate the clothes inside a drum creating turbulence to clean them. However, rotating machineries might involve problems like misalignment, unbalanced masses leading to vibration and noise which are unavoidable. A great challenge for the fabrication of the washing machine is to carefully eliminate these ill effects.

2. DETAILED SET UP

Figure 1 shows the front view of the fabricated pedal powered washing machine. It consists of a shaft (length 1 m, inner diameter = 0.04 m, outer diameter = 0.45 m) which is connected to the sprocket of the cycle. The shaft rotates when the cycle is pedalled. The inner drum with

Springer Link

The Constrained Single-Row Facility Layout Problem with Repairing Mechanisms

Nature-Inspired Methods for Metaheuristics Optimization pp 359-383 | Cite as

- Zahnupriya Kalita (1)
- Dilip Datta (1) Email author (ddatta@tezu.ernet.in)

1. Department of Mechanical Engineering, Tezpur University, , Tezpur, India

Chapter
First Online: 18 January 2020

- 355 Downloads

Part of the Modeling and Optimization in Science and Technologies book series (MOST, volume 16)

Abstract

The single-row facility layout problem (SRFLP), which deals with the placement of some facilities along a row by minimizing the overall material flow cost among them, is usually studied as an unconstrained problem allowing the placement of the facilities arbitrarily without any restriction. But a practical SRFLP instance may require to respect certain constraints imposed on the arrangement of its facilities. Such an SRFLP model, which can be termed as a *constrained* SRFLP (cSRFLP), is studied here by requiring to place some facilities in fixed locations, and/or in predefined orders with/without allowing the arrangement of any other facility in between two ordered facilities. The handling of such a complex problem generally requires a specialized algorithm incorporating some problem-specific information for intelligent search. But the development of an algorithm needs expertise, from which practitioners often suffer. Hence, it is shown here how the cSRFLP can be tackled using a general-purpose algorithm with some repairing mechanisms outside the algorithm for forcibly satisfying the constraints of the problem. Employing a permutation-based genetic algorithm for this purpose, the potentiality of the proposed procedure is demonstrated by applying it to a set of cSRFLP instances of different sizes.

Keywords

Combinatorial optimization Facility layout problem Constraint Repairing mechanism Genetic algorithm

Stability of Female Bicyclists on Sudden Braking

Modeling, Simulation and Optimization pp 153-163 | Cite as

- Dilip Datta (1) Email author (ddatta@tezu.ernet.in)
- Arpeeta Saikia (1)
- Zahnupriya Kalita (1)

1. Department of Mechanical Engineering, Tezpur University, , Tezpur, India

Conference paper
First Online: 18 March 2021

- 30 Downloads

Part of the Smart Innovation, Systems and Technologies book series (SIST, volume 206)

Abstract

Females are generally more prone of falling down from bicycles. Although bicycle is being analyzed on different aspects over the years, the exact science behind that instability is not yet known. Analyzing the seating arrangement in a bicycle and the nature of riding it, the present work explores the technical reasons behind the lower stability of female bicyclists on sudden braking, and subsequently proposes a scientific solution to the problem. The solution is an additional mechanism, fixed under the saddle arrangement without interfering the existing design of a bicycle, which tilts the saddle nose up and down automatically in order to prevent the forward sliding of the rider on the saddle surface during riding as well as to allow her comfort mounting and dismounting.

Keywords

Bicycle Stability Female bicyclist Sudden braking

This is a preview of subscription content, log in to check access.

References

1. Baeyens, L., Vermeersch, E., Bourgeois, P.: Bicyclist's vulva: observational study commentary: attitudes to women's bicycling have changed. Br. Med. J. (BMJ) **325**(7356), 138–139 (2002)

Stability of Bicycle at Low Speed

Modeling, Simulation and Optimization pp 165-175 | Cite as

- Dilip Datta (1) Email author (ddatta@tezu.ernet.in)
- Zahnupriya Kalita (1)
- Sudipta Saikia (1)

1. Department of Mechanical Engineering, Tezpur University, , Tezpur, India

Conference paper
First Online: 18 March 2021

- 32 Downloads

Part of the Smart Innovation, Systems and Technologies book series (SIST, volume 206)

Abstract

Science behind riding a bicycle is still not well known, particularly how the bicycle remains in an upright position during riding. The stability of the bicycle gets reduced gradually with decreasing speed, and finally it falls down below a particular low speed or when it is at rest. It is observed that female, inexperienced, and aged riders are generally more prone to fall down from bicycles at low speed. But such issues are not yet addressed in literature. Hence, performing a systematic analysis of stability, the present study first focuses on exploring the technical reasons behind the instability of a bicycle at a low speed, and then to propose a technical solution for improving the stability of the bicycle. The solution is an additional mechanism, attached on the frame of a bicycle without interfering the existing design of the bicycle, which automatically turns back the front wheel in the vertical plane of the bicycle so as to help the rider to balance the bicycle, particularly at a low speed when the front wheel gets turned largely from the vertical plane of the bicycle upon pedaling.

Keywords

Bicycle Stability Low speed

This is a preview of subscription content, log in to check access.

References

1. Abagnale, C., Cardone, M., Iodice, P., Strano, S., Terzo, M., Vorrano, G.: Derivation and validation of a mathematical model for a novel electric bicycle. In:

TEQIP III

NATIONAL CONFERENCE FOR STUDENTS ON ADVANCES IN MECHANICAL ENGINEERING

DEPARTMENT OF MECHANICAL ENGINEERING
ASSAM ENGINEERING COLLEGE

CERTIFICATE OF PARTICIPATION

This is to certify that

Barnali Chowdhury of **Tezpur University**

has participated and successfully prsented a paper in TEQIP-III sponsored **"National Conference for Students on Advances in Mechanical Engineering"** organized by Department of Mechanical Engineering, Assam Engineering College on 6th of March 2020.

DR. SUDIP KUMAR DEB	DR. PRADIP BAISHYA	DR. RANJIT KUMAR DUTTA
	TEQIP III Cordinator	Prof. & HOD

Polymers Composites | OPEN ACCESS | 1 Oct 18
Development of Various Industrial Lime Sludge Waste-Filled Hybrid Polymeric Composites for Environmental Sustainability

Authors: Authors and affiliations
Sabahi Kasthuri

Chapter
First Online: 27 September 2018
519 Downloads
Part of the Materials Horizons: From Nature to Nanomaterials book series (SMHNN)

Abstract

A potentially hazardous industrial waste material in our society is lime sludge which is sourced mainly from various industries (fertilizer, paper, sugar and soda ash) and generally disposed off in dumpyards or used in manufactured land filling—both causing pollution. Hence, an alternative idea of environmental sustainability is by reusing lime sludge as reinforcing agent in polymeric composites. In this line of thought, lime sludge waste is used as in HDPE to HDPE and epoxy matrices in order to investigate the effects of lime sludge on its composite properties. This would ultimately, throw light on the feasibility and commercial viability of lime sludge waste in polymeric composites. In the present work, lime sludge waste filled HDPE composites and maleic anhydride-grafted polyethylene (MAPE) as compatibilizer for effective adhesion at the filler/matrix boundary. Lime sludge waste was also used as filler in conjunction with randomly dispersed and woven coir fiber reinforced HDPE composites along with 3 wt% MAPE as compatibilizer. It is observed the properties such as flexural strength and mechanical rigidity (tensile and flexural) of the lime sludge infused composites improved with filler addition. The tensile strength increased up to 20 wt% filler addition due to effective reinforcement; however, the tensile strength decreased due to particle agglomeration. Additionally, lime sludge is used as filler in short and long coir fibre added epoxy composites. It is found that lime sludge content of 6 wt% results in superior tensile strength in coir fibre reinforced epoxy composites. In general, lime sludge is found to improve the bending strength and mechanical rigidity (tensile and flexural modulus) with increasing filler weight fraction. Thus, the reuse of lime sludge filler in polymeric composites not only results in the enhancement of various mechanical properties, but also reduces pollution, decreases the cost of the composites and improves the commercial viability of lime sludge waste.

Keywords

Lime Sludge Maleic Anhydride grafted Polyethylene (MAPE) Coir Fiber (CF)
Filler Weight Fraction Rigid Filler Particles

These keywords were added by machine and not by the authors. This process is experimental and the keywords may be updated as the learning algorithm improves.

This is a preview of subscription content, log in to check access.

Bibliography

1. Assessment of utilization of industrial solid wastes in cement manufacturing (2006) Technical report on programme objective series PROBES/103/2006-2007, Central Pollution Control Board (Govt. of India)
Google Scholar
2. Wiegand PE, Unwin JP (1994) Alternative management of pulp and paper in-dustry solid wastes. Tappi J 77(4):91–97
Google Scholar CrossRef
3. Torkaborhani AM, Haghighat N, Shadparvar V (2010) Effect of paper mill lime sludge as an acid soil amendment. Sci Res Essays 5(24):3929–3936
Google Scholar
4. Evanylo GK, Daniels WL (1999) Paper mill sludge composting and compost utilization. Compost Sci Utilization 7(4):30–39
CrossRef Google Scholar
5. Kwon S, Kim KJ, Kim H, Kundu PP, Kim TJ, Lee YK, Lee BH, Choe S (2005) Tensile property and interfacial debonding in the sabic-filled HDPE, LDPE, and LLDPE composites. Polymer 47(4):5901–5909
CrossRef Google Scholar
6. Bartczak Z, Argon A, Cohen R, Weinberg M (1999) Toughness mechanism in semi-crystalline polymer blends: II. High-density polyethylene toughened with calcium carbonate filler particles. Polymer 40(9):2347–2365
CrossRef Google Scholar
7. Zuiderduin W, Westzaan C, Huetink J, Gaymans R (2003) Toughening of polypropylene with calcium carbonate particles. Polymer 44(1):261–275
CrossRef Google Scholar
8. Kim KJ, White JL, Shin SE, Choe S (2004) Effects of stearic-acid coated talc, CaCO3, and mixed talc/CaCO3 particles on the rheological properties of polypropylene compounds. J Appl Polym Sci 93(5):2105–2113
CrossRef Google Scholar
9. Kim HS, Lee BH, Choi SW, Kim S, Kim HJ (2007) The effect of types of maleic anhydride-grafted polypropylene (MAPP) on the interfacial adhesion properties of bio-flour-filled polypropylene composites. Compos A Appl Sci Manuf 38(6):1473–1482
CrossRef Google Scholar
10. Yang HS, Kim HJ, Park HJ, Lee BJ, Hwang TS (2007) Effect of compatibilizing agents on rice husk flour reinforced polypropylene composites. Compo Struct 77(1):45–55
CrossRef Google Scholar
11. Kashyap S, Datta D (2017) Industrial Lime Sludge waste—HDPE composites—a study of their mechanical, thermal, and morphological properties. J Thermoplast Compos Mater. https://doi.org/10.1177/0892705717718489
CrossRef Google Scholar
12. Kashyap S, Datta D (2018) Evaluation of steric acid modified industrial lime sludge waste as a filler in high density polyethylene composites. J Polym Eng 38(4):333–341
CrossRef Google Scholar
13. Acha BA, Aranguren MI, Marcovich NE, Reboredo MM (2005) Composites from PMMA modified thermosets and chemically treated wood flour. Polym Eng Sci 45(5):599–1010
CrossRef Google Scholar
14. Jain SH, Anand MP, Clarke SJ, Pantony SR (2005) Modified polyester resins for natural fibre composites. Compos Sci Technol 65(3):565–573
CrossRef Google Scholar
15. Wu CS (2005) Improving polylactic/starch biocomposites by grafting polylactide with acrylic acid—characterization and biodegradability assessment. Macromol Biosci 5(4):356–364
CrossRef Google Scholar
16. Martí-Ferrer F, Vilaplana F, Ribes-Greus A, Benedito-Borrás A, Sanz-Box C (2006) Flour rice husk as filler in block copolymer polypropylene–effect of different coupling agents. J Appl Polym Sci 99(4):1823–1833
CrossRef Google Scholar
17. Tserki V, Matzinos P, Panayiotou C (2006) Novel biodegradable composites based on treated lignocellulosic waste flour as filler. Part II. Development of biodegradable composites using treated and compatibilized waste flour. Compos A Appl Sci Manuf 37(9):1231–1238
CrossRef Google Scholar
18. Pan L, Deng Z, Nan CW, Li M (2019) Thermal, electrical and mechanical properties of plasticized polymer electrolytes based on PEO/P (VDF-HFP) blends. Electrochim Acta 484(2):1015–1020
CrossRef Google Scholar
19. Kim TD, Oh TG, Oh ST, Moon IH (2001) Thermal conductivity of Ni–Cu composites at various temperatures. Mater Lett 51(5):420–424
CrossRef Google Scholar
20. Gracia JI, Evans RE, Palmer RJ, Johnson NJ (1987) Toughened composites. STP 937:397–412
Google Scholar
21. Linn JY, Angi EJ, Hwang LF, Wilcox BC (1988) Toughening composites by matrix modification. Fleet Eng 44:1027
Google Scholar
22. Bijwe J, Logani CM, Tewari US (1990) Influence of fillers and fiber reinforcement on abrasive-wear resistance of polymer composites. Wear 138(1–2):77–94
CrossRef Google Scholar
23. Wang J, Gu M, Songhao B, Ge S (2005) Investigation of the influence of MoS2 filler on the tribological properties of carbon fiber reinforced nylon 1010 composites. Wear 259(1–6):774–779
CrossRef Google Scholar
24. Mir SS, Nafea N, Hasan M, Hasan K, Hassan A (2005) Improvement of physico-mechanical properties of coir fiber reinforced polypropylene composites by fiber chemical treatment. Mater Des 32:421–427
CrossRef Google Scholar
25. Nam TH, Ogihara S, Tung NH, Kobayashi S (2011) Effect of alkali treatment on interfacial and mechanical properties of coir fiber reinforced poly (butylene succinate) biodegradable composites. Compos B Eng 42(6):1648–1656
CrossRef Google Scholar
26. Salmah H, Russell CM, Supri AG (2009) Compatibilization of polypropylene/ethylene propylene diene terpolymer/kaolin composites: the effect of maleic anhydride-grafted-polypropylene. J Phys Sci 20(1):91–107
Google Scholar
27. Zhou Z, Xu M, Yang Z, Li X, Shao D (2014) Effect of maleic anhydride grafted polyethylene on the properties of chopped cotton fiber/wood plastic composites. J Retail Plast Compos 33(5):1210–1215
CrossRef Google Scholar
28. Satyanarayana KG, Guimarães JL, Wypych F (2007) Studies on lignocellulosic fibers of Brazil. Part I: source, production, morphology, properties and applications. Compos Part A Appl Sci Manuf 38(7):1694–1709
CrossRef Google Scholar
29. Jayabal S, Sathiyamurthy S, Loganathan KT, Kalyanasundaram S (2010) Effect of soaking time and concentration of NaOH solution on mechanical properties of coir–polyester composites. Bull Mater Sci 33(4):397–374
CrossRef Google Scholar
30. Morandim-Giannetti AA, Agnelli JAM, Lanças BZ, Magaludnos R, Casarin SA, Bettini SHP (2012) Lignin as additive in polypropylene/coir composites: Thermal, mechanical and morphological properties. Carbohydr Polym 87(4):2563–2568
Google Scholar
31. Lei Y, Wu Q, Yao F, Xu Y (2007) Preparation and properties of recycled HDPE/natural fiber composites. Compos A Appl Sci Manuf 38(7):1664–1674
CrossRef Google Scholar
32. Yao F, Wu Q, Lei Y, Xu Y (2008) Rice straw fiber-reinforced high-density polyethylene composite: Effect of fiber type and loading. Ind Crops Prod 28(1):63–72
CrossRef Google Scholar
33. Ayrilmis N, Jarusombuti S, Fueangvivat V, Bauchongkol P, White RH (2011) Coir fiber reinforced polypropylene composite panel for automotive interior applications. Fibers Polym 12(7):919
CrossRef Google Scholar
34. Rosman HD, Tay GS, Kumar RN, Abdubkar A, Ismail H, Ishak ZAM (1999) Polypropylene hybrid composites: a preliminary study on the use of glass and coconut fiber as reinforcements in polypropylene composites. Polym Plas Technol Eng 38(5):907–1011
CrossRef Google Scholar
35. Bettini SHP, Brondo ABLC, Augusto JS, Antunes LA, Moraes PL, Condotta R, Bosse BC (2010) Investigation on the use of coir fiber as alternative reinforcement in polypropylene. J Appl Polym Sci 118(5):2842–2848
CrossRef Google Scholar
36. Brahmakumar M, Pavithran C, Pillai RM (2005) Coconut fibre reinforced polyethylene composites: effect of natural waxy surface layer of the fibre on fibre/matrix interfacial bonding and strength of composites. Compos Sci Technol 65(3–4):563–569
CrossRef Google Scholar
37. Bisoyi M, Mohanty S, Nayak SK (2009) Influence of organically modified nanoclay on the performance of pineapple leaf fiber-reinforced polypropylene nanocomposites. J Appl Polym Sci 114(5):2892–2903
CrossRef Google Scholar
38. Nayak SK, Mohanty S, Samal SK (2010) Influence of interfacial adhesion on the structural and mechanical behavior of PP-banana/glass hybrid composites. Polym Compos 31(7):1241–1257
CrossRef Google Scholar
39. Satapathy S, Nando GB, Jose J, Nag A (2008) Mechanical properties and fracture behavior of short pet fiber-waste polyethylene composites. J Retail Plast Compos 47(5):1367–1384
CrossRef Google Scholar
40. Satapathy S, Nando GB, Nag A, Raju KVSN (2011) HDPE-fly ash/waste fly ash Composites. J Appl Polym Sci 120(5):4283–4297
CrossRef Google Scholar
41. Satapathy S, Nag A, Nando GB (2012) Effect of electron beam irradiation on the mechanical, thermal, and dynamic mechanical properties of fly ash and nanostructured fly ash waste polyethylene hybrid composites. Polym Compos 33(3):369–379
CrossRef Google Scholar
42. Pardo SG, Bercal C, Arce A, Abad MJ, Cano J (2010) Rheological, thermal, and mechanical characterization of fly ash-thermoplastic composites with different coupling agents. Polym Compos 31(4):1724–1730
CrossRef Google Scholar
43. Satapathy S, Kothapalli RVS (2018) Mechanical, dynamic mechanical and thermal properties of banana fiber/recycled high density polyethylene biocomposites filled with flyash constituents. J Polym Environ 26(5):2020–2033
CrossRef Google Scholar
44. Malkapuram R, Kumar V, Negi YS (2009) Recent development in natural fiber reinforced polypropylene composites. J Retail Plast Compos 28(10):1169–1189
CrossRef Google Scholar
45. Ramprasath R, Jayabal S (2016) Particle swarm and simulated annealing based intuitive search optimization of flexural behaviors in bioparticles impregnated coir fiber–vinyl ester composites. Polym Compos 37(6):1763–1774
CrossRef Google Scholar
46. Rajeeswaraswaran S, Jayabal S (2016) A lexicographic multi objective genetic algorithm for optimization of mechanical properties of coir-nanogap impregnated coir–polyester composites. Polym Compos 37(5):844–853
CrossRef Google Scholar
47. Mythily C, Pu Z, Kukutschová J, Qi S, Jiang X, Zheng X, Yin R, Vaculík M, Heliová M, Lu Y (2015) Jute fibers and powdered hazelnut shells as natural fillers in non-asbestos organic non-metallic friction composites. Mater Des 51:827–835
CrossRef Google Scholar
48. Akkoniet B, Akpinz M, Shahvan A (2015) Mechanical properties of palm fibre reinforced recycled HDPE. Adv Mater Sci Eng 2015:1–7
CrossRef Google Scholar
49. Yao Z, Xia M, Ge L, Chen T, Li H, Ye Y, Zheng H (2014) Mechanical and thermal properties of polypropylene composites filled with CaCO3 and shell-waste derived bio-fillers. Fibers Polym 15(7):1478–1487
CrossRef Google Scholar
50. Muthu J, Priscilla J, Odedci A, Kuppen N (2017) Characterization of coir fibre hybrid composites reinforced with clay particles and glass spheres. J Compos Mater 0:1–15. https://doi.org/10.1177/0021998317734268
CrossRef Google Scholar
51. Khademieslam H, Kalaiye M (2016) Evaluation of the bending strength, impact strength, and morphological properties of wheat straw fiber/paper mill sludge/polypropylene composites. BioResources 11(2):2934–2960
CrossRef Google Scholar
52. Knight OW (1960) Polyethylene. In: Polymer toughening. Marcel! Dekker Inc, Monticello, NY 12701-5983, USA, pp 99–193
Google Scholar
53. Leong Y, Bakar A, Ishak Z, Ariffin A, Pukanszky B (2004) Comparison of the mechanical properties and interfacial interactions between talc, kaolin, and calcium carbonate filled polypropylene composites. J Appl Polym Sci 94(6):2326–2336
CrossRef Google Scholar

Copyright information

© Springer Nature Singapore Pte Ltd. 2018

About this chapter

Check for updates

Cite this chapter as:
Kashyap S., Datta D. (2018) Development of Various Industrial Lime Sludge Waste-Filled Hybrid Polymeric Composites for Environmental Sustainability. In: Sidhu S., Bains P., Saxena P., Sadasivuni K. (eds) Polymer-Based Nanocomposites: Materials Horizons: From Nature to Nanomaterials. Springer, Singapore. https://doi.org/10.1007/978-981-13-2417-8_10

First Online 27 September 2018
Print ISBN 978-981-13-2416-1
Online ISBN 978-981-13-2417-8
Publisher Name Springer, Singapore
DOI https://doi.org/10.1007/978-981-13-2417-8_10
eBook Packages Chemistry and Materials Science (R0)
Chemistry and Material Science (R0)

Buy this book on publisher's site
Reprints and Permissions

Chapter EUR 24.95 Price excludes VAT (India)
DOI: 10.1007/978-981-13-2417-8_10
Instant PDF download
Readable on all devices
Own it forever
Exclusive offer for individuals only
Tax calculation will be finalised during checkout
Buy Chapter
eBook EUR 93.08
Softcover Book EUR 109.99
Hardcover Book EUR 149.99
Learn about institutional subscriptions
Cite chapter

Chapter EUR 24.95 Price excludes VAT (India)
DOI: 10.1007/978-981-13-2417-8_10
Instant PDF download
Readable on all devices
Own it forever
Exclusive offer for individuals only
Tax calculation will be finalised during checkout
Buy Chapter
eBook EUR 93.08

Over 10 million scientific documents at your fingertips
Academic Edition

Home Impressum Legal information Privacy statement California privacy statement How we use cookies Manage cookies/Do not sell my data Accessibility Contact us

SPRINGER NATURE
© 2020 Springer Nature Switzerland AG. Part of Springer Nature.
Not logged in - Tripura University (TRIPURA) (20.500.11866.1) - Agartala (3000100000) - UGC Fed Account (3000130000) - HELP Library Consortium (3001239) (3000130000) - Information and Library Network (INFLIBNET) Centre (3000175000)
141.105.69.240

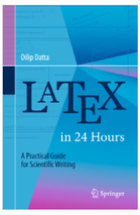

© 2017

LaTeX in 24 Hours

A Practical Guide for Scientific Writing

Authors (view affiliations)
Dilip Datta

Provides insight into LaTeX for scientific writers with little or no prior technical experience
Presents easy and understandable exercises and examples to get to grips with LaTeX fast
Demystifies the intricacies of working with LaTeX for academic writing

Textbook

1 Citations
8.1m Downloads

eBook EUR 32.09
Price includes VAT (India)

- ISBN: 978-3-319-47831-9
- Instant PDF download
- Readable on all devices
- Own it forever
- Exclusive offer for individuals only
- Tax calculation will be finalised during checkout

Buy eBook

Softcover Book EUR 39.99

Learn about institutional subscriptions

Table of contents (24 chapters) | About this book | Reviews

Page 1 of 2 Search within book

Front Matter PDF
Pages i-xxv

Introduction
Dilip Datta
Pages 1-8

Fonts Selection
Dilip Datta
Pages 9-14

Formatting Texts I
Dilip Datta
Pages 15-25

Formatting Texts II
Dilip Datta
Pages 27-36

Page Layout and Style
Dilip Datta
Pages 37-47

Listing and Tabbing Texts
Dilip Datta
Pages 49-58

Table Preparation I
Dilip Datta
Pages 59-70

Table Preparation II
Dilip Datta
Pages 71-80

Figure Insertion
Dilip Datta
Pages 81-90

Figure Drawing
Dilip Datta
Pages 91-100

Equation Writing I
Dilip Datta
Pages 101-112

Equation Writing II
Dilip Datta
Pages 113-123

User-Defined Macros
Dilip Datta
Pages 125-136

Bibliography with LaTeX
Dilip Datta
Pages 137-140

Bibliography with the BIBTeX Program
Dilip Datta
Pages 141-151

Lists of Contents and Index
Dilip Datta
Pages 153-160

Miscellaneous I
Dilip Datta
Pages 161-170

Miscellaneous II
Dilip Datta
Pages 171-180

Letter and Article
Dilip Datta
Pages 181-190

Page 1 of 2

Over 10 million scientific documents at your fingertips

Academic Edition

Home | Impressum | Legal information | Privacy statement | California privacy statement | How we use cookies | Manage cookies/Do not sell my data | Accessibility | Contact us

SPRINGER NATURE

© 2020 Springer Nature Switzerland AG. Part of Springer Nature.
Not logged in · Tezpur University (3000060537) - Convener, UGC-Infonet Digital Library Consortium (3000132959) - UGC Trial Account (3000178880) - DBT e-Library Consortium (DeLCON) (3000183443) - Information and Library Network (INFLIBNET) Centre (3994475188) · 14.139.219.244

Time Series Analysis of Manufacturing Defects – A Case of Refrigerator Liner Manufacturing

Barnali Chowdhury [1] and Sudip Kumar Deb[2]

[1]*Department of Mechanical Engineering , Tezpur University, Tezpur, India.*
[2]*Department of Mechatronics Engineering, Assam Engineering College,Gauhati University Guwahati, India,*

[1]barnali@tezu.ernet.in
[2]sudipkumardeb@gmail.com

Abstract

Defects play a significant role in enhancing the performance of a product and improving the productivity of an organization. Further, defects cannot be isolated or completely removed from a process or a product but can only be reduced. Defect data analysis are being done using commonly used tools namely cause–effect diagram, Pareto analysis, Failure Modes and Effects Analysis etc. since the time when enhancing productivity and reducing cost of poor quality were given due importance. However, these are inadequate to ascertain any persistence behavior or significant correlation among the defect data and cannot provide any forecast based on the existing situation. This inadequacy of commonly used tools in carrying out such effective and exploratory data analysis may be overcome by using time series approach. Hence in this paper, a humble attempt has been made to analyze manufacturing defect data using time series approach and discover significant correlations among them, which would further enable to understand, forecast trend and diagnose manufacturing process problems at a grave depth.

Keywords -Time series, rejection data, forecast, liner manufacturing.

Analysis of Performance Parameters of a Shell and Tube Heat Exchanger using Design of Experiments

Bikshya Saikia[1] and Barnali Chowdhury[2]

[1]*Department of Mechanical Engineering, Tezpur University, Tezpur, India.*
[2]*Department of Mechanical Engineering, Tezpur University, Tezpur, India.*

[1]bsaikia221@gmail.com
[2]barnali@tezu.ernet.in

Abstract

A heat exchanger is important equipment used for the regulation of heat in a wide range of domestic and industrial processes and as a means of waste heat recovery. Therefore it is necessary to find out the optimum combination of parameters that influence the performance of heat exchangers. Experimental analysis is the most basic form of analysis of the performance parameters of a system. However such an analysis has certain limitations and may not always give the desired results. Hence in this work an attempt has been made to carry out a statistical analysis of a shell and tube heat exchanger in order to determine the significant parameters that affect its performance. The performance parameters of the heat exchanger namely log mean temperature difference and effectiveness are analysed with the help of a statistical tool called the Design of Experiments (DOE). Mathematical models are then developed and optimum parameters are obtained.

Keywords –Heat exchangers, DOE, statistical analysis, optimization.

Springer Link

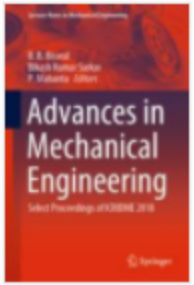

Advances in Mechanical Engineering pp 709-716 | Cite as

Performance Analysis of a Coal-Fired Open Cycle MHD Plant at Constant Subsonic Inlet Nozzle Mach Number with Variation in Nozzle–Area Ratio

Authors | Authors and affiliations

Prabin Haloi, Tapan Kumar Gogoi

Conference paper
First Online: 17 January 2020

738
Downloads

Part of the Lecture Notes in Mechanical Engineering book series (LNME)

Academic Science

DIIF

Conference Info

Reference No.:NITTTR323

2nd International Conference on Engineering Technology, Science and Management Innovation (ICETSMI-2017)

Venue-
National Institute of Technical Teachers Training & Research (NITTTR),
MHRD,Govt of India, Chandigarh, India
on 15th January 2017

Certificate of Presentation

This is to certify that

B.Chowdhury
Department of Mechanical Engineering, Tezpur University, Tezpur, Assam, India

Presented a paper titled as

"Cause-Effect Diagram Versus System Dynamic Model – A case study of Manufacturing Defects analysis"

Organized by Conference Info in Association with Academic Science at
National Institute of Technical Teachers Training & Research(NITTTR),
MHRD, Govt of India, Chandigarh, India
on 15th January 2017

Dr K. Agarwal
Editor, Academic Science

Convener

2021/5/28 22:10
SHOT ON POCO F1
POCO

National Conference on

SUSTAINABLE MECHANICAL ENGINEERING: TODAY AND BEYOND

SMETB 2017

March 25-26, 2017

Department of Mechanical Engineering, Tezpur University, Assam, India

This is to certify that Prof./Dr./Mr./Ms. Barnali Chowdhury *of* Tezpur University *participated and presented a paper titled* Analysis of manufacturing defects using FMEA - a step towards defect prevention. *in the* ***National Conference on SUSTAINABLE MECHANICAL ENGINEERING: TODAY AND BEYOND****, 2017 held at Tezpur University , Assam , India.*

SMETB 2017

(Dr. Partha P. Dutta)	(Prof. Tapan K. Gogoi)	(Dr. Seikh M. Kamal)
Chairman	Organizing Secretary	Joint Organizing Secretary

POCO
SHOT ON POCO F1
2021/5/28 22:11

INTERNATIONAL CONFERENCE

on

Sustainable Approaches in Food Engineering and Technology

(SAFETy-2021)

24th-25th June, 2021

Certificate

BARNALI CHOWDHURY

This is to certify that Dr./Mr./Ms. ..... has participated as Oral Presenter *..... at SAFETy-2021, organized by the Department of Food Engineering & Technology, Tezpur University, Assam, India, and Department of Food Science & Technology, University of Georgia, Georgia (US) in Association with AFST(I) Tezpur Chapter during 24th-25th June, 2021.*

Title: Design and analysis of a water pumping device - A solution for hilly terrains

Author(s): Chowdhury, B., Maitra, S., Das, M. & Krishna, K.

Dr. Amit Baran Das	Dr. Abhinav Mishra	Prof. Nandan Sit	Prof. Manpreet Singh
Organizing Secretary	Organizing Secretary	Chairperson	Chairperson
TEZPUR UNIVERSITY	UNIVERSITY OF GEORGIA	TEZPUR UNIVERSITY	UNIVERSITY OF GEORGIA

International Conference on Recent Innovations and Developments in Mechanical Engineering *NIT Meghalaya, Shillong, India, November 8 – 10, 2018*
Paper No. IC-RIDME18: 163

PERFORMANCE ANALYSIS OF MIXED CONVECTION IN T-SHAPED GEOMETRY FOR ENTROPY GENERATION USING LATTICE BOLTZMANN METHOD

Arupjyoti Das[1], Shikha Bhuyan[2*]
[1]Department of Mechanical Engineering, Tezpur University, Tezpur, PIN - 784028, India
[2]Department of Mechanical Engineering, Tezpur University, Tezpur, PIN - 784028, India

ABSTRACT
The present work focuses on solving differentially heated top lid driven T shaped cavity for three different velocities which experiences mixed convection using lattice Boltzmann method. The behavior of streamlines, isotherms and entropy generation maps are extensively studied taking three fluids namely air (Pr=0.71), ammonia (Pr=1.38) and water (Pr=6.13) for three different cases of Ri=0.1, Ri=1 and Ri=10. Richardson number and Prandtl number were found to be greatly influential on the fluid flow and heat diffusion inside the cavity. It was found that increasing Prandtl number increases the average Nusselt number while increasing the Richardson number decreases the average Nusselt number. The entropy generation was seen to be more concentrated at a few locations near the wall since the entropy generation due to temperature difference is more prominent than the entropy generation due to viscous dissipation.

Keywords: *Mixed convection, Lattice Boltzmann Cavity, T shaped Cavity, Entropy generation*

1. INTRODUCTION

Due to its tremendous application in practical world, study on mixed convection with lid-driven flows in enclosures has been on demand for more than a couple of decades now. It has been extensively explored for designing solar collectors, cooling of electronic devices, air conditioning vents and ducts, drying technologies etc. A literature review on the subject shows that cavity shape is a pertinent parameter of the analysis of mixed convection. An in-depth analysis on fluid flow and heat transfer in square and rectangular cavities driven by shear and buoyancy has been done. However, a dearth is observed in the study of T-shaped cavity.

Hatami et al. [1] studied mixed convection heat transfer of nano fluids in a T-shaped lid-driven porous cavity. They revealed the significant effects of shape and dimensions of the T-shaped cavity on the heat transfer efficiency and Nusselt number and optimized the geometry of T-shaped cavity for studying the effect of the constant coefficients (such as Re, Ri and Pr etc.) on the Nu, isotherm and streamlines in the cavity. A study on natural convection in an inclined T-shaped cavity was reported by Rouijaa et al. [2]. They found that increase of inclination angle was not favorable for heat transfer augmentation. Similar type of work was done by Amraqui et al.[3] considering radiation effect inside a T-shape cavity. Their investigation concluded that increment of Ra number enhanced heat transfer rate. Mojumder et al [4] studied the combined effect of Re and Gr on mixed convection in a lid driven T-shaped cavity. They found that higher Re strengthens overall flow inside the cavity. It also produces a stronger and larger buoyancy-driven vortex. Increased Gr number results in higher Nu along the wall. Roy et al. [5] examined entropy generation during mixed convection within the lid driven square cavity for various thermal boundary conditions. According to the best knowledge, entropy generation due to mixed convection in lid-driven T-shaped cavity has not been analyzed yet by anyone else with the constraints and conditions presented in this paper.

2. PROBLEM FORMULATION

Differentially heated T shaped cavity as shown in figure 1 is taken for the present study. The top lid of the cavity is considered to be moving with velocity $U_{L.}$ The problem is solved for three different fluids viz air (Pr=0.71), Ammonia (Pr=1.38) and Water (Pr=6.13) for three different cases of Ri = 0.1, Ri=1 and Ri=10.

*Corresponding author: Shikha Bhuyan, Department of Mechanical Engineering, Tezpur University
Email id: shikha5@tezu.ernet.in
Contact No.: 9707583444

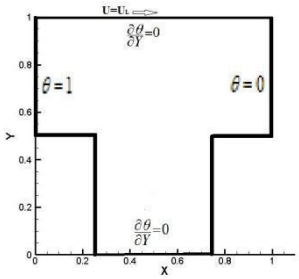

Fig. 1: Differentially heated T shaped cavity with moving top lid

3. METHODOLOGY AND VALIDATION

3.1 Numerical Procedure

Lattice Boltzmann method has been applied for numerical solution of the problem. The cavity has been divided into fine nodes and D2Q9 model has been applied for the transfer of the information between the nodes. Full way bounce back boundary condition has been applied for solving the problem.

The fully discretized Boltzmann equation with the BGK collision operator (eqn 1) replaces Navier–Stokes equation in CFD calculations. The value of τ directly determines the transport coefficients such as viscositv and heat diffusivitv.

$$f_i(x+c_i\Delta t, t+\Delta t)-f_i(x,t)=\frac{\Delta t}{\tau}\left(f_i^{eq}-fi\right) \quad (1)$$

For natural convection, the momentum and energy equations are coupled, both should be updated simultaneously. The flow is driven by temperature or density gradient, i.e., buoyancy force. Hence, there is an extra force term needed to be considered in solving Lattice Boltzmann equation. For natural convection, the Bousinessq approximation reads,

$$F=\rho g\,\beta\,(T-T_{ref}) \quad (2)$$

Here we calculate the term gβ by the Rayleigh number definition as shown in eqn 3 and 4.

$$\Rightarrow Ra=\frac{g\beta\Delta TH^3}{\alpha\nu} \quad (3)$$

$$\Rightarrow g\beta=\frac{Ra*\alpha\nu}{\Delta TH^3} \quad (4)$$

In Lattice Boltzmann method LB equation with the force term becomes

$$f_i\left(x+c_i\Delta t, t+\Delta t\right)-f_i\left(x,t\right)=\frac{\Delta t}{\tau}\left(f_i^{eq}-fi\right)+F_i \quad (5)$$

Where,

$$F_i=3w(k)g\,\beta\theta e_y \quad (6)$$

$$\theta=\frac{T-T_{cold}}{T_{hot}-T_{cold}} \quad (7)$$

The local volumetric rate of entropy generation, S_{gen} (W/m^{3}K), is given as follows

$$S''_{gen}=\frac{k}{T^2}\left[\left(\frac{dT}{dx}\right)^2+\left(\frac{dT}{dy}\right)^2\right]+\frac{\mu}{T}\left[2\left(\left(\frac{du}{dx}\right)^2+\left(\frac{dv}{dy}\right)^2\right)+\left(\frac{du}{dy}+\frac{dv}{dx}\right)^2\right] \quad (8)$$

3.2 Code validation

Differentially heated cavity is taken as a benchmark solution for testing the present code. The problem is based on a square cavity filled with air (Pr = 0.71). The results for streamlines and isotherms have been compared with the results obtained by Dixit et. al [6] and for entropy generation with Magheribi et. al [7]. Figure 2, figure 3 and figure 4 shows that the results obtained are in agreement with results obtained previously.

Table 1: Average Nusselt number comparision

Rayleigh Number	Grid size	Nu_{avg} (Current work)	Nu_{avg} (Previous work [6])
10^3	64 X 64	1.126	1.121
10^4	64 X 64	2.291	2.286
10^5	256 X 256	4.547	4.546

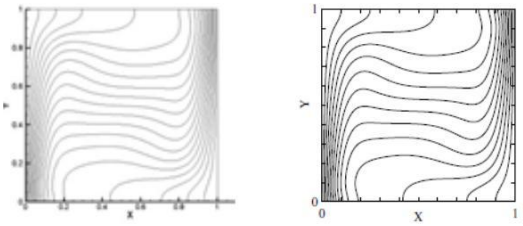

(a) (b)

Fig. 2: Isotherms for Ra=10^5 (a) result [6] (b) present work

*Corresponding author: Shikha Bhuyan, Department of Mechanical Engineering, Tezpur University
Email id: shikha5@tezu.ernet.in
Contact No.: 9707583444

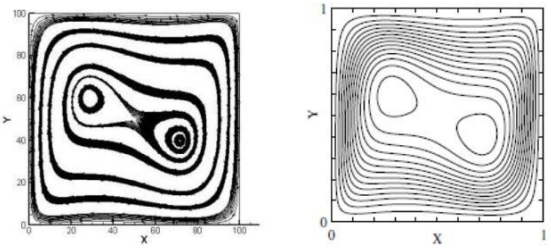

(a) (b)

Fig. 3: Streamlines for Ra=10^5(a) result [6] (b) present work

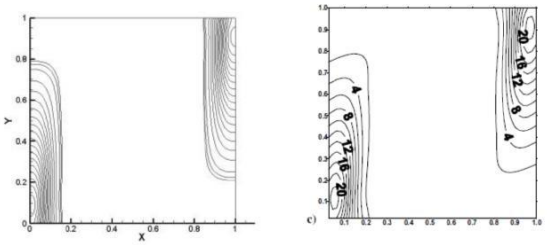

(a) (b)

Fig. 4: Entropy generation for Ra=10^5(a) result [7] (b) present work

4. RESULTS AND DISSCUSSION

4.1 Streamlines inside the cavity

It can be seen from figure 5 that as we decrease the Richardson number the vortices inside the lid increases. It is perceived that for Ri=10, there was only one major vortex and the effect of the lid movement on the lower half of the T shaped duct was not very proficient. As we decrease the Ri to 1 a second vortex with opposite rotational effect develops inside the lower half of the T shaped duct and a small secondary vortex on the bottom left corner of the top half of the T duct. As we decrease the Ri, these secondary and tertiary vortices grow further. It is seen from the streamlines that the center of the primary vortex shifts towards the right of the cavity by increasing the value of Pr. It can be attributed to the fact that when the Pr of the fluid is increased the value of viscosity also increases. It is seen that by increasing the Pr for lower Ri =0.1 value the tertiary vortex near the bottom left corner of the top half becomes further developed. It can be seen that for the same Ri value the thinning of boundary layer occurs with an increase in Ra (Gr*Pr) resulting in steeper velocity and temperature gradients.

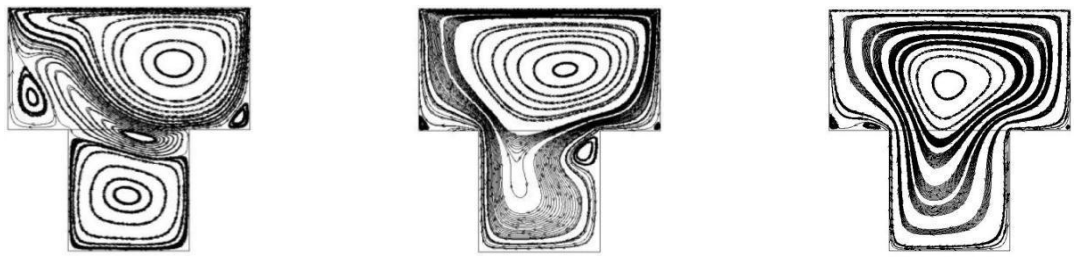

(a) Air

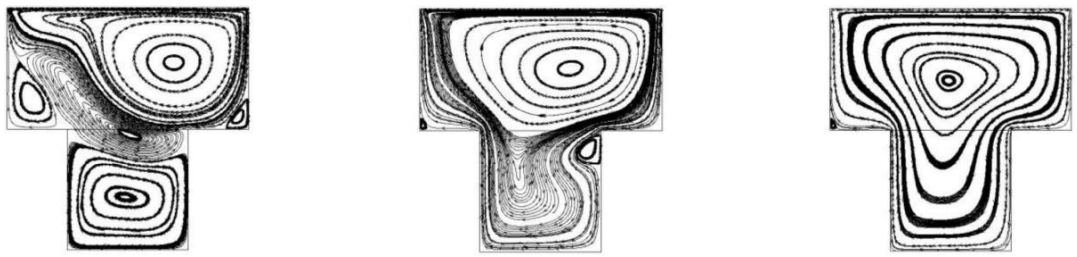

(b) Ammonia

*Corresponding author: Shikha Bhuyan, Department of Mechanical Engineering, Tezpur University
Email id: shikha5@tezu.ernet.in
Contact No.: 9707583444

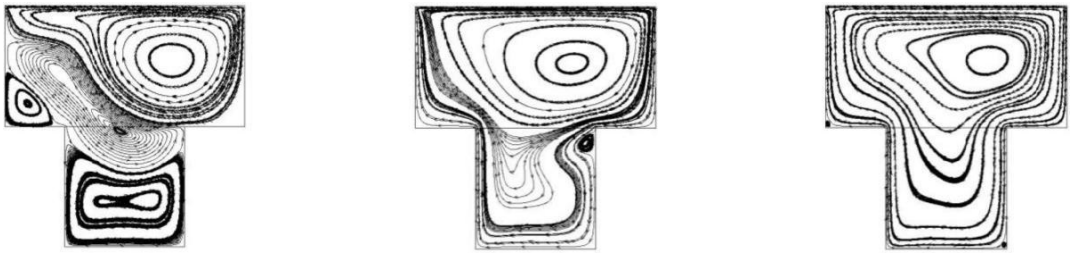

(c) Water

Fig. 5: Streamlines for Ri=0.1, Ri=1, Ri=10

4.2 Isotherms inside the cavity

The thermal effect of increasing the Ri can been seen in figure 6. Due to the formation of secondary and tertiary eddies in case of Ri=0.1, the isotherm are clustered in the top left half of the cavity and the bottom left half of the cavity. Since in cases of Ri=1 and Ri=10 the top lid velocity has lesser effect on the cavity, the isotherms can be seen moving towards the top right side of the cavity. Thermal gradient increases as Pr increases and the isothermal lines become denser at the walls. For high Pr, the isotherms disappear from the center of the cavity. This is due to confining the thermal boundary layer in a small region for highly viscous fluid. These lines become more concentrated from the Ri= 0.1 to Ri=10.

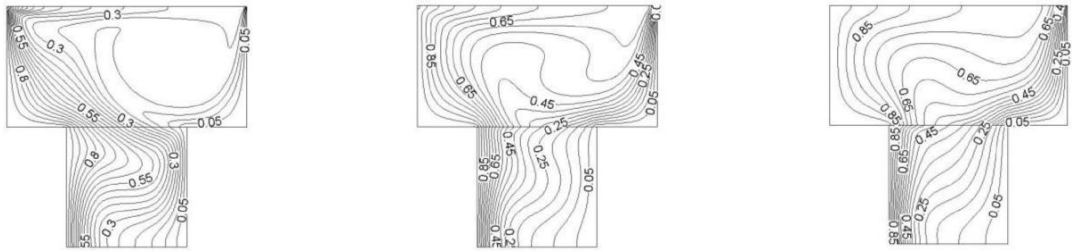

(a) Air

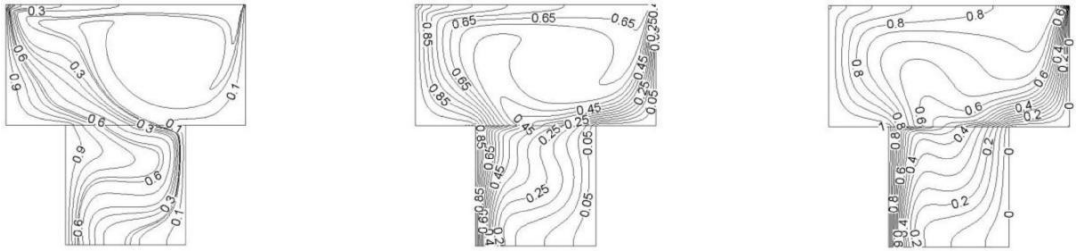

(b) Ammonia

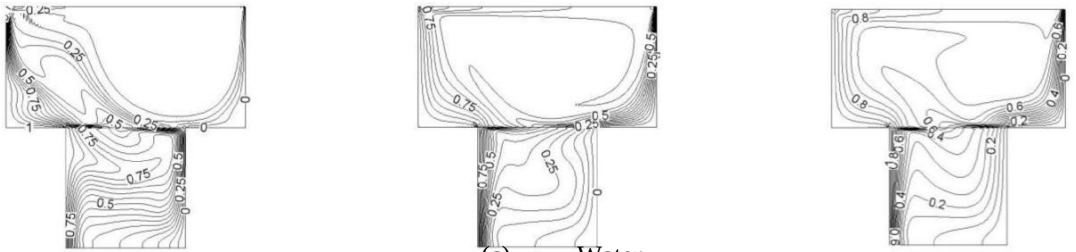

(c) Water

Fig. 6: Isotherms for Ri=0.1, Ri=1, Ri=1

*Corresponding author: Shikha Bhuyan, Department of Mechanical Engineering, Tezpur University
Email id: shikha5@tezu.ernet.in
Contact No.: 9707583444

4.3 Entropy generation inside the cavity

Figure 7 shows the effect of variable Ri and Pr on the local S_{gen} inside the cavity. For Ri=0.1 it is seen that greater entropy is generated on the top upstream side of the cavity than on the left side. This can be attributed to the formation of the large secondary and tertiary vortices and the concentration of the isotherms on the upper left side of the cavity in case of Ri=0.1. It is also seen that for higher Pr the S_{gen} is higher especially in the region nearer to the wall. It is attributed to increasing of the Ra as we increase the Pr. It is also seen that for higher Ri the S_{gen} is higher in the bottom left part and the upper left part of the cavity, this feature can be explained by the clustering of the isotherms in the these parts. It is also seen that there is entropy generation in right part of the bottom half of the cavity and this entropy disappears for Ri=10 which can be attributed to the disappearance of the secondary eddy in case of Ri=10.

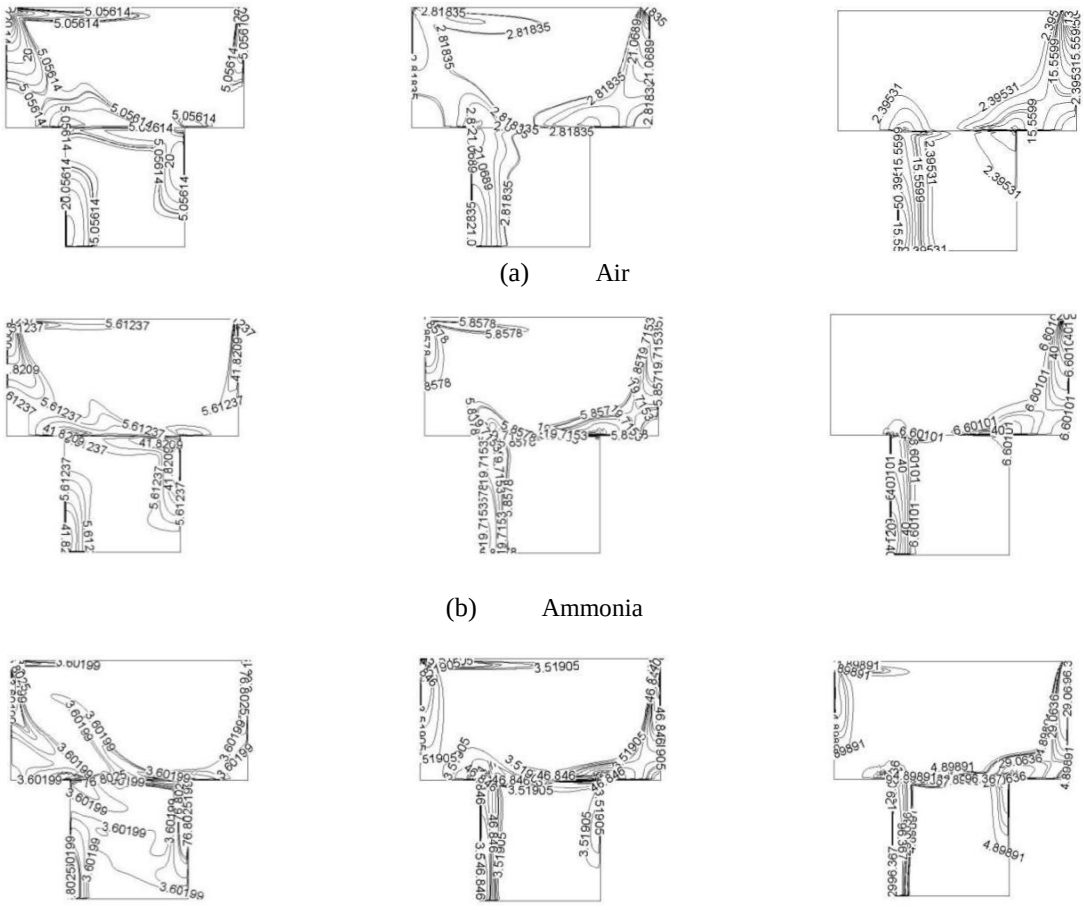

(a) Air

(b) Ammonia

(c) Water

Fig. 7: Entropy Generation for Ri=0.1, Ri=1, Ri=10

4.4 Average Entropy generation

The S_{gen} inside the cavity increases by increasing Pr as shown in Figure 8. This increase in S_{gen} is because of increasing thermal gradient with increasing value of Pr.

Therefore, it is possible to reduce the S_{gen} number using a low Pr fluid. It is also seen that the average entropy generation decreases with the increase in Ri as the degree of randomness

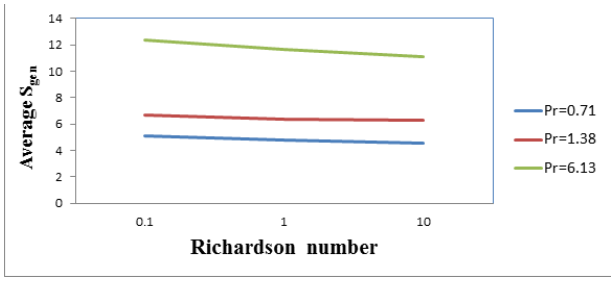

Fig. 8: Average entropy generation to the Richardson number

*Corresponding author: Shikha Bhuyan, Department of Mechanical Engineering, Tezpur University
Email id: shikha5@tezu.ernet.in
Contact No.: 9707583444

expected with high velocity flow is greater than the lower velocity flow.

4.5 Average Nusselt number

The average Nusselt number for different fluids, at the heated wall and cold wall against the different Richardson number (0.1, 1 and 10) are displayed in the figures (9 and 10) below. It is seen that for increasing Prandtl number the average Nusselt number values increase significantly. It is because for lower Pr the heat diffuses quickly. It is also seen that the average Nu is higher for the cold side than the hot side in case when Ri=1and Ri=10 but in case of Ri=0.1, it is seen that the Nu in the hot side of the plate is higher than the cold side. It can be attributed to the formation of the secondary vortex near the hot side of the wall due to mixing takes place and convection becomes more dominant as compared to the other cases. It is also seen that when the Ri increases the Nu decreases. It is due to the fact that with increase in Ri in both cases of the hot side of the cavity and the cold side of the cavity the effect of forced convection slowly decreases and the fluid mixing becomes less.

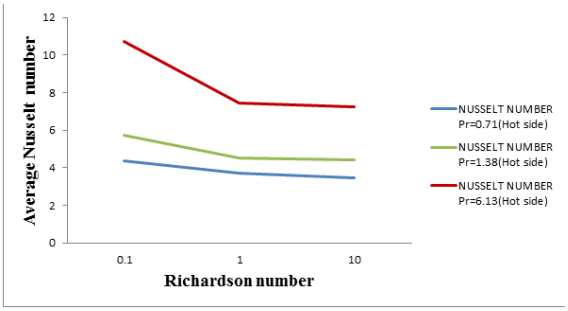

Fig. 9: Variation of average Nu (hot side) to the Richardson number

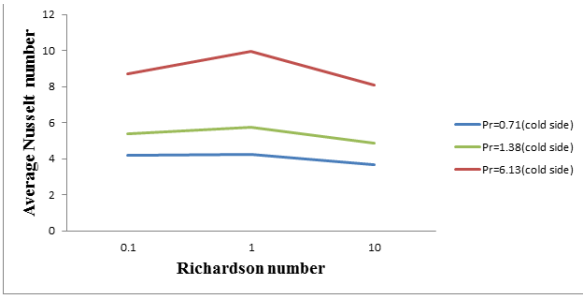

Fig. 10 Variation of average Nu (cold side) to the Richardson number

5. CONCLUSIONS

The present study can be concluded with the following points:

i) It can be seen that for the same Ri number value especially in case of higher Re the thinning of boundary layer occurs with an increase in Pr resulting in steeper velocity and temperature gradients. It is attributed to the fact that when we increases the Pr value for the same Gr value, the Ra number increases and as a result the convection of the fluid increases.

ii) When the Ri increases the entropy generation increases. When the Ri number changes from Ri=0.1 to Ri=1 the entropy generation increases by 5 percent.

iii) When the Pr increases from Ri= 1 to Ri= 10, entropy generation increases by 95 percent. The entropy generation inside the cavity increases by increasing Pr. This increase in entropy generation is because of increasing thermal gradient with increasing value of Pr. Therefore, it is possible to reduce the entropy generation number using a low Pr fluid.

iv) It is seen that cooling will be best at Ri= 1, since the Nusselt number is maximum at this value and the entropy generation is low.

v) When the Richardson number increases the Nusselt number decreases it is due to the fact that with increase in Richardson number, the effect of forced convection slowly decreases and as a result the fluid mixing also decreases. However at Ri=1 the Nusselt number in the cold side is found to be highest

6. REFERENCES

[1] Hatami, M., Zhou, J., Geng, J., Song, D.& Jing,D., 2017, Optimization of a lid-driven T-shaped porous cavity to improve the nanofluids mixed convection heat transfer, Journal of Molecular Liquids, Volume 231, 620-631

[2] Rouijaa H., Alami M. E., 2011, Natural convection in an inclined T-shaped cavity, Fluid Dynamics and Materials Processing , Volume 7(1) , 57-70

[3] S.Amraqui, A. Mezrhab, C.Abid, 2011, Computation of coupled surface radiation and natural convection in an inclined T-form cavity, Energy conversion and Management, Volume 52, 1166-1174

[4] Mojumder, S., Saha, S., Saha, S. & Mamun, M. A., 2015, Combined effect of Reynolds and Grashof numbers on mixed convection in a lid-driven T-shaped

*Corresponding author: Shikha Bhuyan, Department of Mechanical Engineering, Tezpur University
Email id: shikha5@tezu.ernet.in
Contact No.: 9707583444

cavity filled with water-Al_2O_3 nanofluid, Journal of Hydrodynamics , Volume 27, 782-794

[5] Roy, M., Roy, S., Basak, T., 2015, Analysis of entropy generation on mixed convection in square enclosures for various horizontal or vertical moving wall, International Communications in Heat and Mass Transfer, Volume 268,258-266

[6] Dixit, H. N., Babu, V, 2006, Simulation of high Rayleigh number natural convection in a square cavity using the lattice Boltzmann method, International Journal of Heat and Mass Transfer , Volume 49, 727–739

[7] Magherbi, M., Abbassi, H. and Abrahim, B., 2003, Entropy generation at the onset of natural convection, International Journal of Heat and Mass Transfer, Volume 46, 3441–3450

[8] Mohamad, A. A., 2011, Lattice Boltzmann Method: Fundamentals and Engineering Applications with Computer Codes, Springer-Verlag London Limited, London, UK

NOMENCLATURE

a	Length of specimen (m)
c	Lattice Velocity (m/s)
F	Force (N)
g	Acceleration due to gravity (m/s^2)
Gr	Grasshof number
Nu	Nusselt Number (dimensionless)
Pr	Prandtl Number (dimensionless)
Ra	Rayleigh Number (dimensionless)
Re	Reynolds Number (dimensionless)
Ri	Richardson Number (dimensionless)
S	Entropy (J/K)
T	Temperature (K)
T_{hot}	Temperature of hot plate (K)
u	X directional velocity of fluid (m/s)
v	Y directional velocity of fluid (m/s
w	Weight function (dimensionless)

Greek Symbols

α	Thermal diffusivity (m^2/s)
β	Coefficient of thermal expansion (1/K)
ρ	Density (kg/m^3)
μ	Dynamic viscosity (kg/ms)
τ	Relaxation time (dimensionless)
ϕ	Irreversibility (dimensionless)
Ω	BGK collision operator (dimensionless)

Superscripts

(eq)	Equilibrium state

Subscripts

avg	Average
gen	Generation
i	Lattice index

*Corresponding author: Shikha Bhuyan, Department of Mechanical Engineering, Tezpur University
Email id: shikha5@tezu.ernet.in
Contact No.: 9707583444

ASPECTS OF MODERN ASSAMESE

EDITED BY
SIDDHINATH BARUAH
PRATIMA K BORAH

Aspects of Modern Assamese, a collection of several Research Papers on various grammatical aspects of Modern Assamese. Editors: **Madhumita Barbora** and **Gautam K Borah**. [A project carried out as part of the SAP-DRS II Project awarded by the University Grants Commission, New Delhi to Dept of English and Foreign Languages, Tezpur University]

Published by
Bhabani Books, an imprint of Bhabani Offset Pvt. Ltd.
Bhabani Complex, Hatishila, Panikhaiti, Guwahati - 781026
Phone: 0361-2524056, 2528155 Fax: 0361-2450797
E-mail: bhabani@bhabani.com

In association with
Department of English and Foreign Languages
Tezpur University, Napaam, Tezpur - 784-28
(Under UGC's SAP-DRS II, 2015-2020)

First Edition: 2016

ISBN: 978-81-931983-3-9

Copyright: Registrar, Tezpur University

All rights reserved
No part of this editions of the book shall be reproduced, stored in a retrieval system, or transmitted in any form or by any means, electronic, photocopying, recording or otherwise, without the prior written permission of Registrar, Tezpur University

Cover Design: Sanjeev Deka

Printed in India at
Bhabani Offset Pvt. Ltd.
Bhabani Complex, Hatishila, Panikhaiti, Guwahati - 781026, Assam
Phone: 0361-2524056, 2528155 Fax: 0361-2450797
E-mail: bhabani@bhabani.com, Website:www.bhabani.com

Contents

Assamese: Socio-Historical Background 1
Madan M Sarma

The Indeterminacy of Bare Noun in Assamese and Its Determination 25
Gautam K Borah

The Agentive Ergativity in Assamese 65
Madhumita Barbora and *Diganta K Nath*

The Ingresssive Progressive Aspect in Assamese 84
Gautam K Borah

The Fuzzy Boundary Between Projected and Potential Realities and *iba* 92
Gautam K Borah

Genitive Subjects in Assamese 100
Diganta K Nath

Causative Constructions in Assamese 115
Madhumita Barbora

The Particle *ze:* a Clitic, a *Wh*-Operator or a Complementizer? 133
Madhumita Barbora

(Non-Finite) Clausal Complementation and Assignment of Case in Assamese 153
Diganta K Nath

The Scope of Negation in Assamese 180
Kailash Sharma

The Meaning of *ma:ne*: a conversational filler, a structural necessity and a cognitive endowment 192
Suranjana Barua

The Indeterminacy of the Bare Noun in Assamese and Its Determintion

Gautam K Borah

Preamble

In the present chapter I try to focus on the indeterminacy of bare nouns in Assamese and how they are determined. The way this is done in the language radically differs from the way it is done in a language like English.

The paper has the following structure.

1. The Indeterminate Bare Noun

2. Numerical Determination of the Bare Noun in Assamese: the indefinite and the definite classifier phrase

2.1 The Indefinite classifier phrase

2.2 The Definite classifier phrase

2.3 Greenberg (1974), Allan (1977), and the word order underlying the classifier phrases in Assamese

The Agentive Ergativity in Assamese

Madhumita Barbora
Diganta Kumar Nath

1. Introduction

Many languages show a patterning of syntactic behaviour that calls for a distinction between the system of Case and Case-marking. A Case system is the system of *Case features* conventionally labeled as nominative/ergative, accusative/ absolutive, dative, instrumental and so on. These Case features are associated in individual languages with language specific Case-markings. There is no common consensus among researchers who have used these labels, or even among those who have tried to articulate explicit criteria. The basic intuition regarding Nominative Case is that it is the Case of subjects. If a language has two distinct Cases associated with subjects, one inflected and the other uninflected, Nominative refers to the Case of the uninflected one. Ergative is the Case of inflected subjects of transitive verbs in a language where subjects of intransitive verbs are uninflected. Hindi is an Ergative language in which two distinct Cases are

The Ingressive Progressive Aspect in Assamese

Gautam K Borah

1. Introduction

In the current chapter we propose an ingressive progressive aspect for Assamese. We, thus, try to show in the paper that in addition to a usual progressive aspect, which focuses on the progression of an action, Assamese has also an aspect to focus rather on the beginning of an action that is going to continue. In the existing accounts of Assamese the presence of such an aspect in the language has, however, not been recognized.

2. Aspect is the grammatical form used by a speaker in viewing an action with considerations as duration and completion (Comrie 1976, Dahl 2000). A basic aspectual distinction is that of *perfectivity* and *imperfectivity*. In Perfective the situation is presented as a complete whole, as if viewed *externally*, with sharp boundaries (e.g. *He locked the door*). In Imperfective, on the other hand, the action is viewed

The Fuzzy Boundary Between Projected and Potential Realities and *iba*

Gautam K Borah

1. Introduction

In the present chapter we try to show that the future tense in Assamese is part of the modal system. The reason seems to be the fact that the borderline between futurity and modality is fuzzy.

2. Language is a constrcution of not just factual reality, that is, the known past and the ongoing present, but it is also a constrcution of non-factual reality, i.e. (a) what is going to happen or what is becoming realized (e.g. *They will come here again tomorrow*), or (b) what has the potential of becoming realized (e.g. *They should come here again tomorrow*).

Causative Constructions in Assamese

Madhumita Barbora

1. Introduction

The present paper is an investigation into the causative constructions in Assamese. Morphological causatives are productive in Assamese. Like most Indic languages Assamese seems to have two causative morphemes: *–a:* CAUS1 and *–owa:* CAUS2. Intransitive, transitive and di-transitive verbs can derive causative verbs and valency rise determines a causative clause. Derived transitive and di-transitive clauses indicate both direct and indirect causation. CAUS1 constructions vary from CAUS2 constructions. The CAUS2 constructions take an obligatory oblique argument whereas the oblique argument in CAUS1 it is optional.

The Particle *ɛɛ*: a Clitic, a Wh- operator or a Complementizer?

Madhuparna Barkati

1. Introduction

Springer Link

Advances in Applied Mechanical Engineering pp 81-89 | Cite as

Exergy Modelling of a Coal-Fired MHD Power Plant

Authors | Authors and affiliations

Prabin Haloi, Tapan Kumar Gogoi

Conference paper
First Online: 02 February 2020

637
Downloads

Part of the Lecture Notes in Mechanical Engineering book series (LNME)

Springer Link

Corridor Allocation as a Constrained Optimization Problem Using a Permutation-Based Multi-objective Genetic Algorithm

Nature-Inspired Methods for Metaheuristics Optimization pp 335-358 | Cite as

- Zahnupriya Kalita (1)
- Dilip Datta (1) Email author (ddatta@tezu.ernet.in)

1. Department of Mechanical Engineering, Tezpur University, , Tezpur, India

Chapter
First Online: 18 January 2020

- 1 Citations
- 409 Downloads

Part of the Modeling and Optimization in Science and Technologies book series (MOST, volume 16)

Abstract

The corridor allocation problem (CAP) seeks the optimum arrangement of given facilities along two sides of a central corridor. The CAP is so far handled as an unconstrained optimization problem without imposing any restriction on the placement of the facilities. In practice, however, some facilities may need to satisfy certain constraints on their placement. Accordingly, a constrained bi-objective CAP (cbCAP) model is proposed here, where some facilities are restricted to fixed, same and/or opposite rows. Realizing the difficulties to any algorithm for handling such a combinatorial problem, a cbCAP specific permutation-based genetic algorithm (cbCAP-pGA) with specialized operators is also proposed for solving the cbCAP model by generating only feasible solutions. In the numerical experimentation, the cbCAP-pGA is found capable in searching promising solutions even for a set of large-size benchmark instances.

Keywords

Combinatorial optimization Corridor allocation problem Genetic algorithm

This is a preview of subscription content, log in to check access.

References

SONA COLLEGE OF TECHNOLOGY
Learning is a Celebration!

SONA COLLEGE OF TECHNOLOGY

An Autonomous Institution | Approved by AICTE | ISO 9001 : 2015 Certified | NAAC Accredited - A Grade
All Eligible Programmes NBA Accredited | Affiliated to Anna University, Chennai

Junction Main Road, Salem - 636 005. Tamil Nadu. India.
Phone: +91 427 4099 999 | www.sonatech.ac.in

63 Years of Excellence in EDUCATION AND INDUSTRY

Certificate of Presentation

Awarded to

DR.BARNALI CHOWDHURY, Tezpur University, Assam

for presenting a research paper titled

TIME SERIES ANALYSIS OF MANUFACTURING DEFECTS – A CASE OF REFRIGERATOR LINER MANUFACTURING

at the International Virtual Conference on APPLIED SCIENCE, TECHNOLOGY MANAGEMENT AND LANGUAGE STUDIES (ASTMLS - 2020) on 11th & 12th December, 2020.

[Associate Sponsors]

IEEE · IETE · The Institution of Engineers (India) · ISTE · ICI

Coordinator
Dr. D. Senthilkumar
Professor & Head / Mechanical, Dean - Students Affair
Sona College of Technology

Convenor
Dr.S.Chandrasekar
Dean - Research and Development
Sona College of Technology

Patron
Dr. S.R.R. Senthilkumar
Principal
Sona College of Technology

Certificate of Appreciation

International Congress on

Advances in Materials Science and Engineering (CAMSE-2020)

www.camse.in

December 28-30, 2020

This is to certify that

Dr. Barnali Chowdhury, Tezpur University, Tezpur, Assam, India has participated and presented a research paper titled **Optimizing thermoforming of refrigerator liners to reduce liner rejection rate- a case study using fractional factorial design of experiments** in the International Conference - **CAMSE-2020** held in Virtual format in association with **Shobhit University Gangoh** and Technically supported by **STEM-Research Society** and **Dr. B. R. Ambedkar National Institute of Technology, Jalandhar, Punjab.**

Dr. Tarun K. Sharma
Organizing Chair

In association with

Dr. Om Prakash Verma
Organizing Co-Chair

Proceedings in LNME Series

Springer

Technically Supported by:

Smart Innovation, Systems and Technologies 206

Biplab Das
Ripon Patgiri
Sivaji Bandyopadhyay
Valentina Emilia Balas *Editors*

Modeling, Simulation and Optimization

Proceedings of CoMSO 2020

KES International

Springer

Editors
Biplab Das
Department of Mechanical Engineering
National Institute of Technology
Silchar, Assam, India

Sivaji Bandyopadhyay
National Institute of Technology Silchar
Silchar, India

Ripon Patgiri
Department of Computer Science
and Engineering
National Institute of Technology Silchar
Silchar, Assam, India

Valentina Emilia Balas
Aurel Vlaicu University of Arad
Arad, Romania

ISSN 2190-3018 ISSN 2190-3026 (electronic)
Smart Innovation, Systems and Technologies
ISBN 978-981-15-9828-9 ISBN 978-981-15-9829-6 (eBook)
https://doi.org/10.1007/978-981-15-9829-6

© The Editor(s) (if applicable) and The Author(s), under exclusive license to Springer Nature Singapore Pte Ltd. 2021
This work is subject to copyright. All rights are solely and exclusively licensed by the Publisher, whether the whole or part of the material is concerned, specifically the rights of translation, reprinting, reuse of illustrations, recitation, broadcasting, reproduction on microfilms or in any other physical way, and transmission or information storage and retrieval, electronic adaptation, computer software, or by similar or dissimilar methodology now known or hereafter developed.
The use of general descriptive names, registered names, trademarks, service marks, etc. in this publication does not imply, even in the absence of a specific statement, that such names are exempt from the relevant protective laws and regulations and therefore free for general use.
The publisher, the authors and the editors are safe to assume that the advice and information in this book are believed to be true and accurate at the date of publication. Neither the publisher nor the authors or the editors give a warranty, expressed or implied, with respect to the material contained herein or for any errors or omissions that may have been made. The publisher remains neutral with regard to jurisdictional claims in published maps and institutional affiliations.

This Springer imprint is published by the registered company Springer Nature Singapore Pte Ltd.
The registered company address is: 152 Beach Road, #21-01/04 Gateway East, Singapore 189721, Singapore

Contents

1 **Modelling and Forecasting of Solar Radiation Data: A Case Study** 1
Somila Hashunao, Hano Sunku, and R. K. Mehta

2 **Thermal Performance Study of Bamboo and Coal Co-gasification in a Downdraft Gasifier** 15
Monoj Bardalai, Banabir Das, PP Dutta, and Sadhan Mahapatra

3 **Effects of Gurney Flap and Suction Slots on the Aerodynamics of a NACA0012 Airfoil** 29
Sumit Shankar Sarvankar, Anindita Apurbaa Phukan, Abhijeet Konwar, and Paragmoni Kalita

4 **Effects of Numerical Dissipation and Dispersion on Computing the Convection of a Sharp Scalar Cone** 43
Shiv Bhawan Shivhare, Paragmoni Kalita, and Prabin Haloi

5 **Usage of Internet of Things in Home Automation Systems: A Review** 57
Suman Majumder, Sangram Ray, Chinmoy Ghosh, and Shreyasi Datta

6 **Dynamic Analysis of Rotating FRP Composite Cantilever Beam** 73
Diju Kumar Baro and Sachindra Mahto

7 **Online Tool Wear Monitoring Using Low-Cost Data Acquisition System and LabVIEW™ Program** 87
Banarsi Pandey, Binit Kumar Jha, and Sachindra Mahto

8 **Product Priority Problem: A Multi-objective Optimization Approach for Product Development Based on Customers' Priority** 101
Sidharth Sarmah and Dilip Datta

9 **Approximating Non-intersecting Closed Curves Through Four-Bar Linkage Mechanism** 115
Dilip Datta, Chiranjeeb Deb, Abhishek Hafila, and Debajani Das

10 **Optimization of Crude Oil Preheating Process Using Evolutionary Algorithms** 129
Dimbalita Deka and Dilip Datta

11 **Combined Crack and Unbalance Response Simulation for a Spinning Rotor** 143
Pranjal Borah, Sandeep Singh, and Sutanu Samanta

12 **Stability of Female Bicyclists on Sudden Braking** 153
Dilip Datta, Arpeeta Saikia, and Zahnupriya Kalita

13 **Stability of Bicycle at Low Speed** 165
Dilip Datta, Zahnupriya Kalita, and Sudipta Saikia

14 **Impact of Helical Coil Insert in the Absorber Tube of Parabolic Trough Collector** 177
Oveepsa Chakraborty, Biplab Das, and Rajat Gupta

15 **Integral-Tilt-Derivative Controller Based Performance Evaluation of Load Frequency Control of Deregulated Power System** 189
Sandhya Kumari, Gauri Shankar, and Biplab Das

16 **Six Sigma Enablers for Incoming Material Quality Improvement and Their Interaction in Supplier Domain for Indian Manufacturing Scenario** 201
Sudeep Kumar Pradhan, Ravi Reosekar, and Srikanta Routroy

17 **MLGARTC: Machine Learning Based Genetic Approach in RSSI Tree Climbing Path Improvisation of the Mobile Anchor's Using K-Means Clustering of Wireless Sensor Network** 213
P. Thilagavathi and J. Martin Leo Manickam

18 **Modeling Performance and Power on Disparate Platforms Using Transfer Learning with Machine Learning Models** 231
Amit Mankodi, Amit Bhatt, Bhaskar Chaudhury, Rajat Kumar, and Aditya Amrutiya

19 **A Novel Effective Single Sensor MPPT Technique for a Uniform and Partially Shaded Solar PV System via MSCA Approach** 247
Manoja Kumar Behera, Lalit Chandra Saikia, Satish Kumar Ramoji, Biswanath Dekaraja, Sanjeev Kumar Bhagat, and Naladi Ram Babu

20 **Classification of Sequence Data Using LSTM: An Application on Chaotic Sequences** 261
S. Shailesh, M. Anantha Krishnan, and M. V. Judy

21 **Modeling and Simulation of a Multi-area Hydro-thermal Interconnected System Using FOPI$^{\alpha}$ Controller for Integrated Voltage and Frequency Control** 275
Biswanath Dekaraja, Lalit Chandra Saikia, Satish Kumar Ramoji, Naladi Ram Babu, Sanjeev Kumar Bhagat, and Manoja Kumar Behera

22 **Dye Sensitized Solar Cell Parameter Extraction Using Particle Swarm Optimization** 287
Soumik Chakraborty, Ranjith G. Nair, and Lalu Sehan

23 **Modeling and Simulation of an Isolated CCGT and DSTS Plant Using BWO Optimized PI$^{\lambda}$D$^{\mu}$ Controller for Amalgamated Control of Voltage and Frequency** 297
Satish Kumar Ramoji, Lalit Chandra Saikia, Biswanath Dekaraja, Naladi Ram Babu, Sanjeev Kumar Bhagat, and Manoja Kumar Behera

24 **Mathematical Analysis on the Behaviour of Tumor Cells in the Presence of Monoclonal Antibodies Drug** 311
Biplab Dhar and Praveen Kumar Gupta

25 **LFC of a Solar Thermal Integrated Thermal System Considering CSO Optimized TI-DN Controller** 323
Naladi Ram Babu, Lalit Chandra Saikia, Sanjeev Kumar Bhagat, Satish Kumar Ramoji, Biswanath Dekaraja, and Manoja Kumar Behra

26 **Maiden Application of Hybrid Particle Swarm Optimization with Genetic Algorithm in AGC Studies Considering Optimized TIDN Controller** 335
Sanjeev Kumar Bhagat, Lalit Chandra Saikia, Dhenuvakonda Koteswara Raju, Naladi Ram Babu, Satish Kumar Ramoji, Biswanath Dekaraja, and Manoja Kumar Behra

27 **Enhancement of Reactive Power Reserve Using Salp Swarm Algorithm** 347
Nibha Rani and Tanmoy Malakar

28 **Weld Imperfection Classification by Texture Features Extraction and Local Binary Pattern** 367
Rajesh V. Patil and Y. P. Reddy

29 **Simulation and Behavior of Vertically Oriented Planar Structure** 379
Vikram S. Singh and Keshav K. Sangle

30 Automated Analysis and Classification of Sleep Stages Based on Machine Learning Techniques from a Dual-Channel EEG Signal 391
Santosh Kumar Satapathy, D. Loganathan, and Rupalin Nanda

31 Optimal Controller Design for LFC in Power System 405
Himangshi Changmai and Mrinal Buragohain

32 Comparative Study of Optimal Controller Application on Nonlinear Systems 417
Niku Borgohain and Mrinal Buragohain

33 Multi-class Weld Defect Detection and Classification by Support Vector Machine and Artificial Neural Network 429
Rajesh V. Patil, Y. P. Reddy, and Abhishek M. Thote

34 Time Series Forecasting Using Markov Chain Probability Transition Matrix with Genetic Algorithm Optimisation 439
Gurdeep Saini, Naveen Yadav, Biju R. Mohan, and Naganj Naik

35 Modeling Drivers of Machine Learning in Health care Using Interpretive Structural Modeling Approach 453
Pooja Gupta and Ritika Mehra

36 Studies on the Optical and Structural Properties of Exfoliated Graphene Oxide 465
Nipom Sekhar Das, Koustav Kashyap Gogoi, and Avijit Chowdhury

37 Deep Learning for Maize Crop Deficiency Detection 473
Subodh Bansal and Anuj Kumar

38 Improvement in Fault Clearance Time of the Cascaded H-Bridge Multilevel Inverter Using Novel Technique Based on Frequency Detection 485
Hillol Phukan and Jiwanjot Singh

39 Impact and Scope of Electric Power Generation Demand Using Renewable Energy Resources Due to COVID-19 495
Manish Kumar, Muralidhar Nayak Bhukya, Anshuman, and Sachin

40 Demand Side Management-Based Load Frequency Control of Islanded Microgrid Using Direct Load Control 503
Subash Chandra Sahoo, Abdul Latif, Satyajeet Naidu, Shruti Patel, Ranjan Kumar, and Dulal Chandra Das

41 Dynamics of a Class of Modified Leslie-Gower Predator-Prey Model with Strong Allee Effect on Prey and Non-monotonic Rational Functional Response 515
Udai Kumar and Partha Samthi Mandal

42 Mathematical Modelling, Design and Simulation of a Bipedal Walker 531
Randheer Singh, Vikas Kukshal, and Vinod Singh Yadav

43 A Simple Approach to Enhance the Performance of Traditional P&O Scheme Under Partial Shaded Condition by Employing Second Stage to the Existing Algorithm 545
Muralidhar Nayak Bhukya, Manish Kumar, and Shobha Rani Depuru

44 One-Dimensional Model for Removal of Volatile Organic Compound Propane in a Catalytic Monolith 557
Umang Bedi and Sanchita Chauhan

45 Neural Machine Translation: Assamese–Bengali 571
Sahinur Rahman Laskar, Partha Pakray, and Sivaji Bandyopadhyay

46 An Overview of Crossover Techniques in Genetic Algorithm 581
Joseph L. Pachuau, Arnab Roy, and Anish Kumar Saha

47 Escalating Demand, Present and Future Status on Hybrid Electric Vehicles 599
Manish Kumar, Muralidhar Nayak Bhukya, Anshuman, and Sachin

48 Analysis and Control of Civilian Aircraft Model Using Simulink [PECS] 2020 613
Utkarsh Sharma and Sudhir Nadda

49 Factors Affecting the Efficiency of Solar Cell and Technical Possible Solutions to Improve the Performance 623
Muralidhar Nayak Bhukya, Manish Kumar, Vipin, and Chandervanshi

50 Order Reduction of Linear Time Invariant Large-Scale System by Improved Mixed Approximation Method 635
Pragati Shrivastava Deb and G. Leena

51 Seven Level Enhanced Modified T-type Multilevel Inverter (MLI) with Reduce Part Count 645
Hillol Phukan, Tamiru Debela, and Jiwanjot Singh

52 Controller Design for Dynamic Stability and Performance Enhancement of Renewable Energy Systems 657
Isha Rajput, Jyoti Verma, and Hemant Ahuja

53 A Note on Lyapunov Krasvoskii Funtional for Discrete Time Delayed Systems 671
Vipin Chandra Pal, Sudipta Chakraborty, Avadh Pati, and Gurpreet Singh

54 **Bidirectional DC-DC Buck-Boost Converter for Battery Energy Storage System and PV Panel** 681
Krishna Kumar Pandey, Mahesh Kumar, Amita Kumari, and Jagdish Kumar

55 **Performance Comparison of DSTATCOM and PV Fed DSTATCOM for Mitigation of Power Quality Problems** 695
Gurpreet Singh, Yash Pal, and Anil Kumar Dahiya

56 **Numerical Simulation of Blocked Blood Vessel for Early Diagnosis of Coronary Artery Disease** 711
Sandip Saha, Pankaj Biswas, and Sujit Nath

57 **Green Supplier Selection: An Empirical Investigation** 723
Sudipta Ghosh, Chiranjib Bhowmik, Madhab Chandra Mandal, and Amitava Ray

58 **Solar-Driven Potassium Formate Liquid Desiccant Dehumidification System with Thermal Energy Storage** 737
A. Sai Kaushik and Satya Sekhar Bhogilla

59 **Performance Studies with Trapezoidal, Sinusoidal and Square Corrugated Aluminium Alloy (AlMn1Cu) Plate Ducts** 751
Partha Pratim Dutta, Hirakjyoti Kakati, Monoj Bardalai, and Polash P. Dutta

60 **A Survey on Bloom Filter for Multiple Sets** 775
Lilapati Waikhom, Saburima Nayak, and Ripon Patgiri

61 **Topology Optimization of Structures Using Higher Order Finite Elements in Analysis** 791
Sougata Mukherjee, Dongcheng Lu, Subhrajit Dutta, Balaji Raghavan, Piotr Breitkopf, and Manyu Xiao

Author Index 801

Chapter 2
Thermal Performance Study of Bamboo and Coal Co-gasification in a Downdraft Gasifier

Monoj Bardalai, Banabir Das, PP Dutta, and Sadhan Mahapatra

Abstract In this study, bamboo and coal co-gasification is carried out in a downdraft gasifier at different blending ratios. The study mainly focuses on the flame front propagation rate (FFPR), bed movement, effective front propagation, tar concentration and particulate concentration in the producer gas. Three different air mass fluxes namely $\Phi 1$, $\Phi 2$, $\Phi 3$ were used to perform the gasification process. The experimental results show that flame front propagation increases upto 10 wt.% coal, after which it starts decreasing for further increase of coal percentages in the feedstock for all air mass fluxes. Rate of bed movement also shows the similar trend as flame front propagation except at $\Phi 3$. The effective propagation rate increases upto 10–20 wt.% coal beyond which the increment is insignificant for all air mass fluxes. In all air mass fluxes, the tar concentration decreases while the concentration of particulate increases by increasing coal percentages in the feedstock.

2.1 Introduction

Coal has been one of the mostly utilised fossil fuel as the source of energy. The increased use of coal creates pollution by producing green house gases such as CO_2, CO etc, whcih has become the threat for the living beings in the earth. Moreover, coal is not a renewable source of energy and it is going to be finished in the near future. Therefore, total or partial replacement of coal by some other easily available renewable sources of energy has become the major concern for the researchers in the energy sector. Biomass is one of the easily available material which has the potential to replace coal upto a certain extent. As India is an agricultural based country, biomass is abundantly found in most of the places. The main components of biomass are the organic substances derived from animals and plants. The waste products obtained from the agro-industries and municipal are also considered as biomass [1]. The

M. Bardalai (✉) · B. Das · P. Dutta · S. Mahapatra
Tezpur University, Assam, India
e-mail: monojtezu@gmail.com

© The Author(s), under exclusive license to Springer Nature Singapore Pte Ltd. 2021

B. Das et al. (eds.), *Modelling, Simulation and Optimization*, Smart Innovation, Systems and Technologies 206, https://doi.org/10.1007/978-981-15-9829-6_2

Chapter 59
Performance Studies with Trapezoidal, Sinusoidal and Square Corrugated Aluminium Alloy (AlMn1Cu) Plate Ducts

Partha Pratim Dutta, Hirakjyoti Kakati, Monoj Bardalai, and Polash P. Dutta

Abstract Superior heat transfer is possible in corrugated aluminium alloy plate heat transferring devices due to high turbulence generated by fluid flowing over it. Therefore, a standard *k-ε* turbulence model coupled with heat transfer in fluid model was employed to study performance of three corrugated channels. This study covers an investigation of 2-D heat transfer and fluid flow through sinusoidal, square, and trapezoidal corrugated ducts. The fluid used in the analysis was air with a density of 1.225 kg/m^3. The air with an inlet temperature of 380 K was passed through the channel (between the corrugated plates) and in the process, air transfers heat to the plates. On outside of the channel made of corrugated plates was maintained at room temperature. Variations of Nusselt number (Nu), change of velocity and pressure drop with the arc length of the corrugated channel have been computed for three geometries. It was observed that Nu variation from the inlet to outlet for trapezoidal, sinusoidal and square ducts were 52–71, 49–65 and 46–61 respectively. Velocity variations were found to be of 2–2.58, 2–2.35 and 2–2.30 m/s in the channels respectively. The pressure drops from the entry to exit were found 1.33 Pa, 1.7 Pa and 2.28 Pa for trapezoidal, square and sinusoidal channels respectively.

Nomenclature

G_k	The conversion of turbulence kinetic energy for mean velocity gradients (m^2/s^2)
K	Kelvin
k	Turbulent kinetic energy (m^2/s^2)
kg/s	Kilogram/second
kW/m^2	Kilowatt/metre^2
mm	Millimetre
Nu	Nusselt number

P. P. Dutta · H. Kakati · M. Bardalai (✉) · P. P. Dutta
Department of Mechanical Engineering, Tezpur University, Assam, India
e-mail: monojezu@gmail.com

© The Author(s), under exclusive license to Springer Nature Singapore Pte Ltd. 2021

B. Das et al. (eds.), *Modelling, Simulation and Optimization*, Smart Innovation, Systems and Technologies 206, https://doi.org/10.1007/978-981-15-9829-6_59

Green Energy and Technology

Om Prakash
Anil Kumar

Solar Drying Technology

Concept, Design, Testing, Modeling, Economics, and Environment

Springer

Editors
Om Prakash
Department of Mechanical Engineering
Birla Institute of Technology, Mesra
Ranchi, Jharkhand, India

Anil Kumar
Department of Energy (Energy Centre)
Maulana Azad National Institute of Technology
Bhopal, Madhya Pradesh, India

ISSN 1865-3529 ISSN 1865-3537 (electronic)
Green Energy and Technology
ISBN 978-981-10-3832-7 ISBN 978-981-10-3833-4 (eBook)
DOI 10.1007/978-981-10-3833-4

Library of Congress Control Number: 2017940696

© Springer Nature Singapore Pte Ltd. 2017
This work is subject to copyright. All rights are reserved by the Publisher, whether the whole or part of the material is concerned, specifically the rights of translation, reprinting, reuse of illustrations, recitation, broadcasting, reproduction on microfilms or in any other physical way, and transmission or information storage and retrieval, electronic adaptation, computer software, or by similar or dissimilar methodology now known or hereafter developed.
The use of general descriptive names, registered names, trademarks, service marks, etc. in this publication does not imply, even in the absence of a specific statement, that such names are exempt from the relevant protective laws and regulations and therefore free for general use.
The publisher, the authors and the editors are safe to assume that the advice and information in this book are believed to be true and accurate at the date of publication. Neither the publisher nor the authors or the editors give a warranty, express or implied, with respect to the material contained herein or for any errors or omissions that may have been made. The publisher remains neutral with regard to jurisdictional claims in published maps and institutional affiliations.

Printed on acid-free paper

This Springer imprint is published by Springer Nature
The registered company is Springer Nature Singapore Pte Ltd.
The registered company address is: 152 Beach Road, #21-01/04 Gateway East, Singapore 189721, Singapore

Contents

Part I Concept of Solar Drying

Fundamental Concepts of Drying 3
S. Vijayan, T.V. Arjunan, and Anil Kumar

Solar Drying Systems 39
Jan Banout

Characteristics of Different Systems for the Solar Drying of Crops 69
Brian Norton

Fundamental Mathematical Relations of Solar Drying Systems 89
Stamatios Babalis, Elias Papanicolaou, and Vassilios Belessiotis

Advancement in Greenhouse Drying System 177
Anil Kumar, Harsh Deep, Om Prakash, and O.V. Ekechukwu

Part II Design and Testing of Solar Drying Systems

Design Analysis and Studies on Some Solar Drying Systems 199
Vinod Kumar Sharma and Cosmas Ngozichukwu Anyanwu

Thermal Testing Methods for Solar Dryers 215
Shobhana Singh

Exergy Analysis of Solar Dryers 239
Anil Kumar, Saurabh Ranjan, Om Prakash, and Ashish Shukla

Part III Modeling of Solar Drying Systems

Mathematical Modeling of Solar Drying Systems 265
Rajendra C. Patil and Rupesh R. Gawande

Drying Kinetics in Solar Drying 317
Raquel de Pinho Ferreira Guiné and Maria João Barroca

Mathematical and Computational Modeling Simulation of Solar Drying Systems 357
Rebecca Rose Milczarek and Fatima Sierre Alleyne

Numerical Techniques for Evaluating the Performance of Solar Drying Systems 381
Kamnesh Kant, Atul Sharma, and Amritanshu Shukla

Simulation of Food Solar Drying 403
Inês N. Ramos, Teresa R.S. Brandão, and Cristina L.M. Silva

Applications of Soft Computing in Solar Drying Systems 419
Om Prakash, Saurabh Ranjan, Anil Kumar, and P.P. Tripathy

Part IV Environomical Impact of Solar Drying Systems

Economics of Solar Drying 441
Deepali Atheaya

Techno-economic Analysis of Solar Dryers 463
S. Selvanayaki and K. Sampathkumar

Economic Analysis of Various Developed Solar Dryers 495
Om Prakash, Saurabh Ranjan, Anil Kumar, and Ravi Gupta

Economic Analysis of Hybrid Photovoltaic-Thermal (PV-T) Integrated Indirect-Type Solar Dryer 515
Sujata Nayak and Kapil Narwal

Energy Analysis of the Direct and Indirect Solar Drying System 529
Om Prakash, Anil Kumar, Prashant Singh Chauhan, and Daniel I. Onwude

Part V Innovations in Solar Drying

Energy Conservation Through Recirculation of Hot Air in Solar Dryer 545
Kamaruddin Abdullah

Development and Performance Study of Solar Air Heater for Solar Drying Applications 579
Partha Pratim Dutta and Anil Kumar

Thermal Energy Storage in Solar Dryer 603
Ajay Kumar Kaviti and Harsh Deep

Development of Phase Change Materials (PCMs) for Solar Drying Systems 619
Anand Jain, Anil Kumar, A. Shukla, and Atul Sharma

Development and Performance Study of Solar Air Heater for Solar Drying Applications

Partha Pratim Dutta and Anil Kumar

Abstract Open sun drying for drying of rural agro-based produces is an age-old practice for preservation as well as for the use of dried products in the future. However, open sun drying takes longer duration, and thus, it gives inconsistent quality for drying of agro-based produces. Hence, solar dryer emerges as a device to overcome the demerits of the open sun dryer and incorporates its advantage to the maximum extent. Different improved designs of solar air heater cum dryers are available to get efficient solar drying. The present investigation explores general theoretical thermodynamic performance studies of some improved solar air heater for drying applications. It follows with a detailed thermal performance studies of an improved hemispherical protruded solar air heater. The protrusion height (e) varied as 2.4, 3.0, and 3.7 mm, and the long way length (p) varied as 24, 36, and 52 mm, respectively. The effect of $\frac{e}{D}$ (0.055, 0.045, 0.035) of hemispherical protruded absorber on constant $\frac{p}{e} = 12$ had been observed. It was seen that maximum thermal efficiency of 82% is achievable for $\frac{p}{e} = 12$ and $\frac{e}{D} = 0.055$. Moreover, with $\frac{e}{D}$, value of 0.035 and 0.055 gives maximum and minimum effective efficiency (74 and 64%), respectively, at 12,000 Reynolds number. From economic analysis, it has been estimated that if 400 m^2 of black tea processing factory galvanized roof were converted by using black painting, plywood insulation, and tempered glass enclosure to convert it into a solar air heater, then average 20% of conventional thermal energy for black tea drying may be saved. The annual carbon dioxide reduction of 2189 t is achievable by using improved solar air heater. The payback period of the hybrid renewable thermal energy-based system is less than 15 months, and the benefit-cost ratio is 1:1.

Keywords Solar drying • Improved solar air heater • Hemispherical protrusion • Payback period

P.P. Dutta (✉)
Department of Mechanical Engineering, Tezpur University, Tezpur 784028, India
e-mail: ppdutta06@gmail.com

A. Kumar
Department of Energy (Energy Centre), Maulana Azad National Institute of Technology, Bhopal 462003, Madhya Pradesh, India

© Springer Nature Singapore Pte Ltd. 2017

O. Prakash, A. Kumar (eds.), *Solar Drying Technology*, Green Energy and Technology, DOI 10.1007/978-981-10-3833-4_21

Chapter 4
Effects of Numerical Dissipation and Dispersion on Computing the Convection of a Sharp Scalar Cone

Shiv Bhawan Shivhare, Paragmoni Kalita, and Prabin Haloi

Abstract This work presents a classical study on the numerical-dissipation and dispersion behaviors of upwind and central space-discretization schemes. For this purpose, pure convection of a sharp scalar cone is simulated by numerically solving the two-dimensional convection-diffusion equation with zero physical diffusion. The velocity field is so chosen that the scalar cone rotates about the origin. The numerical solutions are carried out on the finite-volume framework, where the interface fluxes are approximated by the first-order upwind (FOU), second-order central difference (CDS2), and Quadratic Upstream Interpolation for Convective Kinematics (QUICK) schemes. Although in the absence of physical dissipation, the cone should rotate without any decay of its amplitude, it is found that the different numerical-flux schemes result in different declining rates of amplitude. This is attributed to different levels of numerical dissipation of the schemes. In addition, it is seen that the numerical dispersions of the schemes result in the change of phase of the scalar being convected, yielding spurious numerical oscillations. The present study compares the FOU, CDS2, and QUICK schemes in the finite-volume computation of the convection-diffusion equation vis-à-vis their numerical dissipation and dispersion. The study demonstrates that among the lot, the FOU scheme is the most dissipative and the QUICK scheme is the least dissipative. On the other hand, the CDS2 scheme is the most dispersive. The aforementioned observations with the FOU and CDS2 schemes are substantiated with finite-difference computation of the governing equation using these schemes for approximating the space derivatives.

4.1 Introduction

The generic convection-diffusion equation is a classic model equation for many fluid transport problems [1, 2]. Accordingly, the importance of the convection-diffusion equation as a model transport equation has attracted various research works related

S. B. Shivhare · P. Kalita (✉) · P. Haloi
Department of Mechanical Engineering, Tezpur University, Tezpur, Assam 784028, India
e-mail: paragmk@tezu.ernet.in

© The Author(s), under exclusive license to Springer Nature Singapore Pte Ltd. 2021

B. Das et al. (eds.), *Modeling, Simulation and Optimization*, Smart Innovation, Systems and Technologies 206, https://doi.org/10.1007/978-981-15-9829-6_4

to its solution methodology, convergence, and accuracy [3–5]. In the numerical solutions of these equations, the accuracy of discrete approximations to the first-order spatial derivatives associated with the convection terms immensely influences the overall exactness of the computed solution itself. Further, it has been seen that the numerical stability and accuracy of computation greatly depend on the numerical dissipation and dispersion of schemes used to discretize the first-order space derivatives of the convection-diffusion equation [6–10]. Consequently, research works were also conducted to analyze the numerical dissipation and dispersion of finite-difference schemes for solving linear and nonlinear convection-diffusion equations [11, 12]. The present work carries out an explicit comparative study on the numerical dissipation and dispersion behaviors of three such schemes used for discretizing the convection terms in the Finite-Volume Method (FVM).

Based on the direction of stencil selection the spatial-discretization schemes for convective terms can be classified as central and upwind. An upwind scheme chooses an asymmetric stencil with a higher number of points from the direction upstream of the associated convective velocity. On the other hand, the central schemes choose symmetric stencils irrespective of the direction of convection. In the Finite-Difference Method (FDM) method, an upwind approximation of a convection term contains an even-order derivative as the leading-error term. The even-order derivative in the leading error acts like artificial dissipation. Conversely, a central FDM approximation of a convection term contains an odd-order derivative in its leading error. This results in the tendency for higher numerical dispersion in the case of central schemes. These contrasting nature of the two types of schemes provides the motivation for the present work to carry out a quantitative comparison of the dissipative and dispersive nature of upwind and central schemes applied for finite-volume discretization of convective terms. The schemes chosen for the present study are the first-order upwind (FOU), second-order central difference (CDS2), and the Quadratic Upstream Interpolation for Convective Kinematics (QUICK) schemes. The FVM computations with the FOU and CDS2 schemes are also compared with the corresponding FDM results to demonstrate the consistency of the present findings. It is to be noted that the present results might be relevant in various applications of theoretical and practical applications [6, 12, 13].

The physical problem for the study involves a sharp scalar cone rotating about the origin in the absence of physical dissipation. Therefore, the cone must be ideally convected without any change of its amplitude. However, artificial dissipation of a numerical scheme results in the gradual diminishing of the amplitude. It is needless to mention that the most dissipative scheme results in the highest rate of decrease in amplitude. The present work shows a direct comparison of the dissipative nature of the various schemes in terms of the amplitudes computed at a given instant of time by each scheme. The difference in numerical dispersion caused by each scheme is also presented through three-dimensional (3D) contour plots of the cone profile computed at a given instant of time.

This paper is organized into five sections. Section 4.2 presents the governing equations and the problem statement. The basic FVM discretization of the governing equation and the FOU, CDS2, and QUICK schemes to approximate the convective

flux across a cell-interface are presented in Sect. 4.3. The dissipative and dispersive natures of the schemes are compared in Sect. 4.4 before making the concluding remarks in Sect. 4.5.

4.2 The Governing Equation and the Problem Statement

The two-dimensional (2D) convection-diffusion equation for any scalar $\varnothing$ is given by

$$\frac{\partial \varnothing}{\partial t} + u\frac{\partial \varnothing}{\partial x} + v\frac{\partial \varnothing}{\partial y} = \Gamma\left(\frac{\partial^2 \varnothing}{\partial x^2} + \frac{\partial^2 \varnothing}{\partial y^2}\right), \tag{4.1}$$

where u and v are the velocity components along the x- and y-directions, respectively, and Γ is the physical-dissipation coefficient.

The present work considers pure convection of the scalar $\varnothing$, i.e., the physical-diffusion coefficient $\Gamma = 0$. It is evident that in the absence of physical viscosity, the cone should be convected undistorted. The initial distribution of $\varnothing$ is considered as a sharp cone with a Gaussian profile that is given by [6]

$$\varnothing(x, y, t = 0) = a \times \exp\left[-\eta\left\{(x - x_c)^2 + (y - y_c)^2\right\}\right], \tag{4.2}$$

where $a = 5$, $\eta = 1500$, $x_c = -0.25$, and $y_c = 0$. Equation (4.1) is to be solved subject to the initial condition given by Eq. (4.2) in the domain $-0.5 \leq x \leq 0.5$ and $-0.5 \leq y \leq 0.5$. The velocity components are taken as $u = -y$ and $v = x$, such that the initial profile rotates about the origin with an angular velocity of $\omega = 1$ about the origin. From Eq. (4.2) one can find that the initial amplitude of $\varnothing$ is equal to $a = 5$ at $x = x_c$ and $y = y_c$. The numerical solution is sought at the instant when the cone completes one complete revolution, i.e., at time $t = 2\pi$. For the numerical solution time integration is carried out by using first-order Euler-explicit scheme with a time step of $\Delta t = 1 \times 10^{-3}$. The spatial discretization is done by various schemes in the FDM and FVM formulations presented in Sect. 4.3.

4.3 The Numerical Methods

The governing equation is discretized in the FDM and FVM frameworks. Sections 4.3.1 and 4.3.2 present the discretization of Eq. (4.1) using the finite-difference and finite-volume approaches. The numerical schemes used for the spatial discretization are described within each subsection. It may be noted that in the absence of physical dissipation, Eq. (4.1) reduces to

$$\frac{\partial \varnothing}{\partial t} + u\frac{\partial \varnothing}{\partial x} + v\frac{\partial \varnothing}{\partial y} = 0 \tag{4.3}$$

4.3.1 Discretization Using FDM

Using the first order Euler-explicit method for time integration, the semi-discrete form of Eq. (4.3) becomes

$$\frac{\varnothing^{n+1} - \varnothing^{n}}{\Delta t} + f^{n} = 0, \tag{4.4}$$

where the superscript n refers to any time level at an instant t and $n+1$ is the time level at the instant $t + \Delta t$ and $f = u\frac{\partial \varnothing}{\partial x} + v\frac{\partial \varnothing}{\partial y}$ is the spatial function. With reference to Fig. 4.1, the fully-discrete form of Eq. (4.4) at any arbitrary node (i, j) in the computational domain is given by

$$\begin{aligned}
&\frac{\varnothing_{i,j}^{n+1} - \varnothing_{i,j}^{n}}{\Delta t} + u_{i,j}^{n}\left(\frac{\partial \varnothing}{\partial x}\right)_{i,j}^{n} + v_{i,j}^{n}\left(\frac{\partial \varnothing}{\partial y}\right)_{i,j}^{n} = 0 \\
&\varnothing_{i,j}^{n+1} = \varnothing_{i,j}^{n} - \Delta t\left[u_{i,j}^{n}\left(\frac{\partial \varnothing}{\partial x}\right)_{i,j}^{n} + v_{i,j}^{n}\left(\frac{\partial \varnothing}{\partial y}\right)_{i,j}^{n}\right],
\end{aligned} \tag{4.5}$$

where $u_{i,j}^{n}$ and $v_{i,j}^{n}$ are the x- and y-velocity components at the node (i, j) at the time level n, and $\left(\frac{\partial \varnothing}{\partial x}\right)_{i,j}^{n}$ and $\left(\frac{\partial \varnothing}{\partial y}\right)_{i,j}^{n}$ are the discrete approximations of $\frac{\partial \varnothing}{\partial x}$ and $\frac{\partial \varnothing}{\partial y}$ at the

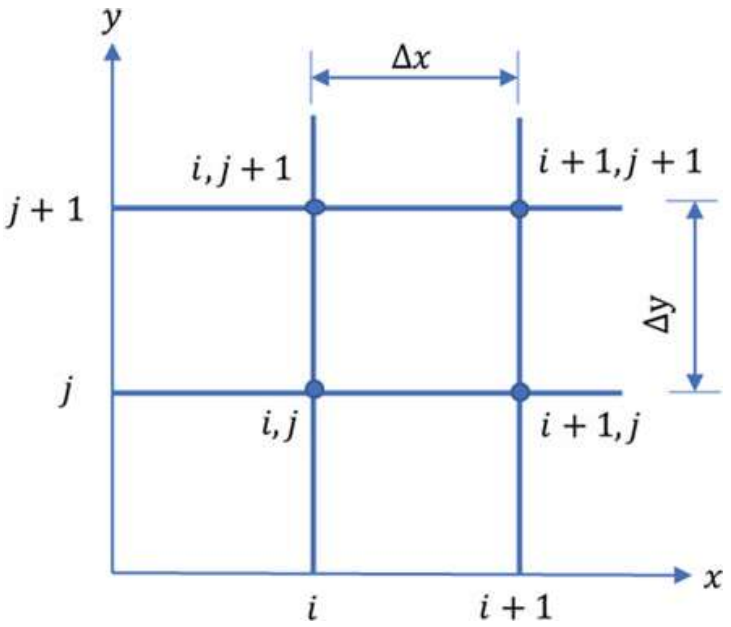

Fig. 4.1 Nodes for the FDM framework

node (i, j) at the time level n. The final form of Eq. (4.5) depends on the scheme used to discretize the spatial derivatives. In the present work, the FOU and CDS2 schemes are used for the discrete approximations of $\left(\frac{\partial \varnothing}{\partial x}\right)_{i,j}^{n}$ and $\left(\frac{\partial \varnothing}{\partial y}\right)_{i,j}^{n}$. It is to be marked that for the present problem the convection terms are linear since $u_{i,j}^{n} = -y_{i,j}$ and $v_{i,j}^{n} = x_{i,j}$.

The FOU Scheme in FDM
The discrete approximation of $\frac{\partial \varnothing}{\partial x}$ with the FOU scheme at arbitrary node (i, j) at the time level n is given by

$$\left(\frac{\partial \varnothing}{\partial x}\right)_{i,j}^{n} = \begin{cases} \frac{\varnothing_{i,j}^{n} - \varnothing_{i-1,j}^{n}}{\Delta x} & \text{if } u_{i,j}^{n} > 0 \\ \frac{\varnothing_{i+1,j}^{n} - \varnothing_{i,j}^{n}}{\Delta x} & \text{otherwise} \end{cases}, \tag{4.6}$$

where Δx is the grid spacing along the x-direction. Similarly $\left(\frac{\partial \varnothing}{\partial y}\right)_{i,j}^{n}$ is given by

$$\left(\frac{\partial \varnothing}{\partial y}\right)_{i,j}^{n} = \begin{cases} \frac{\varnothing_{i,j}^{n} - \varnothing_{i,j-1}^{n}}{\Delta y} & \text{if } v_{i,j}^{n} > 0 \\ \frac{\varnothing_{i,j+1}^{n} - \varnothing_{i,j}^{n}}{\Delta y} & \text{otherwise} \end{cases} \tag{4.7}$$

where Δy is the grid spacing along the y-direction. Equations (4.6) and (4.7) can be used in Eq. (4.5) in order to obtain the fully-discrete form of Eq. (4.3) using the FOU scheme.

The CDS2 Scheme in FDM
In the CDS2 approximation, $\left(\frac{\partial \varnothing}{\partial x}\right)_{i,j}^{n}$ and $\left(\frac{\partial \varnothing}{\partial y}\right)_{i,j}^{n}$ are given by

$$\left(\frac{\partial \varnothing}{\partial x}\right)_{i,j}^{n} = \frac{\varnothing_{i+1,j}^{n} - 2\varnothing_{i,j}^{n} + \varnothing_{i-1,j}^{n}}{2\Delta x}, \tag{4.8}$$

$$\left(\frac{\partial \varnothing}{\partial y}\right)_{i,j}^{n} = \frac{\varnothing_{i,j+1}^{n} - 2\varnothing_{i,j}^{n} + \varnothing_{i,j-1}^{n}}{2\Delta y}. \tag{4.9}$$

One obtains the fully-discrete form of Eq. (4.3) by using the CDS2 scheme after plugging Eqs. (4.8) and (4.9) in Eq. (4.5).

4.3.2 Discretization Using FVM

For applying the FVM, Eq. (4.3) is first converted into conservation form by applying the continuity equation for an incompressible flow as

$$\frac{\partial \varnothing}{\partial t} + \frac{\partial (\varnothing u)}{\partial x} + \frac{\partial (\varnothing v)}{\partial y} = 0$$

$$\frac{\partial \varnothing}{\partial t} + \nabla.\left(\varnothing \vec{V}\right) = 0, \tag{4.10}$$

where $\nabla = \hat{i}\frac{\partial}{\partial x} + \hat{j}\frac{\partial}{\partial y}$ and $\overrightarrow{V} = \hat{i}u + \hat{j}v$. Now Eq. (4.10) is integrated over a finite volume centered at any arbitrary node (I, J) as shown in Fig. 4.2. The integration yields

$$\int\limits_{\Omega_{I,J}} \frac{\partial \varnothing}{\partial t} \mathrm{d}\Omega + \int\limits_{\Omega_{I,J}} \nabla.\left(\varnothing \vec{V}\right) \mathrm{d}\Omega = 0, \tag{4.11}$$

where $\Omega_{I,J}$ is the cell volume. After applying Gauss's Divergence theorem to convert the volume integral associated with the divergence operator in Eq. (4.11) into a surface integral, the equation takes the following form:

$$\int\limits_{\Omega_{I,J}} \frac{\partial \varnothing}{\partial t} \mathrm{d}\Omega + \int\limits_{S_{I,J}} \left(\varnothing \vec{V}\right).\mathrm{d}\overrightarrow{S} = 0, \tag{4.12}$$

where $S_{I,J}$ refers to the control surface of the finite volume centered at the node (I, J) and $\mathrm{d}\overrightarrow{S}$ is an elementary surface vector on the control surface. Equation (4.12) is fully discretized on the FVM framework by introducing the concept of volume averaging with the first-order Euler explicit method of time integration as

$$\frac{\overline{\varnothing}_{I,J}^{n+1} - \overline{\varnothing}_{I,J}^{n}}{\Delta t} \times \Omega_{I,J} + \sum_{k=1}^{N_{\mathrm{F}}} \varnothing_k (V_n)_k S_k = 0$$

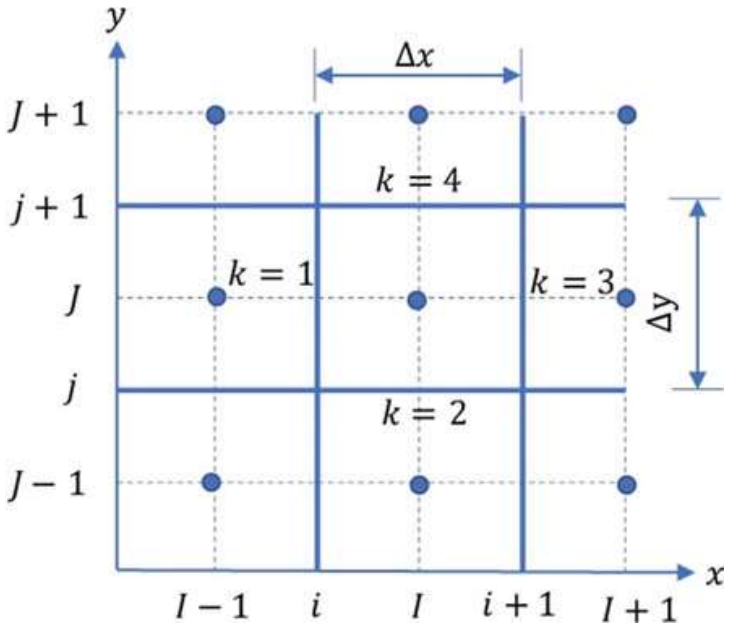

Fig. 4.2 Finite volume cells, with (I, J) representing the index of a cell centroid and (i, j) representing the index of a cell vertex

Table 4.1 Normal velocities and surface areas at the cell-interfaces

Face number (k)	Average velocity $(V_n)_k$	Surface area (S_k)
1	$\frac{u_{i,j+1}+u_{i,j}}{2}$	$-\Delta y$
2	$\frac{v_{i,j}+v_{i+1,j}}{2}$	$-\Delta x$
3	$\frac{u_{i+1,j}+u_{i+1,j+1}}{2}$	Δy
4	$\frac{v_{i+1,j+1}+v_{i,j+1}}{2}$	Δx

$$\overline{\varnothing}_{I,J}^{n+1} = \overline{\varnothing}_{I,J}^{n} - \frac{\Delta t}{\Omega_{I,J}} \times \left[\sum_{k=1}^{N_F} \varnothing_k (V_n)_k S_k \right], \tag{4.13}$$

where $\overline{\varnothing}_{I,J}^{n}$ is the volume-averaged value of $\varnothing$ at any time level n over the cell, centred at the node (I, J), N_F is the number of faces of the finite volume, and V_n is the velocity normal to the cell-interface. With reference to Fig. 4.2, for the present problem $N_F = 4$. The term $\varnothing_k (V_n)_k$ is termed the flux across the kth cell-face. It is to be observed from Eq. (4.13) that while the cell-averaged values of $\varnothing$ are stored and updated at the cell-centroids, the fluxes need to be calculated based on the values of $\varnothing$ and V_n at the cell-interfaces. Accordingly, different numerical-flux schemes are used to approximate the fluxes across the cell-interfaces based on the cell-averaged values of $\varnothing$.

The velocity $(V_n)_k$ and face-area terms (S_k) for the cell centered at (I, J) are listed in Table 4.1. It is to be noted that the width of control volume is taken as unity.

The following discussion presents the FOU, CDS2, and QUICK schemes for computing the flux across an arbitrary cell-interface on the FVM framework.

The FOU, CDS2, and QUICK Schemes in FVM

In the FOU scheme, the interface-flux is obtained based on the cell-averaged value of $\varnothing$ from the cell located upstream of the cell-interface. The CDS2 scheme approximates the value of $\varnothing$ at a cell-interface as the average of the cell-averaged values of $\varnothing$ in the cells sharing that face. The QUICK scheme offers a higher-order accuracy by choosing an upwind-biased stencil. The formulae to evaluate $\varnothing_k^n$ at the four faces of a finite-volume centered at the node (I, J) are listed in Table 4.2.

4.4 Results and Discussion

The profile of the scalar is computed by time marching after one complete revolution of the cone, i.e., at $t = 2\pi$. This section first presents the results with the FDM approach followed by the results with the FVM approach.

Table 4.2 The expressions for scalar variable at the cell-faces using FOU, CDS, and QUICK schemes

k	Value of the scalar variable for the kth face $\left(\varnothing_k^n\right)$				
	FOU		CDS2	QUICK	
	If $(V_n)_k \geq 0$	Else		If $(V_n)_k \geq 0$	Else
1	$\varnothing_{I-1,J}^n$	$\varnothing_{I,J}^n$	$\frac{\varnothing_{I-1,J}^n + \varnothing_{I,J}^n}{2}$	$\frac{6}{8}\varnothing_{I-1,J}^n + \frac{3}{8}\varnothing_{I,J}^n - \frac{1}{8}\varnothing_{I-2,J}^n$	$\frac{6}{8}\varnothing_{I,J}^n + \frac{3}{8}\varnothing_{I-1,J}^n - \frac{1}{8}\varnothing_{I+1,J}^n$
2	$\varnothing_{I,J-1}^n$	$\varnothing_{I,J}^n$	$\frac{\varnothing_{I,J-1}^n + \varnothing_{I,J}^n}{2}$	$\frac{6}{8}\varnothing_{I,J-1}^n + \frac{3}{8}\varnothing_{I,J}^n - \frac{1}{8}\varnothing_{I,J-2}^n$	$\frac{6}{8}\varnothing_{I,J}^n + \frac{3}{8}\varnothing_{I,J-1}^n - \frac{1}{8}\varnothing_{I,J+1}^n$
3	$\varnothing_{I,J}^n$	$\varnothing_{I+1,J}^n$	$\frac{\varnothing_{I,J}^n + \varnothing_{I+1,J}^n}{2}$	$\frac{6}{8}\varnothing_{I,J}^n + \frac{3}{8}\varnothing_{I+1,J}^n - \frac{1}{8}\varnothing_{I-1,J}^n$	$\frac{6}{8}\varnothing_{I+1,J}^n + \frac{3}{8}\varnothing_{I,J}^n - \frac{1}{8}\varnothing_{I+2,J}^n$
4	$\varnothing_{I,J}^n$	$\varnothing_{I,J+1}^n$	$\frac{\varnothing_{I,J}^n + \varnothing_{I,J+1}^n}{2}$	$\frac{6}{8}\varnothing_{I,J}^n + \frac{3}{8}\varnothing_{I,J+1}^n - \frac{1}{8}\varnothing_{I,J-1}^n$	$\frac{6}{8}\varnothing_{I,J+1}^n + \frac{3}{8}\varnothing_{I,J}^n - \frac{1}{8}\varnothing_{I,J+2}^n$

4.4.1 Results with the FDM Approach

The computations are carried out on a 101×101 grid. Figure 4.3 shows the initial profile of the scalar on the FDM framework. It is important to note that the figure plots the local values of $\varnothing$ calculated at the discrete nodes as shown in Fig. 4.1, which clearly shows the sharp cone with Gaussian profile.

The profile of the scalar computed at $t = 2\pi$ computed by using the FOU scheme is shown in Fig. 4.4. It can be observed by comparing Fig. 4.4 with Fig. 4.3 that the FOU scheme results in diminishing of the sharp cone almost into a flat surface after one revolution itself. It is known that for time-marching problems, numerical dissipation results in exponential decay of solution amplitude with time. The present observation is a clear indication of the highly dissipative nature of the FOU scheme. Further Fig. 4.4 shows that there is negligible numerical oscillation in the scalar profile computed by the FOU scheme, which suggests that the scheme is trivially dispersive.

The scalar profile after one revolution of the cone computed by using the CDS2 scheme on the FDM approach is shown in Fig. 4.5. It can be observed from the figure that the CDS2 scheme does not cause a reduction of the amplitude as much as the FOU scheme. However, significant numerical oscillations are observed in the scalar profile, indicating the higher numerical dispersion caused by the CDS2 scheme compared with the FOU scheme

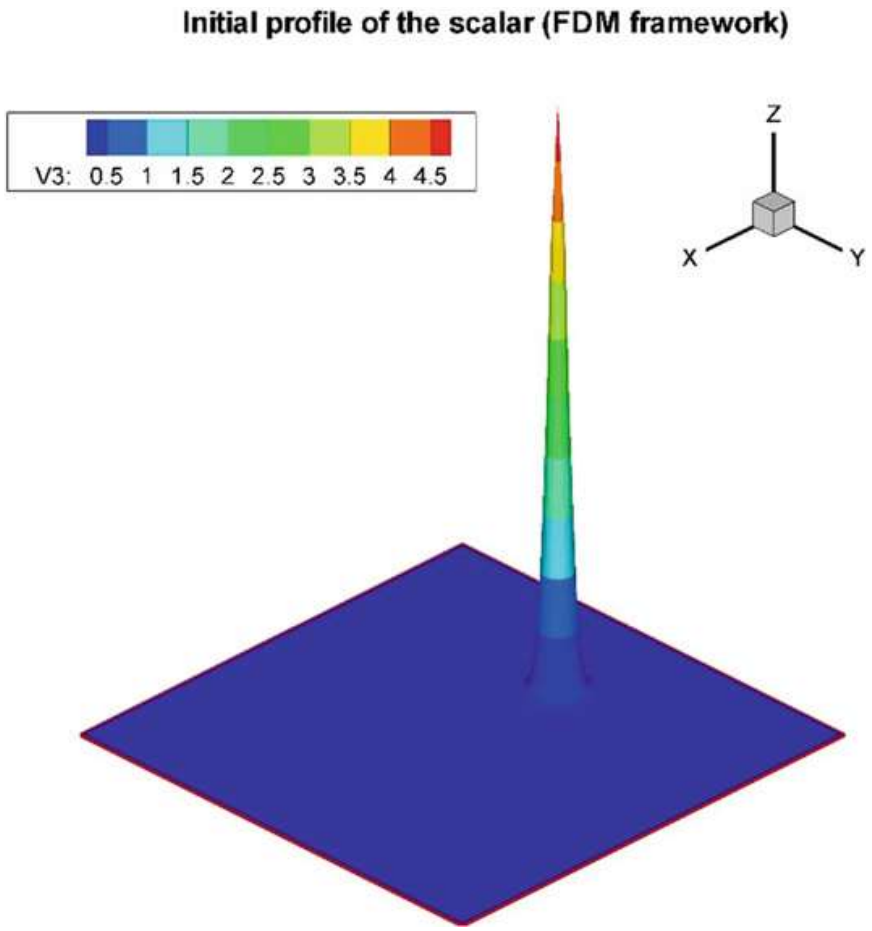

Fig. 4.3 The initial profile of the scalar on the FDM framework

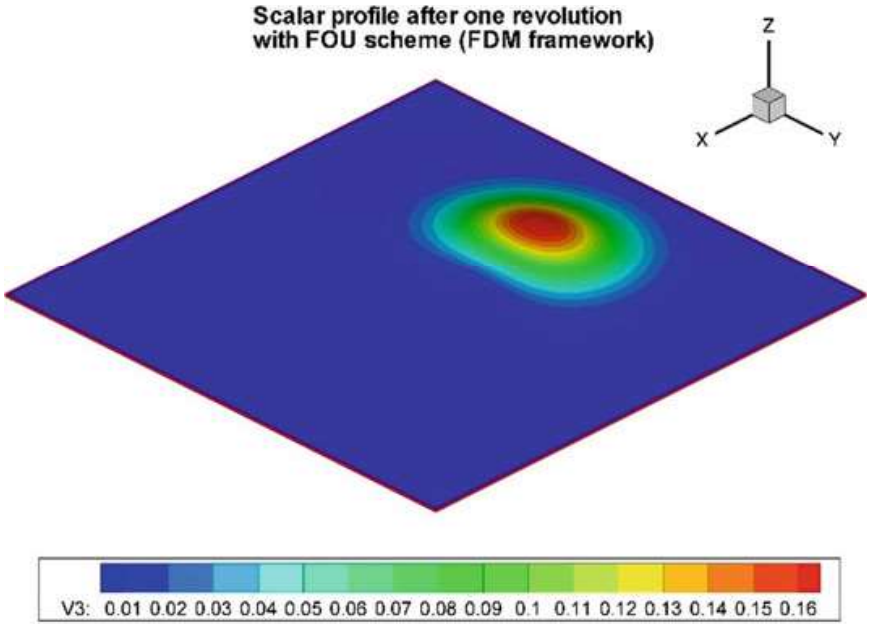

Fig. 4.4 Scalar profile after one revolution computed by using the FOU scheme on the FDM framework

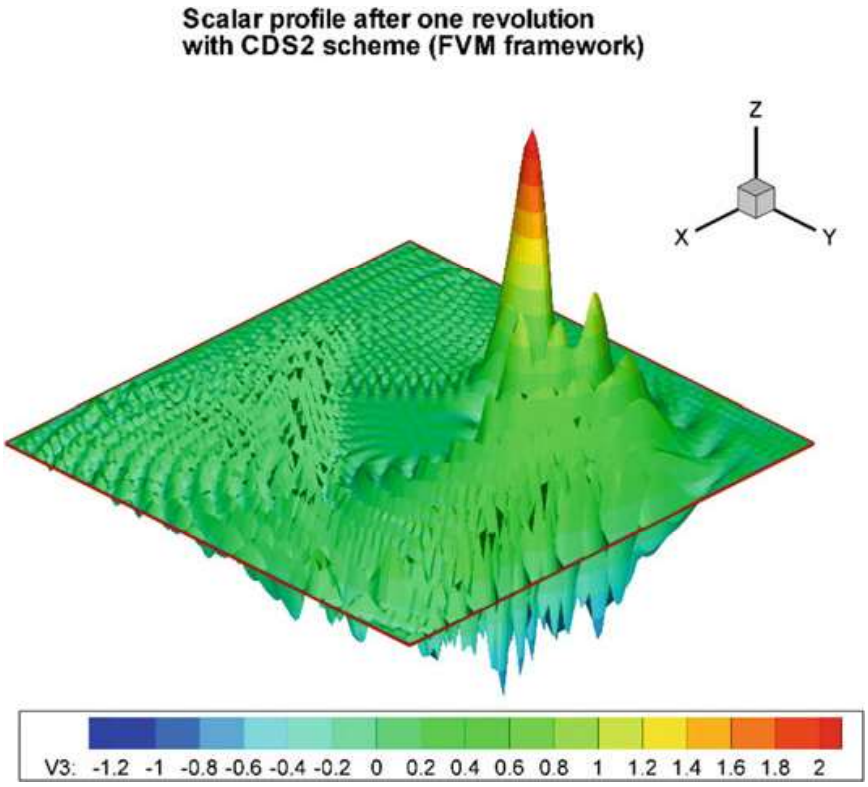

Fig. 4.5 Scalar profile after one revolution computed by using the CDS2 scheme on the FDM framework

4.4.2 Results with the FVM Approach

The computations are carried out on a grid with 100 × 100 cells. The initial profile will be similar to Fig. 4.3, with the only exception being that in this case the profile is plotted based on the cell-averaged values of ∅ over each cell compared with the FDM approach where the local values of ∅ are plotted. In fact, all the plots for the FVM formulation show the cell-averaged profile of ∅ over the computational domain.

The present computations find that the scalar profile after one revolution of the cone computed by using the FOU scheme on the FVM approach is very much similar to Fig. 4.4 and hence not included in the paper for the paucity of space. Further, the scalar profile obtained by using the CDS2 scheme on the FVM approach is found to be analogous to Fig. 4.5 and hence not shown in the paper in order to avoid redundancy. Figure 4.6 shows the scalar profile after one revolution of the cone computed by using the QUICK scheme on the FVM approach. Figure 4.6 indicates that the QUICK scheme offers the least level of numerical dissipation among the three schemes and less numerical dispersion compared with the CDS2 scheme, albeit it offers higher numerical dispersion compared with the FOU scheme.

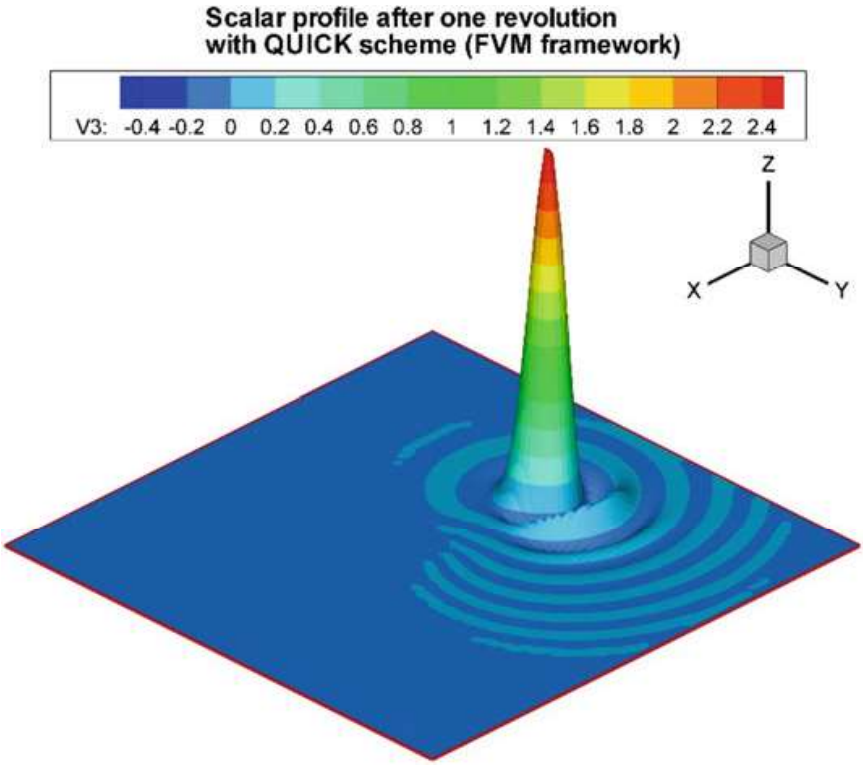

Fig. 4.6 Scalar profile after one revolution computed by using the QUICK scheme on the FVM framework

4.4.3 Quantitative Comparison of the Dissipative and Dispersive Effects

A quantitative comparison of the dissipative and dispersive effects of the schemes is presented in Table 4.3 that shows the maximum and minimum values of the scalar after one complete revolution of the cone. The scheme that computes the highest value of the scalar after convection is the least dissipative. The scheme that computes the least value of the scalar after convection is the most dispersive. It may be noted that the initial maximum and minimum values of the scalar are 5 and 0, respectively. Table 4.3 shows that both the FOU and CDS2 schemes in the FDM framework perform significantly close to their FVM counterparts. In a strict sense, the FOU and

Table 4.3 The maximum and minimum computed values of the scalar after one revolution

Framework	Scheme	Maximum value of $\varnothing$	Minimum value of $\varnothing$
FDM	FOU	0.170665	0
	CDS2	2.19567	−1.3924
FVM	FOU	0.17131	0
	CDS2	2.204791	−1.3895
	QUICK	2.637973	−0.58329

CDS2 schemes are less dissipative than their FDM counterparts. The FOU shows no numerical dispersion, whereas the CDS2 on the FVM framework is less dispersive compared with its performance in the FDM framework. It is also noteworthy that the QUICK scheme shows to be the least dissipative and moderately dispersive among the three schemes tested on the FVM framework.

4.5 Conclusions

The present study shows that while computing the pure convection of a sharp scalar cone, the FOU scheme results in the highest rate of amplitude reduction with time, thereby exhibiting the most dissipative behavior, but zero numerical dispersion in both the FDM and FVM frameworks. On the other hand, the CDS2 scheme is less dissipative compared with the FOU scheme, though it is more dispersive than the latter scheme on both the FDM and FVM frameworks. Both the schemes on the FVM formulations perform almost similar to their FDM counterparts. However, in a stricter sense, the FVM formulations of both FOU and CDS2 schemes are less dissipative than their FDM counterparts. Even the numerical dispersion exhibited by the CDS2 scheme on FVM framework is marginally less compared with the corresponding FDM result. The QUICK scheme that is used for higher-order accurate computation of fluxes in the FVM approach, exhibits significantly less numerical dissipation and dispersion than the CDS2 scheme.

References

1. Dehghan, M.: Weighted finite difference techniques for the one-dimensional advection–diffusion equation. Appl. Math. Comput. **147**(2), 307–319 (2004)
2. Nazir, T., Abbas, M., Ismail, A.I.M., Majid, A.A., Rashid, A.: The numerical solution of advection–diffusion problems using new cubic trigonometric B-splines approach. Appl. Math. Model. **40**(7–8), 4586–4611 (2016)
3. Wan, X., Xiu, D., Karniadakis.: Stochastic solutions for the two-dimensional advection-diffusion equation. SIAM J. Sci. Comput. **26**(2), 578–590 (2004)
4. Gu, X., Huang, T., Ji, C., Carpentieri, B., Alikhanov, A.A.: Fast iterative method with a second-order implicit difference scheme for time-space fractional convection–diffusion equation. J. Sci. Comput. **72**, 957–985 (2017)
5. Li, M., Zheng, Z., Pan, K.: An extrapolation full multigrid algorithm combined with fourth-order compact scheme for convection–diffusion equations. Adv. Differ. Equ. **2018**, 178 (2018)
6. De, A.K., Eswaran, V.: Analysis of a new high resolution upwind compact scheme. J. Comput. Phys. **218**, 398–416 (2006)
7. John, V., Knobloch, P.: On spurious oscillations at layers diminishing (SOLD) methods for convection–diffusion equations: part I-A review. Comput. Methods Appl. Mech. Eng. **196**, 2197–2215 (2007)
8. Tian, Z.F.: A rational high-order compact ADI method for unsteady convection–diffusion equations. Comput. Phys. Commun. **182**, 649–662 (2011)
9. Appadu, A.R., Djoko, J.K., Gidey, H.H.: A computational study of three numerical methods for some advection-diffusion problems. Appl. Math. Comput. **272**, 629–647 (2016)

10. Brandner, M., Knobloch, P.: Some remarks concerning stabilization techniques for convection-diffusion problems. In: Programs and Algorithms of Numerical Mathematics, pp. 35–46. Institute of Mathematics CAS, Prague (2019)
11. Lantz, R.B.: Quantitative evaluation of numerical diffusion (truncation error). Soc. Petrol. Eng. J. **11**, 315–320 (1971)
12. Suman, V.K., Sengupta, T.K., Prasad, C.J.D., Mohan, K.S., Sanwalia, D.: Spectral analysis of finite difference schemes for convection diffusion equation. Comput. Fluids **150**, 95–114 (2017)
13. Silavwe, D.D., Brink, I.C., Wallis, S.G.: Assessment of some numerical methods for estimating the parameters of the one-dimensional advection–dispersion model. Acta Geophys. **67**, 999–1016 (2019)

Lecture Notes in Mechanical Engineering

Shripad Revankar
Swarnendu Sen
Debjyoti Sahu *Editors*

Proceedings of International Conference on Thermofluids

KIIT Thermo 2020

Springer

Editors
Shripad Revankar
Purdue University
West Lafayette, IN, USA

Swarnendu Sen
Jadavpur University
Kolkata, West Bengal, India

Debjyoti Sahu
Kalinga Institute of Industrial Technology
Bhubaneswar, Odisha, India

ISSN 2195-4356 ISSN 2195-4364 (electronic)
Lecture Notes in Mechanical Engineering
ISBN 978-981-15-7830-4 ISBN 978-981-15-7831-1 (eBook)
https://doi.org/10.1007/978-981-15-7831-1

© Springer Nature Singapore Pte Ltd. 2021
This work is subject to copyright. All rights are reserved by the Publisher, whether the whole or part of the material is concerned, specifically the rights of translation, reprinting, reuse of illustrations, recitation, broadcasting, reproduction on microfilms or in any other physical way, and transmission or information storage and retrieval, electronic adaptation, computer software, or by similar or dissimilar methodology now known or hereafter developed.
The use of general descriptive names, registered names, trademarks, service marks, etc. in this publication does not imply, even in the absence of a specific statement, that such names are exempt from the relevant protective laws and regulations and therefore free for general use.
The publisher, the authors and the editors are safe to assume that the advice and information in this book are believed to be true and accurate at the date of publication. Neither the publisher nor the authors or the editors give a warranty, expressed or implied, with respect to the material contained herein or for any errors or omissions that may have been made. The publisher remains neutral with regard to jurisdictional claims in published maps and institutional affiliations.

This Springer imprint is published by the registered company Springer Nature Singapore Pte Ltd.
The registered company address is: 152 Beach Road, #21-01/04 Gateway East, Singapore 189721, Singapore

Contents

Fluid Dynamics

Large Eddy Simulation Modeling in 2D Lid-Driven Cavity 3
Banamali Dalai and Manas Kumar Laha

Numerical Study on Flow Over Two Inline Triangular Cylinders—Influence of Gap Ratio on Vortex Shedding 13
Manu Sivan and S. Ajith Kumar

Fluid–Structure Interaction Modelling of Physiological Loading-Induced Canalicular Fluid Motion in Osteocyte Network 25
Rakesh Kumar, Abhishek Kumar Tiwari, Dharmendra Tripathi, Niti Nipun Sharma, and Milan Khadiya

Generation of Temperature Profile by Artificial Neural Network in Flow of Non-Newtonian Third Grade Fluid Through Two Parallel Plates 39
Vijay Kumar Mishra, Sumanta Chaudhuri, Jitendra K. Patel, and Arnab Sengupta

Fluid Flow and Heat Transfer

Fluid Flow and Heat Transfer Characteristics for an Impinging Jet with Various Angles of Inclination of Impingement Surface 53
Jublee John Mili, Tanmoy Mondal, and Akshoy Ranjan Paul

Implementation of Improved Wall Function for Buffer Sub-layer in OpenFOAM 61
R. Lakshman, Jha Rahul Binod, and Ranjan Basak

Numerical Simulation of Low Reynolds Number Gusty Flow Past Two Side-By-Side Circular Cylinders 71
Yagneshkumar A. Joshi, Deep Pandya, Rameshkumar Bhoraniya, and Atal Bihari Harichandan

Comparative Analysis of Inlet Boundary Conditions for Atmospheric Boundary Layer Simulation Using OpenFOAM 79
R. Lakshman, Nitin Pal, and Ranjan Basak

Parametric Analysis of Coupled Thermal Hydraulic Instabilities in Forced Flow Channel Using Reduced-Order Three-Zone Model 87
Daya Shankar, Harabindu Debnath, and Indira Kar

Numerical Simulation of a Single-Pass Parallel Flow Solar Air Heater with Circular Fins Using S2S Radiation Model 101
Praveen Alok, Sai Charan Teja Javvadi, Pavan Kumar Konchada, and G. Raam Dheep

High-Speed Flow

Parametric Study of Blast Wave Formation in a Shock Tube 115
Sachin Pullil, N. Vaibhav, R. Sanjay, and S. R. Nagaraja

Intermittent Afterburner Engagement Leading to Single Engine Landing in a Typical Bypass Military Aero Engine 125
Saroj Kumar Muduli, Subrata Kumar Rout, Benudhar Sahoo, and P. C. Mishra

Numerical Simulation of Interaction of Blast Wave Generated from Cannon with Wall at Different Pressure Ratio 137
Ansab Khan, Abhishek Kundu, and Akshoy Ranjan Paul

Review on Hypersonic SSTO Engine (HSE) with Variable Diffusers, Double Annular Combustors and N_2O-Oxygen Enhancer 145
Vedant Gupta, S. S. Godara, and B. Tripathi

Modified Method of Characteristics for Analysing Cold Flow in Bell-Type Rocket Nozzle 157
S. Panigrahi, P. S. Maity, Gyan Sagar Sinha, D. Dangi, and Atal Bihari Harichandan

Aerodynamics

Performance Analysis of NACA4412 Airfoil with Gurney Flap 167
Ankit Kumar, Pooja Chambdar, Gyan Sagar Sinha, and Atal Bihari Harichandan

Effect of Ground Clearance and Air Temperature on Drag and Lift for NACA 2412 Airfoil 177
Prakash Ghose and Rishitosh Ranjan

Aerodynamic Characteristics of a Square Cylinder: Effect of Dissimilar Leading Edges 189
Akhil S. Nair, S. Ajith Kumar, K. Arun Kumar, and R. Ajith Kumar

Numerical Investigation of Various Wake Patterns in Flow Past Two Side-By-Side Cylinders 199
P. Pandey, D. Singh, P. Das, D. Ghosh, and Atal Bihari Harichandan

Multiphase Flow and Phase Change Material

Effects of Joules Heating and Soret Number on Double-Diffusive Mixed Convection Flow in an Enclosed Square Cavity 209
A. Satheesh, C. G. Mohan, P. Padmanathan,
and Agarwal Anmol Pallav Kumar

Dimethyl Adipate-Based Microencapsulated Phase Change Material with Silica Shell for Cool Thermal Energy Storage 225
Vedanth Narayan Kuchibhotla, G. V. N. Trivedi, and R. Parameshwaran

Estimation of Parameter in Non-Newtonian Third-Grade Fluid Problem by Artificial Neural Network Under Noisy Data 235
Vijay Kumar Mishra, Sumanta Chaudhuri, Jitendra K. Patel,
and Arnab Sengupta

Role of PCM in Solar Photovoltaic Cooling: An Overview 245
Pragati Priyadarshini Sahu, Abhilas Swain, and Radha Kanta Sarangi

Second Law and Cycle Analysis

Enhancement of Boiling Heat Transfer Using Surfactant Over Surface with Mini-Channels 263
Abhilas Swain, Radha Kanta Sarangi, Satya Prakash Kar, P. C. Sekhar,
and Sandeep Swain

An Analytical Investigation of Pressure-Driven Transport and Heat Transfer of Non-Newtonian Third-Grade Fluid Flowing Through Parallel Plates 275
Sumanta Chaudhuri, Paromita Chakraborty, Rajen Das, Amitesh Ranjan,
and Vijay Kumar Mishra

Design and Analysis of a Naturally Ventilated Fog Cooled Greenhouse Integrated with Solar Desalination System 287
Md Iftikar Ahmed, Sk Arafat Zaman, and Sudip Ghosh

Performance Assessment of a Steam Gasification-Based Hybrid Cogeneration System 297
Sk Arafat Zaman, Dibyendu Roy, and Sudip Ghosh

Heat and Mass Transfer

Experimental Study of Thermal Contact Conductance for Selected Interstitial Materials 309
Mohammad Asif and Alok Kumar

Boiling Front and Boiling Temperature in Microchannels Under Non-uniform Heat Flux Distribution 319
Radha Kanta Sarangi, Abhilas Swain, Satya Prakash Kar, and P. C. Sekhar

Natural Convection Heat Transfer on the Strip Heaters Flushed on the Vertical Flat Plate: A Numerical Study 329
Akurathi Rupendra Siva Prasad, Medisetti Venkata Krishna, and Pradeep S. Jakkareddy

Pool Boiling Heat Transfer Using Isopropyl Alcohol and Ammonium Chloride Surfactant 343
Sandeep Swain, Abhilas Swain, and Satya Prakash Kar

Numerical Simulation on Impact of a Liquid Droplet on a Deep Liquid Pool for Low Impact Velocities 353
Vineet Kumar Tiwari, Tanmoy Mondal, and Akshoy Ranjan Paul

Enhancement of Thermal Performance of Parabolic Trough Collector Using Cavity Receiver 363
Bilkan John Hemrom, Uttam Rana, and Aritra Ganguly

Laminar Mixed Convection Over a Rotating Vertical Hollow Cylinder Exposed in the Air Medium 375
Basanta Kumar Rana and Jnana Ranjan Senapati

Computational Analysis of Static Flow Instabilities in Supercritical Natural Circulation Loop 387
Santosh Kumar Rai, Pardeep Kumar, and Vinay Panwar

Effect of Loop Geometry on the Flow Dynamics of a Single-Phase Natural Circulation Loop 397
Ritabrata Saha, Koushik Ghosh, Achintya Mukhopadhyay, and Swarnendu Sen

Refrigeration and Air Conditioning

A Comparative Analysis Between Indoor and Outdoor Thermal Comfort Parameters of Railway Pantry Car 411
Md. Sarfaraz Alam, Arunachalam Muthiah, and Urmi Salve

Performance Optimization of an Air Conditioning System at Different Mass Flow Rates and Temperatures 417
Taliv Hussain, Adnan Hafiz, Sameer Raza, Abdur Rahman, Tabrez Ahmed, and Pragati Agarwal

Thermo-physical Investigation of Vegetable Oil-Based Nano-lubricant 425
Om Prakash, Ashwani Kumar, and Subrata Kumar Ghosh

Numerical Analysis of Laser-Assisted Cryopreservation of Biological Tissues 435
Saurabh Das and Satya Prakash Kar

Combustion Analysis

Experimental and Numerical Study of Temperature Distribution on Float Glass Along the Wall 447
Raj Kumar Mishra, Ankit Dasgotra, Mahesh Kumar Tiwari, Akhilesh Gupta, Ravi Kumar, and Pavan K. Sharma

Numerical Study on Crude Oil Pool Fire Behavior in an Enclosure . . . 455
Avinash Chaudhary, Mahesh Kumar Tiwari, Akhilesh Gupta, and Surendra Kumar

Thermal and Emissions Characteristics of Pressurized Kerosene Stoves with Selected Commercial Burners 465
Gyan Sagar Sinha, Lav K. Kaushik, and P. Muthukumar

Experimental Study on Elevated Methanol Pool Fires in a Compartment 473
Mahesh Kumar Tiwari, Akhilesh Gupta, Ravi Kumar, Raj Kumar Mishra, Avinash Chaudhary, and Pavan K. Sharma

Soot Formation Characteristic of Impinging Diesel and Biodiesel Blended Sprays at Diesel Engine-Like Conditions 481
Sanaur Rehman and Shah Shahood Alam

Effect of Inlet Swirl and Turbulence Levels on Combustion Performance in a Model Kerosene Spray Gas Turbine Combustor 493
Prakash Ghose and A. Datta

Performance and Emission Analysis of CI Engine Fueled with Waste Cooking Biodiesel Blends at Different Compression Ratios 505
Rahul Mohanty and Vinod Kotebavi

Effect of Compression Ratio on Thermal Efficiency and Cycle-by-Cycle Variation of a Biogas-Fueled SI Engine 515
Santosh Kumar Hotta, Anil Kumar Rout, and Niranjan Sahoo

CFD Simulation of Gasoline and Methanol Combustion in a Twin Spark IC Engine 525
Praveen Alok and Debjyoti Sahu

Thermofluids in Energy Applications

Performance Study on Flat Plate Solar Water Heater with Copper Nanoparticles 539
R. Praveen Bharathwaj, M. B. Varun Pradeep, Joe Jones Raju, A. Satheesh, and P. Padmanathan

Experimentation with a Solar Air Heater Coupled with Evacuated Tubes and Heat Pipes 555
P. Devasena, D. Dimple, A. Varshith, K. Anvesh Reddy, and Vinod Kotebavi

Design of Low-Cost Solar Powered E-Rickshaw: A Case Study 561
Daya Shankar, Manisha Biswas, and Rupa Datta

Integrated MSW to Energy and Hot Water Generation Plant for Indian Cities: Thermal Performance Prediction 569
Pradip Mondal, Shambhunath Barman, and Samiran Samanta

Thermal Performance Evaluation of an Improved Biomass Cookstove for Domestic Applications 579
Raktimjyoti Barpatragohain, Niyarjyoti Bharali, and Partha Pratim Dutta

Experimental Investigation of Paddy Drying in Rotating Fluidized Bed in Static Geometry 591
Rishiraj Purkayastha, Pavitra Singh, Abinash Mahapatro, Alok Kumar, and Pinakeswar Mahanta

Conjugate Heat Transfer Analysis of Solar Cooker Cavity Using CFD Approach 601
Sudhansu Sekhar Sahoo, Prasanta Kumar Satapathy, Pravat Kumar Parhi, Auroshis Rout, and Sanju Thomas

Thermofluids in Materials and Manufacturing

Experimentation with Thermally Stable Mesoporous Silica Powder and Its CO_2 Adsorption 613
Sanjib Barma and Bishnupada Mandal

Experimentation with Thermo-mechanically Stable Epoxy Composite Reinforced with Palm Fiber 621
Jnanaranjan Kar, Arun Kumar Rout, Priyadarshi Tapas Ranjan Swain, and Alekha Kumar Sutar

A Review on Materials Used for Combustion in Porous Radiant Burners 633
Gyan Sagar Sinha, Lav K. Kaushik, and P. Muthukumar

Thermal Analysis of Al 7075-T651 During High-Speed Machining 643
P. Chandrasekhar, Sudipta Chand, Radha Kanta Sarangi, Satya Praksah Kar, and Abhilas Swain

Analysis of Heat Transfer Coefficient in Turning Process 655
Ramanuj Kumar, Amlana Panda, Ashok Kumar Sahoo, and Deepak Singhal

Thermal Performance Evaluation of an Improved Biomass Cookstove for Domestic Applications

Raktimjyoti Barpatragohain, Niyarjyoti Bharali, and Partha Pratim Dutta

Abstract Biomass fuels are normally burnt inefficiently using the traditional cookstoves in rural areas. The uncontrolled harmful emissions released due to the combustion of biomass cause various respiratory problems to the users. Thus in order to overcome such problems related to the traditional cookstove, an improved biomass cookstove is proposed in the present study. An effort is made to design and fabricate an improved biomass cookstove to study various heat losses from it and performance parameters. Water boiling test (WBT) was conducted for understanding the overall performance of the improved stove. Results of WBT were compared with a commercially available biomass cookstove. The average thermal efficiency while boiling 7.5 L water was ~33%, whereas the average thermal efficiency in case of the commercial stove was ~23%. While boiling 7.5 L water in this improved stove, the performance was better than the commercial stove with respect to specific fuel consumption. The maximum level of CO was detected around 20 ppm during the start and it reduced to 5 ppm as combustion progressed. Both the values for CO_2/CO and indoor air quality were within acceptable limit.

Keywords Improved cookstove · Biomass combustion · Thermal performance · Water boiling test · Emission

Nomenclature

w_v	Mass of water vaporized (g)
$P1_i$	Mass of pot of water before test (g)
$P1_f$	Mass of pot of water after test (g)
Δt_c	Time to boil (min)
t_i	Time at start of test (min)

R. Barpatragohain · N. Bharali · P. P. Dutta (✉)
Department of Mechanical Engineering, Tezpur University, Napaam, Sonitpur, Assam 784028, India
e-mail: ppdutta06@gmail.com

© Springer Nature Singapore Pte Ltd. 2021

S. Revankar et al. (eds.), *Proceedings of International Conference on Thermofluids*, Lecture Notes in Mechanical Engineering,
https://doi.org/10.1007/978-981-15-7831-1_54

Lecture Notes in Mechanical Engineering

K. M. Pandey
R. D. Misra
P. K. Patowari
U. S. Dixit *Editors*

Recent Advances in Mechanical Engineering

Select Proceedings of ICRAME 2020

Springer

Editors
K. M. Pandey
National Institute of Technology Silchar
Silchar, India

R. D. Misra
National Institute of Technology Silchar
Silchar, India

P. K. Patowari
National Institute of Technology Silchar
Silchar, India

U. S. Dixit
Indian Institute of Technology Guwahati
Guwahati, India

ISSN 2195-4356 ISSN 2195-4364 (electronic)
Lecture Notes in Mechanical Engineering
ISBN 978-981-15-7710-9 ISBN 978-981-15-7711-6 (eBook)
https://doi.org/10.1007/978-981-15-7711-6

© The Editor(s) (if applicable) and The Author(s), under exclusive license to Springer Nature Singapore Pte Ltd. 2021
This work is subject to copyright. All rights are solely and exclusively licensed by the Publisher, whether the whole or part of the material is concerned, specifically the rights of translation, reprinting, reuse of illustrations, recitation, broadcasting, reproduction on microfilms or in any other physical way, and transmission or information storage and retrieval, electronic adaptation, computer software, or by similar or dissimilar methodology now known or hereafter developed.
The use of general descriptive names, registered names, trademarks, service marks, etc. in this publication does not imply, even in the absence of a specific statement, that such names are exempt from the relevant protective laws and regulations and therefore free for general use.
The publisher, the authors and the editors are safe to assume that the advice and information in this book are believed to be true and accurate at the date of publication. Neither the publisher nor the authors or the editors give a warranty, expressed or implied, with respect to the material contained herein or for any errors or omissions that may have been made. The publisher remains neutral with regard to jurisdictional claims in published maps and institutional affiliations.

This Springer imprint is published by the registered company Springer Nature Singapore Pte Ltd.
The registered company address is: 152 Beach Road, #21-01/04 Gateway East, Singapore 189721, Singapore

Contents

AI-Based ANN Modeling of Performance–Emission Profiles of CRDI Engine under Diesel-Karanja Strategies 1
P. Sandeep Varma, Subrata Bhowmik, Abhishek Paul, Pravin Ashok Madane, and Rajsekhar Panua

ANFIS Prediction of Performance and Exhaust Emission Characteristics of CRDI Engine Fueled with Diesel–Butanol Strategies 11
Vivek Kumar Mishra, Subrata Bhowmik, Abhishek Paul, Ajay Yadav, and Rajsekhar Panua

Development and Workspace Study of a 4-PP Planar Parallel XY Positioning Stage Using SMA Actuators 21
Rutapurna Choudhury, Deep Singh, Anuj Kumar, Yogesh Singh, and Chinmaya Kumar Sahoo

Review of the Hybrid H-Savonius Rotor's Design and Performance 33
D. Sarkar, A. R. Sengupta, P. Bhadra, S. Alam, and B. Debnath

Energy Storage Using Sensible Heat Storage Media: Thermal and Economic Considerations 41
Laxman Mishra, Abhijit Sinha, Prasanta Majumder, and Rajat Gupta

Convective Flow of Nanofluid and Nanoencapsulated Phase Change Material Through Microchannel Heat Sink for Passive Cooling of Microelectronics 51
Manoj Kumar, Vikram Bisht, Sheshang Singh Chandel, Sumit Sinha-Ray, and Pradeep Kumar

Fabrication of Treated and Untreated Coconut Fibre-Reinforced Epoxy-Based Composites of Different Fibre Content and Comparison of Their Tensile and Flexural Strengths 61
U. Deka, M. Bhuyan, C. Borah, S. Kakoti, and R. K. Dutta

Study on Gate Location and Gate Number for Manufacturability of Polymer Gears 71
Bikram Singh Solanki, Harpreet Singh, and Tanuja Sheorey

Fuzzy-PID Control of Hydro-motor Speed Used in Heavy Earth Moving Machinery 83
Shivdutt Sarkar, Mohit Bhola, Harsha Rowdur, and N. Kumar

Phase Change in an Enclosure Under Different Combinations of Boundary Wall Condition: A Numerical Study 95
Bhaskar Ranjan Tamuli, Sujit Nath, and Dipankar Bhanja

Finite Element Modelling of Electromagnetic Crimping of Copper-Stainless Steel Tube-to-Tube Joint 105
Deepak Kumar, Sachin D. Kore, and Arup Nandy

Optimization of Protrusions for an Impinging Jet on a Curved Surface 117
Alankrita Singh and B. V. S. S. S. Prasad

Numerical Analysis on a Selection of Horn Material for the Design of Cylindrical Horn in Ultrasonic Machining 127
Gaddakesh Kumar Chandan and Chinmaya Kumar Sahoo

Emission Studies on a Diesel Engine Fueled with Mixed Biodiesel Produced from Non-edible Oils 137
Bhabani Prasanna Pattanaik, Chandrakanta Nayak, and Rahul Dev Misra

Recent Advancement in Electromagnetic Forming Processes 147
Sagar Pawar, Sachin D. Kore, and Arup Nandy

Review on Pool Boiling Heat Transfer Enhancement by Surface Fabrication Using Various Surface Coating Methods 157
Sonali Priyadarshini Das, Raghavendra Singh, and Rahul Dev Misra

Comparative Study of Extended and Unscented Kalman Filters for Estimating Motion States of an Autonomous Vehicle-Trailer System 165
Hussein F. M. Ali, Nader A. Mansour, and Youngshik Kim

Numerical Study on Material Flow Behaviour in Friction Stir Welding of Low Carbon Steel 175
Pardeep Pankaj, Abhishek Bhardwaj, Avinish Tiwari, Lakshmi Narayan Dham, and Pankaj Biswas

Comparing Wettability and Frictional Performance of Laser Micro-machined Discrete and Continuous Textures 185
V. Kashyap and P. Ramkumar

Influence of Heat Input on Bead Geometry in Metal Inert Gas Welded Thick P91 Steel 193
Lakshmi Narayan Dham, Pardeep Pankaj, and Pankaj Biswas

Opportunities and Challenges in Nanoparticles Formation by Electrical Discharge Machining 203
Irshad Ahamad Khilji, Sunil Pathak, Siti Nadiah Binti Mohd Saffe, Shatarupa Biswas, and Yogesh Singh

Preheating Path Selection Through Numerical Analysis of Laser-Aided Direct Metal Deposition 211
Dhiraj Raj, Bipul Das, and Saikat Ranjan Maity

Robust Synthesis of Path Generating Four-Bar Mechanism 221
Sanjay B. Matekar and Ajay M. Fulambarkar

Predicting the Surface Roughness in Single Point Incremental Forming 233
Manish Omon, Vinay Sharma, and Soumen Mandal

Prediction of Droplet Size Distribution For Viscoelastic Liquid Sheet 243
Saurabh Sharma, Debayan Dasgupta, Sujit Nath, and Dipankar Bhanja

Linear Stability Analysis of Viscoelastic Liquid Sheet in Presence of Moving Gas Medium 251
Debayan Dasgupta, Saurabh Sharma, Sujit Nath, and Dipankar Bhanja

Development of Feature Extraction-Based Currency Recognition System Using Artificial Neural Network 259
Deep Singh, Rahul Kumar, Rutuparna Choudhury, Ashutosh Padhan, and Yogesh Singh

Design and Fabrication of Android Application-Based Grass Cutter Robotic System 271
Rutuparna Choudhury, Deep Singh, Anuj Kumar, and Yogesh Singh

Review on Various Coating Techniques to Improve Boiling Heat Transfer 283
Amatya Bharadwaj and Rahul Dev Misra

Effect of Particulate Type Reinforcements on Mechanical and Tribological Behavior of Aluminium Metal Matrix Composites: A Review 295
V. S. S. Venkatesh and Ashish B. Deoghare

A Review on Solar Drying Applications Using Latent Heat as Energy Storage Media 305
Supreme Das, Agnimitra Biswas, and Biplab Das

Finite Element Analysis of Stamping Process of Maraging Steel Built-Up Wing Panel of a Missile 319
P. Sridhar Reddy, B. V. R. Reddy, S. R. Maity, and K. M. Pandey

Effect of Non-uniform Heating on Forced Convective Flow Through Asymmetric Wavy Channel 333
Sumit Kumar Mehta and Sukumar Pati

Effect of Sintering Temperatures on Mechanical Properties of AA7075/B4C/Graphite Hybrid Composite Fabricated by Powder Metallurgy Techniques 343
Guttikonda Manohar, Saikat Ranjan Maity, and Krishna Murari Pandey

Natural Convection from Two Cylinders in an Enclosure with Sinusoidal Bottom Wall: A Numerical Study 351
Dhrijit Kumar Deka, Gopal Chandra Pal, Sukumar Pati, and Pitambar R. Randive

Identification of Parameters for Ultrasonic Machining (USM) on Drilling of Graphene Oxide/Pineapple Leaf Filler-Reinforced Epoxy Hybrid Composite Using TODIM Method 361
Angkan Bania and Saikat Ranjan Maity

Optimization of Planetary Gearbox Using NSGA-II 367
Abhishek Parmar, P. Ramkumar, and K. Shankar

Conjugate Heat Transfer Analysis for Flow Through Microduct Subjected to Non-uniform Heating 377
Abhijit Borah and Sukumar Pati

Micro Electrical Discharge Milling of Titanium: Effects of Voltage and Tool Rotation Speed 387
Siddhartha Kar, Pallab Sarmah, and Pramod Kumar Patowari

Bio-plastic from Yam—An Ecofriendly Prospective 397
Susheel Kumar, S. K. Pattanayak, and Krishna Murari Pandey

Application of Box-Behnken Method for Multi-response Optimization of Turning Parameters for DAC-10 Hot Work Tool Steel 407
Sunil Kumar, Saikat Ranjan Maity, and Lokeswar Patnaik

Cost Analysis of an Off-Grid Solar/Wind/Battery Based Renewable Energy System for Variable Load 417
Sujeet Singh, Krishna Murari Pandey, and K. K. Sharma

Design and Development of a Mini Sugarcane Harvester 427
M. A. Nagarjun, N. C. Mahendra Babu, and Manjunath M. Ullegaddi

Simulation and Experimental Performance Studies of a Computerized Spark Ignition Engine 441
Pritam Jyoti Saikia, Partha Pratim Dutta, and Pangmoni Kalita

Machinability Study of Rubber using USM for Microdrilling 455
Pallab Sarmah, Tapas Debnath, and Pramod Kumar Patowari

Design, Fabrication and Experimentation of Aqua Silencer for Diesel Genset 463
Neelutpal Ghosh, Sameer S. Gajghate, Sagnik Pal, and Swapan Bhaumik

Numerical Analysis OF PCM Within a Square Enclosure Having Different Wall Heating Conditions 477
Pallab Bhattacharjee, Sujit Nath, and Dipankar Bhanja

Numerical Modelling and Thermohydraulic Analysis of Circular Pipe Having Internal Vortex Generators 487
Binay Bhushan Bora, Mohd Zeeshan, Sujit Nath, and Dipankar Bhanja

Effect of Non-uniform Heating on Electroosmotic Flow Through Microchannel 499
T. Sujith, Sumit Kumar Mehta, and Sukumar Pati

Temperature-Dependent Random Frequency of Functionally Graded Spherical shells—A PCE Approach 509
Vaishali and S. Dey

Microwave Processing of Polymer Matrix Composites: Review of the Understanding and Future Opportunities 517
Tejas Pramod Naik, Ram Singh Rana, Inderdeep Singh, and Apurbba Kumar Sharma

A Comparative Study on the Hydrodynamic and Heat Transfer Behaviour of Conical Fluidized Bed with that of a Columnar Pressurized Circulating Fluidized Bed 531
Hiralh Jyoti Das, Rituraj Sailia, and Pinakeswar Mahanta

Study of the Effect of Welding Current on Heat Transfer and Melt Pool Geometry on Mild Steel Specimen Through Finite Element Analysis 545
Mohd Aslam and Chinmaya Kumar Sahoo

Study of Granular Food Material Drying in a Pilot-Scale Rotating Fluidized Bed with Static Geometry Dryer 555
Pavitra Singh, Pankaj Kalita, Pinakeswar Mahanta, and Hiralh Jyoti Das

Experimental Evaluation of Sand-Based Sensible Energy Storage System 563
Prasant, Sujit Roy, Biplab Das, and Sumita Debbarma

Purification of Biogas for Methane Enrichment Using Biomass Biochar and Biochar–Clay Composite 573
Deep Bora, Lepakshi Barbora, and Pinakeswar Mahanta

Experimental Investigation of Drying Characteristics of Tea in a Conical Bubbling Fluidized Bed Dryer 583
Plabon Tamuly, Hiralch Jyoti Das, and Pinakeswar Mahanta

Design and Development of a *XY* Positioning Stage Using Shape Memory Alloy Spring Actuator 593
Ashutosh Padhan and Yogesh Singh

Selective Etching of Aluminium 6068 Using Photochemical Machining 601
Jaswant Kumar, Tapas Debnath, and Promod Kumar Patowari

Microstructure and Mechanical Characterisation of Friction Stir Welded Inconel 718 Alloy 611
Sanjay Raj, Pardeep Pankaj, and Pankaj Biswas

Effect of Dual-Height Plate Fins on Phase Change Material Cooling Technique: An Experimental Study 619
Maibam Romio Singh, Avis Giri, and Pradip Lingfa

Dynamic Analysis of Parametrically Excited Coupled Beam-Based Piezoelectric Energy Harvester 631
Ranit Roy, Anshul Garg, and Santosha Kumar Dwivedy

An Overview of Wire Electrical Discharge Machining (WEDM) 643
Shatarupa Biswas, Yogesh Singh, and Manidipto Mukherjee

Comparative Analysis of Combustion Noise, Performance and Emission of LTC Diesel Engine with Multiple Injections 653
Sanjoy Biswas and Achintya Mukhopadhyay

Radial Basis Function-Based Probabilistic First-Ply Failure Analyses of Composite Spherical Shells 667
Himanshu Prasad Raturi, Subrata Kushari, and Sudeep Dey

Experimental Investigation of Dimensional Deviation of Square Punches Cut by Wire EDM of A286 Superalloy 677
Subhankar Saha, Saikat Ranjan Maity, and S. Dey

Multi-optimization of μ-EDMed Arrayed Microrods Using Gray Relational Analysis 685
A. K. Singh, T. J. Singh, R. Pongen, and Promod Kumar Patowari

Detection of Fault in a Bevel Gearbox Under Varying Speed Conditions 697
Vikas Sharma, Anand Parey, Abhimanyu Pratap Singh, Atanu Paul, and Yogesh Singh

CFD Analysis of the Performance of an H-Darrieus Wind Turbine Having Cavity Blades 711
Y. Kumar, A. R. Sengupta, Agnimitra Biswas, H. M. S. M. Mazarbhuiya, and Rajat Gupta

The Effect of Negative Hardening Coefficients on Yield Surface Evolution 721
Praveen Kumar and Sivasambu Mahesh

Influence of Camber Ratio and Thickness Ratio on the Airfoil Performance 729
Sujit Roy, Biplab Das, and Agnimitra Biswas

Development of Modified Cyclic Plasticity Model to Simulate Cyclic Behaviour for SA333C–Mn Steel Under LCF Loading Conditions 739
Vibhanshu Pandey, Partha Pratim Dey, Niloy Khutia, and Suneel K. Gupta

High Speed Impact Studies of Kevlar Fabric with and without STF 749
M. Chinnapandi, Ajay Kathyar, Tandra Nandi, and R. Velmurugan

Comparative Study of Nano and Micro Fillers in EPDM/Silicone Rubber for Outdoor Insulator Application 761
S. Bhavya, Unnam Mahesh, R. Velmurugan, and R. Sarathi

Machinability Study for Slot Cutting on Glass Using Ultrasonic Machining Process 771
Anand Mohan Singh, Ranjan Majhi, and Pramod Kumar Patowari

Mechanical Design of a Modular Underwater Rov for Surveillance and Cleaning Purpose 779
Abhimanyu Pratap Singh, Atanu Paul, Yogesh Singh, and Koena Mukherjee

Large Eddy Simulation of Turbulent Slot Jet Impingement on Heated Flat Plate 795
Ghulam Rabbani and Dushyant Singh

Numerical Solution of Foreign-Gas Film Cooling in Supersonic Flow 807
Hitesh Sharma, Dushyant Singh, and Ashutosh Kumar Singh

Deposition of Tungsten and Copper Particle on CFRP Composite 815
Rashed Mustafa Mazarbhuiya and Maneswar Rahang

Performance Improvement of Turbine Blade Using Flow Control Techniques: A Review 823
Hussain Mahamed Sahed Mostafa Mazarbhuiya, Agnimitra Biswas, and Kaushal Kumar Sharma

Parametric Analysis for Machining of Stainless Steel AISI (SS-430) Using Photo Chemical Machining 829
Gaijinlin Gangmei, Jaswant Kumar, Tapas Debnath, and Promod Kumar Patowari

Fabrication and Characterization of Ramie Fiber Based Hybrid Composites 839
Kamnjit Kapila, Sutanu Samanta, and Sushen Kirtania

Multiphase Numerical Modeling of PCM Integrated Solar Collector 849
Bharat Singh Negi, Satyender Singh, and Sushant Negi

Computer-Aided Analysis of Solidification Time and its Effect on Hardness for Aluminium Copper Alloy 861
Sasmita Tripathy and Goutam Sutradhar

Attribute of SiC Powder Additive Mixed EDM on Machining Performance and Surface Integrity Aspects of Inconel 625 869
Ankan Das, Bhavani Tharra, V. V. N. Siva Rao Sammeta, and John Deb Barma

Enhancement of Thermal Performance of Microchannels Using Different Channel Wall Geometries: A Review 881
Dipak Debbarma, K. M. Pandey, and Abhishek Paul

Experimental Investigations of Beeswax Based Composite Phase Change Material 891
Durgesh Kumar Mishra, Sumit Bhowmik, and Krishna Murari Pandey

Investigation on Thermo-hydraulic Performance of Channel with Various Shapes of Rib Roughness: A Review 901
M. K. Sahu, Kumari Ambe Verma, and K. M. Pandey

Interfacial Instabilities in Rotating Hele-Shaw Cell: A Review 911
Akhileshwar Singh, Krishna Murari Pandey, and Yogesh Singh

Performance Analysis of a Scramjet Combustor with Cavity for Mach Numbers 3.0, 3.25 and 3.50 with Hydrogen as a Fuel 919
Namrata Bordoloi, K. M. Pandey, and K. K. Sharma

Study of Fuel Injection Systems in Scramjet Engine—A Review 931
Kumari Ambe Verma, K. M. Pandey, and K. K. Sharma

A Quantitative and Qualitative Review of Sustainable Manufacturing 941
Tejendra Singh and Jinesh Kumar Jain

Simulation and Experimental Performance Studies of a Computerized Spark Ignition Engine

Pritam Jyoti Saikia, Partha Pratim Dutta, and Paragmoni Kalita

Abstract The present work is simulation and experimental performance analysis of a single cylinder spark ignition engine. The simulation model was prepared as a MATLAB code consisting of various input parameters like bore, stroke, compression ratio, spark angle, load, RPM, fuel–air equivalence ratio, inlet pressure, temperature, valve timings, etc. The model uses Wiebe's heat release model, Annand's heat transfer model and Blair's friction model in order to predict the properties with respect to crank angle. Using these data, various performance parameters like brake power, brake thermal efficiency, torque and brake specific fuel consumption were determined by varying the engine speeds, equivalence ratios and loads. The results obtained by simulation were verified by an experimental analysis on a four-stroke single cylinder Honda GX200 computerized Spark Ignition engine. It was observed that the trends in variation of the performance parameters were similar for both the simulation and experimental data. Brake power, torque and brake thermal efficiency were higher in the simulation model whereas brake specific fuel consumption was higher for experimental data. Maximum values of brake power obtained were 2.33 kW for simulation and 1.85 kW for experiment both at 2780 RPM for an engine load of 2.1 kg. Maximum values of torque obtained were 7.35 N m for simulation and 6.35 N m for experiment both at 2780 RPM at an engine load of 2.1 kg. Maximum values of brake thermal efficiency were 13.8% for simulation and 11.3% for experiment both at 2769 RPM for engine load of 1.9 kg. Maximum values of brake specific fuel consumption were 1.92 kg/kWh for simulation and 2.8 kg/kWh for experiment both at 2874 RPM for an engine load of 0.5 kg.

P. J. Saikia · P. P. Dutta (✉) · P. Kalita
Mechanical Engineering, Tezpur University, Tezpur, India
e-mail: ppdutta064@gmail.com

P. J. Saikia
e-mail: psaikia755@rediffmail.com

P. Kalita
e-mail: paragmoni@gmail.com

© The Editor(s) (if applicable) and The Author(s), under exclusive license to Springer Nature Singapore Pte Ltd. 2021

K. M. Pandey et al. (eds.), *Recent Advances in Mechanical Engineering*, Lecture Notes in Mechanical Engineering, https://doi.org/10.1007/978-981-15-7711-6_45

Advances in
SCIENCE AND TECHNOLOGY
Volume II
Write to us at
info.india@mheducation.com
Mc Graw Hill
www.mheducation.co.in
ISBN-13: 978-93-90491-11-7
ISBN-10: 93-90491-11-8
Advances in
SCIENCE AND TECHNOLOGY
Volume II
Kakati | Phukan
Rajbongshi | Bora
Mc Graw Hill
Mc Graw Hill
50 Years
Advances in
SCIENCE AND TECHNOLOGY
Volume II
Edited by
Bharat Kakati
Biswa Ranjan Phukan
Tapan Rajbongshi
Dhiraj Bora

23 Mathematical Modelling of Withering Characteristics of Tea Leaves in Assam, India

Anindita Sharma[1,*] and Partha P. Dutta[1]

[1] Department of Mechanical Engineering, Tezpur University, Tezpur, 784028, Assam
[*] E-mail: aninditat3302@gmail.com

Abstract

Tea is regarded as one of the most consumed drinks around the globe. The processing of tea consists of many stages. Withering is the first step in tea manufacturing. It is a partial drying process of green tea leaf. The moisture content in tea leaves after withering plays a vital role in the subsequent stages of tea processing, hence aiding the final product quality. An attempt is made in this work to mathematically determine the tea withering characteristics by giving special attention to the climatic condition of Assam, India. Three temperatures of 25 °C, 30 °C and 35 °C and five relative humidities of 70%, 75%, 80%, 85% and 90% are considered for the estimation of withering characteristics of tea leaf. Simulations are carried out in MATLAB for all the conditions by keeping one parameter constant at a time. The initial moisture content and the total withering time (*t*) are assumed to be 75% and 10 h respectively. It is observed that the moisture content (MC) reduces at a quicker rate at lower values of humidity as compared to that in high humidity. At 25 °C and 90%, the decrease in moisture content is gradual and comes down to the required value of around 50%. The goodness of fit results for this set of conditions gives the value of R^2 as 0.9227.

Keywords: Tea leaf, Withering, Moisture content, Temperature, Humidity

1. INTRODUCTION

Tea is regarded as one of the most consumed drinks around the globe. Assam produces around 52% of the total tea production in India, which is the largest [1]. The withering of fresh tea leaves is the first and obligatory step in tea manufacturing. It is partial drying of tea leaves. Moisture estimation plays a vital part in tea processing. Withering makes the leaves flabby and decreases the moisture content. Both physical as well as chemical changes take place in withering. The physical changes in the tea leaves that happen during withering are called as physical withering. The tea leaves also undergo certain biochemical changes in this process. This is termed as chemical withering of the leaves. A certain degree of withering has to be attained in order to roll the leaves well. The moisture content generally reduces to around 50% during withering [2]. An attempt is made in this work to mathematically determine the tea withering characteristics by giving emphasis to temperature and relative humidity in agreement with the climatic conditions of Assam, India.

Studies have been made on the drying behaviour of different types of leaves like purple basil leaves [3], olive leaves [4], nettle leaves [5], peppermint leaves [6], curry leaves [7] and so on. There has been considerable research on the drying aspect of tea leaves. However, less work has been done on tea leaf withering [8]. A producer gas fired dryer was used to estimate the thin-layer drying kinetics of fermented tea for temperature and velocity range of 80-110 °C and 0.5-0.75 m/s respectively. The Modified Page model gave satisfactory results for this case with diffusivity constant of 0.746×10^{-5} m^2/s, activation energy of 52.104 kJ/mol and 19.01 MJ/kg energy consumption of made tea [9]. Page model gave best microwave drying characteristics of Assam CTC tea at power levels of 180, 360, 540, 720 and 900 W [10]. A one-dimensional heat and mass transfer mathematical model was developed to simulate moisture content of tea leaves during trough withering. The experimental values tallied with that of

28 Experimental Investigation of Thin Layer Drying Kinetics of *Garcinia pedunculata* Dried in a Forced Convection Environmental Chamber

Pooja Dutta [1,*], Partha Pratim Dutta[1] and Paragmoni Kalita[1]

[1] Mechanical Engineering, Tezpur University, Tezpur, 784028, Assam
[*] E-mail: poojadutta1324@gmail.com

Abstract

Drying is by far the most effective and the ancient way of storing food products. The removal of moisture from a material is termed as drying. The present work focuses on finding the kinetics of *Garcinia pedunculata* (GP) in a forced convection Environment Chamber (Model-REC-22038A2T, Make: RELCO, India). Six samples of GP were taken, each weighing 1kg were considered for experiment. The experiment was carried out for different relative humidity keeping the temperature constant. It was found that 40% RH at 40°C took less time when compared with other relative humidity. The moisture content was found to reduced to 10% (wb) from initial moisture content of 90% (wb) in the environmental chamber. The best chosen drying model was found to be Two Term model out of the seven selected ones.

Keywords: Garcinia Pedunculata, Environmental Chamber, Drying Kinteics, Moisture Ratio

1. INTRODUCTION

Drying is one of the most primitive and essential way to store agricultural fruits for food security and safety. It is simply done by removing moisture from the products that needs to be stored for future use. Drying of food and farming items is essential for preservation and storage, easy handling, and decrease in the transportation cost[1-3]. Open sun drying still continues to be the most popular and cheap method in the tropical region. But when the quality of the product is considered it is not a good way to dry. Researchers from many decades have tried to develop alternative to overcome this difficulty. They have designed and developed different solar dryers for wide variety of agricultural products like chilli, ginger, turmeric, pineapple, cherry tomatoes, banana and herbs and spices [4, 12].

Garcinia pedunculata medicinal characteristics exert influence on human body when taken with food. It increases digestion, cleanses urine and feces, acts as cardiac tonic, relieves constipation, relieves abdominal colic pain, cures tumours of abdomen, cough and cold, asthma, worm infestation, indigestion, vomiting, hemorrhoids etc. It played an important role in the treatment of various diseases such as diabetic, Alzheimer's and normal aging [13,14]. The fruit is a rich source of secondary metabolites with a wide range of biological and pharmacological activities including xanthones, flavonoids, benzophenones, lactones and phenolic acids [15]. North East India (NER) climate conditions and soil are suitable for the cultivation of agricultural seasonal fruits like *Garcinia pedunculata*. The tree starts bearing flowers by September-October and ripens in April. As the fruit is seasonal, it becomes very important to dry this product and store for future use. These products are traditionally sun dried in Assam. GP is traditionally sun dried in Assam, India. Open sun drying has drawbacks such as accumulation of dirt, infestation of pests, bacterial pollution and rain spoilage. In this way, dried items are unhygienic and very often inappropriate for human consumption. To overcome these effects we have carried our experiment in a forced convection environmental chamber. In a variety of dryers, experimental investigation and mathematical modelling of the thin layer drying kinetics of different types of fruits and medicinal plants was carried out. Clearly from the literature we can draw a close conclusion that the drying kinetics of GM in a forced convection environmental chamber.

31 A Comparative Thermal Performance Studies between Two Different Configurations of Absorber Plates in a Double Pass Solar Air Heater using CFD and Experimental Analysis

Partha Pratim Dutta[1]* and Priyom Goswami[1]

[1] Department of Mechanical Engineering, Tezpur University, Tezpur, 784028, Assam
*E-mail: ppdutta06@gmail.com

Abstract

A comparative study between two different absorber pates (i.e. a flat plate and a corrugated plate) of a solar air heater (SAH) is taken into consideration. The comparative analysis is done using two different approaches; CFD (Computational Fluid Dynamics) and experimental. CFD analysis is done using CFD tool ANSYS Fluent 19.1 Academic Version. To discretize the governing equations for heat transfer and also the continuity equations the Finite Volume Method (FVM) is used. The k-ε turbulence model is used for numerical solutions. Keeping all the dimensions as well as the working environment same for both the cases of SAH, the flat plate double pass solar air heater is analyzed using ANSYS whereas the corrugated plate double pass solar air heater is solved by experimental analysis. For both the cases the experimental as well as simulation, the flow rate of air is maintained constant at 0.08 kg/s. By comparing the experimental results and ANSYS results it can be seen that there is a significant improvement in the efficiency of a double pass solar air heater with corrugated plate. Temperature at the outlet of the solar air heater was 322.4 K. The maximum outlet temperature was 326.6 K for a mass flow rate of 0.08 kg/s at radiation level of 1192 W/m^2. Similarly, the pressure drop at the outlet is 0.837 Pa.

Keywords: Solar Thermal Absorber Plate, Solar Energy, Double pass, Corrugated Plate Absorber

1. INTRODUCTION

Suitable design of Solar Air Heaters (SAHs) is a very vital stage for its optimal performance as well as specific applications. Ekechukwu and Norton studied on the principle of operations, constructions and on various designs of SAHs. Based on running modes, they classified SAHs as active, passive and hybrid [1]. SAH are classified based on tracking and non-tracking mechanism, with the use of Phase Changing Materials (PCM) as well as rock bed, for the purpose of heat storage. When air is heated in various spaces of ducts and finally delivered to one end for the purpose of heating applications are termed as active SAH. The heat storage system can also be embedded in the case of active SAH so that it can be used even after sunset for some time. Passive SAH are simple, cost-effective (i.e. less expensive as compared to the active one), and are rugged in construction as reported by Tyagi et al. [2]. SAH are classified in terms of single pass, double pass and multi-pass depending on the flow pattern of SAH. If the air flows in a way such that it flows either from above or below the absorber plate, then it is known as single pass SAH. If the flow passes through two passages, then it is a double pass SAH. This may be further classified into parallel and counter pass SAH. If air passes through the upper side of the absorber plate, it reduces the top heat loss of the SAH to the environment in contrast to the flow through the lower side of the absorber plate. Nonetheless, side edge and bottom losses can be reduced by using materials with lower thermal conductivity such as wood or foam. For the case of the top cover, a glass with low absorptivity and high transmissivity is used. Apart from all these design parameters, the researchers are more inclined towards designing a better absorber plate for better efficiency [3-5].

Dovic et al. [6] developed a reliable tool for investigation of advantages and disadvantages of the new chevron type of corrugated absorber relative to the flat type one. They obtained and guidelines for a corresponding prototype design. Reliability of the simulations was verified through the comparison with the experimental measurements on a collector with tubes. The presented models allowed investigations on the influence of different geometric

32 Modelling and Performance Analysis of Improved Biomass Cook Stove

R. J. B. Gohain[1] and P. P. Dutta[1]

[1]Department of Mechanical Engineering, Tezpur University, Tezpur, 784028, Assam
E-mail: raktim3856@gmail.com

Abstract

Biomass as fuel in furnace for domestic and industrial heating is becoming a very good and efficient alternative thermal energy source to overcome the conventional energy crisis. Due to the uncontrolled harmful emissions released by combustion of biomass in domestic cook stove, it causes various respiratory problems to the users. Thus in order to overcome all these various problems related to traditional cook stove, improved biomass cook stove has been developed. Proper designing and various performance parameters plays a very important role in increasing the overall thermal performance and efficiency of the cook stove. In this study an improved biomass cook stove has been modeled, designed and fabricated to study the various heat losses related to improved biomass cook stove.

The second part of the study consists of experimental analysis of the fabricated design incorporated with a heat recovery system. Water Boiling Test (WBT) was conducted to study the overall performance of the stove. Results were compared with a commercially available biomass cook stove. The overall thermal efficiency was found to be better than the commercial stove i.e. 35 % in case of the fabricated model and 22% in case of the commercial stove.

Keywords: Biomass, Cook stove, Performance Analysis

1. INTRODUCTION

Fossil fuel like coal has been extensively used for decades for heat and power generation in various industrial and domestic purposes [1]. But it has impacted our environment with emissions and with the depletion of the fossil fuels an alternative source of energy had to be adopted. So much effort has been given to obtain sustainable ways of generating power by reducing emission but maintaining generation [2]. Biomass is a suitable renewable energy which could overcome this crisis. Biomass is considered as an inexpensive source of thermal energy generation. Complete combustion of biomass releases carbon dioxide in the atmosphere but biomass is considered as a carbon neutral source because it recaptures same amount of carbon in growing [3].

People generally burn biomass in two ways. Either they use wood burning stove or they use biomass furnace. The simplest method is to use a wood-burning stove, an enclosed metal box made from something like cast iron, with opening doors at the front where the fuel is loaded up and a small smokestack called a flue to carry away carbon dioxide, smoke, steam, and so on. This generally provides heat in a single room, much like a traditional coal fire. A biomass furnace is a more sophisticated option that can heat an entire building. While wood-burning stoves have to be manually filled up with logs, biomass furnaces are often completely automated, they have a large fuel hopper on the side that automatically tops up the furnace whenever necessary [9]. The furnace's ability to run on a particular type of biomass depends on several factors such as moisture content, energy content, density and size. Chip/pellet size is important because any fuel type put into the hopper must be able to flow through the system. For example, the energy content of a wood chip is the same as an equal weight wood pellet made from the same material.

34 Design and Modelling of a Parabolic Trough Solar Collector

S. S. Begum*, H. Jangid, A. P. Goswami and P. P. Dutta

Department of Mechanical Engineering, Tezpur University, Tezpur, 784028, Assam
*E-mail: sahana.shehnaz@gmail.com

Abstract

A parabolic trough solar collector (PTC) was designed and modelled through for evaporation and condensation semi filtered waste water. The collector of the PTC is made up of aluminium and is coated with reflective films. The focus of this PTC is at a distance of 0.4934 m from the base of the trough. The receiver of the PTC is a copper tube with inner diameter 0.025 m and outer diameter 0.026 m, lies at the focus of the parabolic trough. The receiver is enclosed in a glass tube of inner diameter 0.05 m so as to trap the heat inside the enclosure and hence acts as an insulator. Water in the copper tube of the solar collector is heated by multiple solar radiations reflected by the solar collector. The relationships among different variables have been studied in the environmental conditions of Tezpur University campus. The measured solar radiation values were in the range of 650 W/m^2 to 750 W/m^2 . The concentration ratio of the given PTC is estimated as 13.90 and the optical and thermal efficiencies are 0.5391 and 0.5214 respectively. To maintain water temperature at 100°C through the absorber, mass flow rate should be kept at around 0.0027 kg/s with a useful heat gained around 790 W. The relationship between useful heat gained and solar intensity is linear. Thermal losses increase with temperature at constant solar radiation. But heat losses decrease with increase the solar intensity, keeping absorber temperature constant. With an increase in the inlet temperature of water in the PTC, thermal losses increase, thereby, decreasing its thermal efficiency. At low inlet temperature levels, the exergetic efficiency takes values close to zero, because the operating temperature levels (inlet and outlet) are close to the ambient temperature and there is no significant margin for the production of work.

Keywords: Parabolic trough, Modelling, Radiation, Efficiency

1. INTRODUCTION

Water and energy are vital for sustaining life on earth and assist the modern world. Saving water and energy is currently of utmost importance to the mankind. Scarcity of water is a serious challenge that many regions are facing, and it is now becoming even worse due to the increasing water demand brought by the industrial development in different countries. Meanwhile, the untreated industrial waste water effluent and municipal discharge have again magnified the problem. Treating water is the process of improving the quality of water to make it acceptable for a specific end-use. This may be drinking, industrial use, use in irrigation, water recreation and many more. Water treatment either safely removes the contaminants and other undesirable components or their concentrations are reduced to desirable values to make the water fit for further use. At the same time, with the increase in manpower and machines, the need of energy has also increased. The depletion of fossil fuels has led to the discovery and use of different renewable energy sources as a part of sustainable development. The water treatment process can be carried out using sustainable techniques to gain maximum advantage in the field of resource conservation.

A solar parabolic trough collector (PTC) may be used to purify contaminated water through evaporation and condensation processes. Since the heat source to vaporize contaminated water is purely from concentrated solar thermal energy, therefore the greenhouse gases emissions are negligible. Moreover, a low-cost water treatment setup is required in many parts of the world where there is a clean water scarcity but plenty of solar radiation, making the sludge water fit for reuse. The PTC, because of its smaller absorber surface area can generate higher temperature difference more efficiently than a single flat plate collector. It can be made by bending a sheet of a

Contents

Preface vi

1. Microstructural, Optical and Photocatalytic Properties of Cu-Doped ZnO Nanocrystals 1
Amarjyoti Kalita and Manos P. C. Kalita

2. Analysis of Rainfall Events in Northeast Region of India 7
Ashok Singh, Samir Thakur and Nirab C. Adhikary

3. pH Dependent Structural and Morphological Modifications of Protein Thin Film 13
Bijay Kumar Sah and Sarathi Kundu

4. Nonlinear Solitary and Shock Wave Propagation in Positron Beam Driven Multicomponent Plasma 17
B. Boro, A. N. Dev, B. K. Saikia and N. C. Adhikary

5. Sheath Profiles in a Three Component Plasma Containing Tsallis Distributed Electrons 25
Dima Rani Borgohain

6. MoS_2 Quantum Dots Synthesis and Their Size Modulation by Pulsed Laser Ablation in Liquid 30
Gobinda Pradhan, Partha P Dey and Ashwini Kumar Sharma

7. Simulation of Nanofluid Filled Inside a Porous Square Cavity Heated Partially on the Bottom Wall in Presence of Magnetic Field 35
L. Jino, A. Vanav Kumar

8. Design and Fabrication of an Optical Metrology System for the Measurement of Scattering and Reflectance Properties of Biological Tissues 43
Ankur Gogoi, Madhumita Devi, Rajdeep Nath and Jyoti P. Gogoi

9. Study of Structural, Electronic and Interaction Mechanism of Functionalized Carbon Nanotubes with Oxygen 49
Samir Thakur, Sankar M. Borah, Ashok Singh and Nirab C. Adhikary

10. Giant Kerr Nonlinearity and Slow Light via EIT in Three-level Semiconductor Quantum Well Nanostructures 55
Nitu Borgohain, Dipankar Sarmah, Harshajit Kalita and Abdulla Al Amin

11. Anomalous Scaling Behavior of Cu Film via Pulsed Laser Deposition and Correlation with SPR Properties 61
Rahul Kesarwani, Partha P Dey and Alika Khare

12. Microstructural and Optical Properties of Vacuum Deposited Polyaniline (PANI) on Nano Si Structure 69
Pranjal Nath, Deepali Sarkar

13. Spectroscopic Measurement of Magnetic Field in High Density Plasma 74
Subir Biswas

14. Systematic Study of Ground State Deformation Effects on Fusion Cross Sections 79
Tapan Rajbongshi

15. Optical and Electrical Properties of Cation Exchanged Hybrid Semiconductor Nanowires 85
Ritun Chakraborty

16. Recent Advances in the Development of Nanostructure Polyaniline: A Review 90
Mausumi Das

17. Forces on Dust Grains in Low Pressure Laboratory Complex Plasma 94
Bharat Kakati

18. Formation of Pyrrole Sandwich and Multidecker Complexes via Cation···π Interaction: A Density Functional Study 100
Bapan Saha, Sangeeta Das, Ondrila Deb, Shrutimala Baruah and Priyanka Paul

19. Some Applications of Fixed Point Theorem in Fuzzy Boundary Value Problems 108
Nilakshi Goswami and Bijoy Patir

20. Spiky Wave in Dusty Plasma with Dust Charge Variation Having Nonthermal Ions 115
Banajit Sarmah, Anuradha Devi and Jnanjyoti Sarma

21. A Mathematical Model to Establish the Interactive Glucose Insulin Dependence in Presence of Externally Ingested Glucose (G_{IG}–I_{IG}–E Model) 122
Anuradha Devi and Ranjan Kalita

22. Preliminary Study on the Fish Species, Their Feeding Habit and Water Quality of Tharong River, Kokrajhar, Assam 127
Sanraja Machahary and Bronson Kumar Khangembam

23. Mathematical Modelling of Withering Characteristics of Tea Leaves in Assam, India 133
Anindita Sharma and Partha P. Datta

24. Investigation on the Emission Performance of a CI Engine Fuelled by Biodiesels and Their Blends 139
Madhurjya Saikia, Bichitra Bikash, Dilip Kumar Bora and Kalyan Kalita

25. Effect of Solution Treatment Temperature and Soaking Time on Hardness of Al-Mg-Si-Sn Alloy 145
Monoj Baruah, Hrishikesh Bhattacharyya, H. Gohain and Anil Borah

26. Design and Fabrication of a Refrigeration System Operated with LPG 150
Kamaldeep Kalita, Santanu Talukdar, Suraj Singha, Mousam Handique, Deepjyoti Barmanand Khemraj Newar

27. Investigating the Effect of Furnace Cooling on Hardness of 2xxx Series Aluminium Alloy Micro-Alloyed with 0.04 wt% of Titanium 156
Manash Bhuyan, Nang Kingkham Chowpi, Eliza Maibangsa, Anurag Sarma, Anil Borah

28. Experimental Investigation of Thin Layer Drying Kinetics of Garcinia pedunculata Dried in a Forced Convection Environmental Chamber 161
Pooja Datta, Partha Pratim Datta and Paragmoni Kalita

29. Design and Fabrication of Portable Rice Grain Separator cum De-Husker 166
Pranjal Sarma, Raktim Ranjan Baruah, Jitul Kumar Rabha, Pratik Chakraborty, Ankash Barman, Reeshav Raj Barman

30. Multi-response Optimization for Koroch Bio-diesel using Taguchi-Grey Relational Analysis 172
Prasanta Kr. Choudhury, Dilip Kr. Bora

31. A Comparative Thermal Performance Studies between Two Different Configurations of Absorber Plates in a Double Pass Solar Air Heater using CFD and Experimental Analysis 178
Partha Pratim Dutta and Priyom Goswami

32. Modelling and Performance Analysis of Improved Biomass Cook Stove 184
R. J. B. Gohain and P. P. Dutta

33. Benefits of Upwind Differencing Scheme over Central Differencing Scheme while Numerically Solving Convection-dominated Diffusion Problems 189
S. Bhawan Shivhare 189

34. Design and Modelling of a Parabolic Trough Solar Collector 197
S. S. Begum, H. Jangid, A. P. Goswami and P. P. Datta 197

35. Study on Sustainable Design against Rocking 204
Gitartha Kalita and Pranjal Sarma

36. An Assessment of Sick Building Syndrome: A Survey of Hospitals in North Lakhimpur, Assam, India 211
Parinita Baruah and Gitartha Kalita

37. A Survey on Vehicular Ad-hocNetwork (VANET) 216
Mausumi Barooah and Nabanita Das

38. Cancer Sample Classification from microRNA Gene Expression Data: An Empirical Study 224
Dikme Chisil B. Marak and Anindya Halder

39. Segmentation of Brain MRI using Unsupervised and Semi-supervised Techniques 232
Nur Akon Talukdar and Anindya Halder

40. Automatic Removal of Pectoral Muscle from Mediolateral Oblique View Mammograms 239
Rubul Kumar Bania, Anindya Halder

41. Prediction of Air Pollutants using Spatiotemporal Big Data, Methods of Machine Learning and Deep Learning and their Application on Human Health and Environment: A Study 245
Shrabani Medhi and Minakshi Gogoi

42. An Approach of Online Handwriting Bangla Character Recognition 251
Subhash Banishtha

43. English to Aputani Machine Translation using Statistical Method 257
Debayan Chakraborty and Koj Sambyo

44. Design and Analysis of Brain Tumor Detection System using Convolutional Neural Networks in MRI Images 263
Deepjyoti Kalita and Anindita Barman

45. Analysis and Enhancing of ECG Signal using Optimal Moving Average and DFT Filtering, Performance Evaluation using RSME and CC Measures 268
Smriti Rekha Baruah and Pallab Sarma

46. 5G as a Potential Communication Network for Autonomous Vehicles – A Literature Survey 275
Nandan Acharjee, Syed Mobrur Ahmed, Satyasuchi Bhattacharyya and G Aruna

47. Energy Plantations from the Modern Bioenergy Standpoint: Crucial Issues and Policy Requirements in India 280
Mayur Mazoom Phukan and Plaban Bora

48. Feasibility of Vegetable Oil as Transformer Oil: A Review 284
Sami Kakati, Jyotishmanya Kakoti, and Nabajit Dev Choudhury

49. Design, Construction and Technology Transfer of a Low-Cost Solar Fish Dryer 293
Shah M. Hussain, Bipul Kr. Kakati and Biswa Ranjan Phukan

50. Status and Importance of Postharvest Management of Horticultural Crops 298
Ajai Kr. Pandey, Ghan Shyam Abrol, Ng. Piloo and Amit Kumar

51. A Qualitative Study of the Concept of Post Purchase Consumer Regret and its Importance in Case of Online Purchase of White Goods 311
Anannya Boruah and Sinmoy Goswami

52. A Conceptual Study on Metacognition and its Role in Music Experience and Music Marketing 316
Manmit Mahanta and Sinmoy Goswami

53. Critical Analysis of the Impact of Artificial Intelligence in the Service Industry 324
Samajjwal Mohan Dev Sarma and Mukalesh Barua

54. Self Help Groups and Rural Development: With Special Reference to Nagaon District, Assam 330
Pingki Sarma

Spectrum Vol.1 No.1

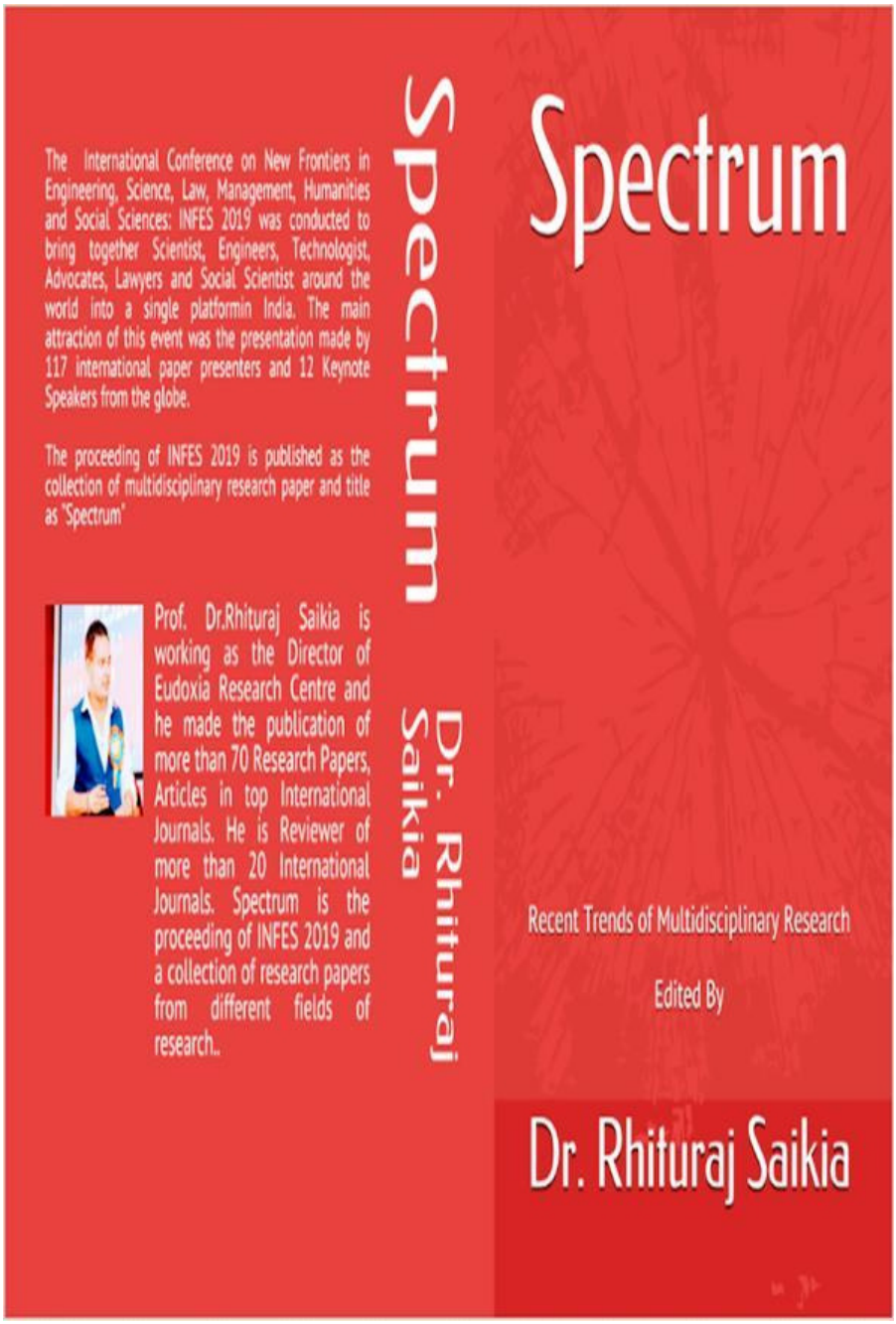

CONTENT

SL/NO	Title of the Paper	Author Name	Page No.
1	SYNTHESIS AND CHARACTERIZATION OF STARCH CAPPED CuS NANOSTRUCTURES ON LOW MOLAR CONCENTRATION	S.KR. NATH[1] & P.K. KALITA[2]	11-21
2	STUDY OF INDUSTRIAL LIME SLUDGE WASTE FILLED COIR-JUTE REINFORCED POLYESTER HYBRID COMPOSITES	SATADRU KASHYAP[1], DIPYAMAN GOGOI[2]	22-37
3	A DATA-BASED SOFTWARE DESIGN FOR BIODIVERSITY ASSESSMENT IN SILCHAR	SHIRSHENDU DEB	38-51
4	DETERMINATION OF EFFICACY OF BIOPESTICIDE AGAINST CHILLI APHID (*APHIS GOSSYPII)*BASED ON LC_{50} VALUES	TANJIL RAHMAN[1], SWAGATA SAIKIA[2]	53-59
5	RESERVATION SYSTEM IN INDIA	BATOTSI KRI	60-66
6	"A COMPARATIVE STUDY OF THE PERFORMANCE MANAGEMENT SYSTEM ADOPTED BY TWO ORGANIZATIONS BELONGING TO THE PRIVATE AND PUBLIC TELECOM SECTOR".	DEBOSREE SARMA	67-82
7	ANALYZING WORKABILITY OF MAKE IN INDIA – INITIATIVE AND ITS IMPACT ON INDIAN ECONOMY	PROF. (DR.) SATISH CHANDER SHARMA	83-93
8	PERCEPTION OF BLOCKCHAIN TECHNOLOGY BY BANKING PROFESSIONALS	MD. ABDULLAH AL MAHMUD	94-108

ISBN:9798647282972

STUDY OF INDUSTRIAL LIME SLUDGE WASTE FILLED COIR-JUTE REINFORCED POLYESTER HYBRID COMPOSITES

Satadru Kashyap[1], Dipyaman Gogoi[2]

Department of Mechanical Engineering, Tezpur University
Napaam, Sonitpur District, Assam – 784028
Email: satadru@tezu.ernet.in

Abstract:

Today, the focus of material science has shifted from the conventional materials to composite materials, due to their better properties, low cost, light weight, easy processing and their ability to be tailor made for specific purposes. Recently, natural fibres are being used in composites in order to test their worthiness as reinforcement materials and due to their biodegradability. In this study, an industrial waste in the form of lime sludge from the paper industry is also added as filler in natural fibre based polymeric composites i.e. coir-jute reinforced unsaturated polyester composites. Initially, a comparison was carried out between unfilled and lime sludge filled hybrid composites of coir and jute. It was observed that the tensile strengths of the filled composites were superior to that of their unfilled composites. Subsequently, the fibre combinations of jute and coir are varied in the ratios of 1:1, 1:2 and 2:1 respectively while the lime sludge content was fixed at 6 wt%. The tensile and flexural strengths of the samples were measured for the composites. It was observed that the tensile and flexural strengths were the highest when the fibre ratios are 1:1 and the fibre content is highest i.e. 30 wt %.

Keyword: hybrid composites, lime sludge, tensile strength, flexural strength

 ISBN:9798647282972

s.kashyap@tezu.ernet.in
IP Address: 157.42.210.197

Chapter 30
Optimization of Cutting Parameters for AISI H13 Tool Steel by Taguchi Method and Artificial Neural Network

Hrishikesh Pathak
Tezpur University, India

Rakesh Doley
Tezpur University, India

Sanghamitra Das
Tezpur University, India

Satadru Kashyap
Tezpur University, India

ABSTRACT

In the present study an attempt has been made to investigate the effect of cutting parameters (cutting speed, feed rate, and depth of cut) on surface roughness and material removal rate (MRR) during dry turning operation of AISI H13 tool steel as per Taguchi's experimental design technique using an L9 orthogonal array. Signal to noise ratio (S/N) results and Analysis of Variance (ANOVA) were employed in order to investigate the optimal and significant cutting characteristics of H13 tool steel respectively. This paper focuses on optimizing the cutting parameters for minimum surface roughness and maximum MRR of H13 tool steel using high speed steel (HSS) as the cutting tool during turning. The results indicated that feed has a significant influence on surface finish and depth of cut on MRR when turning operation was carried out with HSS cutting tool. An artificial neural network model and regression equations were also developed to obtain minimum surface roughness and maximum MRR at different cutting conditions.

INTRODUCTION

Surface finish is a major factor in the functional performance of machined components. The main aim in today's manufacturing industry is to enhance production efficiency and safety of the products. Product quality and production efficiency can be obtained through lower surface roughness and higher material removal rate while machining. Thus, it is very important to identify the factors affecting surface quality. Among these factors machining conditions play the most significant role.

DOI: 10.4018/978-1-7998-0414-7.ch030

Copyright © 2020, IGI Global. Copying or distributing in print or electronic forms without written permission of IGI Global is prohibited.

Development of Various Industrial Lime Sludge Waste-Filled Hybrid Polymeric Composites for Environmental Sustainability

Satadru Kashyap and Dilip Datta

Abstract A potentially hazardous industrial waste material in our society is lime sludge which is sourced mainly from various industries (fertilizer, paper, sugar and soda ash) and generally disposed off in dumpyards or used in unauthorized land filling—both causing pollution. Hence, an alternative idea of environmental sustainability is by reusing lime sludge as reinforcing agent in polymeric composites. In this line of thought, lime sludge waste is used as filler in HDPE and epoxy matrices in order to investigate the effects of lime sludge on its composite properties. This would ultimately, throw light on the feasibility and commercial viability of lime sludge reuse in polymeric composites. Mechanical properties of HDPE composites are studied with maleic anhydride-grafted polyethylene (MAPE) as compatibilizer for effective adhesion at the filler/matrix boundary. Lime sludge waste was also used as filler in conjunction with randomly dispersed short coir fibre reinforced HDPE composites along with 5 wt% MAPE as compatibilizer. It is observed the properties such as flexural strength and mechanical rigidity (tensile and flexural) of the lime sludge infused composites improved with filler addition. The tensile strength increased up to 20 wt% filler addition due to effective reinforcement; however, beyond that the tensile strength decreased due to particle agglomeration. Additionally, lime sludge is used as filler in short and long coir fibre added epoxy composites. It is found that lime sludge content of 6 wt% results in superior tensile strength in coir fibre reinforced epoxy composites. In general, lime sludge is found to improve the bending strength and mechanical rigidity (tensile and flexural modulus) with increasing filler weight fraction. Thus, the reuse of lime sludge filler in polymeric composites not only results in the enhancement of various mechanical properties, but also reduces pollution, decreases the cost of the composites and improves the commercial viability of lime sludge waste.

S. Kashyap (✉) · D. Datta
Department of Mechanical Engineering, Tezpur University, Napaam 784028, Assam, India
e-mail: satadru@tezu.ernet.in

D. Datta
e-mail: ddatta@tezu.ernet.in

© Springer Nature Singapore Pte Ltd. 2018

S. S. Sidhu et al. (eds.), *Futuristic Composites*, Materials Horizons: From Nature to Nanomaterials, https://doi.org/10.1007/978-981-13-2417-8_10